



Homogenization of pseudoparabolic reaction- diffusion-mechanics systems

Multiscale modeling, well-posedness and convergence rates

Arthur J. Vromans

Faculty of Health, Science and Technology

Mathematics

DOCTORAL THESIS | Karlstad University Studies | 2019:19

Homogenization of pseudoparabolic reaction- diffusion-mechanics systems

Multiscale modeling, well-posedness and convergence rates

Arthur J. Vromans

Homogenization of pseudoparabolic reaction-diffusion-mechanics systems -
Multiscale modeling, well-posedness and convergence rates

Arthur J. Vromans

DOCTORAL THESIS

Karlstad University Studies | 2019:19

urn:nbn:se:kau:diva-72926

ISSN 1403-8099

ISBN 978-91-7867-033-8 (print)

ISBN 978-91-7867-038-3 (pdf)

© The author

Distribution:
Karlstad University
Faculty of Health, Science and Technology
Department of Mathematics and Computer Science
SE-651 88 Karlstad, Sweden
+46 54 700 10 00

Print: Universitetstryckeriet, Karlstad 2019

WWW.KAU.SE

Homogenization of pseudoparabolic reaction-diffusion-mechanics systems: multiscale modeling, well-posedness and convergence rates

PROEFSCHRIFT

ter verkrijging van de graad van doctor aan de Technische
Universiteit Eindhoven, op gezag van de rector magnificus
prof.dr.ir. F.P.T. Baaijens,
voor een commissie aangewezen door het College voor
Promoties, in het openbaar te verdedigen op vrijdag 6
september 2019 om 16:00 uur

door

Arthur Johannes Vromans

geboren te Vlaardingen

Dit proefschrift is goedgekeurd door de promotoren en de samenstelling van de promotiecommissie is als volgt:

voorzitter:	prof.dr.	M.G.J. van den Brand
1 ^e promotor:	prof.dr.habil.	A. Muntean (Karlstads Universitet)
2 ^e promotor:	prof.dr.	M.A. Peletier
copromotor(en):	dr.ir.	A.A.F. van de Ven
leden:	prof.dr.	J. Zeman (České vysoké učení technické v Praze)
	prof.dr.ir.	J. Padding (Technische Universiteit Delft)
	prof.dr.	I.S. Pop (Universiteit Hasselt)
adviseur(s):	dr.	M. Lind (Karlstads Universitet)
	dr.rer.nat.	O.T.C. Tse

Het onderzoek of ontwerp dat in dit proefschrift wordt beschreven is uitgevoerd in overeenstemming met de TU/e Gedragscode Wetenschapsbeoefening.

Contents

1	Introduction	3
1.1	Background, motivation and research objectives	4
1.2	Outline of the dissertation	6
2	Preliminaries	9
2.1	Function spaces	10
2.2	Inequalities and embedding results	12
2.3	Basic solvability results	19
2.4	Two-scale convergence	19
2.5	Periodic homogenization via two-scale convergence	23
3	Modeling and Simulation of Concrete Corrosion – a Mixture Theory Perspective	31
3.1	Introduction	32
3.2	Derivation of a mixture-theory-based concrete corrosion model	35
3.3	Dimension reduction: 1-D model of a concrete plate-layer .	44
3.4	Numerical method	50
3.5	Quest for realistic numerical behavior	51
3.6	Conclusion	59
3.7	Appendix: Asymptotic ϵ -small solutions to System D	61
4	Weak Solvability of a Pseudoparabolic System	71
4.1	Introduction	72
4.2	Formulation of the model equations	74
4.3	Main existence result	76
4.4	Proof of Theorem 4.2	81

4.5	Proof of Theorem 4.1	97
4.6	Numerical exploration of allowed parameter sets	98
4.7	Conclusion	107
4.8	Appendix: Existence of solutions to discrete-time system	107
4.9	Appendix: Derivation of discrete-time quadratic inequalities	113
5	Homogenization and Corrector Estimates	119
5.1	Introduction	120
5.2	Notation and problem statement	123
5.3	Main results	129
5.4	Upscaling procedure	132
5.5	Corrector estimates via asymptotic expansions	147
5.6	Upscaling and convergence speeds for a concrete corrosion model	154
5.7	Appendix: Determining κ , $\tilde{\kappa}$ and exponents l , λ and μ	156
6	Upscaling Non-linear Pseudoparabolic-like Systems on Vanishing Thin Multidomains	161
6.1	Introduction	162
6.2	Preliminaries	164
6.3	Main results	168
6.4	Simultaneous homogenization and dimension reduction for (6.1)	171
6.5	Corrector estimates	182
6.6	A comment on the case $p = 2$	187
6.7	Conclusions	189
6.8	Appendix: An approximation scheme of (U_ϵ, V_ϵ)	190
7	Conclusions and recommendations	203
	List of symbols	207
	Bibliography	211
	About the author	225
	Summary	227
	List of publications	229
	Acknowledgements	233

Abstract

In this dissertation, parabolic-pseudoparabolic equations are proposed to couple chemical reactions, diffusion, flow and mechanics in heterogeneous materials using the framework of mixture theory. The weak solvability is obtained in a one dimensional setting for the full system posed in a homogeneous domain—a formulation which we have obtained using the classical mixture theory. To give a glimpse of what each component of the system does, we illustrate numerically that approximate solutions according to the Rothe method exhibit realistic behaviour in suitable parameter regimes. The periodic homogenization in higher space dimensions is performed for a particular case of the initial system of partial differential equations posed in perforated domains. Besides obtaining upscaled model equations and formulas for computing effective transport coefficients, we also derive corrector/convergence estimates which delimitate the precision of the upscaling procedure. Finally, the periodic homogenization is performed for a thin vanishing multidomain. Corrector estimates are obtained for a comb-like domain placed on a thin plate in a monotone operator setting for pseudoparabolic equations.

Keywords: Reaction-diffusion-mechanics system, parameter delimitation, parabolic-pseudoparabolic equations, weak solvability, Rothe method, periodic homogenization, corrector estimates, vanishing thin domains

MSC Subject Classification (2010): Primary: 35B27, 35K70
Secondary: 35A01, 35B30, 35J60, 35K57, 41A25

Introduction

1.1 Background, motivation and research objectives

The starting point of this work is a partly dissipative model that consists of a nonlinearly coupled parabolic-pseudoparabolic system of partial differential equations based on the classical theory of mixtures, which is coupled with a nonlinear, non-monotonic ordinary differential equation. This way we model explicitly the evolution of the mechanics of the material and keep track of both chemical changes in volume fractions and moisture- and heat-induced mechanical displacements in the presence of small-wavelength oscillations. Such kind of partial differential equation structure arises when modeling geothermal flows and designing devices for the harvesting of geothermal energy (see [43], [44], [95], [98]), acid attack on concrete (see [6], [9], [14], [26], [32], [53], [56], [57], [101], [102], [103]), as well as in the design of solar cells (see [7], [51], [63]).

Interestingly, there is no general solvability theory for such systems; see [70], [71], [92], [128]. One reason for this is that it is not clear-cut how balance laws for multi-physics naturally couple with each other (i.e. often the constitutive laws for the structure of the transport fluxes are debatable; see for example [17], [31], [47], [81], [94], [104], [109], [145]). As typical feature of what we have in mind, the weak solvability of the system cannot be ensured in the absence of the pseudo-parabolic regularization (arising from e.g. a Kelvin-Voigt viscoelasticity model [21]). Preliminary studies on remotely resembling evolution systems with pseudo-parabolic terms are [15], [25], [33], [50], [55], [107], [108], [112], [115].

Since it is not clear-cut how balance laws for multi-physics naturally couple each other, any chosen coupling is a modeling choice. While determining which model is appropriate for the problem at hand, one must, therefore, take the philosophy of modeling into account. A model is a tool for addressing predetermined questions. These questions are essential in choosing a known model or creating a new model as the length-scales, time-scales, quantities and errors used within the questions determine which concepts fit a model description. The model description itself can be contradictory, missing information, or not having the right level of complexity. For a mathematical model described by partial differential equations, these description problems arise when checking the existence, uniqueness, dependence on parameters, and shape/behavior of the solution. Passing this mathematical validation step means that the model is consistent in some parameter region, but not necessarily yielding physical behaviour. For example, if the model yields negative mass or blow up in certain quantities, then the model needs additional

physical constraints, which can severely restrict the parameter region even further. Passing this physical validation step means that the model can be used to describe the physical problem, but not necessarily that the model gives an accurate description of the real situation. Experimental validation against known data of the problem yields how accurate the model describes the problem. At each validation step it is determined whether the model is appropriate for answering the questions. Only when a model passes all validation steps, it can be deemed useful to answer the chosen predetermined questions.

This dissertation addresses the derivation and the mathematical and physical validation of a multi-physics model for in particular a concrete corrosion problem, but it is also related to generalizations where multi-physics scenarios are involved.

The main questions, which we address in this dissertation, are:

Q1: Under which assumptions on the non-linearities can we ensure the weak solvability of the well-posedness of the nonlinearly coupled parabolic-pseudoparabolic system describing the interplay between flow, diffusion, mechanical deformation and chemical reactions?

Q2: To which extent do the model parameters delimitate the existence (and eventually also the stability) of the target weak solutions?

Q3: In an attempt to handle the durability of large scale heterogeneous multi-structures, to which extent can the upscaling of alike coupled systems be done? Is the pseudo-parabolic part of the system hindering the upscaling or is its presence rather an advantage?

Q4: Can the upscaling of our PDE systems be controlled in terms of corrector/convergence estimates?

Q5: In the specific case of a nonlinearly coupled parabolic-pseudoparabolic system posed in a perforated domain lying on a vanishing thin layer, can then the upscaling be performed also in a controlled manner (in terms of corrector/convergence estimates)?

In this work, we give partial answers to these questions. Most of the results are published or accepted for publication; we refer the reader to [136], [137], [142], [140], [143].

1.2 Outline of the dissertation

Chapter 2

This chapter contains a brief summary of known basic results used in this dissertation. The main parts of this chapter are about function spaces, two-scale convergence, periodic homogenization, general inequalities and embedding results.

Chapter 3

In this chapter, we built a 3-D continuum mixture model describing the corrosion of concrete with sulfuric acid. Essentially, the chemical reaction transforms slaked lime (calcium hydroxide) and sulfuric acid into gypsum releasing water. The model incorporates the evolution of chemical reaction, diffusion of species within the porous material and mechanical deformations. We apply this model to a 1-D problem of a plate-layer between concrete and sewer air. The influx of slaked lime from the concrete and sulfuric acid from the sewer air sustains a gypsum-creating chemical reaction (*sulfatation or sulfate attack*). The combination of the influx of matter and the chemical reaction causes a net growth in the thickness of the gypsum layer on top of the concrete base. The model allows for the determination of the plate layer thickness $h = h(t)$ as function of time, which indicates both the amount of gypsum being created due to concrete corrosion and the amount of slaked lime and sulfuric acid in the material. We identify numerically the existence of a parameter regime for which the model yields a non-decreasing plate layer thickness $h(t)$. Also we investigate the robustness of the model with respect to changes in the model parameters.

Chapter 4

In this chapter, we study the weak solvability of a nonlinearly coupled system of parabolic and pseudo-parabolic equations describing the interplay between mechanics, chemical reactions, diffusion and flow modelled within a mixture theory framework via energy-like estimates and Gronwall inequalities. In analytically derived parameter regimes, these estimates ensure the convergence of discretized-in-time partial differential equations. Additionally, we test and extend numerically these regimes. Especially, the size of the time-interval in which physical behaviour is observed, has our focus with emphasis on its dependence on selected parameters.

Chapter 5

In this chapter, we determine corrector estimates, which quantify the convergence speed of the upscaling of a pseudo-parabolic system containing drift

terms incorporating the separation of length scales with relative size $\epsilon \ll 1$. To achieve this goal, we exploit a natural spatial-temporal decomposition, which splits the pseudo-parabolic system into an elliptic partial differential equation and an ordinary differential equation coupled together. We obtain upscaled model equations, explicit equations for effective transport coefficients, as well as corrector estimates delimitating the quality of the upscaling. Finally, for special cases, we show convergence speeds for global times, i.e. $t \in \mathbf{R}_+$, by using time intervals expanding to the whole of \mathbf{R}_+ simultaneously with passing to the homogenization limit $\epsilon \downarrow 0$.

Chapter 6

In this chapter, we modify the pseudo-parabolic problem in two ways. First, we make the system of equations nonlinear with the use of monotone operators. Second, we change the domain to a simply-connected set of periodically placed parallel cylinders on a substrate, such that the thickness of the individual cylinders, the spacing between the cylinders, and the thickness of the substrate tend to 0 as ϵ tends to 0. This domain represents a geometry used in solar cell production. For this nonlinear pseudo-parabolic problem, we obtain upscaled model equations, explicit equations for effective transport coefficients, as well as corrector estimates delimitating the quality of the upscaling.

Chapter 7

This chapter is the final chapter of the dissertation. It describes briefly the results we accomplished in this dissertation (in relation to questions Q1-Q5 from Section 1.1), the conclusions we can draw from them and what type of research directions seem natural extensions or complements of the results presented in this dissertation.

Preliminaries

2.1 Function spaces

In this section, we give the definition and associated norms and also inner products in the case of Hilbert spaces for all the function spaces used in this dissertation. For general theory about these function spaces and their inter-relations, we recommend [20], [48], [79], [121], and [146].

For simplicity, we assume that every domain $\Omega \subset \mathbf{R}^d$ for $d \in \mathbf{N}$ is equipped with the Lebesgue measure $d\mathbf{x}$. Moreover, we assume that $p \in [1, \infty]$ and $n \in \mathbf{N}$ unless otherwise stated.

We start with the function spaces of continuous functions.

The space $C^n(\Omega)$ is the set of all functions $f : \Omega \rightarrow \mathbf{R}$ such that all derivatives up to and including n -th order exists and are continuous on Ω .

The space $C^\infty(\Omega)$ is defined as $\bigcap_{n \in \mathbf{N}} C^n(\Omega)$.

The associated norms are $\|f\|_{C^n(\Omega)} := \sum_{0 \leq |\alpha| \leq n} \sup_{\mathbf{x} \in \Omega} |D^\alpha f(\mathbf{x})|$.

Related are the continuous functions with compact support.

The space $C_c^n(\Omega)$ is the set of all functions $f : \Omega \rightarrow \mathbf{R}$ such that all derivatives up to and including n -th order exist and are continuous on Ω and there is a compact set $\mathbb{K} \subset \Omega$ such that f is 0 on $\Omega \setminus \mathbb{K}$.

The space $C_c^\infty(\Omega)$, also denoted as $\mathcal{D}(\Omega)$, is defined as $\bigcap_{n \in \mathbf{N}} C_c^n(\Omega)$.

Their associated norms are identical to the norms of $C^n(\Omega)$.

When one takes integrability as a more important property than continuity, one arrives naturally to the Lebesgue spaces.

The Lebesgue space $L^p(\Omega)$ for $p \in [1, \infty)$ is defined as the set of functions $f : \Omega \rightarrow \mathbf{R}$ such that the norm $\|f\|_{L^p(\Omega)} := \int_\Omega |f(\mathbf{x})|^p d\mathbf{x}$ exists and is finite and with the identification of functions that only differ on null-sets.

The Lebesgue space $L^\infty(\Omega)$ is defined as the set of functions $f : \Omega \rightarrow \mathbf{R}$ such that the norm $\|f\|_{L^\infty(\Omega)} := \text{esssup}_{\mathbf{x} \in \Omega} |f(\mathbf{x})|$ exists and is finite and with the identification of functions that only differ on null-sets.

The Lebesgue space $L^2(\Omega)$ is also a Hilbert space with respect to the inner product $(f, g)_{L^2(\Omega)} = \int_\Omega f(\mathbf{x})g(\mathbf{x})d\mathbf{x}$.

Moreover, the space $L^p_{loc}(\Omega)$ is defined as the set of all functions $f \in L^p(\Omega)$ such that f has compact support within Ω , i.e. there is a compact set $\mathbb{K} \subset \Omega$ such that f is 0 on $\Omega \setminus \mathbb{K}$.

Related to the Lebesgue spaces are the Sobolev spaces.

The Sobolev space $W^{1,p}(\Omega)$ is defined as the set of functions $f \in L^p(\Omega)$ such that there exists a function $\mathbf{g} \in L^p(\Omega)^d$ which satisfies

$$\int_{\Omega} f \nabla \phi \cdot \mathbf{n} d\mathbf{x} = - \int_{\Omega} \phi \mathbf{g} \cdot \mathbf{n} d\mathbf{x} \text{ for all } \phi \in C_c^\infty(\Omega) \text{ and for all } \mathbf{n} \in \mathbf{R}^n.$$

The Sobolev spaces $W^{n,p}(\Omega)$ for $n \geq 1$ are defined recursively as the set of functions $f \in W^{n-1,p}(\Omega)$ such that there exists a function $D^\alpha f \in W^{n-1,p}(\Omega)^d$ for all $|\alpha|_1 = 1$.

The associated norms are $\|f\|_{W^{n,p}(\Omega)} := \left(\sum_{0 \leq |\alpha|_1 \leq n} \|D^\alpha f\|_{L^p(\Omega)}^p \right)^{\frac{1}{p}}$ for $p \in [1, \infty)$ and $\|f\|_{W^{n,\infty}(\Omega)} := \max_{0 \leq |\alpha|_1 \leq n} \text{esssup}_{\mathbf{x} \in \Omega} |D^\alpha f(\mathbf{x})|$.

The Sobolev space $W^{n,2}(\Omega)$ is also a Hilbert space with respect to the inner product $(f, g)_{W^{n,2}(\Omega)} = \int_{\Omega} \sum_{0 \leq |\alpha|_1 \leq n} D^\alpha f(\mathbf{x}) \cdot D^\alpha g(\mathbf{x}) d\mathbf{x}$. This Hilbert space can also be denoted as $H^n(\Omega)$.

The Lebesgue spaces $L^p(\Omega)$ can now be interpreted as $W^{0,p}(\Omega)$.

Moreover, the space $W_0^{n,p}(\Omega)$ is the closure of $C_c^n(\Omega)$ with respect to the norm $\|\cdot\|_{W^{n,p}(\Omega)}$.

A special set of function spaces are those of periodic functions.

Let G be a closed subset of the group of all translations on \mathbf{R}^d such that the quotient group \mathbf{R}^d/G can be identified with a finite subset Y of \mathbf{R}^d that is not a null-set.

A function f is called Y -periodic if $f = f \circ g$ for all mappings $g \in G$.

The space $C_{\#}^n(Y)$ is the space of all Y -periodic functions in $C^n(Y)$.

The space $L_{\#}^p(Y)$ is the space of all Y -periodic functions in $L^p(Y)$.

The space $W_{\#}^{n,p}(Y)$ is the space of all Y -periodic functions in $W^{n,p}(Y)$.

The space $W_{\#}^{n,p}(Y)/\mathbf{R}$ is the space of all Y -periodic functions in $W^{n,p}(Y)$ with $\int_Y f(\mathbf{x}) d\mathbf{x} = 0$.

The associated norms of these periodic function spaces are those of their non-periodic counterparts.

More complicated function spaces to construct are the Bochner spaces, which are function spaces of functions that take values in other function spaces instead of \mathbf{R} .

Let \mathbb{B} denote a Banach space. A Bochner space is in general a space of functions $f : \Omega \rightarrow \mathbb{B}$. A Bochner space can only be a Hilbert space if \mathbb{B} is a Hilbert space, which we denote by \mathbb{H} for differentiation with Banach spaces. Let $\mathbb{B}_1(\Omega)$ and \mathbb{B}_2 be Banach spaces and $\mathbb{H}_1(\Omega)$ and \mathbb{H}_2 be Hilbert spaces. In general The Bochner space $\mathbb{B}_1(\Omega; \mathbb{B}_2)$ is a Banach space of functions for which

the following norm exists and is finite: $\|f\|_{\mathbb{H}_1(\Omega; \mathbb{B}_2)} = \|\|f\|_{\mathbb{B}_2}(\mathbf{x})\|_{\mathbb{H}_1(\Omega)}$.

The Bochner space $\mathbb{H}_1(\Omega; \mathbb{H}_2)$ is a Hilbert space of functions for which the following norm exists and is finite: $\|f\|_{\mathbb{H}_1(\Omega; \mathbb{H}_2)} = \|\|f\|_{\mathbb{H}_2}(\mathbf{x})\|_{\mathbb{H}_1(\Omega)}$. We refrain from writing the inner product in general form as this form depends on the choice of $\mathbb{H}_1(\Omega)$.

The following two spaces are examples of Bochner spaces:

The Bochner space $W^{2,3}(\Omega; L^5(0,1))$ is a Banach space of functions for which the following norm exists and is finite:

$$\begin{aligned} \|f\|_{W^{2,3}(\Omega; L^5(0,1))} &= \|\|f\|_{L^5(0,1)}(\mathbf{x})\|_{W^{2,3}(\Omega)} \\ &= \left(\sum_{0 \leq |\alpha|_1 \leq 2} \int_{\Omega} \left| D^{\alpha} \int_0^1 |f(\mathbf{x}, t)|^5 dt \right|^{\frac{3}{5}} d\mathbf{x} \right)^{\frac{1}{3}}. \end{aligned}$$

The Bochner space $L^2(\Omega; H^1(0,1))$ is a Hilbert space of functions for which the following norm exists and is finite: $\|f\|_{L^2(\Omega; H^1(0,1))} = \|\|f\|_{H^1(0,1)}(\mathbf{x})\|_{L^2(\Omega)} =$

$\left(\int_{\Omega} \left| \int_0^1 |f(\mathbf{x}, t)|^2 + \left| \frac{\partial f(\mathbf{x}, t)}{\partial t} \right|^2 dt \right|^2 d\mathbf{x} \right)^{\frac{1}{2}}$. Moreover, the inner product is given by $(f, g)_{L^2(\Omega; H^1(0,1))} = \int_{\Omega} \int_0^1 f(\mathbf{x}, t)g(\mathbf{x}, t) + \frac{\partial f(\mathbf{x}, t)}{\partial t} \frac{\partial g(\mathbf{x}, t)}{\partial t} dt d\mathbf{x}$.

2.2 Inequalities and embedding results

In this section, we list a number of inequalities that we found useful in our work as well as a selection of embedding results between function spaces. These inequalities and embedding results can be found in [20] and [48].

Inequality 1 (Triangle). *Let \mathbb{X} denote a vector space with a norm $\|\cdot\|$, then the norm must satisfy (by definition)*

$$\left| \|a\| - \|b\| \right| \leq \|a + b\| \leq \|a\| + \|b\| \quad (2.1)$$

for $a, b \in \mathbb{X}$.

Inequality 2 (Cauchy-Schwartz). *Let \mathbb{X} denote a vector space with an inner product (\cdot, \cdot) and a corresponding norm $\|\cdot\|$, then the inner product of two vectors $a, b \in \mathbb{X}$ is bounded.*

$$|(a, b)| \leq \|a\| \|b\| \quad (2.2)$$

Inequality 3 (Young's). Let $a, b \in \mathbf{R}^+$, let $\eta > 0$ and let $p, q \in [1, \infty]$ satisfy $1/p + 1/q = 1$ then holds

$$ab \leq \frac{\eta^p a^p}{p} + \frac{b^q}{q\eta^q}. \quad (2.3)$$

Inequality 4 (Hölder's). Let $p_1, p_2, \dots, p_n \in [1, \infty]$ satisfy $\sum_{j \leq n} 1/p_j = 1$, and let $u_j \in L^{p_j}(\Omega)$ for all $j \leq n$, then

$$\int_{\Omega} \prod_{j \leq n} |u_j| \, d\mathbf{x} \leq \prod_{j \leq n} \|u_j\|_{L^{p_j}(\Omega)}. \quad (2.4)$$

Inequality 5 (Minkowski's). Let $p \in [1, \infty]$ and $u, v \in L^p(\Omega)$, then the triangle inequality is satisfied by the integral norm of L^p -spaces.

$$\|u + v\|_{L^p(\Omega)} \leq \|u\|_{L^p(\Omega)} + \|v\|_{L^p(\Omega)} \quad (2.5)$$

Inequality 6 (Hanner's). Let $p \in [1, \infty)$, let $u, v \in L^p(\Omega)$ and let $\|\cdot\|$ denote the norm of $L^p(\Omega)$, then a parallelogram rule like inequality for the integral norm of L^p spaces can be obtained

$$\|u + v\|^p + \|u - v\|^p \diamond (\|u\| + \|v\|)^p + \|\|u\| - \|v\|\|^p \quad (2.6)$$

with the relational operator \diamond defined as

$$\diamond \begin{cases} \geq & \text{for } p \in [1, 2], \\ = & \text{for } p = 2, \\ \leq & \text{for } p \in [2, \infty). \end{cases} \quad (2.7)$$

Inequality 7 (Clarkson's). *Let $p, q \in [1, \infty]$ satisfy $1/p + 1/q = 1$, let $u, v \in L^p(\Omega)$, and let $\|\cdot\|$ denote the norm of $L^p(\Omega)$, then*

$$\left\| \frac{u+v}{2} \right\|^{\max\{p,q\}} + \left\| \frac{u-v}{2} \right\|^{\max\{p,q\}} \leq \left(\frac{\|u\|^p + \|v\|^p}{2} \right)^{\max\{p,q\}/p}. \quad (2.8)$$

Inequality 8 (Generalized Mean). *Let $\mathbf{x}, \mathbf{w} \in \mathbf{R}_+^n$ with $\|\mathbf{w}\|_1 = 1$. Introduce*

$$\mathcal{M}_p(\mathbf{x}) = \begin{cases} \min\{\mathbf{x}\} & \text{for } p = -\infty, \\ \left(\sum_{i=1}^n w_i x_i^p \right)^{1/p} & \text{for } p \in \mathbf{R} \setminus \{0\}, \\ \prod_{i=1}^n x_i^{w_i} & \text{for } p = 0, \\ \max\{\mathbf{x}\} & \text{for } p = \infty. \end{cases} \quad (2.9)$$

If $p < q$, then $\mathcal{M}_p(\mathbf{x}) \leq \mathcal{M}_q(\mathbf{x})$. Note, the unweighted version has $w_i = 1/n$. Moreover, equality only occurs when $\mathbf{x} = x_1 \mathbf{1}$.

Inequality 9 (Equivalence of p -norms on \mathbf{R}^n). *Let $0 < p < q$, then we have the equivalence inequalities $|\cdot|_q \leq |\cdot|_p \leq n^{1/p-1/q} |\cdot|_q$.*

Inequality 10 (Jensen's). *Let f be a positive Lebesgue-integrable function on Ω with $|\Omega| < \infty$ and let ψ be a convex function on the range of f , then*

$$\psi \left(\frac{1}{|\Omega|} \int_{\Omega} f(\mathbf{x}) d\mathbf{x} \right) \leq \frac{1}{|\Omega|} \int_{\Omega} \psi(f(\mathbf{x})) d\mathbf{x}. \quad (2.10)$$

Inequality 11 (Continuous Gronwall). *Let x, u and v be real continuous functions defined in $[a, b]$, $v(t) \geq 0$ for $t \in [a, b]$. We suppose that on $[a, b]$ we have the inequality*

$$x(t) \leq u(t) + \int_a^t v(s)x(s) ds. \quad (2.11)$$

Then

$$x(t) \leq u(t) + \int_a^t v(s)u(s) \exp\left(\int_s^t v(r)dr\right) ds \quad (2.12)$$

in $[a, b]$. If u is constant, then

$$x(t) \leq u \exp\left(\int_a^t v(r)dr\right). \quad (2.13)$$

Inequality 12 (Discrete Gronwall #1). Suppose $h \in (0, H)$. Let (x^k) , (y^{k+1}) and (z^k) for $k = 0, 1, \dots$ be sequences in \mathbf{R}_+ satisfying

$$y^k + \frac{x^k - x^{k-1}}{h} \leq A + z^{k-1} + Bx^k + Cx^{k-1} \quad \text{and} \quad \sum_{j=0}^{k-1} z^j h \leq Z$$

for all $k = 1, 2, \dots$ with constants A, B, C and Z independent of h satisfying

$$A > 0, \quad Z > 0, \quad B + C > 0, \quad \text{and} \quad BH \leq 0.6838,$$

then

$$x^k \leq \left(x^0 + Z + A \frac{C + 1.6838B}{C + B} kh\right) e^{(C+1.6838B)kh} \quad \text{and}$$

$$\sum_{j=1}^k y^j h \leq (x^0 + Z + A kh) e^{(C+1.6838B)kh}.$$

Inequality 13 (Discrete Gronwall #2). Let $c > 0$ and (y_k) , (g_k) be sequences of positive numbers satisfying

$$y_k \leq c + \sum_{0 \leq j < k} g_j y_j \quad \text{for } k \geq 0,$$

then

$$y_k \leq c \exp\left(\sum_{0 \leq j < k} g_j\right) \quad \text{for } k \geq 0.$$

Lemma 2.1 (Inclusion inequality). *Let Ω be an open connected subset of \mathbf{R}^n with $|\Omega| < \infty$, let $1 \leq p_0 \leq p_1 \leq \infty$ then $L^{p_1}(\Omega) \subset L^{p_0}(\Omega)$ by the inequality*

$$\frac{1}{|\Omega|^{\frac{1}{p_0}}} \|u\|_{L^{p_0}(\Omega)} \leq \frac{1}{|\Omega|^{\frac{1}{p_1}}} \|u\|_{L^{p_1}(\Omega)} \quad (2.15)$$

which holds for all $u \in L^{p_1}(\Omega)$.

Lemma 2.2 (Infinity limit). *Let Ω be an open connected subset of \mathbf{R}^n with $|\Omega| < \infty$, let $p \in [1, \infty)$ and $u \in L^\infty(\Omega)$, then holds*

$$\|u\|_{L^p(\Omega)} \rightarrow \|u\|_{L^\infty(\Omega)} \text{ as } p \rightarrow \infty. \quad (2.16)$$

Remark that $u \in L^p(\Omega)$ holds by the inclusion inequality, see Lemma 2.1.

Theorem 2.3 (Interpolation inequality). *Let $r \in [s, t] \subseteq [1, \infty]$ satisfy*

$$\frac{1}{r} = \frac{\theta}{s} + \frac{1-\theta}{t} \quad (2.17)$$

for some $\theta \in [0, 1]$ and let $u \in L^s(\Omega) \cap L^t(\Omega)$, then $u \in L^r(\Omega)$ and

$$\|u\|_{L^r(\Omega)} \leq \|u\|_{L^s(\Omega)}^\theta \|u\|_{L^t(\Omega)}^{1-\theta}. \quad (2.18)$$

Theorem 2.4 (Gagliardo-Nirenberg interpolation). *Let Ω be a connected open subset of \mathbf{R}^n with a Lipschitz boundary, let $q, r \in [1, \infty]$, $m \geq 0$ integer and $u \in L^q(\Omega)$ with $D^\alpha u \in L^r(\Omega)$ for $|\alpha|_1 = m$. Suppose there exists a $p \in [1, \infty]$ and $j \geq 0$ integer such that*

$$\frac{1}{p} - \frac{j}{n} = \beta \left(\frac{1}{r} - \frac{m}{n} \right) + \frac{1-\beta}{q} \quad \text{for } \beta \in \left[\frac{j}{m}, 1 \right] \quad (2.19)$$

is satisfied, then there exist constants $C_1, C_2 < \infty$ depending on Ω and p, q, r, j, k and n such that the following inequality holds

$$\|D^\gamma u\|_{L^p(\Omega)} \leq C_1 \|D^\alpha u\|_{L^r(\Omega)}^\beta \|u\|_{L^q(\Omega)}^{1-\beta} + C_2 \|u\|_{L^s(\Omega)} \quad (2.20)$$

with $|\gamma|_1 = j$ and $s > 0$ arbitrary.

Theorem 2.5 (Sobolev inequality). *Let Ω be a connected open subset of \mathbf{R}^n , let $1 \leq p < q < \infty$, $k \geq 0$ integer and $u \in W^{k,p}(\Omega)$. Suppose there exists an $l \in (0, k)$ integer such that*

$$\frac{1}{q} - \frac{l}{n} = \frac{1}{p} - \frac{k}{n} \quad (2.21)$$

is satisfied, then there exists a constant $C < \infty$ depending on Ω and p, q, k, l and n such that the following inequality holds.

$$\|u\|_{W^{l,q}(\Omega)} \leq C \|u\|_{W^{k,p}(\Omega)} \quad (2.22)$$

Theorem 2.6 (Rellich-Kondrachov). *Let Ω be an finite open interval or a connected open subset of \mathbf{R}^n with a Lipschitz boundary and $|\Omega| < \infty$, then there exists a constant $C < \infty$ depending on Ω and p such that the inequality*

$$\|u\|_{L^q(\Omega)} \leq C \|u\|_{W^{1,p}(\Omega)} \quad (2.23)$$

holds for

$$\begin{aligned} q \in [1, p^*] & \quad \text{if } p < n, \\ q \in [p, \infty) & \quad \text{if } p = n, \\ q = \infty & \quad \text{if } p > n, \end{aligned} \quad (2.24)$$

where $1/p^ = 1/p - 1/n$.*

Moreover, these embeddings are compact except for two cases: 1. $q = p^$ for $p < n$ and 2. $q = \infty$ for $p > n$. For $p > n$, we have the compact embedding of $W^{1,p}(\Omega)$ in $C(\overline{\Omega})$.*

Theorem 2.7 (Friedrich's inequality). *Let Ω be an open connected subset of \mathbf{R}^n with $|\Omega| < \infty$, let $p \in [1, \infty)$, $k \geq 0$ integer and $u \in W_0^{k,p}(\Omega)$, then we have*

$$\|u\|_{L^p(\Omega)}^p \leq |\Omega|^{pk} \sum_{|\alpha|_1=k} \|D^\alpha u\|_{L^p(\Omega)}^p. \quad (2.25)$$

Theorem 2.8 (Poincaré inequality). *Let Ω be an open connected subset of \mathbf{R}^n between two parallel hyperplanes separated by a distance d , let $p \in [1, \infty)$ and $u \in W_0^{1,p}(\Omega)$, then*

$$\|u\|_{L^p(\Omega)}^p \leq \frac{d^p}{p} \|\nabla u\|_{L^p(\Omega)}^p. \quad (2.26)$$

Theorem 2.9 (Poincaré-Wirtinger inequality). *Let Ω be a connected convex open subset of \mathbf{R}^n with $|\Omega| < \infty$ and C^1 -boundary. Let $p \in [1, \infty)$ and $u \in W^{1,p}(\Omega)$. Then there exists a constant $C < \infty$ depending only on p and Ω such that*

$$\left\| u - \frac{1}{|\Omega|} \int_{\Omega} u(\mathbf{x}) d\mathbf{x} \right\|_{L^p(\Omega)}^p \leq C \text{diam}(\Omega)^p \|\nabla u\|_{L^p(\Omega)}^p. \quad (2.27)$$

Theorem 2.10 (Trace inequality for $n \geq 2$). *Let Ω be an open connected subset of \mathbf{R}^n for $n \geq 2$ with $|\Omega| < \infty$ and Lipschitz boundary $\partial\Omega$, let $p \in [1, \infty]$ and $u \in W^{1,p}(\Omega)$, then there exists a constant C depending only on p and Ω such that the following inequality holds*

$$\|u|_{\partial\Omega}\|_{L^p(\partial\Omega)} \leq C \|u\|_{W^{1,p}(\Omega)} \quad (2.28)$$

where $u|_{\partial\Omega}$ denotes the function u restricted to the boundary of Ω .

Proposition 2.11 (Trace inequality for $n = 1$). *Let Ω be an open bounded interval, $p \in [1, \infty]$ and $u \in W^{1,p}(\Omega)$. Then the following inequality holds*

$$\|u|_{\partial\Omega}\|_{L^p(\partial\Omega)} \leq p^{1/p} \|u\|_{L^p(\Omega)}^{1/q} \left\| \frac{\partial u}{\partial x} \right\|_{L^p(\Omega)}^{1/p}, \quad (2.29)$$

where $u|_{\partial\Omega}$ denotes the function u restricted to the boundary of Ω and q satisfies $1/p + 1/q = 1$.

2.3 Basic solvability results

For results concerning the weak solvability of elliptic equations and systems, we refer the reader to for example [20], [121]. What concerns weak/strong solutions for parabolic equations, we have mainly used the method by Rothe. Our main references are [40], [48], [74], [121], [129]. Last but not least, we were very much inspired by the work of Showalter and co-authors, e.g. [15], [107], [128], and others, e.g. [43], [50], [55], [112], [115] in the framework of pseudo-parabolic equations. In Chapter 6, we use a similar framework, when monotone operators are used. We refer the reader to [8], [28], [58], [85], [127], [130], [146].

2.4 Two-scale convergence

Our work in Chapter 5 and Chapter 6 relies essentially on the use of the concept of two-scale convergence. Two-scale convergence is a method invented in 1989 by G. Nguetseng, see [99], and further development by G. Allaire, see [4], and many other authors. This method removes many technicalities by basing the convergence itself on functional analytic grounds as a property of functions in certain spaces. In some sense the function spaces natural to periodic boundary conditions have nice convergence properties of their oscillating continuous functions. This is made precise in the First Oscillation Lemma:

Lemma 2.12 (‘First Oscillation Lemma’). *Let $\Omega \subset \mathbf{R}^d$ be a connected domain and let $Y \subset \mathbf{R}^d$ be a parallelepiped given by $Y = [0, l_1] \times \dots \times [0, l_d]$. Let $B_p(\Omega, Y)$, $1 \leq p < \infty$, denote any of the spaces $L^p(\Omega; C_{\#}(Y))$, $L^p_{\#}(\Omega; C(\bar{Y}))$, $C(\bar{\Omega}; C_{\#}(Y))$. Then $B_p(\Omega, Y)$ has the following properties:*

1. $B_p(\Omega, Y)$ is a separable Banach space.
2. $B_p(\Omega, Y)$ is dense in $L^p(\Omega \times Y)$.
3. If $f(\mathbf{x}, \mathbf{y}) \in B_p(\Omega, Y)$. Then $f(\mathbf{x}, \mathbf{x}/\epsilon)$ is a measurable function on Ω such that

$$\left\| f\left(\mathbf{x}, \frac{\mathbf{x}}{\epsilon}\right) \right\|_{L^p(\Omega)} \leq \|f(\mathbf{x}, \mathbf{y})\|_{B_p(\Omega, Y)}. \quad (2.30)$$

4. For every $f(\mathbf{x}, \mathbf{y}) \in B_p(\Omega, Y)$, one has

$$\lim_{\epsilon \rightarrow 0} \int_{\Omega} f\left(\mathbf{x}, \frac{\mathbf{x}}{\epsilon}\right) d\mathbf{x} = \frac{1}{|Y|} \int_{\Omega} \int_Y f(\mathbf{x}, \mathbf{y}) d\mathbf{y} d\mathbf{x}. \quad (2.31)$$

5. For every $f(\mathbf{x}, \mathbf{y}) \in B_p(\Omega, Y)$, one has

$$\lim_{\epsilon \rightarrow 0} \int_{\Omega} \left| f\left(\mathbf{x}, \frac{\mathbf{x}}{\epsilon}\right) \right|^p d\mathbf{x} = \frac{1}{|Y|} \int_{\Omega} \int_Y |f(\mathbf{x}, \mathbf{y})|^p d\mathbf{y} d\mathbf{x}. \quad (2.32)$$

See Theorems 2 and 4 in [86].

However, the application of the First Oscillation Lemma is not sufficient as it cannot be applied to weak solutions nor to gradients. Essentially the concept of two-scale convergence overcomes these problems by extending the First Oscillation Lemma in a weak sense, see [116].

Two-scale convergence: definition and results

For each function $c(t, \mathbf{x}, \mathbf{y})$ on $(0, T) \times \Omega \times Y$, we introduce a corresponding sequence of functions $c_{\epsilon}(t, \mathbf{x})$ on $(0, T) \times \Omega$ by

$$c_{\epsilon}(t, \mathbf{x}) = c\left(t, \mathbf{x}, \frac{\mathbf{x}}{\epsilon}\right) \quad (2.33)$$

for all $\epsilon \in (0, \epsilon_0)$, although two-scale convergence is valid for more general class of bounded sequences of functions $c_{\epsilon}(t, \mathbf{x})$.

Introduce the notation $\nabla_{\mathbf{y}}$ for the gradient in the \mathbf{y} -variable. Moreover, we introduce the notations \rightarrow , \rightharpoonup , and $\xrightarrow{2}$ to point out strong convergence, weak convergence, and two-scale convergence, respectively. See List of Symbols for more notation.

The two-scale convergence was first introduced in [99] and popularized with the seminal paper [4], in which the term two-scale convergence was actually coined. For our explanation we use both the seminal paper [4] as the modern exposition of two-scale convergence in [86]. From now on, p and q are real numbers such that $1 < p < \infty$ and $1/p + 1/q = 1$.

Definition 2.13. Let $(\epsilon_h)_h$ be a fixed sequence of positive real numbers¹ converging to 0. A sequence (u_{ϵ}) of functions in $L^p(\Omega)$ is said to two-scale converge to a limit $u_0 \in L^p(\Omega \times Y)$ if

$$\int_{\Omega} u_{\epsilon}(\mathbf{x}) \phi\left(\mathbf{x}, \frac{\mathbf{x}}{\epsilon}\right) d\mathbf{x} \rightarrow \frac{1}{|Y|} \int_{\Omega} \int_Y u_0(\mathbf{x}, \mathbf{y}) \phi(\mathbf{x}, \mathbf{y}) d\mathbf{y} d\mathbf{x}, \quad (2.34)$$

for every $\phi \in L^q(\Omega; C_{\#}(Y))$.

See Definition 6 on page 41 of [86].

¹when it is clear from the context we will omit the subscript h

Remark 2.1. Definition 2.13 allows for an extension of two-scale convergence to Bochner spaces $L^r(I; L^p(\Omega \times Y))$ for $r > 1$ of the additional variable $t \in I$ by having the regularity $u_\epsilon \in L^p(I \times \Omega)$, $u_0 \in L^p(I \times \Omega \times Y)$ and $\phi \in L^s(I; L^q(\Omega; C_\#(Y)))$ for $1/r + 1/s = 1$. Moreover (2.34) changes into

$$\int_I \int_\Omega u_\epsilon(t, \mathbf{x}) \phi\left(t, \mathbf{x}, \frac{\mathbf{x}}{\epsilon}\right) d\mathbf{x} dt \rightarrow \frac{1}{|Y|} \int_I \int_\Omega \int_Y u_0(t, \mathbf{x}, \mathbf{y}) \phi(t, \mathbf{x}, \mathbf{y}) d\mathbf{y} d\mathbf{x} dt. \quad (2.35)$$

This Bochner-like extension is well-defined because for y -independent u_0 limits two-scale convergence is identical to weak convergence.

Note, for $r \neq p$ convergence (2.35) is valid for the regularity $u_\epsilon \in L^r(I; L^p(\Omega))$, $u_0 \in L^r(I; L^p(\Omega \times Y))$ and $\phi \in L^s(I; L^1(\Omega; C_\#(Y)))$ for $s = \frac{r}{r-1}$.

For $r = \infty$ we need $\phi \in ba_{ac}(I; L^1(\Omega; C_\#(Y)))$, where $ba_{ac}(I)$ denotes $L^\infty(I)^*$ as the dual of $L^\infty(I)$ can be identified with the set of all finitely additive signed measures that are absolutely continuous with respect to dt on I .

With the Bochner version of Definition 2.13 introduced in Remark 2.1, we can give the Sobolev space version of Definition 2.13.

Definition 2.14. Let $r, p \in [1, \infty)$, $s = \frac{r}{r-1}$, and $q = \frac{p}{p-1}$. A sequence (u_ϵ) of functions in $W^{1,r}(I; L^p(\Omega))$ is said to two-scale converge to a limit $u_0 \in W^{1,r}(I; L^p(\Omega \times Y))$ if both

$$\int_I \int_\Omega u_\epsilon(t, \mathbf{x}) \phi\left(t, \mathbf{x}, \frac{\mathbf{x}}{\epsilon}\right) d\mathbf{x} dt \rightarrow \frac{1}{|Y|} \int_I \int_\Omega \int_Y u_0(t, \mathbf{x}, \mathbf{y}) \phi(t, \mathbf{x}, \mathbf{y}) d\mathbf{y} d\mathbf{x} dt, \quad (2.36a)$$

$$\int_I \int_\Omega \frac{\partial u_\epsilon}{\partial t}(t, \mathbf{x}) \phi\left(t, \mathbf{x}, \frac{\mathbf{x}}{\epsilon}\right) d\mathbf{x} dt \rightarrow \frac{1}{|Y|} \int_I \int_\Omega \int_Y \frac{\partial u_0}{\partial t}(t, \mathbf{x}, \mathbf{y}) \phi(t, \mathbf{x}, \mathbf{y}) d\mathbf{y} d\mathbf{x} dt \quad (2.36b)$$

hold for every $\phi \in L^s(I; L^q(\Omega; C_\#(Y)))$. Or in short notation

$$u_\epsilon \xrightarrow{2} u_0 \text{ in } L^r(I; L^p(\Omega)) \text{ and } \frac{\partial u_\epsilon}{\partial t} \xrightarrow{2} \frac{\partial u_0}{\partial t} \text{ in } L^r(I; L^p(\Omega)). \quad (2.37)$$

We now list several important results concerning the two-scale convergence, which can all be extended in a natural way for Bochner spaces, see Section 2.5.2 in [106] or Section 1.1.5 of [116].

Proposition 2.15. Let (u_ϵ) be a bounded sequence in $W^{1,p}(\Omega)$ for $1 < p \leq \infty$ such that

$$u_\epsilon \rightharpoonup u_0 \text{ in } W^{1,p}(\Omega). \quad (2.38)$$

Then $u_\epsilon \xrightarrow{2} u_0$ and there exist a subsequence ϵ' and a $u_1 \in L^p(\Omega; W_{\#}^{1,p}(Y)/\mathbf{R})$ such that

$$\nabla u_{\epsilon'} \xrightarrow{2} \nabla u_0 + \nabla_{\mathbf{y}} u_1. \quad (2.39)$$

Proposition 2.15 for $1 < p < \infty$ is Theorem 20 in [86], while for $p = 2$ it is identity (i) in Proposition 1.14 in [4]. On page 1492 of [4] it is mentioned that the $p = \infty$ case holds as well. The case of interest for us here is $p = 2$.

Proposition 2.16. *Let (u_ϵ) and $(\epsilon \nabla u_\epsilon)$ be two bounded sequence in $L^2(\Omega)$. Then there exists a function $u_0(\mathbf{x}, \mathbf{y})$ in $L^2(\Omega; H_{\#}^1(Y))$ such that, up to a subsequence, $u_\epsilon \xrightarrow{2} u_0(\mathbf{x}, \mathbf{y})$ and $\epsilon \nabla u_\epsilon \xrightarrow{2} \nabla_{\mathbf{y}} u_0(\mathbf{x}, \mathbf{y})$. See identity (ii) in Proposition 1.14 in [4].*

Corollary 2.17. *Let (u_ϵ) be a bounded sequence in $L^p(\Omega)$, with $1 < p \leq \infty$. There exists a function $u_0(\mathbf{x}, \mathbf{y})$ in $L^p(\Omega \times Y)$ such that, up to a subsequence, $u_\epsilon \xrightarrow{2} u_0(\mathbf{x}, \mathbf{y})$, i.e., for any function $\psi(\mathbf{x}, \mathbf{y}) \in \mathcal{D}(\Omega; C_{\#}^\infty(Y))$, we have*

$$\lim_{\epsilon \rightarrow 0} \int_{\Omega} u_\epsilon(\mathbf{x}) \psi\left(\mathbf{x}, \frac{\mathbf{x}}{\epsilon}\right) d\mathbf{x} = \frac{1}{|Y|} \int_{\Omega} \int_Y u_0(\mathbf{x}, \mathbf{y}) \psi(\mathbf{x}, \mathbf{y}) d\mathbf{y} d\mathbf{x}. \quad (2.40)$$

See Corollary 1.15 in [4].

Note, that Propositions 2.15 and 2.16 are straightforwardly extended to Bochner spaces by applying the two-scale convergence notions of Remark 2.1 and Definition 2.14 instead of the notion from Definition 2.13.

Theorem 2.18. *Let (u_ϵ) be a sequence in $L^p(\Omega)$ for $1 < p < \infty$, which two-scale converges to $u_0 \in L^p(\Omega \times Y)$ and assume that*

$$\lim_{\epsilon \rightarrow 0} \|u_\epsilon\|_{L^p(\Omega)} = \|u_0\|_{L^p(\Omega \times Y)}. \quad (2.41)$$

Then, for any sequence (v_ϵ) in $L^q(\Omega)$ with $\frac{1}{p} + \frac{1}{q} = 1$, which two-scale converges to $v_0 \in L^q(\Omega \times Y)$, we have that

$$\int_{\Omega} u_\epsilon(\mathbf{x}) v_\epsilon(\mathbf{x}) \tau\left(\mathbf{x}, \frac{\mathbf{x}}{\epsilon}\right) d\mathbf{x} \rightarrow \int_{\Omega} \frac{1}{|Y|} \int_Y u_0(\mathbf{x}, \mathbf{y}) v_0(\mathbf{x}, \mathbf{y}) \tau(\mathbf{x}, \mathbf{y}) d\mathbf{y} d\mathbf{x}, \quad (2.42)$$

for every τ in $\mathcal{D}(\Omega, C_{\#}^\infty(Y))$. Moreover, if the Y -periodic extension of u belong to $L^p(\Omega; C_{\#}(Y))$, then

$$\lim_{\epsilon \rightarrow 0} \left\| u_\epsilon(\mathbf{x}) - u_0\left(\mathbf{x}, \frac{\mathbf{x}}{\epsilon}\right) \right\|_{L^p(\Omega)} = 0. \quad (2.43)$$

See Theorem 18 in [86].

These results generalize properties 3, 4 and 5 of the First Oscillation Lemma in such a way that the convergence applies to weak solutions, products and gradients and it even guarantees that the convergence is strong for oscillating continuous functions. Hence, two-scale convergence can be seen as a tool for homogenization (upscaling, averaging, correctors).

2.5 Periodic homogenization via two-scale convergence

The homogenization method tries to describe macroscale behaviour from given microscale behaviour. Consequently, there are at least two scales present in a description of the microscale behaviour: \mathbf{y} of the microscale and \mathbf{x} of the macroscale. Hence, Bochner spaces are crucial function spaces in homogenization.

Different kinds of homogenization techniques exist due to different types of microscale structures causing the microscale behaviour. For understanding different kinds of homogenization techniques good starting references are [72], [84], [100]. We restrict ourselves to periodic homogenization and base our results on [26], [29], [30], [68], [97].

Let $g_1, \dots, g_n \in \mathbf{R}^n$ denote a set linearly independent vectors at the microscale. Introduce the set $\bar{Y} \subset \mathbf{R}^n$ as $\{\sum_{i=1}^n t_i g_i \mid t_i \in [0, 1] \text{ for all } i\}$ and take $Y = \text{Int}(\bar{Y})$. Let $\Omega \subset \mathbf{R}^n$ be an open simply-connected bounded domain at the macroscale. The set Y is a domain and it is a representation of the quotient $\mathbf{R}^n / \mathbb{T}(g_1, \dots, g_n)$, where $\mathbb{T}(g_1, \dots, g_n)$ is a closed subgroup of the translation group \mathbb{T}_n on the microscale domain \mathbf{R}^n . Hence, $\mathbb{T}(g_1, \dots, g_n)$ is equal to the set of mappings

$$\mathcal{T}_{\mathbf{g}} : \mathbf{R}^n \rightarrow \mathbf{R}^n \quad \mathbf{y} \mapsto \mathbf{y} + \mathbf{g}, \quad (2.44)$$

where $\mathbf{g} = \sum_{i=1}^n N_i g_i$ with $N_i \in \mathbf{Z}$ for all $i \in \{1, \dots, n\}$.

Remark 2.2. *The domain Y can be seen as a square on a chess board, that has been stretched, squeezed and rotated.*

Since Y describes a domain at the microscale, we introduce the parameter ϵ as the (homogeneous) scale separation variable such that a distance of 1 at the microscale represents a distance of ϵ in the macroscale. Implicitly, it is assumed that the microscale is embedded in the macroscale. Hence, we assume $\mathbf{y} = \mathbf{x}/\epsilon$. This allows us to use the translation group $\mathbb{T}(g_1, \dots, g_n)$ to tile Ω with copies of Y . Consequently, the boundary of Ω might split a translated copy of Y into multiple parts. Even though, such a situation can be treated, we assume that this does not occur. Moreover, we assume there is

a sequence of $(\epsilon_k)_{k=1}^\infty$ such that $\epsilon_k > 0$, $\epsilon_k \downarrow 0$ and for all ϵ_k any intersection of $\bar{\Omega}$ with a translated copy of \bar{Y} at the ϵ_k -microscale is either empty or the entire translated copy of \bar{Y} .

Remark 2.3. *The region $\bar{\Omega}$ can be seen as a region that can be created by taking unions of adjacent translated copies of \bar{Y} .*

We introduce two types of boundaries $\partial\Omega = \partial\Omega_{ext}$ and

$$\partial\Omega \cup \partial\Omega_{int}^\epsilon = \bigcup_{\mathcal{T}_g(Y) \subset \Omega} \epsilon \partial(\mathcal{T}_g(Y)), \quad \text{while } \partial\Omega \cap \partial\Omega_{int}^\epsilon = \emptyset. \quad (2.45)$$

The first boundary, $\partial\Omega_{ext}$, are all boundary segments of the separate ϵ -sized translated Y such that these segments coincide with a segment of $\partial\Omega$. Then, by assumption, the external boundary equals $\partial\Omega$. The second boundary, $\partial\Omega_{int}$, contains all boundary segments within Ω of the separate ϵ -sized translated Y in Ω .

We introduce a toy model

$$(\mathbf{P}) : \begin{cases} -\operatorname{div}(\mathbf{A}(\mathbf{x}, \mathbf{x}/\epsilon) \cdot \nabla u_\epsilon) = f(\mathbf{x}, \mathbf{x}/\epsilon) & \text{in } \Omega, \\ u_\epsilon = 0 & \text{on } \partial\Omega, \\ -(\mathbf{A}(\mathbf{x}, \mathbf{x}/\epsilon) \cdot \nabla u_\epsilon) \cdot \mathbf{n}_\epsilon = g(\mathbf{x}, \mathbf{x}/\epsilon) & \text{on } \partial\Omega_{int}^\epsilon, \end{cases} \quad (2.46)$$

where $\mathbf{A} \in L^\infty(\Omega; L^\infty_\#(Y))^{n \times n}$ is uniformly elliptic, $f \in L^2(\Omega; L^2_\#(Y))$, $g \in L^2(\Omega; L^2_\#(\partial Y))$, and \mathbf{n}_ϵ the unit normal vector on ∂Y .

Remark 2.4. *The space $L^p_\#(Y)$ is the set of elements of $L^p(Y) \cap L^p(\mathbf{R}^n)$ such that they are invariant under $\mathbb{T}(\mathbf{g}_1, \dots, \mathbf{g}_n)$. This invariance is called Y -periodic.*

This informal definition can be made more precise with Fourier basis-functions in $L^p(\mathbf{R}^n)$. Although, for $H^1_\#(Y)$, one often uses Y -periodic functions in $C^\infty(\mathbf{R}^n)$, see Section 3.4 in [29]. A proper definition of several periodic function spaces on the microscale can be found in Section B.2 of [68] or in Section 1.1 of [72].

There are many homogenization methods for obtaining the macroscopic behaviour. One method is formal asymptotic expansions. This method takes a formal ansatz and decouples the microscale \mathbf{y} from the macroscale \mathbf{x} . The ansatz and the decoupling make it a non-rigorous method that is very effective in deriving the macroscopic behaviour. Four other methods are convergence methods: Γ -convergence, G -convergence, H -convergence, and two-scale convergence. These methods are rigorous, but also have significant complications

in their applicability. See Appendix A of [68] for an introduction to these convergence methods.

The formal asymptotic expansion method and the two-scale convergence method should yield the same macroscopic behaviour. However, the steps necessary to obtain this result are quite different.

The formal asymptotic expansion method yields a set of related systems, one for obtaining each term in the formal asymptotic expansion ansatz of u_ϵ . Solving these expansion systems can only occur when specific solvability conditions are met. The microscale solvability conditions yield the existence of so called cell functions as solutions of so called cell problems. The macroscopic solvability conditions yield a system describing the macroscopic behaviour, which is the desired upscaled behaviour.

The two-scale method first needs u_ϵ to be a weak solution of (\mathbf{P}) with ϵ -independent a-priori estimates such that u_ϵ has a weak limit u . Using the properties of two-scale convergence, the weak limit implies the existence of a two-scale limit \tilde{u} , such that u is the Y -average of \tilde{u} . Obtaining this two-scale limit is called a compactness step. With the existence of \tilde{u} , we are able to apply two-scale convergence to (\mathbf{P}) , which yields a two-scale limit system. In order to obtain a strong form of this system, one needs to remove the \mathbf{y} -dependence. This removal leads in a natural way to cell functions and cell problems and to a macroscopic system describing the macroscopic behaviour of u .

Both methods yield the same macroscopic system. However, their solutions might be different. Only when the macroscopic system admits only a single solution do they give the same solution.

Even though homogenization tries to obtain the macroscopic behaviour via a macroscopic system, the application of this result to the real world needs an error estimate for finite values of ϵ . Such an error estimate is called a corrector estimate/convergence rate.

Formal asymptotic expansion method

We start with the main ansatz of the formal asymptotic expansion method: it is assumed that there exist functions $u_i(\mathbf{x}, \mathbf{y})$ such that

$$u_\epsilon(\mathbf{x}) = \sum_{i=0}^N \epsilon^i u_i(\mathbf{x}, \mathbf{x}/\epsilon) + \mathcal{O}(\epsilon^N) \quad (2.47)$$

for some $N > 0$, usually $N = 2$. For smooth enough functions $v(\mathbf{x}, \mathbf{y})$ we have the chain rule

$$\nabla v(\mathbf{x}, \mathbf{x}/\epsilon) = \left[\nabla_{\mathbf{x}} v(\mathbf{x}, \mathbf{y}) + \frac{1}{\epsilon} \nabla_{\mathbf{y}} v(\mathbf{x}, \mathbf{y}) \right]_{\mathbf{y}=\mathbf{x}/\epsilon}. \quad (2.48)$$

Inserting Equation (2.47) and Equation (2.48) into (\mathbf{P}) and collecting terms of same ϵ power for $N = 2$, we obtain

$$(\mathbf{P})_0 : \begin{cases} -\operatorname{div}_{\mathbf{y}}(\mathbf{A} \cdot \nabla_{\mathbf{y}} u_0) = 0 & \text{in } \Omega, \\ u_0 = 0 & \text{on } \partial\Omega, \\ -(\mathbf{A} \cdot \nabla_{\mathbf{y}} u_0) \cdot \mathbf{n}_{\epsilon} = 0 & \text{on } \partial\Omega_{int}^{\epsilon}, \end{cases} \quad (2.49a)$$

$$(\mathbf{P})_1 : \begin{cases} -\operatorname{div}_{\mathbf{y}}(\mathbf{A} \cdot [\nabla_{\mathbf{x}} u_0 + \nabla_{\mathbf{y}} u_1]) \\ \quad -\operatorname{div}_{\mathbf{x}}(\mathbf{A} \cdot \nabla_{\mathbf{y}} u_0) = 0 & \text{in } \Omega, \\ u_1 = 0 & \text{on } \partial\Omega, \\ -(\mathbf{A} \cdot [\nabla_{\mathbf{x}} u_0 + \nabla_{\mathbf{y}} u_1]) \cdot \mathbf{n}_{\epsilon} = 0 & \text{on } \partial\Omega_{int}^{\epsilon}, \end{cases} \quad (2.49b)$$

$$(\mathbf{P})_2 : \begin{cases} -\operatorname{div}_{\mathbf{y}}(\mathbf{A} \cdot [\nabla_{\mathbf{x}} u_1 + \nabla_{\mathbf{y}} u_2]) \\ -\operatorname{div}_{\mathbf{x}}(\mathbf{A} \cdot [\nabla_{\mathbf{x}} u_0 + \nabla_{\mathbf{y}} u_1]) = f & \text{in } \Omega, \\ u_2 = 0 & \text{on } \partial\Omega, \\ -(\mathbf{A} \cdot [\nabla_{\mathbf{x}} u_1 + \nabla_{\mathbf{y}} u_2]) \cdot \mathbf{n}_{\epsilon} = g & \text{on } \partial\Omega_{int}^{\epsilon}, \end{cases} \quad (2.49c)$$

The existence of u_0 , u_1 and u_2 follows from the following lemma.

Lemma 2.19. *Let $f \in L^2(\Omega \times Y)$ and $g \in L^2(\Omega \times \partial Y)$ be Y -periodic. Let $\mathbf{A} \in L^{\infty}_{\#}(\Omega \times Y)^{n \times n}$ satisfy $\boldsymbol{\xi} \cdot (\mathbf{A} \cdot \boldsymbol{\xi}) \geq a|\boldsymbol{\xi}|^2$ for all $\boldsymbol{\xi} \in \mathbf{R}^n$ for some $a > 0$. Consider the following boundary value problem for $v(\mathbf{y})$:*

$$\begin{cases} -\nabla_{\mathbf{y}} \cdot (\mathbf{A} \cdot \nabla_{\mathbf{y}} v) = f & \text{in } Y, \\ -(\mathbf{A} \cdot \nabla_{\mathbf{y}} v) \cdot \mathbf{n} = g & \text{on } \partial Y, \\ v \text{ is } Y\text{-periodic.} \end{cases} \quad (2.50)$$

Then the following statements hold:

- (i) *There exists a weak Y -periodic solution $v \in H^1_{\#}(Y)/\mathbf{R}$ to Equation (2.50) if and only if $\int_Y f d\mathbf{y} = \int_{\partial Y} g d\sigma_{\mathbf{y}}$.*
- (ii) *If (i) holds, then the uniqueness of weak solutions is ensured up to an additive constant.*

where $\mathbf{A}^* = \frac{1}{|Y|} \int_Y \mathbf{A} \cdot [1 + \nabla_{\mathbf{y}} \mathbf{W}] d\mathbf{y}$ is the homogenized/averaged tensor \mathbf{A} , $\bar{f} = \frac{1}{|Y|} \int_Y f d\mathbf{y}$ is the homogenized/averaged driving term f , and $\bar{g} = \frac{1}{|\partial Y|} \int_{\partial Y} g d\sigma_{\mathbf{y}}$ is the homogenized/averaged boundary term g .

Two-scale convergence method

We start the two-scale convergence method by recalling that problem (\mathbf{P}) has a weak solution in $H_0^1(\Omega)$ due to the elliptic existence theory. Moreover, due to the regularity of \mathbf{A} , f and g , the elliptic existence theory yields that $\|u_\epsilon\|_{H_0^1(\Omega)}$ is bounded independent of ϵ . This has profound consequences.

Lemma 2.20 (Compactness step). *Let $u_\epsilon \in H_0^1(\Omega)$ be the weak solution of (\mathbf{P}) with $\|u_\epsilon\|_{H_0^1(\Omega)}$ bounded independent of ϵ , then there exists a $u_0 \in H_0^1(\Omega)$ and $u_1 \in L^2(\Omega; H_{\#}^1(Y)/\mathbf{R})$ such that*

$$\begin{cases} u_\epsilon \rightharpoonup u_0 & \text{in } H^1(\Omega), \\ u_\epsilon \xrightarrow{2} u_0 & \text{in } L^2(\Omega \times Y), \\ \nabla u_\epsilon \xrightarrow{2} \nabla_{\mathbf{x}} u_0 + \nabla_{\mathbf{y}} u_1 & \text{in } L^2(\Omega \times Y) \end{cases} \quad (2.56)$$

for a subsequence $(\epsilon') \subset (\epsilon)$.

Proof. Weak convergence follows directly from Eberlein-Šmuljan Theorem. Then the two-scale convergences follow from Proposition 2.15. \square

The compactness step allows one to directly obtain the macroscopic system $(\mathbf{P})_{\mathbf{m}}$, the cell function \mathbf{W} from decomposition (2.54) and the cell problem (2.55).

Theorem 2.21. *Let $u_\epsilon \in H_0^1(\Omega)$ be the weak solution of (\mathbf{P}) and satisfy the conditions of the Compactness step (Lemma 2.20), then there exists a subsequence $(\epsilon') \subset (\epsilon)$ such that $u_\epsilon \xrightarrow{2} u_0$ in $H_0^1(\Omega)$ and u_0 satisfies $(\mathbf{P})_{\mathbf{m}}$ with the homogenized tensor \mathbf{A}^* derived from the cell function $\mathbf{W} \in L^2(\Omega; H_{\#}^1(Y)/\mathbf{R})$ that satisfies the cell problem (2.55).*

Proof. Test (\mathbf{P}) with $\phi(\mathbf{x}, \mathbf{x}/\epsilon) \in H^1(\Omega)$ arbitrarily chosen, such that $\phi(\mathbf{x}, \mathbf{y}) \in L^2(\Omega; H_{\#}^1(Y))$ and $\nabla_{\mathbf{x}} \phi \in \mathcal{D}(\Omega; C_{\#}^\infty(Y))^n$, and integrate over $\Omega \times Y$. Note that ϕ satisfies the conditions of Proposition 2.15. Hence, there is a $\phi_0 \in H^1(\Omega)$ and $\Phi \in L^2(\Omega; H_{\#}^1(Y)/\mathbf{R})$ such that $\nabla \phi_{\epsilon'} \xrightarrow{2} \nabla \phi_0 + \nabla_{\mathbf{y}} \Phi$ for a subsequence $(\epsilon') \subset (\epsilon)$. By applying the divergence theorem, we obtain

$$\int_{\Omega} (\mathbf{A}_\epsilon \cdot \nabla u_\epsilon) \cdot \nabla \phi_\epsilon d\mathbf{x} = \int_{\Omega} f_\epsilon \phi_\epsilon d\mathbf{x} + \int_{\partial \Omega_{int}^\epsilon} g_\epsilon \phi_\epsilon d\sigma_x \quad (2.57)$$

where $\mathbf{A}_\epsilon = \mathbf{A}(\mathbf{x}, \mathbf{x}/\epsilon)$, $f_\epsilon = f(\mathbf{x}, \mathbf{x}/\epsilon)$, $g_\epsilon = g(\mathbf{x}, \mathbf{x}/\epsilon)$, and $\phi_\epsilon = \phi(\mathbf{x}, \mathbf{x}/\epsilon)$. Taking the limit $\epsilon \downarrow 0$ over a subsequence $(\epsilon'') \subset (\epsilon')$, we are allowed to apply Definition 2.13, Corollary 2.17 and Theorem 2.18, which leads to

$$\begin{aligned} & \int_{\Omega} \frac{1}{|Y|} \int_Y (\mathbf{A} \cdot [\nabla_{\mathbf{x}} u_0 + \nabla_{\mathbf{y}} u_1]) \, d\mathbf{y} \cdot \nabla_{\mathbf{x}} \phi_0 \, d\mathbf{x} \\ &= \int_{\Omega} \frac{1}{|Y|} \int_Y f \, d\mathbf{x} \phi_0 \, d\mathbf{y} + \int_{\Omega} \frac{1}{|\partial Y|} \int_{\partial Y} g \, d\sigma_{\mathbf{y}} \phi_0 \, d\mathbf{x}, \end{aligned} \quad (2.58a)$$

$$\int_{\Omega} \frac{1}{|Y|} \int_Y (\mathbf{A} \cdot [\nabla_{\mathbf{x}} u_0 + \nabla_{\mathbf{y}} u_1]) \cdot \nabla_{\mathbf{y}} \Phi \, d\mathbf{x} \, d\mathbf{y} = 0 \quad . \quad (2.58b)$$

Obviously, Equation (2.58a) is the weak version of Equation (2.53). Moreover, inserting decomposition (2.54) into Equation (2.58b) yields the weak version of cell problem (2.55). Hence, u_0 satisfies $(\mathbf{P})_{\mathbf{m}}$. \square

Even though both the two-scale convergence method and the formal asymptotic expansion method yield the same system to which their macroscopic variable u_0 must adhere, there is no guarantee that these solutions are identical. Even more reason for this is the use of a subsequence of (ϵ) in the two-scale convergence method to obtain better properties. This is for two-scale convergence similar to the Eberlein-Šmuljan theorem of weak convergence. It turns out that $(\mathbf{P})_{\mathbf{m}}$ is linear in u_0 . Moreover, it can be shown that \mathbf{A}^* is elliptic, because \mathbf{A} is elliptic. Hence, elliptic existence theory states that $(\mathbf{P})_{\mathbf{m}}$ has a unique weak solution. Thus both methods give the same weak solution.

A natural follow-up to obtaining the macroscopic solution u_0 tries to determine whether $u_\epsilon \rightarrow u_0(\mathbf{x})$ in some space \mathbb{X} . A positive answer would lead to the pursuit of finding a qualitative estimate of this convergence. Thus whether one can find a function $h : \mathbf{R}_+ \rightarrow \mathbf{R}_+$ such that $\|u_\epsilon - u_0(\mathbf{x})\|_{\mathbb{X}} \leq h(\epsilon) \downarrow 0$ as $\epsilon \downarrow 0$. This type of results are called *corrector estimates* and even for our toy problem (\mathbf{P}) it is too complicated to give a quick introduction to corrector estimates. In Chapter 5 actual corrector estimates are derived for pseudo-parabolic systems.

Modeling and Simulation of Concrete Corrosion – a Mixture Theory Perspective

Based on:

A.J. Vromans, A. Muntean, and A.A.F. van de Ven, “A mixture theory-based concrete corrosion model coupling chemical reactions, diffusion and mechanics,” 2018, *Pacific Journal of Mathematics for Industry* **10** 5, online print only.

In this chapter a 3-D continuum mixture model describing the corrosion of concrete with sulfuric acid is built. Essentially, the chemical reaction transforms slaked lime (calcium hydroxide) and sulfuric acid into gypsum releasing water. The model incorporates the evolution of chemical reaction, diffusion of species within the porous material and mechanical deformations. This model is applied to a 1-D problem of a plate-layer between concrete and sewer air. The influx of slaked lime from the concrete and sulfuric acid from the sewer air sustains a gypsum creating chemical reaction (*sulfatation or sulfate attack*). The combination of the influx of matter and the chemical reaction causes a net growth in the thickness of the gypsum layer on top of the concrete base. The model allows for the determination of the plate layer thickness $h = h(t)$ as function of time, which indicates both the amount of gypsum being created due to concrete corrosion and the amount of slaked lime and sulfuric acid in the material. The existence of a parameter regime for which the model yields a non-decreasing plate layer thickness $h(t)$ is identified numerically. The robustness of the model with respect to changes in the model parameters is also investigated.

3.1 Introduction

Forecasting concrete corrosion is a major issue in civil engineering due to its potential of drastically decreasing the lifespan of constructions such as sewers, bridges and dams, see e.g. [42, 118, 123]. As an example, the differences in mechanical properties between gypsum and concrete result in volume expansion, cracking, and decrease in load-bearing capacity of the concrete resulting in compromised structural integrity followed by expensive repairs, construction replacements or even accidents due to (partial) collapse [69, 132] resulting in major costs for society [45, 134].

We focus on three related topics: First, we construct a 3-D continuum mixture model describing concrete corrosion capable of exhibiting realistic behaviour of the growth of a concrete layer due to the formation of gypsum inside the concrete layer. Secondly, we apply the new model to a specific 1-D situation of the concrete layer and investigate the validity of the behavior of this 1-D model with respect to physical constraints and expected physical behavior. Finally, we investigate the parameter dependence of both the time span of realistic behavior and growth of the concrete layer for the 1-D model.

Even though concrete is a heterogeneous material, a lot of research has been

done relying on continuum models, where the heterogeneity details are averaged out. In [94] the reader can find a short historical overview of the use of continuum models in concrete research. Similar to the continuum models from [94], the authors of ref. [104] proposed a composite material model of concrete with an explicit volume division into mortar and aggregate. These models were mostly created to better describe the behavior of concrete under high stresses, and, hence, to predict the cracking behavior observed in the experiments reported in [94, 104]. The mathematical community has addressed this corrosion issue mainly from a single-scale or multiple-scale reaction-diffusion perspective. Usually, the single-scale approach involves one or two moving sharp reaction interfaces [3, 32, 56, 57, 102, 103], while the multiple scale setting prefers exploiting a better understanding of the porosity and tortuosity of the material without involving free boundaries [6, 26, 53]. There are still a number of open issues concerning how poro-mechanics of the material couples with chemical reactions, flow, diffusion and heat transfer hindering a successful forecast of the durability of the concrete exposed to sulfate attack. In this chapter, we are interested in understanding and then predicting eventual critical situations occurring before cracking. Particularly, we want to describe the corrosion of concrete by acid attack [131], which usually leads at a later stage to cracking followed by erosion. The main inspiration source for our problem setting is the basic scenario described in [14] which considers a simple reaction mechanism producing gypsum, without involving the ettringite formation.

In [14] an isothermal acid attack continuum model for sulfuric acid corrosion was proposed with a similar sewer pipe geometry as in our model, but including also the porosity of the gypsum. This model focussed solely on the creation of hydrogen sulfide and sulfuric acid, which reacts at the boundary to create gypsum. The model assumed that almost all the gypsum was created at the boundary separating the uncorroded concrete causing a moving sharp corrosion front penetrating irreversibly the material. We deviate from this model by assuming that the gypsum reaction gradually takes place in the full domain, and that the corrosion front is caused by the penetration of sulfuric acid. In some sense our model can be seen as a description of the moving corrosion front in [14] as a fixed bulk reaction domain, and can, therefore, be idealized into a plate-layer model. To avoid describing the exact growth of the involved phases of the material, we take a modeling route in the spirit of the classical mixture theory.

Figure 3.1 shows the concrete geometry we have in mind. A concrete sewer pipe contains in the air phase acid droplets wanting to react with the concrete to form gypsum. When zooming in on the pipe wall, the curvature vanishes,

which allows for the formulation of a plate layer model of the concrete pipe. We neglect, therefore, the tangential directions and only focus on the normal (z) direction. Hence, a 1-D model can be posed to approximate the concrete corrosion in a simplistic 3-D sewer pipe.

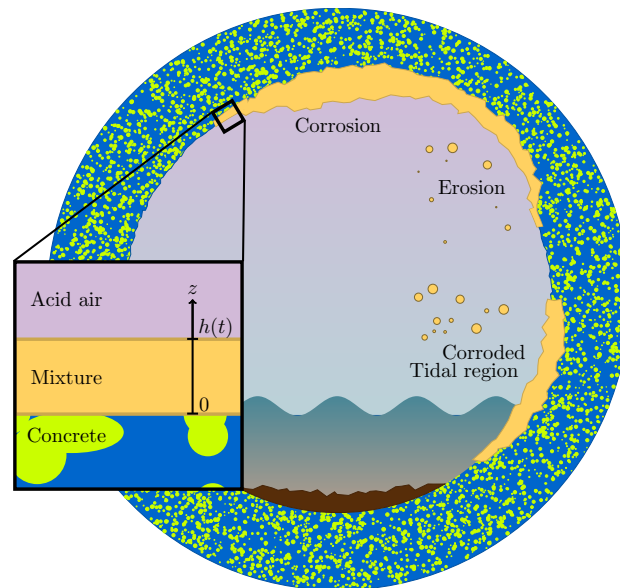


Figure 3.1: A concrete sewer pipe is corroded by sulfuric acid containing air at the top and by the acidic sewage at the tidal region of the sewage-air interface. The sulfuric acid is created by biodegradation of bio-matter in sewage. Extended corrosion leads to erosion of the concrete and potentially to sewer pipe collapse. Our model is meant to describe the beginning of corrosion, as shown in the small square, allowing the simplifications from a pipe to a plate layer, as shown in the large square. This simplification reduces a 3-D concrete corrosion model into a 1-D model only dependent on the spatial variable z . The thickness, $h(t)$, of the mixture layer changes over time due to both influx of material and the chemical reaction in the mixture.

It is worth noting that most of the assumptions mentioned in [14] are taken over here as well. Our model is supposed to reflect the entire corrosion process with no other contributing chemical reactions and species than those explicitly mentioned. Also, the external concentration and influx rates of sulfuric acid and hydrogen sulfide are constant. Both these assumptions are restrictive. For example, competing corrosion reactions and other reacting chemicals, such as nitrates, are present in an actual concrete corrosion process according to [14]. Moreover, in [22] it is explained that experiments show that external concentrations and influx rates are not even approximately constant because flow changes (changing Reynolds number) have enormous influences, which according to [14] could change rates and concentrations with many orders of magnitude. Therefore, the assumptions of ref. [14] are necessary to reduce the complexity of our model. Moreover, we have the additional assumption

that external forces such as gravity are negligible. Further, we assume that the absolute internal pressure of the concrete is only locally deviating in our small scale layer, which allows us to use relative pressure in the concrete.

This chapter is organized as follows. In Section 3.2, we construct several 3-D continuum mixture models of chemical corrosion of concrete. We take into account effective balance laws, diffusion processes, chemical reaction effects, mechanical effects due to elastic and/or viscoelastic stresses, local interactions due to for instance the Stokes drag, and influx from external reservoirs and from domain growth due to a moving corrosion layer. In Section 3.3, we focus on the normal (z) direction to obtain an effective 1-D model of the corroding concrete for one of the constructed models. In Section 3.4, we briefly describe both the code used to simulate the model of Section 3.3 and the validation of this code with respect to the asymptotic expansion solution obtained in Section 3.7. In Section 3.5, we investigate the validity of the numerical behavior of the model of Section 3.3. First, we illustrate the typical behavior of the model and relate it to the expected realistic behavior. Second, we investigate the dependence of the realistic behavior on specific tuples of model parameters. Finally, in the conclusion we summarize our results and discuss the relation of these results with known literature.

3.2 Derivation of a mixture-theory-based concrete corrosion model

The presentation of a continuous 3-component mixture model in this section is based on the theory of mixtures of Bowen in [18].

Preliminaries

Let the index α denote the different constituents of our mixture, $\alpha = 1$ the gypsum (solid), $\alpha = 2$ the lime (solid) and $\alpha = 3$ the acid (fluid). The configuration $\mathbb{G}(t)$ indicates the domain occupied by the mixture body at time $t > 0$ in \mathbf{R}_3 , and $\mathbf{x} = \mathbf{x}(t) \in \mathbb{G}(t)$ is the momentary position of a material point of the mixture body. Let $g(t) \subset \mathbb{G}(t)$ be a generic *element of material volume*, which by definition has no fixed volume. This partial material volume $g(t)$ contains $n_\alpha(g(t))$ molecules of the constituent α with molecular mass M_α . The mass $m_\alpha(g(t))$ of constituent α in $g(t)$ is given by

$$m_\alpha(g(t)) = M_\alpha n_\alpha(g(t)) = \mathcal{M}_\alpha n_\alpha(g(t))/N_A, \quad (3.1)$$

where N_A denotes the Avogadro constant (i.e. 6.022×10^{23} molecules per mole) and \mathcal{M}_α the molar mass of constituent α . The total mass $m(g(t))$ of the mixture in $g(t)$ is given by

$$m(g(t)) = \sum_{\alpha} m_{\alpha}(g(t)). \quad (3.2)$$

A strictly positive integrable function $\rho_{\alpha}(\mathbf{x}, t)$, called the *partial density of component α* , is defined by

$$m_{\alpha}(g(t)) = \int_{g(t)} \rho_{\alpha}(\mathbf{x}, t) \, d\mathbf{x}. \quad (3.3)$$

The density of the mixture in the point (\mathbf{x}, t) is

$$\rho(\mathbf{x}, t) = \sum_{\alpha} \rho_{\alpha}(\mathbf{x}, t). \quad (3.4)$$

Let $\tilde{\rho}_{\alpha}$ be the intrinsic density of component α (i.e. the density of the isolated pure component) and let $\phi_{\alpha}(\mathbf{x}, t)$ be its volume fraction, then

$$\rho_{\alpha}(\mathbf{x}, t) = \tilde{\rho}_{\alpha} \phi_{\alpha}(\mathbf{x}, t), \quad \sum_{\alpha} \phi_{\alpha}(\mathbf{x}, t) = 1 \text{ for all } (\mathbf{x}, t) \in g(t). \quad (3.5)$$

We assume that the constituents of the mixture are incompressible. Hence, the intrinsic densities $\tilde{\rho}_{\alpha}$ are uniform constants.

Balance laws

Following [18] and in analogy with [19] and [95], we describe the time evolution of our 3-component mixture by means of two sets of global balance laws for each component of the mixture: one for mass and one for momentum conservation. We assume that the chemical reaction is an isothermal process; the conservation of energy is then automatically satisfied.

The conservation of the partial mass for component α is formulated as the balance law for the partial density $\rho_{\alpha} = \rho_{\alpha}(\mathbf{x}, t)$ in the form:

$$\frac{d}{dt} m_{\alpha}(g(t)) = \frac{d}{dt} \int_{g(t)} \rho_{\alpha}(\mathbf{x}, t) \, dV = \int_{\partial g(t)} \delta_{\alpha} \nabla \rho_{\alpha}(\mathbf{x}, t) \cdot d\mathbf{S} + \int_{g(t)} R_{\alpha}(\mathbf{x}, t) \, dV. \quad (3.6)$$

In this balance law, the outward flux is given by Fick's law of diffusion, and equals $-\delta_{\alpha} \nabla \rho_{\alpha}$, where δ_{α} is the diffusion coefficient of the α -th component. The production term by chemical reaction R_{α} acts as a source or as a

sink when the constituent is being produced or consumed, respectively, in the chemical reaction. Equation (3.6) indicates that $g(t)$ is not an element of material volume for a single constituent, but it is an element of material volume for the mixture, i.e. for all constituents together. Hence, in Equation (3.6), summing up over α and using that $g(t)$ is an element of material volume for which $m(g(t))$ is constant, we obtain

$$0 = \frac{d}{dt} \int_{g(t)} \rho(\mathbf{x}, t) d\mathbf{x} = \int_{\partial g(t)} \sum_{\alpha} (\delta_{\alpha} \nabla \rho_{\alpha})(\mathbf{x}, t) \cdot d\mathbf{s} + \int_{g(t)} \sum_{\alpha} R_{\alpha}(\mathbf{x}, t) d\mathbf{x}. \quad (3.7)$$

Since a chemical reaction is inherently a mass-conserving process, we obtain $\sum_{\alpha} R_{\alpha} = 0$. Thus this global mass conservation is satisfied if $\sum_{\alpha} \delta_{\alpha} \nabla \rho_{\alpha} = \sum_{\alpha} \delta_{\alpha} \tilde{\rho}_{\alpha} \nabla \phi_{\alpha} = 0$, a compatibility condition for the allowed types of internal diffusion processes. This is satisfied if, for instance, $\delta_{\alpha} = \delta / \tilde{\rho}_{\alpha}$. Hence, $\delta = 0$ (no internal diffusion) would suffice.

Conservation of linear momentum for the component α is formulated as

$$\frac{d}{dt} \int_{g(t)} (\rho_{\alpha} \mathbf{v}_{\alpha})(\mathbf{x}, t) dV = \int_{\partial g(t)} \mathbf{T}_{\alpha}(\mathbf{x}, t) \cdot d\mathbf{S} + \int_{g(t)} \mathbf{B}_{\alpha}(\mathbf{x}, t) dV, \quad (3.8)$$

where $\rho_{\alpha} \mathbf{v}_{\alpha}$ is the linear momentum density of the component α , while the outward flux is given by the partial stress tensor \mathbf{T}_{α} and the production term by the internal linear momentum production \mathbf{B}_{α} . The latter two terms will be specified in the next section. Since in our setting the mechanical processes and flow dynamics are slow, we assume a quasi-static regime. This implies that the inertia term on the left-hand side in Equation (3.8) may be neglected. Moreover, the sum of the internal momentum-production terms \mathbf{B}_{α} must be zero, i.e. $\sum_{\alpha} \mathbf{B}_{\alpha} = 0$, by Newton's third law.

Local equations and jump conditions

The global balance equations can in the usual way, see e.g. [18], be converted into local balance equations and jump conditions across a singular surface $\Sigma(t)$, a surface defined by the location of a discontinuity in a quantity. Thus, we obtain from Equation (3.6) the local partial mass balance equations (or continuity equations):

$$\frac{\partial \rho_{\alpha}}{\partial t} + \operatorname{div}(\rho_{\alpha} \mathbf{v}_{\alpha}) - \delta_{\alpha} \Delta \rho_{\alpha} = R_{\alpha}, \quad (3.9)$$

together with the jump condition at $\Sigma(t)$

$$\llbracket \rho_{\alpha} (\mathbf{V} \cdot \mathbf{n} - \mathbf{v}_{\alpha} \cdot \mathbf{n}) + \delta_{\alpha} \nabla \rho_{\alpha} \cdot \mathbf{n} \rrbracket = 0 \quad (3.10)$$

where $[[\cdot]]$ denotes the outward jump across the surface $\Sigma(t)$, \mathbf{V} the velocity of $\Sigma(t)$, and \mathbf{n} the outward unit normal on $\Sigma(t)$. We rewrite the mass equations by elimination of ρ_α in favour of ϕ_α yielding

$$\frac{\partial \phi_\alpha}{\partial t} + \operatorname{div}(\phi_\alpha \mathbf{v}_\alpha) - \delta_\alpha \Delta \phi_\alpha = \frac{R_\alpha}{\tilde{\rho}_\alpha}. \quad (3.11)$$

Summing Equation (3.11) over all α , we obtain

$$\sum_\alpha \operatorname{div}(\phi_\alpha \mathbf{v}_\alpha) = \sum_\alpha \left(\delta_\alpha \Delta \phi_\alpha + \frac{R_\alpha}{\tilde{\rho}_\alpha} \right) = \sum_\alpha \frac{1}{\tilde{\rho}_\alpha} (\delta \Delta \phi_\alpha + R_\alpha), \quad (3.12)$$

with use of $\delta_\alpha = \delta / \tilde{\rho}_\alpha$. We refer to Equation (3.12) as the *incompressibility condition*. Later we shall use Equation (3.12) to replace one of the three mass equations (e.g. for $\alpha = 2$, and then use $\phi_2 = 1 - \phi_1 - \phi_3$).

Analogously, the quasi-static momentum balance yields

$$\operatorname{div} \mathbf{T}_\alpha + \mathbf{B}_\alpha = 0 \quad (3.13)$$

with the jump condition

$$[[\mathbf{T}_\alpha \cdot \mathbf{n}]] = 0. \quad (3.14)$$

Summing Equation (3.13) over all α and using $\mathbf{T} = \sum_\alpha \mathbf{T}_\alpha$, the total stress tensor, and $\sum_\alpha \mathbf{B}_\alpha = 0$, we find

$$\operatorname{div} \mathbf{T} = 0. \quad (3.15)$$

Before we can evaluate the local momentum equations any further we have to make constitutive assumptions concerning the structure of \mathbf{T}_α and \mathbf{B}_α .

The two solid components, $\alpha = (1, 2)$ are modeled as linearly (visco)elastic media, the stress tensor \mathbf{T}_α of which is given by

$$\mathbf{T}_\alpha = -\phi_\alpha p \mathbf{l} + \mathbf{T}_\alpha^{\text{el}} + \mathbf{T}_\alpha^{\text{vi}}, \quad (3.16)$$

where p is the relative pressure with respect to the inner tube pressure (this pressure term is needed to compensate for the incompressibility assumption), \mathbf{l} the unit tensor, $\mathbf{T}_\alpha^{\text{el}}$ is the linear elastic part and $\mathbf{T}_\alpha^{\text{vi}}$ the linear viscous part. The first one is given by Hooke's law as

$$\mathbf{T}_\alpha^{\text{el}} = \lambda_\alpha \operatorname{Tr}(\mathbf{E}_\alpha) \mathbf{l} + 2\mu_\alpha \mathbf{E}_\alpha \quad \text{for } \alpha \in \{1, 2\}, \quad (3.17)$$

where $\mathbf{E}_\alpha = (\nabla \mathbf{u}_\alpha + (\nabla \mathbf{u}_\alpha)^\top) / 2$ is the linear deformation tensor written in terms of the displacement \mathbf{u}_α , $\operatorname{Tr}(\mathbf{A})$ means the trace of the matrix \mathbf{A} , and λ_α and μ_α are the corresponding Lamé parameters. The viscous part is modeled

such that Equation (3.16) follows the Kelvin-Voigt model, see [21, 91], and has the general structure

$$\mathbb{T}_\alpha^{\text{vi}} = \sum_{\beta=1}^2 \gamma_{\alpha\beta} \mathbb{D}_\beta \quad \text{for } \alpha \in \{1, 2\}, \quad (3.18)$$

where $\mathbb{D}_\alpha = (\nabla \mathbf{v}_\alpha + (\nabla \mathbf{v}_\alpha)^\top)/2$ is the rate of deformation tensor based on the velocity $\mathbf{v}_\alpha = \partial \mathbf{u}_\alpha / \partial t$, while the coefficients $\gamma_{\alpha\beta}$ are material constants that will be further specified below.

The internal linear momentum production represents the *Stokes Drag* [95, eq. (92)], i.e.

$$\mathbf{B}_\alpha^{(SD)} = -\chi_\alpha (\mathbf{v}_\alpha - \mathbf{v}_3) \quad \text{for } \alpha \in \{1, 2\}, \quad (3.19)$$

and

$$\mathbf{B}_3^{(SD)} = \sum_{\beta=1}^2 \chi_\beta (\mathbf{v}_\beta - \mathbf{v}_3), \quad (3.20)$$

such that $\sum_\alpha \mathbf{B}_\alpha^{(SD)} = 0$. For an explicit definition of the material parameter χ_α , we refer to the note [†] in Table 3.1.

The fluid is modeled as an inviscid fluid, possibly modified by an extra linear viscoelastic term, which in general is zero, except for the first of the four systems to be introduced next, i.e.

$$\mathbb{T}_3 = -\phi_3 p \mathbf{I} + \mathbb{T}_3^{\text{vi}}. \quad (3.21)$$

The specification of $\gamma_{\alpha\beta}$ entering the structure of $\mathbb{T}_\alpha^{\text{vi}}$ (cf. Equation (3.18)) differs for the four systems we introduce now:

1. **System A:** This system corresponds best to the evolution systems studied in [136], where conditions for the existence of weak solutions were obtained. Here, the individual constituents are assumed to be viscoelastic, such that the mixture as a whole remains purely elastic. For this, we choose $\gamma_{\alpha\beta} = \gamma_\alpha$ if $\beta = \alpha \in \{1, 2\}$, and $\gamma_{\alpha\beta} = 0$ if $\beta \neq \alpha$, resulting in

$$\mathbb{T}_\alpha^{\text{vi}} = \gamma_\alpha \mathbb{D}_\alpha \quad \text{for } \alpha \in \{1, 2\}. \quad (3.22)$$

Moreover, we take \mathbb{T}_3^{vi} such that

$$\mathbb{T}_3^{\text{vi}} = -\sum_{\alpha=1}^2 \gamma_\alpha \mathbb{D}_\alpha = -\sum_{\alpha=1}^2 \mathbb{T}_\alpha^{\text{vi}}, \quad (3.23)$$

providing that $\mathbb{T}^{\text{vi}} = \sum_{\alpha=1}^3 \mathbb{T}_\alpha^{\text{vi}} = 0$.

2. **System B:** Here, $\gamma_{\alpha\beta} = 0$: the solid components are thus purely elastic and the fluid inviscid.
3. **System C:** As in System A, the solid components are intrinsically viscoelastic, but the fluid is inviscid, so $\mathbf{T}_3 = -\phi_3 p \mathbf{l}$, implying that the mixture as a whole is also viscoelastic. This has consequences for the pressure term p , as can be seen in the 1-D problem described in Section 3.3; see Equation (3.41).
4. **System D:** In this case, we assume that the viscoelastic terms in the stresses are proportional to the differences in shear rates of the two solids so that these stresses are zero if the velocities, or displacements, of the solids are equal. Moreover, we let the sum of the two stresses equal zero and keep the fluid inviscid. Thus, the total stress is purely elastic. This results in the following choice for $\gamma_{\alpha\beta}$

$$\gamma_{11} = \gamma_{22} = \gamma, \quad \text{and} \quad \gamma_{12} = \gamma_{21} = -\gamma. \quad (3.24)$$

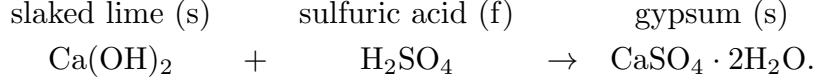
System A is well-posed mathematically (cf. [136]), but is possibly physically incorrect as we are not aware of any physical system with a physically purely elastic mixture, but with viscoelastic constituents. To be precise, the sulfuric acid viscoelastic stress for this models must be defined by the viscoelastic stress of the other components, see (3.23), which seems physically impossible. This was one of the reasons why we abandoned System A, even though it has nice mathematical properties. System B is physically nice, but mathematically it needs an additional viscoelastic term to ensure the existence of weak solutions and FEM approximations. System C combines the strong points of systems A and B. It is physically justified and mathematically sound. However, the mixture is viscoelastic, which is a behavior one would expect on unnaturally large timescales. System D is both mathematically and physically sound, supporting an elastic mixture, which favors timescales compatible with measurements.

The physical derivation of systems A, B, C and D indicate that only system D has the right physical properties at the desired timescales. Hence, from here on we will focus on system D from both analytical and numerical perspectives, for example when we judge solutions to exhibit realistic behaviors. To reduce complexity, we investigate a special situation leading effectively to a 1-D version of system D.

Chemical corrosion of concrete with sulphates

The concrete corrosion we discuss here refers to sulfuric acid reacting with

slaked lime to create gypsum. The reaction mechanism is very complex, leading to ettringite growth, e.g. see [131]. In this chapter, the chemical reaction mechanism takes the simplified form (s: solid, f: fluid)



Hence, the stoichiometric coefficients N_α are $N_1 = 1$ and $N_2 = N_3 = -1$. The chemical reaction, as shown above, is the net reaction and does not reflect the full complexity of all the intermediate steps necessary for this reaction. The complexity is encompassed in a single rate equation. A similar reaction as above but with calcite, CaCO_3 , instead of slaked lime has been treated in [17]. Therefore, we assume a rate equation similar to the one in [17], i.e.

$$r = kF = k\mathcal{L}([\text{H}_2\text{SO}_4] - C_{eq})\mathcal{L}(C_{\max} - [\text{gypsum}]), \quad (3.25)$$

where we denote $\mathcal{L}(u) = u\mathcal{H}(u)$ with \mathcal{H} the Heaviside function, k is the volumetric reaction rate (in $[\text{m}^3/\text{mol}\cdot\text{s}]$), $[f]$ the molar concentration of f , C_{eq} the dissolution equilibrium molar concentration of the sulfuric acid, and C_{\max} the maximum precipitation molar concentration of gypsum.

The mass production term $R_\alpha = R_\alpha(\mathbf{x}, t)$ is given by

$$R_\alpha(\mathbf{x}, t) = N_\alpha \mathcal{M}_\alpha r(\mathbf{x}, t) \quad \text{for } (\mathbf{x}, t) \in g(t), \quad (3.26)$$

which satisfies $\sum_\alpha R_\alpha = 0$. Moreover, Equation (3.26) implies that the volume fraction production can be written as

$$\frac{R_\alpha(\mathbf{x}, t)}{\tilde{\rho}_\alpha} = \frac{\mathcal{M}_\alpha N_\alpha \tilde{k}}{\tilde{\rho}_\alpha} \frac{\tilde{\rho}_1 \tilde{\rho}_3}{\mathcal{M}_1 \mathcal{M}_3} F(\mathbf{x}, t) \quad \text{for } (\mathbf{x}, t) \in g(t), \quad (3.27)$$

with

$$F = \mathcal{L}(\phi_3 - \phi_{3,thr})\mathcal{L}(\phi_{1,sat} - \phi_1), \quad (3.28)$$

where $\phi_{1,sat}$ is the gypsum saturation level, while $\phi_{3,thr}$ represents the sulfuric acid dissolution threshold.

Initial and boundary conditions

We consider a mixture body, placed freely in space, and initially in a homogeneous, undeformed state, free of stress and movement. This yields the initial conditions:

$$\phi_\alpha(\mathbf{x}, 0) = \phi_{\alpha 0}(\mathbf{x}) \quad \text{and} \quad \mathbf{u}_\alpha(\mathbf{x}, 0) = 0 \quad \text{for } (\mathbf{x}, 0) \in g(0), \quad (3.29)$$

where $\phi_{\alpha 0} = \rho_{\alpha 0} / \tilde{\rho}_\alpha$ are prescribed initial concentration values. We wish to point out here that, although $\mathbf{u}_3(\mathbf{x}, 0^+) = 0$, there is a jump in the velocity \mathbf{v}_3 , which is inherent to the quasi-static approximation we used. Due to the influx of material (acid and/or gypsum) across the boundary and the chemical reactions, the domain \mathbb{G} will change as time elapses, i.e. $\mathbb{G} = \mathbb{G}(t)$ as does its boundary $\partial\mathbb{G} = \partial\mathbb{G}(t)$. However, consistent with the small-deformation assumption, the boundary condition may be considered to hold on the undeformed (reference) boundary. The space outside the domain can contain any of the constituents with a concentration ϕ_α^+ . The influx is assumed to be proportional to the concentration difference $[[\phi_\alpha]]$ across $\partial\mathbb{G}$, provided this difference is positive. The boundary is semi-permeable for all constituents α , allowing only one-sided transfer from outside the domain into the domain if $\phi_\alpha^+ > \phi_\alpha|_{\partial\mathbb{G}}$. This leads to the boundary condition (compare with Equation (3.10)), holding for $t > 0$

$$\phi_\alpha(\mathbf{v}_\alpha - \mathbf{V}) \cdot \mathbf{n} + \delta_\alpha \nabla \phi_\alpha \cdot \mathbf{n} = J_\alpha (\mathcal{L}([[\phi_\alpha]])) \quad \text{at } \partial\mathbb{G}, \quad (3.30)$$

where \mathbf{n} denotes the outward normal on $\partial\mathbb{G}$, \mathbf{V} the velocity of the boundary, $[[\phi_\alpha]] = \phi_\alpha^+ - \phi_\alpha$ with ϕ_α^+ the volume fraction of α outside $\partial\mathbb{G}$ and ϕ_α just inside it, while J_α is a material constant. If, on the other hand, for certain α , we have $\phi_\alpha^+ < \phi_\alpha|_{\partial\mathbb{G}}$, then the influx is zero (due to the semi-permeability), leading to the boundary condition¹

$$\nabla \phi_\alpha \cdot \mathbf{n} = 0 \quad \text{at } \partial\mathbb{G}. \quad (3.31)$$

If the outer space contains only one constituent, say β , then Equation (3.31) holds for the two values $\alpha \neq \beta$, but then $\sum_\gamma \phi_\gamma = 1$ yields directly that also $\nabla \phi_\beta \cdot \mathbf{n} = 0$, and thus the second term on the left-hand side of Equation (3.30) vanishes, so that this boundary condition for β becomes

$$\phi_\beta(\mathbf{v}_\beta - \mathbf{V}) \cdot \mathbf{n} = J_\beta \mathcal{L}([[\phi_\beta]]) \quad \text{at } \partial\mathbb{G}, \quad (3.32)$$

the right-hand side of which is greater than zero if $\phi_\beta^+ > \phi_\beta$.

The small piece of sewer pipe can be modeled as a free unloaded body due to the use of the relative pressure term since we assumed the inner pipe pressure to be practically constant over this small piece of sewer pipe. For the free unloaded body that we will consider in this chapter, the boundary is free of stress, which implies

$$\mathbb{T} \cdot \mathbf{n} = \sum_\alpha \mathbb{T}_\alpha \cdot \mathbf{n} = 0 \quad \text{at } \partial\mathbb{G}. \quad (3.33)$$

¹In principle the right-hand side of Equation (3.31) should be $-\phi_\alpha(\mathbf{v}_\alpha - \mathbf{V})/\delta_\alpha$ instead of 0. However, in our linear theory the value 0 is justified due to the scale separation between displacement and the actual size of the domain. See Section 3.3 for the effect of scale separation on the system in the dimension reduction process.

If, for some α , we have $\phi_\alpha^+ < \phi_\alpha$, then the flux is zero and hence, the boundary condition (3.6) reduces to

$$\mathbf{v}_\alpha \cdot \mathbf{n} = \mathbf{V} \cdot \mathbf{n} \quad \text{at } \partial\mathbb{G}. \quad (3.34)$$

However, instead of (3.30) a different boundary condition, particular for the solid constituents ($\alpha = 1, 2$) is used, namely

$$(\nabla_{\mathbf{x}} \mathbf{u}_\alpha \cdot \mathbf{n})^\top \cdot \mathbf{n} = A_\alpha (\mathbf{u}_\alpha - \mathbf{W}) \cdot \mathbf{n} \quad \text{at } \partial\mathbb{G}. \quad (3.35)$$

In Equation (3.35), \mathbf{W} denotes the displacement vector of the boundary such that $\mathbf{V}(t) = d\mathbf{W}/dt$. In [136] it was shown that a finite positive value of A_α is useful to prove existence of a realistic numerical approximation of weak solutions. Note that in the limit $A_\alpha \rightarrow \infty$ the boundary condition $\mathbf{u}_\alpha = \mathbf{W}$ is retrieved. On the other hand, in the opposite limit $A_\alpha \rightarrow 0$ the boundary condition becomes the homogeneous Neumann boundary condition

$$(\nabla_{\mathbf{x}} \mathbf{u}_\alpha \cdot \mathbf{n})^\top \cdot \mathbf{n} = 0, \quad (3.36)$$

which is equivalent to requiring that the partial normal stress of constituent α is zero.

Summary of the model equations

Based on the discussion from the preceding sections, we are now able to formulate complete 3-D systems of equations and boundary conditions for the reacting, diffusing and deforming 3-component continuum mixture. From the four systems presented before, we opt for System D. The internal unknowns (6 in number, of which 3 scalar and 3 vectorial) are $\{\phi_1, \phi_3, \mathbf{u}_1, \mathbf{u}_2, \mathbf{v}_3, p\}$, with $\phi_2 = 1 - \phi_1 - \phi_3$, for which we have a set of balance equations, following from successively the local mass balances, the incompressibility condition and the 3 local momentum balances. Together with the constitutive equations for \mathbf{T}_α and \mathbf{B}_α , given by Equations (3.16) to (3.21) and (3.24), we obtain for $t > 0$

and $\mathbf{x} \in \mathbb{G}$:

$$\frac{\partial \phi_\alpha}{\partial t} + \operatorname{div}(\phi_\alpha \mathbf{v}_\alpha) - \delta_\alpha \Delta \phi_\alpha = \frac{R_\alpha}{\tilde{\rho}_\alpha} \quad \text{for } \alpha \in \{1, 2, 3\}, \quad (3.37a)$$

$$\operatorname{div} \left(\sum_{\alpha=1}^3 \phi_\alpha \mathbf{v}_\alpha \right) - \sum_{\alpha=1}^3 \delta_\alpha \Delta \phi_\alpha = \sum_{\alpha=1}^3 \frac{R_\alpha}{\tilde{\rho}_\alpha}, \quad (3.37b)$$

$$\nabla(-\phi_\alpha p + [\lambda_\alpha + \mu_\alpha] \operatorname{div}(\mathbf{u}_\alpha)) + \mu_\alpha \Delta \mathbf{u}_\alpha = \chi_\alpha (\mathbf{v}_\alpha - \mathbf{v}_3) - \sum_{\beta=1}^3 \gamma_{\alpha\beta} \Delta \mathbf{v}_\beta, \quad \alpha \neq 3, \quad (3.37c)$$

$$\nabla(-\phi_3 p) = - \sum_{\beta=1}^2 [\chi_\beta (\mathbf{v}_\beta - \mathbf{v}_3) + \gamma_{3\beta} \Delta \mathbf{v}_\beta], \quad (3.37d)$$

where $\mathbf{v}_\beta = \partial_t \mathbf{u}_\beta = \partial \mathbf{u}_\beta / \partial t$ for $\beta \in 1, 2$. Combining the three momentum equations, and using that $\sum_{\alpha=1}^3 \phi_\alpha = 1$, we obtain the global momentum equation:

$$\nabla \left(-p + \sum_{\alpha=1}^2 (\lambda_\alpha + \mu_\alpha) \operatorname{div}(\mathbf{u}_\alpha) \right) + \sum_{\alpha=1}^2 \mu_\alpha \Delta \mathbf{u}_\alpha + \sum_{\alpha=1}^3 \sum_{\beta=1}^3 \gamma_{\alpha\beta} \Delta \mathbf{v}_\beta = 0, \quad (3.38)$$

in which the γ -term is zero due to (3.24). Note, the γ -term would only be non-zero for System C as the mixture itself is viscoelastic in this model.

We can replace Equation (3.37d) describing the fluid motion by this global equation, and then determine the pressure p from it with the aid of the stress boundary condition.

The initial conditions are given in Equation (3.29) and the necessary boundary conditions are Equations (3.30), (3.31), (3.33) and (3.35).

3.3 Dimension reduction: 1-D model of a concrete plate-layer

We reduce the 3-D model of Section 3.2 to a simpler 1-D problem, namely a flat plate-layer of concrete of initial thickness H , which is exposed at its upper side to acidic air due to the presence of droplets of sulfuric acid. The bottom of the plate layer is fixed on a rigid ground space of non-reacting concrete having a fixed concentration of lime. The material of the layer (concrete) is a mixture of gypsum ($\alpha = 1$), lime ($\alpha = 2$) and sulfuric acid ($\alpha = 3$). Initially,

i.e. for $t < 0$, the layer is in a homogeneous, undeformed, and stress-free state, where the sulfuric acid has penetrated the concrete and has already partially reacted to create gypsum, such that $\phi_{\alpha 0} > 0$ for $\alpha = (1, 2, 3)$. The external space both below and above the plate is free of stress. As the layer is created in a homogeneous and uniform way, and the acid is in equilibrium, we expect no symmetry breaking. Hence, we can forget about the tangential directions and only focus on the normal (z) direction. Hence, a 1-D plate-layer model is sufficient to model a 3-D sewer pipe as already explained in the Introduction.

From $t > 0$ onwards, the inflow of lime from below and acid from above into the plate takes place and chemical reactions start; here it is assumed that the concentrations ϕ_2^- , of lime in the ground space, and ϕ_3^+ , of acid in the air above the plate, are greater than ϕ_{20} and ϕ_{30} , respectively, resulting in an inflow of lime and acid. Due to the combination of inflow and the chemical reactions, the plate grows, as is experimentally observed in [69, 132], and the thickness of the plate increases to a value $h(t) > H = h(0)$ at time $t > 0$. We consider only a time span from $t = 0$ to a final time t_f in which the growth remains small, i.e. such that $(h(t) - H)/H \ll 1$ holds and our small-deformation assumption is valid. A direct consequence of this assumption is that we may apply the boundary conditions at $z = H$ instead of at $z = h(t)$. All field variables are only dependent on z and t , and the only displacement components are $u_\alpha = u_\alpha(z, t) = \mathbf{u}_\alpha \cdot \mathbf{e}_z$, with \mathbf{e}_z the unit vector in the z -direction. This leads us to our 1-D model, valid for all four systems. Before recapitulating the resulting set of equations, we first use the global equation of equilibrium for the total stress Equation (3.38), which for Systems A, B, and D in the 1-D version reads

$$\partial_z(-p + E_1 \partial_z u_1 + E_2 \partial_z u_2) = 0, \quad (3.39)$$

where $E_{1(2)} = \lambda_{1(2)} + 2\mu_{1(2)}$ is the Young's modulus of the solid constituent. Since the upper plane $z = H$ is free of stress, we have for Systems A, B, and D

$$(-p + E_1 \partial_z u_1 + E_2 \partial_z u_2)(H, t) = 0, \quad (3.40)$$

which, in combination with the equation above, implies that the total stress must be zero everywhere in the plate, yielding

$$p(z, t) = E_1 \partial_z u_1(z, t) + E_2 \partial_z u_2(z, t) \quad \text{for } z \in [0, H] \quad \text{and } t \geq 0. \quad (3.41)$$

This result holds for Systems A, B, and D. For System C an extended expression is found, because in System C the total stress contains a viscoelastic part. Due to this, we get

$$p = E_1 \partial_z u_1 + E_2 \partial_z u_2 + \gamma_1 \partial_z \partial_t u_1 + \gamma_2 \partial_z \partial_t u_2 \quad (3.42)$$

for $z \in [0, H]$ and $t \geq 0$, which further on leads to the expressions $\tilde{\gamma}_{\alpha\beta}$; see Equation (3.46). After the elimination of p from Equations (3.37c) and (3.37d), the set of unknown variables in the one-dimensional model is

$$\{\phi_1, \phi_3, u_1, u_2, v_3\}(z, t), \quad (3.43)$$

for $z \in (0, H)$ and $t \in (0, t_f)$. Reducing Equations (3.37a) to (3.37d) to their 1-D version, eliminating p , and inserting the volume fraction production R_α due to chemical reactions given by Equation (3.27), we obtain the following 1-D model:

$$\partial_t \phi_1 + \partial_z (\phi_1 \partial_t u_1) - \delta_1 \partial_z^2 \phi_1 = \frac{N_1 \tilde{\rho}_3}{\mathcal{M}_3} k F(\phi_1, \phi_3), \quad (3.44a)$$

$$\partial_t \phi_3 + \partial_z (\phi_3 v_3) - \delta_3 \partial_z^2 \phi_3 = \frac{N_3 \tilde{\rho}_1}{\mathcal{M}_1} k F(\phi_1, \phi_3), \quad (3.44b)$$

$$\partial_z (\phi_1 \partial_t u_1 + \phi_2 \partial_t u_2 + \phi_3 v_3) - \sum_{\alpha=1}^3 \delta_\alpha \partial_z^2 \phi_\alpha = S_K K F(\phi_1, \phi_3), \quad (3.44c)$$

$$\partial_t u_1 - \frac{E_1}{\chi_1} \partial_z^2 u_1 - \frac{\gamma_{11}}{\chi_1} \partial_z^2 \partial_t u_1 - \frac{\gamma_{12}}{\chi_1} \partial_z^2 \partial_t u_2 = v_3 - \partial_z \left(\phi_1 \frac{E_1}{\chi_1} \partial_z u_1 + \phi_1 \frac{E_2}{\chi_1} \partial_z u_2 \right), \quad (3.44d)$$

$$\partial_t u_2 - \frac{E_2}{\chi_2} \partial_z^2 u_2 - \frac{\gamma_{22}}{\chi_2} \partial_z^2 \partial_t u_2 - \frac{\gamma_{21}}{\chi_2} \partial_z^2 \partial_t u_1 = v_3 - \partial_z \left(\phi_2 \frac{E_1}{\chi_2} \partial_z u_1 + \phi_2 \frac{E_2}{\chi_2} \partial_z u_2 \right), \quad (3.44e)$$

where $F(\phi_1, \phi_3)$ is given in Equation (3.28), $\delta_\alpha = \delta / \tilde{\rho}_\alpha$, $\phi_2 = 1 - \phi_1 - \phi_3$, and

$$K = \left(\sum_{\alpha=1}^3 \frac{N_\alpha \mathcal{M}_\alpha}{\tilde{\rho}_\alpha} \right) \frac{\tilde{\rho}_1 \tilde{\rho}_3}{\mathcal{M}_1 \mathcal{M}_3} k, \quad S_K = \text{sgn} \left(\sum_{\alpha=1}^3 \frac{N_\alpha \mathcal{M}_\alpha}{\tilde{\rho}_\alpha} \right). \quad (3.45)$$

Moreover, $\gamma_{11} = \gamma_1$, $\gamma_{22} = \gamma_2$, $\gamma_{12} = \gamma_{21} = 0$ for System A, $\gamma_{11} = \gamma_{22} = \gamma_{12} = \gamma_{21} = 0$ for System B, and $\gamma_{11} = \gamma_{22} = -\gamma_{12} = -\gamma_{21} = \gamma$ for System D. For System C one has, due to the additional terms in p , the effective coefficients $\tilde{\gamma}$ defined by

$$\tilde{\gamma}_{11} = (1 - \phi_1) \gamma_1, \quad \tilde{\gamma}_{12} = -\phi_1 \gamma_2, \quad \tilde{\gamma}_{21} = -\phi_2 \gamma_1, \quad \tilde{\gamma}_{22} = (1 - \phi_2) \gamma_2, \quad (3.46)$$

instead of γ . Since these effective coefficients depend on the volume fractions $\phi_{1,2}$ the (numerical) analysis of this system becomes more complicated than for the other systems.

The initial conditions at $t = 0$ are

$$\phi_1 = \phi_{10}, \quad \phi_3 = \phi_{30}, \quad u_1 = u_2 = 0. \quad (3.47)$$

As boundary conditions we have for $t > 0$
at $z = 0$:

$$\partial_z \phi_1 = \partial_z \phi_3 = u_1 = v_3 = 0, \quad \phi_2 \partial_t u_2 = J_2 \mathcal{L}(\llbracket \phi_2 \rrbracket), \quad (3.48)$$

and at $z = H$:

$$\begin{aligned} \partial_z \phi_1 &= \partial_z \phi_3 = 0, & \phi_3 v_3 &= \phi_3 \partial_t h(t) - J_3 \mathcal{L}(\llbracket \phi_3 \rrbracket), \\ \partial_z u_1 &= A_1(u_1 - h(t) + h(t_0)), & \partial_z u_2 &= A_2(u_2 - h(t) + h(t_0)), \end{aligned} \quad (3.49)$$

as they follow from (3.31), (3.32) and (3.35), respectively. We notice that we need in total 9 boundary conditions (2 for each of ϕ_1 , ϕ_2 , u_1 , u_2 and 1 for v_3), as well as an extra condition to determine $h(t)$, so in total 10 conditions.

Dimensionless formulation

We nondimensionalize the fundamental variables, unknowns and parameters by dividing them by a normalization constant to make them dimensionless and $\mathcal{O}(1)$. The normalization constants are denoted as U for the displacement, H for the position, V for the velocity, T for the time, and J for the flux. Material coefficients $\chi_{1,2}$ and $E_{1,2}$ are normalized with respect to the largest value of all constituents, so $\chi = \max\{\chi_1, \chi_2\}$, $E = \max\{E_1, E_2\}$. Moreover, we introduce the small parameter ϵ as the ratio of U and H . This small parameter recalls that our model uses linear deformation theory, in which deformations are small with respect to the size of the domain. We note here that this assumption holds as long as $(h(t) - H)/H = \mathcal{O}(\epsilon)$. Concerning the choice of the time scale T , we have three natural options: *diffusion time scale* $T = U/V$, *reaction time scale* $T = 1/K$, and *inflow time scale* $T = U/J$. If we opt for the diffusion time scale and nondimensionalize Equation (3.44c) making all terms and coefficients of the same order, we obtain $V = HK$ and $J = HK$ yielding $T = U/V = U/J = (U/H)/K = \epsilon/K$, for both the diffusion and the inflow time scale. Consequently, the diffusion time scale is much smaller than the reaction time scale, implying that diffusion is much faster than the reaction, and therefore we opt here for the normalization constant $T = U/V = \epsilon/K$. Analogously, we find from Equation (3.44d) or Equation (3.44e) the relation $EU/H^2 = \chi V$. All this leads to the definitions of the following dimensionless numbers, viz:

$$V = HK, \quad T = \epsilon/K, \quad U = \frac{\chi H^3 K}{E}, \quad J = HK, \quad \text{and} \quad \epsilon = \frac{\chi H^2 K}{E}. \quad (3.50)$$

Looking at the problem at the diffusion time scale regime, we obtain the following nondimensionalized system equations:

$$\partial_t \phi_1 + \epsilon \partial_z (\phi_1 \partial_t u_1) - \epsilon \delta_1 \partial_z^2 \phi_1 = \epsilon \kappa_1 F(\phi_1, \phi_3), \quad (3.51a)$$

$$\partial_t \phi_3 + \epsilon \partial_z (\phi_3 v_3) - \epsilon \delta_3 \partial_z^2 \phi_3 = -\epsilon \kappa_3 F(\phi_1, \phi_3), \quad (3.51b)$$

$$\partial_z (\phi_1 \partial_t u_1 + \phi_2 \partial_t u_2 + \phi_3 v_3) - \sum_{\alpha} \delta_{\alpha} \partial_z^2 \phi_{\alpha} = S_K F(\phi_1, \phi_3), \quad (3.51c)$$

$$\begin{aligned} \chi_1 \partial_t u_1 - E_1 \partial_z^2 u_1 - \gamma_{11} \partial_z^2 \partial_t u_1 - \gamma_{12} \partial_z^2 \partial_t u_2 &= \chi_1 v_3 \\ &\quad - \partial_z (\phi_1 E_1 \partial_z u_1 + \phi_1 E_2 \partial_z u_2), \end{aligned} \quad (3.51d)$$

$$\begin{aligned} \chi_2 \partial_t u_2 - E_2 \partial_z^2 u_2 - \gamma_{22} \partial_z^2 \partial_t u_2 - \gamma_{21} \partial_z^2 \partial_t u_1 &= \chi_2 v_3 \\ &\quad - \partial_z (\phi_2 E_1 \partial_z u_1 + \phi_2 E_2 \partial_z u_2), \end{aligned} \quad (3.51e)$$

where

$$\kappa_{\alpha} = \frac{\mathcal{M}_{\alpha}}{\tilde{\rho}_{\alpha}} \frac{\tilde{\rho}_1}{\mathcal{M}_1} \frac{\tilde{\rho}_3}{\mathcal{M}_3} \frac{k}{K}. \quad (3.52)$$

In these equations all material coefficients q_{α} were made dimensionless in the usual way of $q_{\alpha} = \tilde{q}_{\alpha} q$ and dropping the tildes. Effectively this yields a replacement of coefficients in system (3.44). Inserting the following changes together with the normalization of the variables and unknowns into system (3.44) yields system (3.51):

$$\left\{ \delta_{\alpha} \rightarrow \delta_{\alpha} / KH^2 = \delta / KH^2 \tilde{\rho}_{\alpha}, \chi_{\alpha} \rightarrow \chi_{\alpha} / \chi, E_{\alpha} \rightarrow E_{\alpha} / E, \gamma_{\alpha} \rightarrow \gamma_{\alpha} / \chi H^2 \right\}. \quad (3.53)$$

Due to the nondimensionalization, the domain changes from $(0, H)$ to $(0, 1)$. The initial conditions and most of the boundary conditions do not change their structure. Only the nonzero boundary conditions at the upper boundary (now at $z = 1$) change due to the introduction of the dimensionless boundary displacement function $W(t) = (h(t) - H) / \epsilon H$ such that $W = \mathcal{O}(1)$. The non-homogeneous boundary conditions at $z = 1$ become

$$\phi_3 (\partial_t W(t) - v_3) = J_3 \mathcal{L}([\phi_3]), \quad (3.54a)$$

$$\partial_z u_1 = A_1 (u_1 - W(t)), \quad (3.54b)$$

$$\partial_z u_2 = A_2 (u_2 - W(t)). \quad (3.54c)$$

Integrating Equation (3.44c) from $z = 0$ to $z = 1$, and using (3.48) and (3.49), we obtain a closed expression for $W(t)$ for all $t > 0$ in terms of influxes, the production term by the chemical reaction, and the mismatch of displacement

at the boundary, viz.

$$W(t) = \int_0^t \left[J_2 \mathcal{L}(\llbracket \phi_2(0, s) \rrbracket) + S_K \int_0^1 F(\phi_1(z, s), \phi_3(z, s)) dz \right. \\ \left. + J_3 \mathcal{L}(\llbracket \phi_3(1, s) \rrbracket) - \sum_{\alpha=1}^2 \frac{\phi_\alpha(1, s)}{A_\alpha} \partial_t \partial_z u_\alpha(1, s) \right] ds. \quad (3.55)$$

We note here that in the limiting case $A_{1,2} \downarrow 0$, as then also $\partial_z u_{1,2} \rightarrow 0$, the last term of Equation (3.55) becomes undetermined. In this case we cannot use (3.54b) and (3.54c), which results in the following adapted relation for $W(t)$ (derived analogously to the derivation of Equation (3.55))

$$W(t) = \int_0^t \frac{1}{\phi_3(1, s)} \left[J_2 \mathcal{L}(\llbracket \phi_2(0, s) \rrbracket) + S_K \int_0^1 F(\phi_1(z, s), \phi_3(z, s)) dz \right. \\ \left. + J_3 \mathcal{L}(\llbracket \phi_3(1, s) \rrbracket) - \sum_{\alpha=1}^2 \phi_\alpha(1, s) \partial_t u_\alpha(1, s) \right] ds. \quad (3.56)$$

From both these results we conclude that the first two terms, the influxes with $J_{2,3}$ being positive, yield a positive contribution to $W(t)$ making the layer increase in thickness. Whether or not the second term has an increasing or decreasing effect depends on the sign of S_K ; when, as in our case, $S_K = -1$, the chemical reaction does shrink the layer. At this moment, nothing specific can be said for the last term. However, our numerical results reveal that the effect of this term is small. Thus, we can neglect the fourth term. Consequently, the domain of the layer grows if the magnitude of the J -terms representing expansion through influx is greater than the magnitude of the S_K -term representing decrease of size due to the chemical reaction. Hence, there is a competition effect here.

In Section 3.7, a solution for System D has been obtained as a formal asymptotic expansion in ϵ . The asymptotic expansion is formal as it is not a priori known whether or not this power series has positive radius of convergence in ϵ . The predictive power of a formal asymptotic expansion should not be underestimated, because there exist formal asymptotic expansions, which are diverging, but can be very accurate when only a truncated version of the expansion is used; see the example in Section 1.4.2 on pages 13 and 14 of [66]. This motivated us in the choice of the two J -parameters; see Table 3.1.

3.4 Numerical method

In this section, we solve numerically the systems A, C and D. We omit system B, because a viscoelastic term is needed to obtain a coercive system, such as in system A, for which we have proven the convergence of the time-discrete evolutions to the corresponding weak solution; see [136]. We expect that similar convergence results can be obtained for the systems C and D, as they have a viscoelastic term similar to the one in system A. Also, when solving system D we exclude the Laplacian terms in Equation (3.44c), or stated in another way: the numerical method uses $\delta_\alpha = 0$ for (3.44c). This exclusion is justified by an order analysis of the terms of (3.44c) from the ϕ_α -solutions of (3.44a) and (3.44b), which states that $\sum_{\alpha=1}^3 \delta_\alpha \Delta \phi_\alpha = \mathcal{O}(\sqrt{\epsilon}F)$.

Our code is called `NewGypsum` and it is based on a combination of MATLAB routines. We start off with a Rothe time discretization of the systems A, C and D, which linearizes the systems. Benefitting from the one-dimensional-in-space formulation, solving the linear systems is done automatically by using the built-in boundary value problem (BVP) solvers of MATLAB, see `bvp4c` and `bvp5c`; [76] and [77]. These solvers take a grid, a guess for the solution, and the BVP system as input. Then they automatically readjust the grid and interpolate the guess solution to obtain a starting point for the numerical scheme, controlling a certain error metric to determine the solution based on user-defined-convergence criteria.

The solver `bvp4c` is an implicit Runge-Kutta method using the 3-stage Lobatto IIIa formula with control on the residual [76]. The method is only applicable to linear Lipschitz systems [76]. Fortunately, systems A, C, and D can be shown to satisfy this condition within certain parameter constraints (which we will explain more thoroughly in the next section). For an easy guide in understanding and using `bvp4c` we recommend [126]. Moreover, [126] shows that boundary layer effects are well resolved by the `bvp4c` solver.

The solver `bvp5c` is an implicit Runge-Kutta method using the 4-stage Lobatto IIIa formula with control on the true error [77]. The solver `bvp5c` is more precise than `bvp4c`, but it is also less versatile [77]. This does not pose a problem as our three systems A, C and D still satisfy the applicability conditions for `bvp5c` and `bvp5c` has similar capabilities in handling boundary layers as `bvp4c` [77]. In our case the choice was made to use `bvp5c` as it made our simulations about 27 times faster than when using `bvp4c`.

A more detailed explanation of our `NewGypsum` can be found in section 2.4 of [136]. Moreover, in Appendix 3.7 one can find a validation of the `NewGypsum` routine with a Mathematica simulation of the asymptotic ϵ -expansion solu-

tions derived in the same appendix.

3.5 Quest for realistic numerical behavior

Even though our systems were derived based on first principles in terms of balance/conservation laws, this does not guarantee that all physical constraints are automatically satisfied for large variations in the model parameters. A solution is said to show *realistic behavior* if the following three constraints are satisfied within this framework:

1. The volume fractions should be nonnegative and less than one. From the mathematical analysis point of view we expect that system A behaves poorly when volume fractions become very small. To outlaw this unwanted behavior a positive minimal value ϕ_{\min} is introduced, leading to the requirement

$$0 < \phi_{\min} \leq \phi_{\alpha}(t, z) < 1 \quad (3.57)$$

for all $\alpha \in \{1, 2, 3\}$, for all $z \in (0, 1)$, and for all $t \in (0, t_f)$.

2. A second condition is a demand on the upper bound for the velocity. Fast local deformations are allowed as long as the total contribution to the domain deformation is still small, the stresses remain low and the quasi-static approximation is not violated. Hence, it is natural to cap both the total velocity in the domain and the total spatial change of the velocity in the domain. This is reflected in the condition

$$\|v_3\|_{L^2(t_0, t; H^1(0, 1))}^2 = \int_0^t \left[\int_0^1 \left(v_3(s, z)^2 + (\partial_z v_3(s, z))^2 \right) dz \right] ds < V^2 \quad (3.58)$$

for all $t \in (0, t_f)$.

3. The concrete layer has two boundaries that allow influx. Even though the chemical reaction itself is volume contractive, the combination of influx and chemical reactions must be volume expansive due to the porous nature of gypsum [101]. Hence, the height of the plate-layer must be a nondecreasing function:

$$\partial_t h(t) = \epsilon \partial_t W(t) \geq 0 \quad \text{for all } t \in (0, t_f). \quad (3.59)$$

Realistic behavior is defined as satisfying all three requirements Equations (3.57) to (3.59). We immediately stop a simulation when one of the three inequalities is violated.

Testing for realistic behavior need a realistic range of values for material constants. A-priori such a range is difficult to obtain. Hence, we need a reference set of material constants that are arguably realistic. Based on this set, we seek ranges of values for material constants for which the system exhibits realistic behaviour by satisfying the three inequalities above. Hence, we introduce a reference set of material constants. The values of these constants, and their dimensionless counterparts, dimensionalized with respect to the diffusion time scale, are listed in Table 3.1. The numerical evaluations use a time step Δt , the size of the time interval t_f , and a number of spatial subdivisions, $1/\Delta z$. We choose fixed values $\Delta t = 0.001$, $t_f = 0.500$ and $1/\Delta z = 300$ for these parameters. In the remainder of this chapter we implicitly use the parameter values of Table 3.1, whenever parameter values are not explicitly specified. A spatial-temporal analysis of our benchmark problem with the parameter values of Table 3.1 can be found in Section 2.6 of [136], showing that our reference simulation gives realistic behaviour by satisfying the above three inequalities.

Parameter dependence of found realistic behavior

We aim to determine how the size of the realistic time interval, given in number of numerical iterations N_R , depends on the system parameters. Our definition of realistic behavior contains three constraints, see the beginning of Section 3.5, which can be numerically checked. We investigate the numerical simulation applied to systems A, C and D for a large parameter range, by changing specific parameters in Table 3.1. In this way our results even hold when experimental values with large uncertainties are used for the model parameters if these values with uncertainties remain in the probed region. Out of the 20 model parameters, we will only change specific parameters chosen on basis of their influence on the analytical bounds in the existence proof in [136]. When a bound in this existence proof contains a product of two parameters, then this parameter pair is chosen. All parameters are modified in a double exponential fashion such that large parameter ranges are investigated. Finally, the initial condition $(\phi_{10}, \phi_{20}, \phi_{30})$ is chosen, because it immediately determines whether chemical reactions or influx do occur.

We have chosen to investigate the response of the model with respect to the following parameters and parameter tuples, because these parameters or combinations of parameters are either crucial for System D from a physical perspective or dominant in mathematically derived upper bounds in the existence

Material Constants				Dimensionless Parameters		
	value	(MKS unit)	reference	value	definition	
E_1	$1.60 \cdot 10^9$	(kg/m s ²)	[109]	E_1	0.038	E_1/E
E_2	$4.20 \cdot 10^{10}$	(kg/m s ²)	[145]	E_2	1.00	E_2/E
χ_1	$2.67 \cdot 10^{10}$	(kg/m ³ s)	†	χ_1	1.00	χ_1/χ
χ_2	$2.67 \cdot 10^{10}$	(kg/m ³ s)	†	χ_2	1.00	χ_2/χ
J_2	$0.326 \cdot 10^{-5}$	(m/s)	*	J_2	0.40	J_2/J
J_3	$1.632 \cdot 10^{-5}$	(m/s)	*	J_3	2.00	J_3/J
γ_1	$3.604 \cdot 10^{10}$	(kg/ms)	*	γ_1	0.50	γ_1/γ
γ_2	$3.604 \cdot 10^{10}$	(kg/ms)	*	γ_2	0.50	γ_2/γ
A_1	$0.821 \cdot 10^{-3}$	(1/m)	*	A_1	0.50	A_1/A
A_2	$0.821 \cdot 10^{-3}$	(1/m)	*	A_2	0.50	A_2/A
$\tilde{\rho}_1$	$2.32 \cdot 10^3$	(kg/m ³)	[64]	ϕ_{1sat}	1.00	
$\tilde{\rho}_2$	$2.21 \cdot 10^3$	(kg/m ³)	[64]	ϕ_{3thr}	0.00	
$\tilde{\rho}_3$	$1.84 \cdot 10^3$	(kg/m ³)	[64]	ϕ_{2res}	1.00	
\mathcal{M}_1	0.172164	(kg/mol)	[64]	ϕ_{3res}	1.00	
\mathcal{M}_2	0.074093	(kg/mol)	[64]	κ_1	23.00	Equation (3.52)
\mathcal{M}_3	0.098079	(kg/mol)	[64]	κ_3	13.50	Equation (3.52)
δ	5.10	(kg/m s)	*	δ_1	1.00	δ_1/KH^2
δ_1	$2.20 \cdot 10^{-3}$	(m ² /s)	‡	δ_2	1.05	δ_2/KH^2
δ_2	$2.31 \cdot 10^{-3}$	(m ² /s)	‡	δ_3	1.26	δ_3/KH^2
δ_3	$2.77 \cdot 10^{-3}$	(m ² /s)	‡			
k	$1.00 \cdot 10^{-6}$	(m ³ /mol s)	[9]			
Normalization Constants				Numerical Parameters		
	value	(MKS unit)	definition	value	definition	
H	$1.643 \cdot 10^0$	(m)	$h(0)$	Δt	0.001	
K	$0.816 \cdot 10^{-3}$	(1/s)	Equation (3.45)	t_f	0.5	T_f/T
S_K	-1	(-)	Equation (3.45)	$1/\Delta z$	300	
χ	$2.67 \cdot 10^{10}$	(kg/m ³ s)	χ_1	ϕ_{min}	10^{-5}	
E	$4.20 \cdot 10^{10}$	(kg/m s ²)	E_2	V_{max}	10^6	
T	1.716	(s)	$\chi H^2/E$			
U	$2.300 \cdot 10^{-3}$	(m)	$\chi H^3 K/E$			
V	$1.341 \cdot 10^{-3}$	(m/s)	HK			
J	$0.816 \cdot 10^{-3}$	(m/s)	HK			
γ	$7.208 \cdot 10^{10}$	(kg/m s)	χH^2			
ϵ	0.0014	(-)	$\chi H^2 K/E$			

Table 3.1: Table with numerical values of material constants, normalization constants, dimensionless parameters, and numerical parameters.

* An experimental value of this parameter is unknown to us; we have chosen their values such that their dimensionless values are of order one of magnitude. Specifically, the values of J_2 and J_3 are so large that they guarantee growth of the layer; see also remark just below Equation (3.56).

† We estimated the values of χ_α from Darcy's law with $\chi_\alpha = \mu/k_0$ with μ the dynamic viscosity of sulfuric acid (value of $26.7 \cdot 10^{-3}$ kg/ms, see [52, p. 304-305]) and k_0 the average pore size or permeability (about $1 \mu\text{m}^2 = 10^{-12} \text{m}^2$); see [31, 81].

‡ We used $\delta_\alpha = \delta/\tilde{\rho}_\alpha$ for $\alpha = 1, 2, 3$.

proof in [136]:

$$(\phi_{10}, \phi_{20}, \phi_{30}), \quad \delta, \quad \epsilon, \quad (J_2, \phi_{2,res}) \quad \text{and} \quad (A_1, \gamma_1). \quad (3.60)$$

The parameter pair (A_2, γ_2) should be investigated as well. However, we chose to fix the ratios A_1/A_2 and γ_1/γ_2 , because the dependence on (A_2, γ_2) is expected to be similar to the dependence on (A_1, γ_1) . Similarly, we chose to fix the ratios J_2/J_3 and $\phi_{2,res}/\phi_{3,res}$. Moreover, if parameters are not mentioned to have special values, then these parameters are set to their standard values as listed in Table 3.1.

The existence proof in [136] points out a dependence on the $(\kappa_1, \kappa_3, \phi_{1,sat})$ parameter triple. However, the dependence on $\phi_{1,sat}$, κ_1 and κ_3 is quite subtle: only for $\phi_{1,sat} > \phi_1 \approx \phi_{10}$ the chemical reaction is active and $F > 0$. This has only a relevant effect on the incompressibility condition, because in the first two diffusion equations Equations (3.51a) and (3.51b) the right-hand sides are of $\mathcal{O}(\epsilon)$. This implies that the effect of κ_1 and κ_3 on the simulations is expected to be (negligibly) small. As we made not enough simulations for ϕ_1 above the $\phi_{1,sat}$ threshold value, we can not draw any conclusions concerning its effect on realistic behavior. However, we expect an increasing $\phi_{1,sat}$ to decrease the size of the realistic time interval, as increasing $\phi_{1,sat}$ increases the size of F and, hence, also the size of v_3 .

We investigate the triple $(\phi_{10}, \phi_{20}, \phi_{30})$ using a barycentric triangular grid with grid size 0.1, as shown in Figure 3.2. The performance of the simulations is measured in terms of the number of consecutive iterations yielding realistic behavior. Each number denotes that the first unrealistic behavior occurs at the next iteration, while 500 denotes that no unrealistic behavior has been encountered. This performance value is placed at the grid point of the initial volume fraction values used for obtaining the result. We have added the existence region of [136] to the barycentric plots of Figure 3.2 as a shaded region.

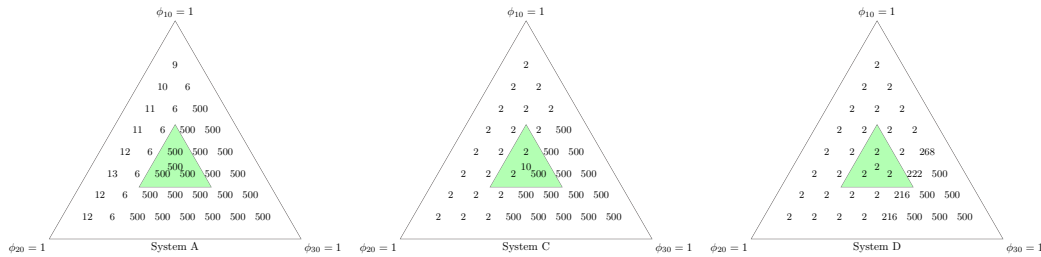


Figure 3.2: Barycentric grid with at each grid point the number of consecutive iterations yielding solutions with realistic behavior for Systems A, C and D, respectively. The volume fraction values of that grid point were used as initial conditions. The shaded central triangle indicates the parameter region for which the existence proof in [136] works for a finite time interval.

The three systems behave differently as one can see from the size of the para-

meter region with 500 iterations. The parametric region pointing at the high acid concentration region is outperforming the other parameter regions in all systems. A high concentration of acid implies that the reaction is slow (i.e. F is small), and consequently, the velocity v_3 remains small. Moreover, also the influx of acid is low or even absent. This results in a relatively small increase of the norm of v_3 , and, therefore, violating the velocity norm upper bound (which is the most critical of the three conditions to violate) takes more time for large values of ϕ_3 . This explains the good performance of this parameter region.

For the determination of the dependence on other parameters the best choice of initial conditions for each system is exactly in the transition region between the regions of small (single digit) and high (500) amount of iterations. In this transition region, the amount of iterations is expected about half way in between 1 and 500 iterations. Any dependence yielding lower or higher amounts of iterations is faithfully represented. Outside this transition region the registration of the dependence is limited to a one-sided deviation of the reference level of amount of iterations, while in this transition region the registration allows for the full two-sided deviation of the reference level of the amount of iterations. We have chosen $(\phi_{10}, \phi_{20}, \phi_{30})$ equal to $(11/30, 11/30, 8/30)$, $(1/3, 1/3, 1/3)$, and $(1/4, 1/4, 1/2)$ for System A, C, and D, respectively.

As for δ and ϵ , we modified their values in an exponential fashion. Again, we recorded the amount of consecutive iterations, N_R , for which the solutions remained realistic. The amount N_R for Systems A, C and D is recorded in Table 3.2 for changes in δ .

System	$\delta = 1.00 \times \text{factor below}$										
	10^{-5}	10^{-4}	10^{-3}	10^{-2}	10^{-1}	1	10	10^2	10^3	10^4	10^5
A	297	304	297	311	311	324	332	338	331	338	338
C	212	222	220	216	218	220	216	212	230	222	212
D	462	462	462	462	464	464	464	464	464	464	464

Table 3.2: Number of consecutive iterations yielding realistic behavior for Systems A, C and D at different values of δ .

For all systems, we see that the size of δ has practically no influence and is, therefore, unimportant in establishing realistic behavior defined in this section. This makes sense because the initial conditions are smooth, which leads to small values of the Laplacian. Hence, δ has only a minor effect on the simulation output.

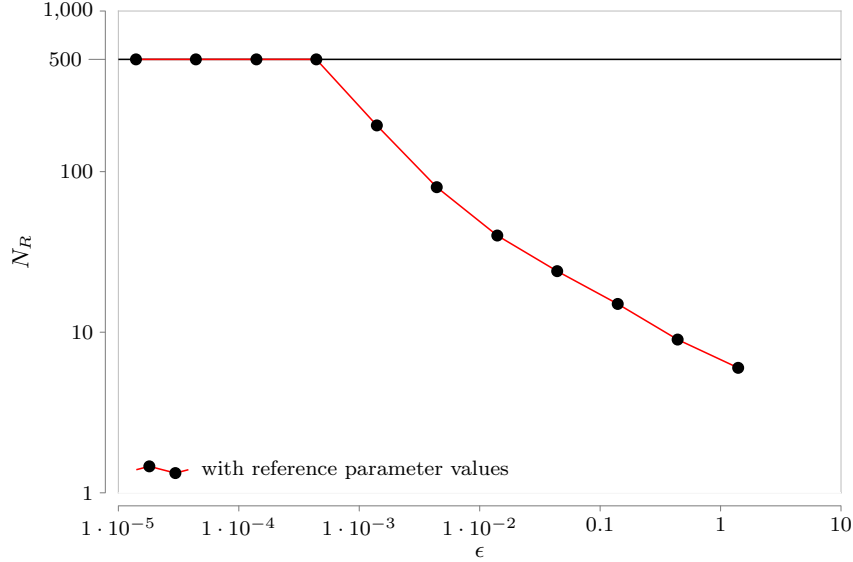


Figure 3.3: Log-log plot of the number of consecutive iterations yielding realistic behavior (N_R) versus the parameter value of ϵ for several systems and initial values. Since the duration of the simulation was limited to 500 iterations, only the unambiguous values smaller than 500 iterations are chosen.

In Figure 3.3, the values of N_R are plotted for systems A, C and D for ϵ equal to 1.4 times a factor equal to all powers of $\sqrt{10}$ between 10^{-2} and 10^3 . Only the unambiguous values of $N_R < 500$, are plotted next to similar simulations executed with the modified parameter values $(\phi_{10}, \phi_{20}, \phi_{30}) = (0.2, 0.3, 0.5)$. The effect of ϵ shows a different performance for $\epsilon \geq 0.0014$ and $\epsilon < 0.0014$, where in the former case the behavior becomes worse for greater values of ϵ . However, one should be aware that only small values of ϵ are acceptable because our model is based on the assumption of linear (small) deformations ($\epsilon \ll 1$). The linear behavior of system D in the log-log plot of Figure 3.3 is a clear power law signal. In Table 3.3, we have listed the power law exponent estimate and its unbiased variance estimate for both initial value data sets. The estimators are explained in detail in section 14.2 of [119]. Essentially, $T_{real} = N_R \Delta t \sim \epsilon^{-0.5}$ is a reasonable hypothesis for System D and it indicates how the validity of our model depends on physical scale separation.

The realistic behavior is affected by changes in J_α , $\alpha \in \{2, 3\}$, as they control the rate of influx and so a major aspect of thickness growth. Increasing the size of J_α gives a corresponding increase in the size of $W(t)$ for large enough J_α . However, for small J_α we cannot expect the same correspondence, because at some point the reaction becomes the dominant contributor. Hence,

System D: (ϕ_{10}, ϕ_{30})	(0.20,0.50)	(0.25,0.50)
$\hat{\alpha}_0$	-0.509	-0.487
$s_{\hat{\alpha}_0}$	0.00854	0.0121
# datapoints	7	7

Table 3.3: Unbiased estimators of α_0 and their standard error for the relationship $T_{real} \sim \epsilon^{\alpha_0}$ describing the dependence of the realistic time interval of System D on the parameter ϵ for two different initial conditions.

for small J_α the growth of $W(t)$ must be independent of J_α , while at large J_α this growth must be in a one-to-one correspondence.

The size of $W(t)$ correlates with the size of J_α , see Equation (3.55). However, Equations (3.48) and (3.49) show that $\partial_t u_2$ and v_3 are related to J_α . The incompressibility condition Equation (3.51c) immediately gives that the norm of v_3 is, then, correlated with the size of J_α . Hence, from Equations (3.51c) and (3.55) we expect for small J_α no dependence between the realistic time interval T_{real} and J_α . At large J_α , we expect an inverse dependence of the realistic time interval T_{real} on J_α . In Figure 3.4 the expected behavior is shown. This figure also shows that the choice of the system (A, C, or D) and the value of $\phi_{\alpha, res}$ has only a minor influence on the realistic behavior.

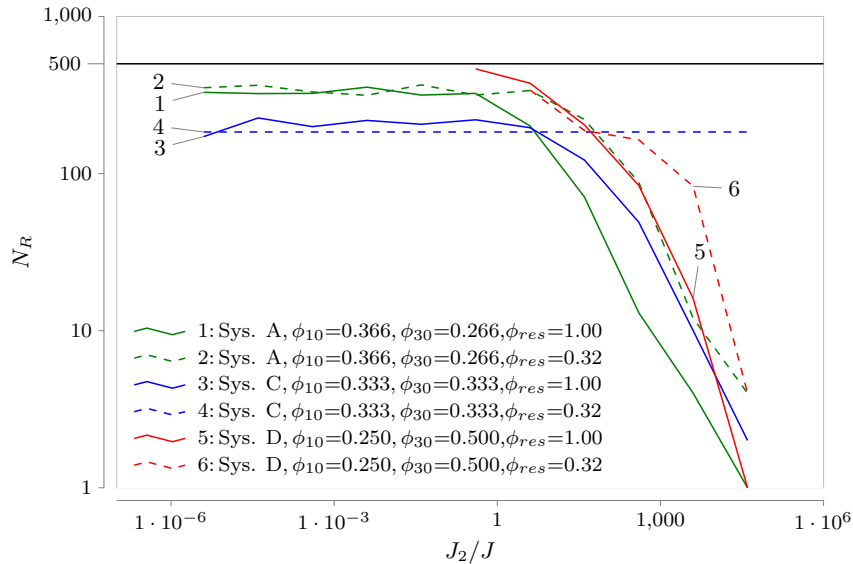


Figure 3.4: Log-log plot of the number of consecutive iterations yielding realistic behavior (N_R) versus the parameter value of J_2 for all three systems at two different values for $\phi_{2, res}$, with $J_3/J = 5 * J_2/J$. Notice the two regions with different performance as expected due to the influence of $W(t)$ on v_3 .

The size of the viscoelastic parameter γ_α has a major effect on the realistic behavior: when γ_α is too small, the system loses coercivity and the numerical program immediately terminates. This happens for all values of $\gamma_\alpha < 0.005$. For large enough values of γ_α the system preserves ellipticity, resulting in stable realistic behavior; see Table 3.4 for System A, C, and D.

	System A				System C				System D			
	$2\gamma_1$				$2\gamma_1$				$2\gamma_1$			
$2A_1$	0.01	0.1	1	10	0.01	0.1	1	10	0.01	0.1	1	10
0.1^5	12	13	57	500	16	17	33	500	410	410	410	412
0.1^4	12	13	57	500	16	17	33	500	410	410	410	412
0.1^3	12	13	59	500	16	17	33	500	410	410	410	412
0.1^2	12	13	59	500	14	17	33	500	410	410	412	412
0.1	10	14	123	500	14	19	38	500	416	416	416	418
1	8	10	324	1	12	14	220	45	462	464	464	464
10	8	1	4	6	10	1	4	8	244	320	308	306
10^2	2	6	8	8	2	4	8	8	1	1	1	1

Table 3.4: Number of consecutive iterations yielding realistic behavior (N_R) for Systems A, C and D, and a set of values for the parameter pair (A_1, γ_1) . The values for $2\gamma_1 < 0.1^3$ were omitted since the system lost coercivity and therefore no simulation was performed. The values for $\gamma_1 = 50$ have been omitted for brevity since they are almost identical to the values for $\gamma_1 = 5$.

The realistic behavior depends also on A_α . When A_α takes large values, then the coupling between $W(t)$ and the displacements u_1 and u_2 becomes strong, leading to a larger value of v_3 , and thus smaller N_R . On the other hand, when A_α is small (say $A_\alpha < 1$), then the boundary condition will behave more like a Neumann boundary condition, having no effect whatsoever on the realistic time interval. Again, we see these behaviors in Table 3.4 for Systems A, C, and D. This behavior agrees with the analytical results from [136] for System A.

For System D, we have used the standard values for the parameters and initial conditions, to calculate the dimensionless thickness growth $W(t)$. In Figure 3.5, the results for a set of ϵ -values are depicted. For $\epsilon \geq 0.0014$ the curve of $W(t)$ has a rotated S shape, whereas for $\epsilon < 0.0014$ the behavior is linear and identically the same for all ϵ . This linear behavior is clearly different for $t/T \approx 0$ and should not be confused with a windowing artifact applied to an S-shaped curve as the linear behavior occurs immediately and

does not show a characteristic decrease in slope as with $\epsilon < 0.0014$. Therefore, it seems there exists a bifurcation value of ϵ at which the system changes the qualitative behavior in $W(t)$ near $t = 0$. A deeper insight in this aspect requires more numerical and theoretical investigations. Future investigations are needed to shed light on this bifurcation behavior.

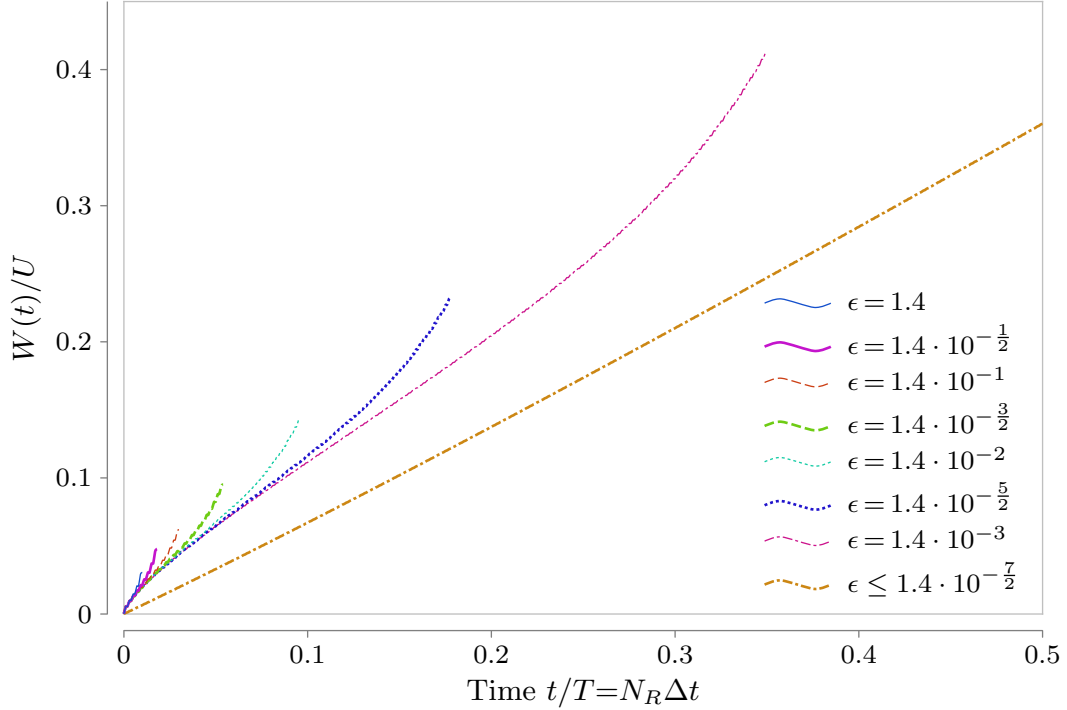


Figure 3.5: A plot of $W(t)$ in System D at different parameter values of ϵ .

3.6 Conclusion

We have derived, based on first principles, several models describing concrete corrosion by taking into account mixture theory, small deformations, compressibility and viscoelastic effects, diffusion, chemical reactions, influx of chemical species and an expanding domain. The most suitable model is System D. For this system, we could obtain the best numerical results with nice power law behaviors, which lead us to the hypothesis that the realistic time interval T_{real} scales as $1/\sqrt{\epsilon}$. Moreover, we could interpret the spatial behavior of all variables by taking into account the physical effects of the chemical reaction and of the influx of reacting materials.

Even though we have derived our systems from first principles, many material constants (δ_α , γ_α , A_α) have either unknown values or are determined at length scales orders of magnitude larger than our simulated domain (e.g. the Young modulus cf. [109]). Consequently, many of our model parameters need to be identified. Better insight in the model parameters is needed. This can be obtained in at least three ways:

- (i) By performing more specific measurements at the length scale of our domain;
- (ii) By upscaling procedures, obtain effective material coefficients at length scales compatible with the measurements;
- (iii) By suitably combining (i) and (ii).

By performing simulations with intentionally large parameter ranges, we localized the uncertainties in the model parameters and probed simultaneously the continuous dependence of the solution to our systems on the choice of parameters. In this way, the behavior of System D is valid, even for the model parameters with large uncertainties. While probing the parameter dependence of our system on 20 different parameters, of which about 10 are indeterminate, we immediately encounter the curse of dimensionality – sampling a high dimensional space² is a sparse operation. A more structured sampling was possible by targeting the variables present in analytical upper bounds derived in [136]. An additional complication is the nonlinear coupling of all unknowns involved concurrently in several physical processes. Such a strong coupling prohibits a fast simulation at a single parameter tuple and creates a complex nonlinear parameter dependence of the solution behavior.

What concerns System D, at least for a short transient time the realistic behavior showed practically constant concentrations due to the slow reaction with respect to the influx. The displacements and velocities seemed consistent with the influx of material, while the thickness of the concrete layer was growing steadily, as expected from real world observations. Moreover, these results coincide with [14] as the plate thickness increases in time and the correct changes in volume fractions were observed. Displacements and velocities could not be related to any quantity in [14], because their reaction occurs in the boundary, while ours occurs in the full domain.

²In our case, the dimensionality is linked to the space of simulations for all possible combinations of parameter values.

The Systems A, C, and D showed strong dependence on several parameters. For all systems the number of consecutive iterations yielding realistic behavior (N_R) is highly dependent on the choice of ϕ_{30} , due to the incompressibility condition, while ϕ_{10} and ϕ_{20} seem unimportant, as long as $\phi_{10} + \phi_{20} = 1 - \phi_{30}$. The diffusion coefficient $\delta > 0$ had no effect on N_R , while the scale separation parameter ϵ greatly influenced N_R for all systems, especially for System D with an apparent power law dependence. The reaction parameters κ_1 , κ_3 , $\phi_{1,sat}$ had no influence on N_R , because ϵ is small and $J_3 > 1$. The flux parameters J_2 and J_3 are unimportant at small values ($J_2 < 1$), while almost in one to one correspondence with N_R at large values ($J_2 > 10$) due to Equation (3.55). The external concentrations ϕ_{res} had almost no influence on N_R , what can be attributed to an under sampling of large values ($\phi_{res} > 0.3$). The viscoelastic parameters γ_1 and γ_2 are important for keeping coercivity. They show a high dependence on N_R for Systems A and C, but almost no dependence for System D. The boundary condition parameters A_1 and A_2 highly influence N_R , but for Systems A and C the behavior seems erratic, except at small values due to the convergence to Neumann boundary conditions. The thickness $W(t)$ for System D becomes larger for smaller values of ϵ , but changes behavior for $\epsilon < 0.0014$, for which $W(t)$ seems independent of ϵ . This behavioral change is unexpected and advocates for additional research. Moreover, the thickness $W(t)$ increases continuously as expected from experiments.

Hence, the important parameters of Systems A, C, and D describing the behavior of N_R are ϕ_{30} , ϵ , J_α , γ_β and A_β for $\alpha \in \{2, 3\}$ and $\beta \in \{1, 2\}$. Moreover, the observed behavior of the thickness $W(t)$ is largely as expected from observations.

3.7 Appendix: Asymptotic ϵ -small solutions to System D

The system (3.51a)-(3.51e) contains the small parameter ϵ , $0 < \epsilon \ll 1$, and we assume that the solution of this system can be expanded as a *Poincaré series* in ϵ , for instance:

$$\phi_\alpha(z, t; \epsilon) = \phi_\alpha^{(0)}(z, t) + \epsilon \phi_\alpha^{(1)}(z, t) + \dots, \quad (3.61)$$

and the same for $u_\alpha(z, t; \epsilon)$ and $v_3(z, t; \epsilon)$.

We substitute these expansions into the equations of system (3.51a)-(3.51e)

and develop them with respect to ϵ . We start with (3.51a), which results in

$$\partial_t \phi_1^{(0)} + \epsilon \left(\partial_t \phi_1^{(1)} + \partial_z \left(\phi_1^{(0)} \partial_t u_1^{(0)} \right) - \delta_1 \partial_z^2 \phi_1^{(0)} - \kappa_1 F(\phi_1^{(0)}, \phi_3^{(0)}) \right) + O(\epsilon^2) = 0. \quad (3.62)$$

The ϵ^0 -term yields $\partial_t \phi_1^{(0)} = 0$. Together with the initial condition $\phi_1^{(0)}(z, 0) = \phi_{10}$, this gives $\phi_1^{(0)}(z, t) = \phi_{10}$ for all $t > 0$ and all $z \in (0, 1)$. If needed, the following equation for the first-order perturbation of ϕ_1 can be used

$$\partial_t \phi_1^{(1)} + \phi_{10} \partial_z \partial_t u_1^{(0)} = \kappa_1 F(\phi_{10}, \phi_{30}) =: \kappa_1 F_0. \quad (3.63)$$

In analogous way we obtain from (3.51b): $\phi_3^{(0)}(z, t) = \phi_{30}$, implying that also $\phi_2^{(0)}(z, t) = 1 - \phi_{10} - \phi_{30} = \phi_{20}$, and

$$\partial_t \phi_3^{(1)} + \phi_{30} \partial_z v_3^{(0)} = -\kappa_3 F_0. \quad (3.64)$$

For the remaining three equations, (3.51c), (3.51d), and (3.51e), we are only interested in the zeroth-order approximation, meaning that we let $\epsilon \rightarrow 0$. From here on, we denote $u_1^{(0)}, u_2^{(0)}, v_3^{(0)}$ simply by u_1, u_2, v_3 ; moreover we use here $S_K = -1$. This reduces these equations to:

$$\partial_z (\phi_{10} \partial_t u_1 + \phi_{20} \partial_t u_2 + \phi_{30} v_3) = -F_0, \quad (3.65a)$$

$$\chi_1 \partial_t u_1 - (1 - \phi_{10}) E_1 \partial_z^2 u_1 + \phi_{10} E_2 \partial_z^2 u_2 - \gamma \partial_z^2 \partial_t (u_1 - u_2) = \chi_1 v_3, \quad (3.65b)$$

$$\chi_2 \partial_t u_2 + \phi_{20} E_1 \partial_z^2 u_1 - (1 - \phi_{20}) E_2 \partial_z^2 u_2 - \gamma \partial_z^2 \partial_t (u_2 - u_1) = \chi_2 v_3 \quad (3.65c)$$

Integrating the first equation to z and using the boundary condition at $z = 0$: $\phi_{20} \partial_t u_2(0, t) = J_2 \mathcal{L}(\phi_{2, res} - \phi_{20}) =: F_1$, we obtain

$$v_3 = \frac{1}{\phi_{30}} (F_1 - F_0 z - \phi_{10} \partial_t u_1 - \phi_{20} \partial_t u_2). \quad (3.66)$$

We eliminate v_3 with use of this relation from the last two equations. After some manipulations we can write these two equations as one matrix equation of the form

$$\mathbf{A} \partial_t \mathbf{u} - \mathbf{B} \partial_z^2 \mathbf{u} - \mathbf{C} \partial_z^2 \partial_t \mathbf{u} = \mathbf{r}, \quad (3.67)$$

with

$$\mathbf{u} = \begin{pmatrix} u_1 \\ u_2 \end{pmatrix}, \quad (3.68a)$$

$$\mathbf{A} = \frac{1}{\phi_{30}} \begin{pmatrix} (\phi_{10} + \phi_{30})\chi_1 & \phi_{20}\chi_1 \\ \phi_{10}\chi_2 & (\phi_{20} + \phi_{30})\chi_2 \end{pmatrix}, \quad (3.68b)$$

$$\mathbf{B} = \begin{pmatrix} (\phi_{20} + \phi_{30})E_1 & -\phi_{10}E_2 \\ -\phi_{20}E_1 & (\phi_{10} + \phi_{30})E_2 \end{pmatrix}, \quad (3.68c)$$

$$\mathbf{C} = \begin{pmatrix} \gamma & -\gamma \\ -\gamma & \gamma \end{pmatrix}, \quad (3.68d)$$

$$\mathbf{r} = \mathbf{r}(z) = \frac{F_1 - F_0 z}{\phi_{30}} \begin{pmatrix} \chi_1 \\ \chi_2 \end{pmatrix}. \quad (3.68e)$$

This system is a linear *pseudo-parabolic* system with constant coefficients for 2 unknown variables: $u_1(z, t)$ and $u_2(z, t)$ and for $z \in (0, 1)$ and $t \in (0, t_f)$. The initial and boundary conditions for this system are $\mathbf{u}(z, 0) = \mathbf{0}$ and

$$\text{at } z = 0, \quad \mathbf{u}(0, t) = \mathbf{J} = \begin{pmatrix} 0 \\ F_1/\phi_{20} \end{pmatrix}, \quad (3.69a)$$

$$\text{at } z = 1, \quad \partial_z \mathbf{u}(1, t) = \mathbf{0}. \quad (3.69b)$$

Moreover, $W(t)$ can be found from (3.56) as

$$W(t) = (F_1 + \phi_{30}\tilde{J}_3 - F_0)t - \phi_{10}u_1(1, t) - \phi_{20}u_2(1, t), \quad (3.70)$$

with $\phi_{30}\tilde{J}_3 := J_3\mathcal{L}(\phi_{3, res} - \phi_{30})$.

For $\chi_1\chi_2\phi_{30} \neq 0$ and $E_1E_2\phi_{30} \neq 0$, we can rewrite the pseudo-parabolic equation above as an initial-boundary-value problem by introducing

$$\mathbf{u}(z, t) = \mathbf{U}_0(z) + \mathbf{J}t + \tilde{\mathbf{u}}(z, t), \quad (3.71)$$

where the first two terms are chosen such that $\tilde{\mathbf{u}}$ satisfies the homogeneous pseudo-parabolic equation

$$\mathcal{D}_{PP}\{\tilde{\mathbf{u}}\} = \partial_t \tilde{\mathbf{u}}(z, t) - \hat{\mathbf{B}} \partial_z^2 \tilde{\mathbf{u}}(z, t) - \hat{\mathbf{C}} \partial_z^2 \partial_t \tilde{\mathbf{u}}(z, t) = \mathbf{0}, \quad (3.72)$$

together with the homogeneous boundary conditions

$$\text{at } z = 0, \quad \tilde{\mathbf{u}}(0, t) = \mathbf{0}, \quad (3.73a)$$

$$\text{at } z = 1, \quad \partial_z \tilde{\mathbf{u}}(1, t) = \mathbf{0}, \quad (3.73b)$$

and the inhomogeneous initial condition

$$\tilde{\mathbf{u}}(z, 0) = -\mathbf{U}_0(z), \quad (3.74)$$

such that the original initial condition $\mathbf{u}(z, 0) = \mathbf{0}$ is still satisfied. In (3.72) $\hat{\mathbf{B}} = \mathbf{A}^{-1}\mathbf{B}$ and $\hat{\mathbf{C}} = \mathbf{A}^{-1}\mathbf{C}$, and , while $\mathbf{U}_0(z)$ is given by

$$\mathbf{U}_0(z) = \mathbf{b}_1 z + \mathbf{b}_2 z^2 + \mathbf{b}_3 z^3, \quad (3.75)$$

with $\mathbf{b}_1 = -2\mathbf{b}_2 - 3\mathbf{b}_3$, $2\mathbf{b}_2 = \hat{\mathbf{B}}^{-1}(\mathbf{J} - \hat{\mathbf{r}}_1)$ and $6\mathbf{b}_3 = -\hat{\mathbf{B}}^{-1}\hat{\mathbf{r}}_0$, where $\hat{\mathbf{r}}(z) = \mathbf{A}^{-1}\mathbf{r}(z) =: \hat{\mathbf{r}}_1 + \hat{\mathbf{r}}_0 z$. Note, \mathbf{A} and \mathbf{B} are invertible because $\chi_1 \chi_2 \phi_{30} \neq 0$ and $E_1 E_2 \phi_{30} \neq 0$, respectively.

For $\gamma \neq -\frac{\chi_1 \chi_2}{\chi_1 + \chi_2} \frac{4}{\pi^2 (2k-1)^2}$ with $k \geq 1$ integer, i.e. $\gamma > 0$ for $\chi_1, \chi_2 > 0$, we write the solution of (3.72) with the homogeneous boundary conditions as a series expansion in sine terms such that the boundary conditions are automatically satisfied of the form

$$\tilde{\mathbf{u}}(z, t) = \sum_{k=1}^{\infty} \mathbf{U}_k(t) \sin(\zeta_k z), \quad (3.76)$$

with $\zeta_k = (2k-1)\pi/2$, while the functions $\mathbf{U}_k(t)$ have to satisfy the ODE

$$\partial_t \mathbf{U}_k(t) + \zeta_k^2 \left(\hat{\mathbf{B}} \mathbf{U}_k(t) + \hat{\mathbf{C}} \partial_t \mathbf{U}_k(t) \right) = \mathbf{0}, \quad (3.77)$$

or, because $\hat{\mathbf{C}} + \zeta_k^{-2} \mathbf{I}$ is invertible due to choice of γ , slightly rewritten as

$$\partial_t \mathbf{U}_k(t) + \mathbf{K}_k \mathbf{U}_k(t) = \mathbf{0}, \quad (3.78)$$

with $\mathbf{K}_k = \left(\hat{\mathbf{C}} + \zeta_k^{-2} \mathbf{I} \right)^{-1} \hat{\mathbf{B}}$ and \mathbf{I} the 2-D unit matrix. This ODE has the fundamental solutions $e^{-\lambda_{1k} t}$ and $e^{-\lambda_{2k} t}$, where λ_{1k} and λ_{2k} are the eigenvalues of the 2x2-matrix \mathbf{K}_k . Hence, $\mathbf{U}_k(t)$ must be of the form

$$\mathbf{U}_k(t) = \mathbf{U}_k \mathbf{C}_k(t), \quad (3.79)$$

where \mathbf{U}_k is the matrix of the eigenvectors of \mathbf{K}_k , i.e.

$$\mathbf{U}_k = \begin{pmatrix} K_{k12} & K_{k12} \\ \lambda_{1k} - K_{k11} & \lambda_{2k} - K_{k11} \end{pmatrix}, \quad (3.80)$$

with K_{kij} the (i, j) entry of \mathbf{K}_k , while

$$\mathbf{C}_k(t) = \begin{pmatrix} c_{k1} e^{-\lambda_{1k} t} \\ c_{k2} e^{-\lambda_{2k} t} \end{pmatrix}, \quad (3.81)$$

with c_{k1} and c_{k2} two unknown constants that will be determined from the condition that

$$\tilde{\mathbf{u}}(z, 0) = \sum_{k=1}^{\infty} \mathbf{U}_k \mathbf{c}_k \sin(\zeta_k z) = -\mathbf{U}_0(z), \quad \mathbf{c}_k = \mathbf{C}_k(0) = \begin{pmatrix} c_{k1} \\ c_{k2} \end{pmatrix}. \quad (3.82)$$

Realizing that $\mathbf{U}_0(z)$ can be expanded in the sine series

$$\mathbf{U}_0(z) = -(2z - z^2)\mathbf{b}_2 - (3z - z^3)\mathbf{b}_3 = S_1(z)\mathbf{b}_2 + S_2(z)\mathbf{b}_3 =: \sum_{k=1}^{\infty} \mathbf{B}_k \sin(\zeta_k z), \quad (3.83)$$

with

$$S_1(z) = -\frac{32}{\pi^3} \sum_{k=1}^{\infty} \frac{1}{(2k-1)^3} \sin(\zeta_k z), \quad S_2(z) = \frac{192}{\pi^4} \sum_{k=1}^{\infty} \frac{(-1)^k}{(2k-1)^4} \sin(\zeta_k z), \quad (3.84)$$

we find

$$\mathbf{c}_k = -\mathbf{U}_k^{-1} \mathbf{B}_k. \quad (3.85)$$

With this result, the solution for $\mathbf{u}(z, t)$ is complete. Recapitulating, we write (3.71) as

$$\mathbf{u}(z, t) = -(2z - z^2)\mathbf{b}_2 - (3z - z^3)\mathbf{b}_3 + \mathbf{J}t + \sum_{k=1}^{\infty} \mathbf{U}_k \mathbf{C}_k(t) \sin(\zeta_k z). \quad (3.86)$$

Finally, we find $v_3(z, t)$ from (3.66) and $W(t)$ from (3.70).

Simulating these results with both Mathematica and MATLAB gave near identical results, except for an unphysical velocity $v_3(z, t)$ in the MATLAB simulation yielding almost negligible small oscillations in time for $u_1(z, t)$, $u_2(z, t)$, and $W(z, t)$. Even though the MATLAB and Mathematica simulations use different approaches, especially for determining the initial velocity $v_3(z, 0^+)$, we can conclude that both simulations are accurate with respect to $u_1(z, t)$, $u_2(z, t)$, and $W(z, t)$, while only the Mathematica simulation shows accurate physical velocities of $v_3(z, t)$. The MATLAB simulations of $u_1(z, t)$, $u_2(z, t)$ and $W(t)$ for different fixed z or t values are shown in Figures 3.6 to 3.10, while the Mathematica plots of $v_3(z, t)$ for different fixed z or t are shown in Figures 3.11 and 3.12, respectively. All simulations are dimensionless.

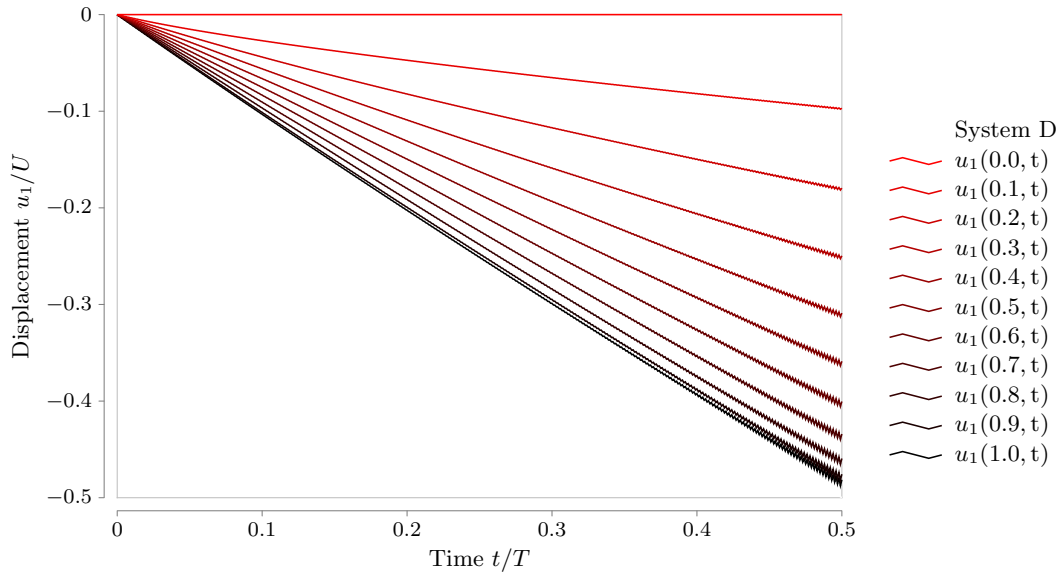


Figure 3.6: MATLAB simulation of $u_1(z, t)$ for $z \in \{0, 0.1, \dots, 0.9, 1\}$ for $A_1 = A_2 = 0$ and the other parameters with the values of Table 3.1. The oscillations in the graphs are due to an unphysical alternating-in-time solution of $v_3(z, t)$ in the MATLAB simulation.

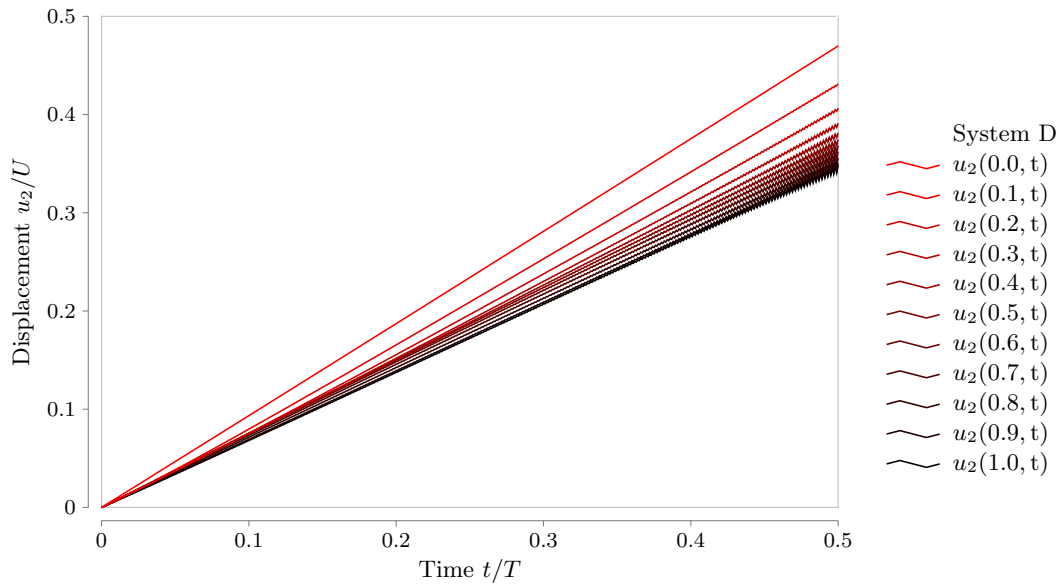


Figure 3.7: MATLAB simulation of $u_2(z, t)$ for $z \in \{0, 0.1, \dots, 0.9, 1\}$ for $A_1 = A_2 = 0$ and the other parameters with the values of Table 3.1. The oscillations in the graphs are due to an unphysical alternating-in-time solution of $v_3(z, t)$ in the MATLAB simulation.

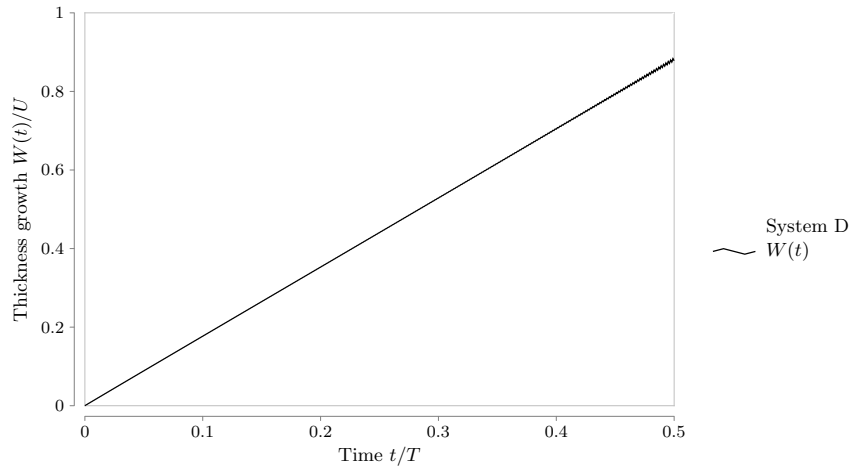


Figure 3.8: MATLAB simulation of $W(t)$ for $A_1 = A_2 = 0$ and the other parameters with the values of Table 3.1. The oscillations in the graphs are due to an unphysical alternating-in-time solution of $v_3(z, t)$ in the MATLAB simulation.

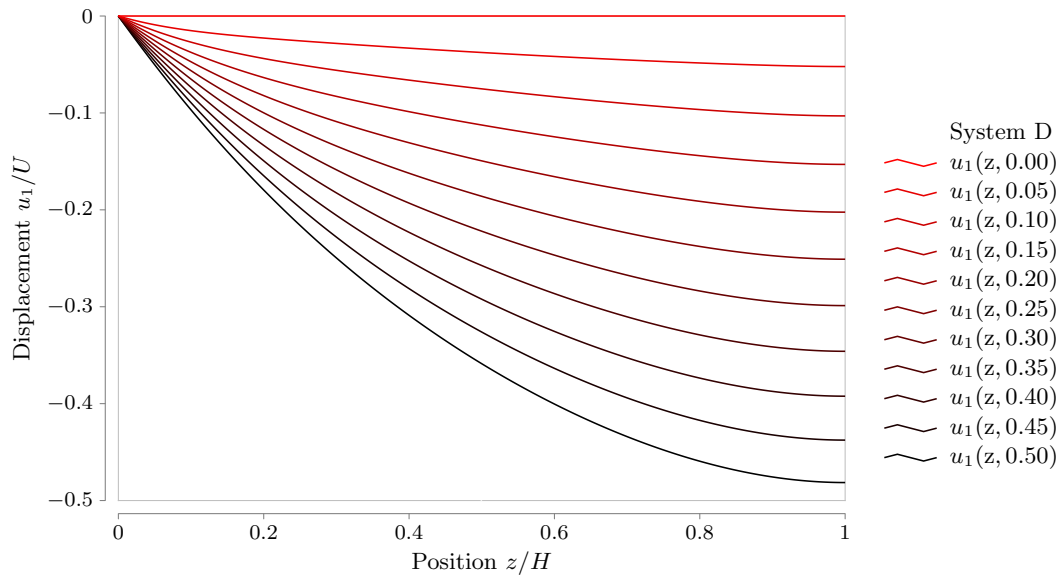


Figure 3.9: MATLAB simulation of $u_1(z, t)$ for $t \in \{0, 0.05, \dots, 0.45, 0.50\}$ for $A_1 = A_2 = 0$ and the other parameters with the values of Table 3.1. The oscillations in the graphs are due to an unphysical alternating-in-time solution of $v_3(z, t)$ in the MATLAB simulation.

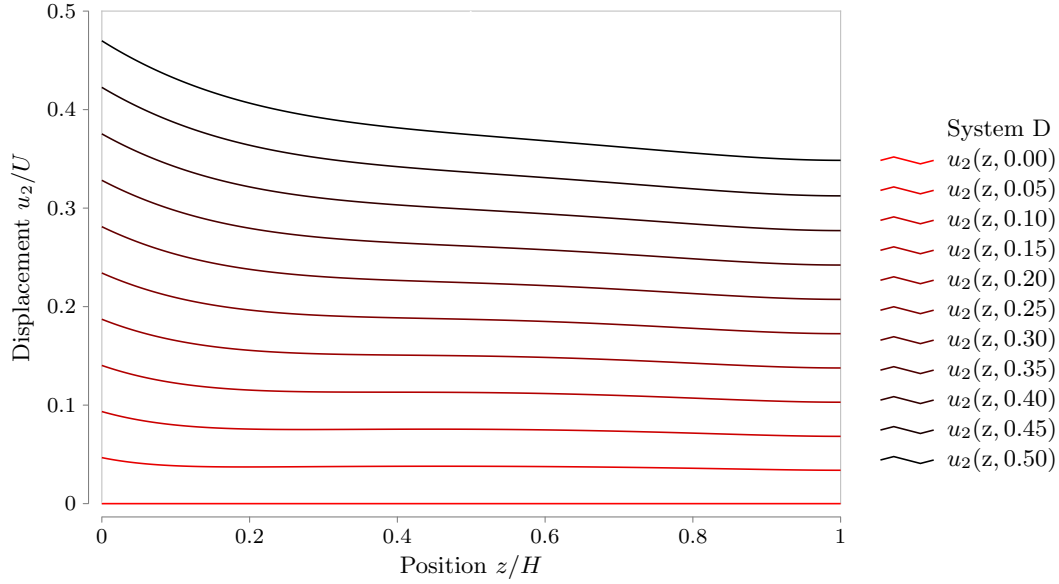


Figure 3.10: MATLAB simulation of $u_2(z, t)$ for $t \in \{0, 0.05, \dots, 0.45, 0.50\}$ for $A_1 = A_2 = 0$ and the other parameters with the values of Table 3.1. The oscillations in the graphs are due to an unphysical alternating-in-time solution of $v_3(z, t)$ in the MATLAB simulation.

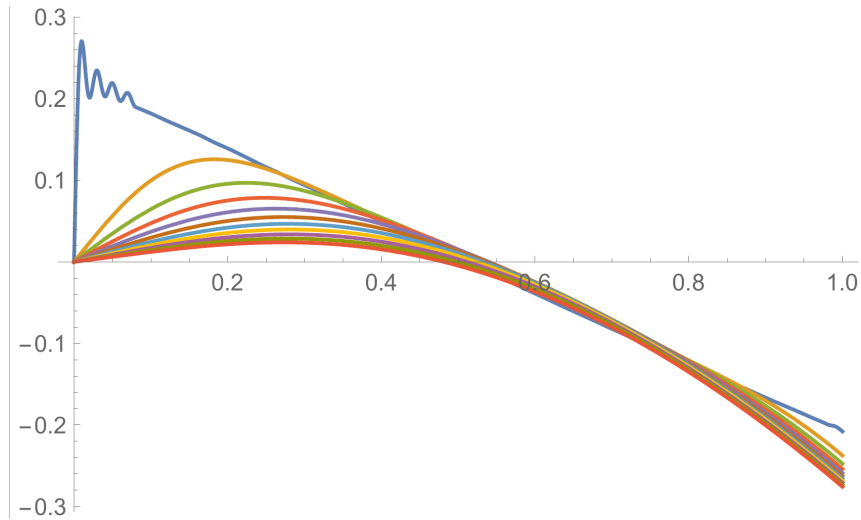


Figure 3.11: Mathematica simulation of $v_3(z, t)$ with from top to bottom $t \in \{0, 0.05, \dots, 0.45, 0.50\}$, respectively, for $A_1 = A_2 = 0$ and the other parameters with the values of Table 3.1. The oscillations in the $t = 0$ graph are artifacts of the inevitable truncation of the infinite sum in Equation (3.86).

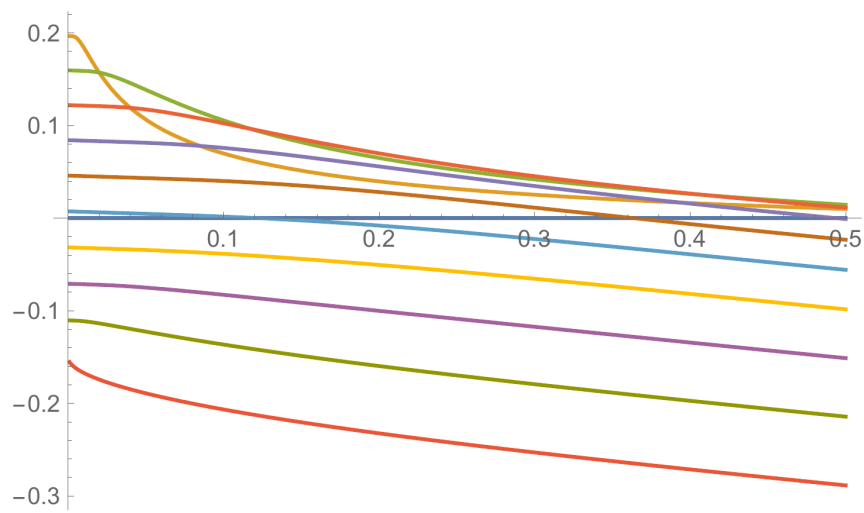


Figure 3.12: Mathematica simulation of $v_3(z, t)$ for $z \in \{0, 0.1, \dots, 0.9, 1\}$ with the order in the same color scheme as in Figure 3.11 for $A_1 = A_2 = 0$ and the other parameters with the values of Table 3.1.

Weak Solvability of a Pseudoparabolic system

Based on:

A.J. Vromans, A.A.F. van de Ven, and A. Muntean, “Existence of weak solutions for a pseudo-parabolic system coupling chemical reactions, diffusion and momentum equations”, *Advances in Mathematic Sciences and Applications*, vol. 28, no. 1, 2019, pp. 273-311

A.J. Vromans, A.A.F. van de Ven and A. Muntean, “Existence of weak solutions for a pseudo-parabolic system coupling chemical reactions, diffusion and momentum equations,” 2017, CASA-report **17-03**

In this chapter the weak solvability of a nonlinearly coupled system of parabolic and pseudo-parabolic equations describing the interplay between mechanics, chemical reactions, diffusion and flow modelled within a mixture theory framework is studied via energy-like estimates and Gronwall inequalities. In analytically derived parameter regimes, these estimates ensure the convergence of discretized-in-time partial differential equations. These regimes are tested and extended numerically. Especially, the dependence of the temporal existence domain of physical behaviour on selected parameters is shown.

4.1 Introduction

We investigate the existence of weak solutions to a system of partial differential equations coupling chemical reaction, momentum transfer and diffusion, cast in the framework of mixture theory [19]. For simplicity, we restrict ourselves to a model with a single non-reversible chemical reaction in a one-dimensional bounded spatial domain $[0, 1]$ enclosed by unlimited (or instantly replenished) reservoirs of the reacting chemicals. The chemical reaction is of the $(N + 1)$ -to-1-type with the reacting chemicals consisting of N solids and a single fluid, while the produced chemical is a solid. New mathematical challenges arise due to the strong nonlinear coupling between all unknowns and their transport fluxes.

Evolution systems can describe physical systems or biological processes via the balances of masses and forces. These type of systems often contain chemical reactions, momentum transfer, diffusion and stresses; see e.g. [25, 44, 53, 108]. Here, the interest lies in capturing the interactions between flows, deformations, chemical reactions and structures. Such a system is, for instance, used in biology to better understand and eventually forecast plant growth and plant development [108], and in structural engineering to describe ambient corrosion, for example sulfate attack in sewer pipes [53], in order to increase the durability of an exposed concrete sample. Our initial interest in this topic originates from mathematical descriptions of sulfate corrosion [14]. The mathematical techniques used for a system describing sulfate attack - when within a porous media (concrete) sulfuric acid reacts with slaked lime to produce gypsum - could be equally well applied to systems sharing similar features (e.g. types of flux couplings and nonlinearities).

At a general level, the system outlined in this chapter is a combination of parabolic equations of diffusion-drift type with production terms by chemical reactions and pseudo-parabolic stress equations containing elastic and viscoelastic terms. On their own, both parabolic equations, cf. [48, 80, 83],

and pseudo-parabolic equations, see [15, 50, 55, 112, 115, 128, 133], are well understood from mathematical and numerical analysis perspectives. However, coupling these objects leads to systems of equations with a less understood structure. Many systems in the literature seem similar to ours at a first glance. A coupling resembling our case appears in [1], but with different nonlinear terms due to the combination of Navier-Stokes and Cahn-Hilliard systems. Other systems do not use chemical reactions or diffusion like in [25], where multi-dimensional Navier-Stokes-like stress equations are used; refer to a composite domain situation [44]; do not use stress equations [53]; contain a hyperbolic stress equation [108]; or have different non-linearities [10]. Furthermore, the techniques we employ are well-established in pseudo-parabolic systems, such as porous media flow models, and are capable of handling non-linearities, non-localities, singularities, degeneracies, and singular limits, see e.g. [23, 24, 49, 93, 113, 114, 125].

We investigate in this chapter the simplest case: a one-dimensional bounded domain. The one-dimensional setting allows one to control the nonlinearities by relying on the embedding $H^1 \hookrightarrow L^\infty$. In higher-dimensions, this embedding does not hold, and hence, nonlinearities become difficult to control. Usually higher regularity in the data can yield higher regularity solutions, which via embedding results such as Rellich-Kondrachov can lead to L^∞ again. If this is not possible, than quite often structural properties such as monotonicity or Lipschitz-continuity of coefficients can lead to sufficient control of the nonlinearities.

The main target here is to probe the parameter region for which the system is weakly solvable. To this aim we search for explicit expressions of a priori parameter-dependent bounds. These bounds delimit the parameter region where the existence of our concept of weak solutions holds. Our numerical simulations show that the existence region is actually larger.

In Section 4.2 we introduce our mathematical model together with a set of assumptions based on which the existence of weak solutions can be proven. In Section 4.3 we present two theorems: the main existence theorem for the continuous-time system with certain physical constraints and an auxilliary existence theorem for the time-discretized version of the system. In Section 4.4 we prove the auxilliary existence theorem and, then, in Section 4.5 we prove the main existence theorem by using the auxilliary existence theorem. In Section 4.6, we validate numerically the existence of solutions and, additionally, we show numerically that the assumptions seem to be more restrictive than necessary. Moreover, we show in what manner the existence of weak solutions depends on certain crucial parameters.

4.2 Formulation of the model equations

Consider a 1-D body, modeled as a d -component ($d \geq 2$) mixture of $(d - 1)$ solid components and one fluid component. The body will deform under the action of chemical reactions. This process is described by a system of partial differential equations (PDEs) and initial and boundary conditions.

We define our system on a time-space domain $[0, T] \times [0, 1]$, where T is the not yet determined final time of the process. The unknowns of our system are two vector functions, $\phi : ([t_0, T] \times [0, 1])^d \rightarrow \mathbf{R}^d$ and $\mathbf{w} : ([t_0, T] \times [0, 1])^{d-1} \rightarrow \mathbf{R}^{d-1}$, and two scalar functions $v : [0, T] \times [0, 1] \rightarrow \mathbf{R}$ and $W : [0, T] \rightarrow \mathbf{R}$. The vector ϕ denotes the volume fractions of the d chemical components active in a target chemical reaction. The vector \mathbf{w} denotes the displacements of the solid mixture components with respect to the initial domain as reference coordinate system. The scalar v denotes the velocity of the fluid. Lastly, the scalar W denotes the domain size. We identify the different components of the vectors with the different chemicals and use the following notation convention: The subscript 1 is related to the produced chemical, the subscript d is related to the fluid, all other subscripts are related to the remaining solid chemicals.

The time evolution of the unknowns is described by the following system of coupled partial differential equations: For $l \in \mathfrak{L} = \{1, \dots, d - 2, d\}$, the index of the reacting chemicals, and $m \in \mathfrak{M} = \{1, \dots, d - 1\}$, the index of the solid chemicals, we have

$$\partial_t \phi_l - \delta_l \partial_z^2 \phi_l + I_l(\phi) \partial_z (\Gamma(\phi)v) + \sum_{m \in \mathfrak{M}} \sum_{i,j=0}^1 \partial_z^i \left(B_{lijm}(\phi) \partial_t^j w_m \right) = G_{\phi,l}(\phi), \quad (4.1a)$$

$$\partial_z (\Gamma(\phi)v) + \sum_{m \in \mathfrak{M}} \sum_{j=0}^1 \partial_z \left(H_{jm}(\phi) \partial_t^j w_m \right) = G_v(\phi), \quad (4.1b)$$

$$\begin{aligned} \partial_t w_m - D_m \partial_z^2 w_m - \gamma_m \partial_z^2 \partial_t w_m + F_m(\phi)v \\ + \sum_{j \in \mathfrak{M}} \sum_{\substack{i+n=0 \\ i,n \geq 0}}^1 \partial_z \left(E_{minj}(\phi) \partial_z^i \partial_t^n w_j \right) = G_{w,m}(\phi), \end{aligned} \quad (4.1c)$$

with constants $\delta_l, D_m, \gamma_m \in \mathbf{R}_+$ and functions $I_l, \Gamma, B_{lijm}, H_{jm}, F_m, E_{minj}, G_{\phi,l}, G_v, G_{w,m}$ that are actually products of functions $f_i(\cdot) \in C^1([0, 1])$,

satisfying

$$f(\boldsymbol{\phi}) = \prod_{i=1}^d f_i(\phi_i). \quad (4.2)$$

Furthermore, we abuse notation with $\|f(\cdot)\|_{C^1([0,1])} \leq f \in \mathbf{R}_+$ for reducing the amount of constants.

Physically, Equation (4.1a) can be interpreted as a generalized reaction-diffusion-advection equation obtained from a mass balance law, Equation (4.1b) can be interpreted as a transport equation indicating the consequences of retaining incompressibility, and Equation (4.1c) is a pseudo-parabolic equation obtained from a generalized momentum balance law.

Note that the system (4.1a) - (4.1c) must satisfy the constraint $\sum_{l=1}^d \phi_l = 1$, the fundamental equation of fractions, which allowed for the elimination of ϕ_{d-1} .

We assume the volume fractions are insulated at the boundary: $\partial_z \boldsymbol{\phi} = 0$ at $z = 0$ and $z = 1$. The boundary at $z = 0$ is assumed to be fixed, while the boundary at $z = 1$ has a displacement $W(t) = h(t) - 1$, where $h(t)$ is the height of the reaction layer at the present time t and $h(0) = 1$. The Rankine-Hugoniot relations, see e.g. [96], state that the velocity of a chemical at a boundary is offset from $\mathbf{V}_0 = 0$ or $\mathbf{V}_1 = \partial_t W(t)$, the velocity of the boundary at $z = 0$ or $z = 1$, respectively, by influx or outflux of this chemical, i.e.

$$\text{at } z = 0 \text{ and } z = 1 \text{ hold } \begin{cases} \phi_m (\mathbf{V}_{0,1} - \partial_t w_m) \cdot \hat{\mathbf{n}} = J_m \mathcal{L}(\phi_{m,res} - \phi_m) \\ \phi_d (\mathbf{V}_{0,1} - v) \cdot \hat{\mathbf{n}} = J_d \mathcal{L}(\phi_{d,res} - \phi_d) \end{cases} \quad (4.3)$$

with $J_d, J_m \geq 0$ for $m \in \mathfrak{M}$, $\phi_{d,res}, \phi_{m,res} \in [0, 1]$ for $m \in \mathfrak{M}$ and $\sum_{j=1}^d \phi_{j,res} = 1$. We assume $\mathcal{L}(\cdot)$, the concentration jump across the boundary, to have the semi-permeable form $\mathcal{L}(f) := f_+$, the positive part of f . Furthermore, we assume all chemicals have only one reservoir. The fluid chemical reservoir is assumed to be at $z = 1$: $\phi_{d,res} \geq 0$ at $z = 1$, $\phi_{d,res} = 0$ at $z = 0$. The solid chemical reservoirs are assumed to be at $z = 0$: $\phi_{m,res} = 0$ at $z = 1$, $\phi_{m,res} \geq 0$ at $z = 0$ for $m \in \mathfrak{M}$. We generalize the Rankine-Hugoniot relations by replacing ϕ_m with $H_{1m}(\boldsymbol{\phi})$ and ϕ_d with $\Gamma(\boldsymbol{\phi})$ in Equation (4.3).

The influx due to the Rankine-Hugoniot relations shows that the displacement $w_m|_{z=1}$ will not be equal to the boundary displacement $W(t)$. This will result in stresses, which we incorporate within a Robin boundary condition at these locations [105, Section 5.3]. Collectively for all $t \in [0, T]$, these boundary

conditions are, for $m \in \mathfrak{M}$, $l \in \mathfrak{L}$, given by

$$\begin{cases} \partial_z \phi_l|_{z=0} = 0, \\ \partial_z \phi_l|_{z=1} = 0, \end{cases} \quad (4.4a)$$

$$\begin{cases} H_{1m}(\phi) \partial_t w_m|_{z=0} = J_m \mathcal{L}(\phi_{m,res} - \phi_m|_{z=0}), \\ \partial_z w_m|_{z=1} = A_m (w_m|_{z=1} - W(t)), \\ v|_{z=0} = 0, \\ \Gamma(\phi) (\partial_t W(t) - v)|_{z=1} = J_d \mathcal{L}(\phi_{d,res} - \phi_d|_{z=1}), \end{cases} \quad (4.4b)$$

where $A_m \in \mathbf{R}$. Additionally there are positive lower bounds for $\Gamma(\phi)$ and all H_{1m} : $\Gamma_\alpha := \inf_{\phi \in \mathcal{I}_\alpha^d} \Gamma(\phi) > 0$ and $H_\alpha := \min_{m \in \mathfrak{M}} \inf_{\phi \in \mathcal{I}_\alpha^d} H_{1m}(\phi) > 0$, with $\mathcal{I}_\alpha = (\alpha, 1 - (d-1)\alpha)$ for all $0 < \alpha < 1/d$. It is worth noting, that in the limit $|A_m| \rightarrow \infty$ one formally obtains Dirichlet boundary conditions. The initial conditions describe a uniform and stationary equilibrium solution at $t = 0$:

$$\phi_l(0, z) = \phi_{l0} \quad \text{and} \quad w_m(0, z) = 0 \quad \text{for all } z \in [0, 1] \quad \text{and} \quad W(0) = 0. \quad (4.5)$$

Restricting our initial conditions to a uniform and stationary equilibrium solution was chosen on a physical ground. Moreover, this choice simplified some arguments. A posteriori, we could have relaxed this condition to for example elements of $H^1(0, 1)$ or $L^2(0, 1) \cap L^\infty(0, 1)$.

Note that $v(0, z) \in H^1(0, 1)$ does not need to be specified as $v(0, z)$ follows from Equations (4.1b), (4.1c), and (4.4a) on $\{0\} \times (0, 1)$.

The system of PDEs including initial and boundary conditions described above is called the *continuous-time system* for later reference in this chapter.

4.3 Main existence result

Introduce $\phi_{\min} \in (0, 1 - C_{1,0}(d-1)/d]$. Moreover, $C_{1,0}$, the optimal Sobolev constant of the embedding $H^1(0, 1) \hookrightarrow C^0[0, 1]$, is given by $C_{1,0} = \coth(1)$, see [144].

We assume that the following set of restrictions is satisfied.

Assumption 4.1.

We assume the parameters of the continuous-time system to satisfy:

- (i) $\delta_l > 0$,

$$(ii) |A_m| < 1,$$

$$(iii) E_{m01j}^2 < \frac{4}{9(d-1)^2} \min\{3/5, \gamma_m(1 - |A_m|)\} \min\{3, \gamma_j(1 - |A_j|)\},$$

$$(iv) 4\Gamma(\phi_0)^2 > (5d - 4)^2 F_m(\phi_0)^2 H_{1j}(\phi_0)^2,$$

$$(v) \phi_{i0} \geq \phi_{\min} \text{ and } \sum_{i \neq \tilde{i}} \phi_{i0} < \frac{1 - \phi_{\min}}{C_{1,0}} \text{ for all } 1 \leq \tilde{i} \leq d, \text{ while } \sum_{i=1}^d \phi_{i0} = 1,$$

$$(vi) (3d - 2)(5d - 4)\gamma_j A_j^2 < 1,$$

$$(vii) 4\gamma_j > (3d - 2)(5d - 4)H_{1m}(\phi_0)^2 / \Gamma(\phi_0)^2.$$

for all $j, m \in \mathfrak{M}$, all $l \in \mathfrak{L}$, and all $i \in \{1, \dots, d\}$.

Additionally, we assume that the parameters are such that there exist positive constants $\eta_{m1}, \eta_{m2}, \eta_{m01j1}, \eta_{m01j2} > 0$ for $j, m \in \mathfrak{M}$ satisfying

$$(viii) \mathfrak{C}_{1m} = 1 - \sum_{j \in \mathfrak{M}} E_{j01m} \frac{\eta_{j01m1}}{2} > 0,$$

$$(ix) \mathfrak{C}_{2m} = \gamma_m(1 - |A_m|) - \frac{\eta_{m1} + \eta_{m2}}{2} - \frac{1}{2} \sum_{j \in \mathfrak{M}} \left(\frac{E_{m01j}}{\eta_{m01j1}} + \frac{E_{m01j}}{\eta_{m01j2}} + E_{j01m} \eta_{j01m2} \right) > 0,$$

$$(x) \frac{7d-5}{\Gamma_{\phi_{\min}}^2} \max_{m \in \mathfrak{M}} \left\{ \frac{H_{1m}^2}{\mathfrak{C}_{2m}} \right\} \sum_{m \in \mathfrak{M}} \left(\frac{\gamma_m^2 |A_m|^2}{2\eta_{m1}} + \frac{F_m^2}{2\eta_{m2}} \right) < 1$$

for all $m \in \mathfrak{M}$.

Note, conditions (i), (ii), (viii) and (ix) are necessary conditions for coercivity in order to obtain a-priori estimates. Conditions (iii), (iv), (vi) and (vii) are necessary conditions for coercivity of a special system in Section 4.8 for the existence of a special physical v^0 , the instantaneous initial velocity field. Condition (v) guarantees the physical condition $\phi^k \in (\phi_{\min}, 1 - (d-1)\phi_{\min})^d$, while condition (x) guarantees boundedness of $\|v\|_{L^2(0,T;H^1(0,1))}$.

Accepting Assumption 4.1, we can now formulate the main result of this chapter.

Theorem 4.1.

Let $d \in \{2, 3, 4\}$ and let the parameters satisfy Assumption 4.1. Then there

exist constants $T > 0$ and $V > 0$ and functions

$$\begin{aligned} \phi_l &\in L^2(0, T; H^2([0, 1])) \cap L^\infty(0, T; H^1(0, 1)) \\ &\quad \cap C^0([0, T]; C^0[0, 1]) \cap H^1(0, T; L^2(0, 1)), \end{aligned} \quad (4.6a)$$

$$v \in L^2(0, T; H^1(0, 1)), \quad (4.6b)$$

$$\begin{aligned} w_m &\in L^\infty(0, T; H^2(0, 1)) \cap C^0([0, T]; C^1[0, 1]) \\ &\quad \cap H^1(0, T; H^1(0, 1)), \end{aligned} \quad (4.6c)$$

$$W \in H^1(0, T), \quad (4.6d)$$

for all $l \in \mathfrak{L}$, $m \in \mathfrak{M}$ such that $(\phi_1, \dots, \phi_{d-2}, \phi_d, v, w_1, \dots, w_{d-1}, W)$ satisfies the weak version of the continuous system (4.1a)-(4.1c), (4.4a), (4.4b), and (4.5), such that

$$(I) \quad \|v\|_{L^2(0, T; L^2(0, 1))} \leq V,$$

$$(II) \quad \|\partial_z v\|_{L^2(0, T; L^2(0, 1))} \leq V,$$

$$(III) \quad \min_{1 \leq l \leq d} \min_{t \in [0, T]} \min_{z \in [0, 1]} \phi_l(t, z) \geq \phi_{\min} \text{ with } \phi_{d-1} = 1 - \sum_{l \in \mathfrak{L}} \phi_l.$$

The proof of this theorem is given in Section 4.5, and consists of the following three steps:

Step 1.

First, we assume conditions (I), (II), and (III) to hold. We discretise the continuous-time system in time with a regular grid of step size Δt , and apply a specific Euler scheme. This is the so-called Rothe method, see [74, 120]. Our chosen discretization is such that the equations become linear elliptic equations with respect to evaluation at time slice $\{t = t_k\}$ and only contain evaluations at time slices $\{t = t_k\}$ and $\{t = t_{k-1}\}$. The time derivative $\partial_t u$ is replaced with the standard first order finite difference $\mathcal{D}_{\Delta t}^k(u) := (u^k - u^{k-1})/\Delta t$, where we use the notation $u^k(z) := u(t_k, z)$. The discretised system has the

form

$$\mathcal{D}_{\Delta t}^k(\phi_l) - \delta_l \partial_z^2 \phi_l^k + I_l(\phi^{k-1}) \partial_z (\Gamma(\phi^{k-1}) v^{k-1}) \quad (4.7a)$$

$$+ \sum_{m \in \mathfrak{M}} \sum_{i=0}^1 \partial_z^i (B_{li0m}(\phi^{k-1}) w_m^{k-1} + B_{li1m}(\phi^{k-1}) \mathcal{D}_{\Delta t}^k(w_m)) = G_{\phi,l}(\phi^{k-1}),$$

$$\sum_{m \in \mathfrak{M}} \partial_z (H_{0m}(\phi^{k-1}) w_m^{k-1} + H_{1m}(\phi^{k-1}) \mathcal{D}_{\Delta t}^k(w_m)) \quad (4.7b)$$

$$+ \partial_z (\Gamma(\phi^{k-1}) v^k) = G_v(\phi^{k-1}),$$

$$\mathcal{D}_{\Delta t}^k(w_m) - D_m \partial_z^2 w_m^k - \gamma_m \partial_z^2 \mathcal{D}_{\Delta t}^k(w_m) + F_m(\phi^{k-1}) v^{k-1} \quad (4.7c)$$

$$+ \sum_{j \in \mathfrak{M}} \sum_{i=0}^1 \partial_z (E_{mi0j}(\phi^{k-1}) \partial_z^i w_j^{k-1} + E_{m01j}(\phi^{k-1}) \mathcal{D}_{\Delta t}^k(w_j)) = G_{w,m}(\phi^{k-1}),$$

with initial conditions Equation (4.5) while the boundary conditions (4.3), (4.4a), and (4.4b) become:

$$\begin{cases} \partial_z \phi_l^k \Big|_{z=0} = 0, \\ \partial_z \phi_l^k \Big|_{z=1} = 0, \end{cases} \quad (4.8a)$$

$$\begin{cases} H_{1m}(\phi^{k-1}|_{z=0}) \mathcal{D}_{\Delta t}^k(w_m) \Big|_{z=0} = J_m \mathcal{L}(\phi_{m,res} - \phi_m^{k-1}|_{z=0}) \\ \partial_z w_m^k \Big|_{z=1} = A_m(w_m^k|_{z=1} - W^k) \\ v^k \Big|_{z=0} = 0 \\ \Gamma(\phi^{k-1}|_{z=1}) (\mathcal{D}_{\Delta t}^k(W) - v^{k-1}) \Big|_{z=1} = J_d \mathcal{L}(\phi_{d,res} - \phi_d^{k-1}|_{z=1}), \end{cases} \quad (4.8b)$$

for $l \in \mathfrak{L}$ and $m \in \mathfrak{M}$, with the notation $W^k := W(t_k)$.

For convenience, we refer to the discretised system (4.7a)-(4.7c), (4.8a), and (4.8b) as the *discrete-time system*.

A powerful property of this discrete-time system is its sequential solvability at time t_k : the existence of a natural hierarchy in attacking this problem. First, we obtain results for Equation (4.7c), then we use these results to obtain results for both Equations (4.7a) and (4.7b). Moreover, the structure of the discrete-time system is that of an elliptic system. Hence, the general existence and uniqueness theory for elliptic systems can be extended directly to cover our situation. One can either apply standard results from ordinary differential equations (ODEs), cf. [110, p.130], or from elliptic theory, cf. Chapter 6 in [48], since the discrete-time system at each time slice $\{t = t_k\}$ can be put into the form $\mathcal{A}(u^k, v^k) = \mathcal{F}^{k-1} v^k$ with \mathcal{A} a continuous coercive bilinear form and \mathcal{F}^{k-1} a continuous operator depending on the previous time slice

$\{t = t_{k-1}\}$ allowing Lax-Milgram to be applied. We take the elliptic theory option. See Section 2.3 for introductory references to elliptic solvability theory.

Step 2.

We prove Theorem 4.2, the discretized version of Theorem 4.1, in Section 4.4 by testing the time-discrete system with specific test functions such that we obtain quadratic inequalities by using conditions (I), (II) and (III). By application of Young's inequality and using Gronwall-like lemmas we obtain energy-like estimates, which are step size Δt -independent upper bounds of the Sobolev norms of the weak solutions. These bounds allow for weakly convergent sequences in Δt small parameter. Moreover, the upper bounds of the energy-like estimates are monotonically increasing functions of T and V , the parameters used in (I), (II) and (III). With these upper bounds, we test whether or not the conditions (I), (II) and (III) can be satisfied: the consistency check of our assumption. This leads to the conditions of Assumption 4.1 to guarantee overlapping regions in (T, V) -space for which Theorem 4.2 holds for Δt small enough, including the conditions (I), (II) and (III). Since $T > 0$ and $V > 0$ only have to exist, it is sufficient to find a non-empty intersection of all the overlapping regions.

Theorem 4.2.

Let $d \in \{2, 3, 4\}$ and let the parameters satisfy Assumption 4.1, then there exist $T > 0$, $V > 0$, $\hat{\tau} > 0$ and $C > 0$ independent of Δt such that for all $0 < \Delta t < \hat{\tau}$ there exists a sequence of functions $(\phi_1^k, \dots, \phi_{d-2}^k, \phi_d^k, v^k, w_1^k, \dots, w_{d-1}^k, W^k)$ for $0 \leq t_k \leq T$ satisfying the weak version of the discrete-time system given by Equations (4.7a)-(4.7c), (4.8a), (4.8b), and (4.5) as well as the following

a priori bounds

$$\sum_{j=0}^k \|\partial_z v^j\|_{L^2(0,1)}^2 \Delta t, \sum_{j=0}^k \|v^j\|_{L^2(0,1)}^2 \Delta t \leq V^2, \quad (4.9a)$$

$$\min_{1 \leq l \leq d} \min_{z \in [0,1]} \phi_l^k(z) \geq \phi_{\min}, \quad (4.9b)$$

$$\|\phi_1^k\|_{H^1(0,1)}, \dots, \|\phi_d^k\|_{H^1(0,1)} \leq C, \quad (4.9c)$$

$$\sum_{j=1}^k \|\phi_1^j\|_{H^2(0,1)}^2 \Delta t, \dots, \sum_{j=1}^k \|\phi_d^j\|_{H^2(0,1)}^2 \Delta t \leq C, \quad (4.9d)$$

$$\sum_{j=1}^k \|\mathcal{D}_{\Delta t}^k(\phi_1^j)\|_{L^2(0,1)}^2 \Delta t, \dots, \sum_{j=1}^k \|\mathcal{D}_{\Delta t}^k(\phi_d^j)\|_{L^2(0,1)}^2 \Delta t \leq C, \quad (4.9e)$$

$$\|w_1^k\|_{H^2}, \dots, \|w_{d-1}^k\|_{H^2(0,1)} \leq C, \quad (4.9f)$$

$$\sum_{j=1}^k \|\mathcal{D}_{\Delta t}^k(w_1^j)\|_{H^1(0,1)}^2 \Delta t, \dots, \sum_{j=1}^k \|\mathcal{D}_{\Delta t}^k(w_{d-1}^j)\|_{H^1(0,1)}^2 \Delta t \leq C, \quad (4.9g)$$

$$|W^k|, \sum_{j=1}^k |\mathcal{D}_{\Delta t}^k(W)|^2 \Delta t \leq C, \quad (4.9h)$$

for all $0 \leq t_k \leq T$, where $\phi_{d-1}^k = 1 - \sum_{l \in \mathcal{L}} \phi_l^k$.

Step 3.

We introduce temporal interpolation functions $\hat{u}(t) = u^{k-1} + (t - t_{k-1})\mathcal{D}_{\Delta t}^k(u)$ on $[t_0, T] \times [0, 1]$. Then we use Theorem 4.2 to show that the interpolation functions are measurable, bounded and converge weakly. With the Lions-Aubin-Simon lemma, see [27, 40], in combination with the Rellich-Kondrachov theorem, see [2, p.143] and [20], we show strong convergence as well. The proof concludes by showing that the weak solution of the time-discrete system converges to a weak solution of the continuous-time system.

Remark 4.1. From now on $\|\cdot\|_{\mathbb{X}(0,1)}$ will be denoted as $\|\cdot\|_{\mathbb{X}}$.

4.4 Proof of Theorem 4.2

The proof of Theorem 4.2 is done in three steps. First, energy bounds are obtained by assuming there exist $\phi_{\min} > 0$, $V > 0$ and $T > 0$ for which the

three inequalities of Theorem 4.2 hold.¹ Second, we apply two discrete variants of Gronwall's inequality to the quadratic inequalities to obtain a-priori estimates independent of Δt . Lastly, we show that $\phi_{\min} > 0$, $V > 0$ and $T > 0$ can be chosen if Assumption 4.1 is satisfied by the parameters of the continuous-time system.

Before we can do these three steps, we must show that the discrete-time system is well-posed. We do this iteratively in k , such that the solution of time slice t_{k-1} implies the well-posedness of the solution of time slice k . Since the initial conditions (4.5) are smooth and v^0 follows from a second order system, we obtain the well-posedness for all $t_k \in [0, T]$. In more detail see Section 4.8.

We obtain the weak form of the discrete-in-time system by multiplying the model equations with a function in $H^1(0, 1)$, integrating over $(0, 1)$ and applying the boundary conditions where needed. We test Equation (4.7a) with ϕ_l^k and $\mathcal{D}_{\Delta t}^k(\phi_l)$, and Equation (4.7c) with w_m^k and $\mathcal{D}_{\Delta t}^k(w_m)$ to obtain the quadratic inequalities below:

$$\begin{aligned}
& \mathcal{D}_{\Delta t}^k \left(\sum_{m \in \mathfrak{M}} \|w_m\|_{L^2}^2 + a_{1m} \|\partial_z w_m\|_{L^2}^2 \right) \\
& \quad + \sum_{m \in \mathfrak{M}} \left[a_{2m}(\Delta t) \|\mathcal{D}_{\Delta t}^k(w_m)\|_{L^2}^2 + a_{3m}(\Delta t) \|\mathcal{D}_{\Delta t}^k(\partial_z w_m)\|_{L^2}^2 \right] \\
& \leq a_4 + \sum_{m \in \mathfrak{M}} \left[a_{5m} \|w_m^k\|_{L^2}^2 + a_{6m} \|\partial_z w_m^k\|_{L^2}^2 + a_{7m} \|w_m^{k-1}\|_{L^2}^2 + a_{8m} \|\partial_z w_m^{k-1}\|_{L^2}^2 \right. \\
& \quad \left. + a_{9m} \|\mathcal{D}_{\Delta t}^k(w_m)\|_{L^2}^2 + a_{10m} \|\mathcal{D}_{\Delta t}^k(\partial_z w_m)\|_{L^2}^2 \right] + a_{11} \|v^{k-1}\|_{L^2}^2 + a_{12} \|\partial_z v^{k-1}\|_{L^2}^2,
\end{aligned} \tag{4.10}$$

¹We would like to point out that for a given time T , which is not defined as the size of the temporal domain for which (I), (II), and (III) in Theorem 1 hold, the common procedure for applying the Rothe method is the procedure as followed in [34], since one can choose sequences Δt decreasing to 0 such that $T/\Delta t$ is an integer. However, in our case we cannot a-priori claim that $T \geq \Delta t$ is satisfied or that $T/\Delta t$ is an integer. We show that there is a delicate relation between T , V and Δt and that a $T > \Delta t$ and $V > 0$, both independent of Δt , for sufficiently small Δt can be chosen from a connected set of (T, V) points for which (I) and (II) hold for all sufficiently small Δt , especially for sequences Δt such that $T/\Delta t$ is an increasing integer. Moreover, one can even choose (T, V) -points independent of Δt such that (I), (II), and (III) in Theorem 1 hold for all Δt sufficiently small and $T/\Delta t$ an increasing sequence of integers.

for all $l \in \mathfrak{L}$

$$\begin{aligned} & \mathcal{D}_{\Delta t}^k (\|\phi_l\|_{L^2}^2) + b_{1l} \|\partial_z \phi_l^k\|_{L^2}^2 + b_{2l} (\Delta t) \|\mathcal{D}_{\Delta t}^k(\phi_l)\|_{L^2}^2 \\ & \leq b_{3l} + b_{4l} \|\partial_z v^{k-1}\|_{L^2}^2 + b_{5l} \|\phi_l^k\|_{L^2}^2 + \sum_{n \in \mathfrak{L}} [b_{6ln} \|\partial_z \phi_n^{k-1}\|_{L^2}^2] \\ & \quad + \sum_{m \in \mathfrak{M}} \sum_{i=0}^1 \left[b_{7lim} \|\partial_z^i w_m^{k-1}\|_{L^2}^2 + b_{8lim} \|\mathcal{D}_{\Delta t}^k(\partial_z^i w_m)\|_{L^2}^2 \right], \end{aligned} \quad (4.11)$$

and

$$\begin{aligned} & \mathcal{D}_{\Delta t}^k \left(\sum_{l \in \mathfrak{L}} \|\partial_z \phi_l\|_{L^2}^2 \right) + \sum_{l \in \mathfrak{L}} \left[c_{1l} \|\mathcal{D}_{\Delta t}^k(\phi_l)\|_{L^2}^2 + c_{2l} (\Delta t) \|\mathcal{D}_{\Delta t}^k(\partial_z \phi_l)\|_{L^2}^2 \right] \\ & \leq c_3 + c_4 \|\partial_z v^{k-1}\|_{L^2}^2 + \sum_{l \in \mathfrak{L}} \left[c_{5l} \|\mathcal{D}_{\Delta t}^k(\phi_l)\|_{L^2}^2 + c_{6l}^k \|\partial_z \phi_l^{k-1}\|_{L^2}^2 \right] \\ & \quad + \sum_{m \in \mathfrak{M}} \sum_{i=0}^1 \left[c_{7im} \|\partial_z^i w_m^{k-1}\|_{L^2}^2 + c_{8im} \|\mathcal{D}_{\Delta t}^k(\partial_z^i w_m)\|_{L^2}^2 \right]. \end{aligned} \quad (4.12)$$

For details of the derivation of these quadratic inequalities and the exact definition of the “a”, “b”, and “c”-coefficients, see Section 4.9.

For coercivity, which is needed to obtain bounds on $\|\mathcal{D}_{\Delta t}^k(w_m)\|_{H^1}$ and $\|\mathcal{D}_{\Delta t}^k(\phi_l)\|_{L^2}$, we need the conditions $a_{2m}(0) - a_{9m} > 0$, $a_{3m}(0) - a_{10m} > 0$ and $c_{1l} - c_{5l} > 0$. It follows that these conditions can be satisfied by choosing the right values for the free parameters η_x if conditions (viii) and (ix) of Assumption 4.1 are satisfied, which is only possible if conditions (i), (ii) and (iii) of Assumption 4.1 are satisfied.

Before we make use of the quadratic inequalities (4.10), (4.11), and (4.12), we refer to two versions of the discrete Gronwall lemma, see [46] and Theorem 4 in [67], which we modified slightly by using the inequalities $1/(1-a) \leq e^{a+a^2} \leq e^{1.6838a}$ for $0 \leq a \leq 0.6838$, and $1+a \leq e^a \leq 1+ae^a$ for $a \geq 0$. These new versions are Inequality 12 and Inequality 13 in Section 2.2.

We are now able to apply Inequality 12 and Inequality 13 to the quadratic inequalities (4.10), (4.11), and (4.12). The result:

Lemma 4.3.

Let $\Delta t \in (0, H)$ with

$$H \leq \min \left\{ \frac{0.6838}{\max_{m \in \mathfrak{M}} \left\{ a_{5m}, \frac{a_{6m}}{a_{1m}} \right\}}, \frac{0.6838}{\min_{l \in \mathfrak{L}} \{b_{5l}\}} \right\}. \quad (4.13)$$

There exist positive constants \tilde{a}_{index} , \tilde{d}_{index} , \tilde{e}_{index} and parameter functions $a(T, V)$, $d_0(T, V)$, $d_1(T, V)$, $d_2(T, V)$, $e_1(T, V)$, and $e_2(T, V)$ such that for all $l \in \mathfrak{L}$, for all $m \in \mathfrak{M}$, and for all $t_k \in [0, T]$ the following estimates hold:

$$\|\phi_l^k\|_{L^2}^2 \leq (\phi_{l0}^2 + e_{2l}(T, V) + e_{1l}(T, V)T)e^{1.6838b_{5l}T}, \quad (4.14a)$$

$$\frac{1}{d-1} \|\partial_z \phi_{d-1}^k\|_{L^2}^2 \leq \sum_{l \in \mathfrak{L}} \|\partial_z \phi_l^k\|_{L^2}^2 \leq d_1(T, V)e^{d_2(T, V)}, \quad (4.14b)$$

$$\frac{1}{d-1} \|\phi_{d-1}^k - \phi_{d-1,0}\|_{L^2}^2 \leq T \frac{d_1(T, V) (1 + d_2(T, V)e^{d_2(T, V)})}{\min_{l \in \mathfrak{L}} \{c_{1l} - c_{5l}\}}, \quad (4.14c)$$

$$\sum_{j=1}^k \sum_{l \in \mathfrak{L}} (c_{1l} - c_{5l}) \left\| \mathcal{D}_{\Delta t}^j(\phi_l) \right\|_{L^2}^2 \Delta t \leq d_1(T, V) \left(1 + d_2(T, V)e^{d_2(T, V)} \right), \quad (4.14d)$$

$$\sum_{m \in \mathfrak{M}} \|w_m^k\|_{L^2}^2 \leq d_0(T, V), \quad (4.15a)$$

$$\sum_{m \in \mathfrak{M}} a_{1m} \|\partial_z w_m^k\|_{L^2}^2 \leq d_0(T, V), \quad (4.15b)$$

$$\sum_{j=1}^k \sum_{m \in \mathfrak{M}} (a_{2m}(0) - a_{9m}) \left\| \mathcal{D}_{\Delta t}^j(w_m) \right\|_{L^2}^2 \Delta t \leq d_0(T, V), \quad (4.15c)$$

$$\sum_{j=1}^k \sum_{m \in \mathfrak{M}} (a_{3m}(0) - a_{10m}) \left\| \mathcal{D}_{\Delta t}^j(\partial_z w_m) \right\|_{L^2}^2 \Delta t \leq d_0(T, V), \quad (4.15d)$$

$$\sum_{j=1}^k \left| \mathcal{D}_{\Delta t}^j(W) \right|^2 \Delta t \leq 2V^2 + \frac{2J_d^2 \phi_{d,res}^2}{\Gamma_{\phi_{\min}}^2} T, \quad (4.16a)$$

$$|W^k|^2 \leq \left(|W^0| + \frac{J_d \phi_{d,res}}{\Gamma_{\phi_{\min}}} T + V\sqrt{T} \right)^2 \quad (4.16b)$$

with

$$d_0(T, V) = ((a_{11} + a_{12})V^2 + 1.6838a_4T) e^{\tilde{d}_{01}T}, \quad (4.17a)$$

$$d_1(T, V) = c_3T + c_4V^2 + (\tilde{d}_{11} + \tilde{d}_{12}T)d_0(T, V), \quad (4.17b)$$

$$d_2(T, V) = \sum_{l \in \mathcal{L}} c_{6l1}V^2 + (\tilde{d}_{21} + \tilde{d}_{22}T)d_0(T, V), \quad (4.17c)$$

$$e_{1l}(T, V) = b_{3l} + \min_{n \in \mathcal{L}} \{b_{6ln}\} d_1(T, V) e^{d_2(T, V)} + \tilde{e}_{11}d_0(T, V), \quad (4.17d)$$

$$e_{2l}(T, V) = b_{4l}V^2 + \tilde{e}_{21}d_0(T, V). \quad (4.17e)$$

and with

$$\tilde{d}_{01} = \max_{m \in \mathfrak{M}} \left\{ a_{7m}, \frac{a_{8m}}{a_{1m}} \right\} + 1.6838 \max_{m \in \mathfrak{M}} \left\{ a_{5m}, \frac{a_{6m}}{a_{1m}} \right\} \quad (4.18a)$$

$$\tilde{d}_{11} = \max_{m \in \mathfrak{M}} \left\{ \frac{c_{80m}}{a_{2m}(0) - a_{9m}} + \frac{c_{81m}}{a_{3m}(0) - a_{10m}} \right\} \quad (4.18b)$$

$$\tilde{d}_{12} = \max_{m \in \mathfrak{M}} \left\{ c_{70m} + \frac{c_{71m}}{a_{1m}} \right\} \quad (4.18c)$$

$$\tilde{d}_{21} = \max_{m \in \mathfrak{M}} \left\{ \frac{\sum_{l \in \mathcal{L}} c_{6l3m}}{a_{2m}(0) - a_{9m}} + \frac{\sum_{l \in \mathcal{L}} c_{6l3m}}{a_{3m}(0) - a_{10m}} \right\} \quad (4.18d)$$

$$\tilde{d}_{22} = \max_{m \in \mathfrak{M}} \left\{ \sum_{l \in \mathcal{L}} c_{6l2m} \left(1 + \frac{1}{a_{1m}} \right) \right\} \quad (4.18e)$$

$$\tilde{e}_{11} = \max_{m \in \mathfrak{M}} \left\{ b_{7l0m} + \frac{b_{7l1m}}{a_{1m}} \right\} \quad (4.18f)$$

$$\tilde{e}_{21} = \max_{m \in \mathfrak{M}} \left\{ \frac{b_{8l0m}}{a_{2m}(0) - a_{9m}} + \frac{b_{8l1m}}{a_{3m}(0) - a_{10m}} \right\} \quad (4.18g)$$

Proof.

The conditions $c_{5l} < c_{1l}$, $a_{9m} < a_{2m}(0)$ and $a_{10m} < a_{3m}(0)$ are satisfied due to conditions (i), (viii) and (ix) of Assumption 4.1, respectively. Apply Inequality 12 to Equation (4.10) in order to obtain all four w^k bounds.

For the bounds of ϕ_{d-1}^k , we use $\sum_{l=1}^d \phi_l^k = 1$ in two ways. First, we apply ∂_z to this identity and use $|x|_1^2 \leq n|x|_2^2$ for $x \in \mathbf{R}^n$ to obtain the upper bound $\sum_{l \in \mathcal{L}} \|\partial_z \phi_l^k\|_{L^2}^2$. Second, we subtract the same identity at time-slice $t = 0$ to obtain an upper bound in $\sum_{l \in \mathcal{L}} (\phi_l^k - \phi_{l,0})$ and, then, apply again $|x|_1^2 \leq n|x|_2^2$ for $x \in \mathbf{R}^n$ using the telescoping series for k to obtain the upper bound $k\Delta t \sum_{j=1}^k \sum_{l \in \mathcal{L}} \|\mathcal{D}_{\Delta t}^k(\phi_{d-1})\|_{L^2}^2 \Delta t$.

All the ϕ -bounds now follow from applying Inequality 12 to Equation (4.11)

and Inequality 13 to Equation (4.12) and inserting the newly obtained w^k bounds.

The use of the Gronwall inequalities are only allowed for Δt small enough, as given by the conditions for H in Inequality 12. \square

Remark 4.2. *The a priori estimates in Lemma 4.3 depend on $T > 0$ and $V > 0$.*

We need to prove that $T > 0$ and $V > 0$ can be chosen for $\Delta t > 0$ small enough. On closer inspection, we see that we can work with upper bounds only.

Lemma 4.4.

Let $0 \leq t_k = k\Delta t \leq T$. Let \mathbf{P}_d be the set of cyclic permutations of $(1, \dots, d)$. The three requirements (I) $\phi_l^k(z) \in [\phi_{\min}, 1 - (d-1)\phi_{\min}]$ for $1 \leq l \leq d$, (II) $\sum_{j=0}^k \|v^j\|_{L^2}^2 \Delta t \leq V^2$, and (III) $\sum_{j=0}^k \|\partial_z v^j\|_{L^2}^2 \Delta t \leq V^2$ are implied by the following two requirements

$$\sum_{j \in \mathfrak{M}} \left\| \phi_{\alpha_j}^k \right\|_{H^1} \leq \frac{1 - \phi_{\min}}{C_{1,0}} \text{ for all } \alpha \in \mathbf{P}_d \text{ and } \sum_{j=0}^k \|\partial_z v^j\|_{L^2}^2 \Delta t \leq V^2, \quad (4.19)$$

where the second requirement is again requirement (III) and with $C_{1,0}$ given by (ii) from Section 4.3.

Proof.

The boundary condition (4.8b) allows the application of the Poincaré inequality to v^k , which gives the bound $\|v^j\|_{L^2} \leq \|\partial_z v^j\|_{L^2}$.

For the constraints on ϕ_l^k we pick arbitrarily an $\alpha \in \mathbf{P}_d$ and start with the inequality $\sum_{j \in \mathfrak{M}} \left\| \phi_{\alpha_j}^k \right\|_{H^1} \leq (1 - \phi_{\min})/C_{1,0}$. This inequality is transformed

by the Sobolev embedding theorem on $[0, 1]$ into $\sum_{j \in \mathfrak{M}} \left\| \phi_{\alpha_j}^k \right\|_{C^0} \leq 1 - \phi_{\min}$.

Hence, we obtain $\inf_{z \in (0,1)} \phi_{\alpha_d}^k \geq \phi_{\min}$ from the volume fraction identity $1 = \sum_{1 \leq l \leq d} \phi_l^k$. Since α was chosen arbitrarily, we conclude that this result holds for all $\alpha \in \mathbf{P}_d$. Hence, $\min_{1 \leq l \leq d} \inf_{z \in (0,1)} \phi_l^k(z) \geq \phi_{\min}$. With the d infima

established it yields that the d suprema follow automatically from the same volume fraction identity. \square

We prove the simultaneous validity of the two inequalities of Lemma 4.4 with elementary arguments based on the Intermediate Value Theorem (IVT) for the

continuous functions given as upper bounds in the inequalities of Lemma 4.3 having parameters T, V as variables.

Lemma 4.5.

Let $2 \leq d \leq C_{1,0}/(C_{1,0} - 1) \approx 4.194528$, $0 < \phi_{\min} \leq 1 - C_{1,0}(d - 1)/d$ and let $\phi^0 = (\phi_{10}, \dots, \phi_{d0}) \in \Phi_d(\phi_{\min}, (1 - \phi_{\min})/C_{1,0})$, where the set $\Phi_d(s, r)$ is defined as the non-empty set of points $(x_1, \dots, x_d) \in \mathbf{R}^d$ satisfying

$$\begin{cases} \sum_{j \neq i} x_j < r & \text{for all } 1 \leq i \leq d, \\ x_i \geq s & \text{for all } 1 \leq i \leq d, \\ \sum_{i=1}^d x_i = 1. \end{cases} \quad (4.20)$$

Then there exist an open simply connected region $\mathbb{S} \subset \mathbf{R}^2$ containing $(0, 0)$ such that

$$(T, V) \in \mathbb{S} \Rightarrow P_{\alpha}(T, V) < \frac{1 - \phi_{\min}}{C_{1,0}} \text{ for all } \alpha \in \mathbf{P}_d, \quad (4.21a)$$

$$(T, V) \in \partial\mathbb{S} \Rightarrow P_{\alpha}(T, V) \leq \frac{1 - \phi_{\min}}{C_{1,0}} \text{ for all } \alpha \in \mathbf{P}_d, \quad (4.21b)$$

$$(T, V) \notin \bar{\mathbb{S}} \Rightarrow P_{\alpha}(T, V) > \frac{1 - \phi_{\min}}{C_{1,0}} \text{ for at least one } \alpha \in \mathbf{P}_d, \quad (4.21c)$$

where $P_{\alpha}(T, V)$ denotes the upper bound of $\sum_{j \in \mathfrak{M}} \|\phi_{\alpha_j}^k\|_{H^1}$ obtained from the a-priori estimates of Lemma 4.3.

Proof.

First, we note that the set $\Phi_d(\phi_{\min}, (1 - \phi_{\min})/C_{1,0})$ is non-empty if the following inequalities are satisfied

$$0 < (d - 1)\phi_{\min} \leq \frac{d - 1}{d} < \frac{1 - \phi_{\min}}{C_{1,0}}. \quad (4.22)$$

This is because $(d - 1)\phi_{\min}$ and $(d - 1)/d$ are the minimal and the maximal value of the sum $\sum_{j \in \mathfrak{M}} x_{\alpha_j}$ over all $\alpha \in \mathbf{P}_d$ when minimizing for each $\alpha \in \mathbf{P}_d$ over all (x_1, \dots, x_d) satisfying $\min_{1 \leq i \leq d} x_i \geq \phi_{\min}$ and $\sum_{i=1}^d x_i = 1$. Hence, we obtain the inequalities

$$0 < \phi_{\min} < 1 - C_{1,0} \frac{d - 1}{d} \leq \frac{1}{d} \quad (4.23)$$

for $2 \leq d < C_{1,0}/(C_{1,0} - 1) \approx 4.194528$ integer.

Second, from Lemma 4.3, $P_\alpha(T, V)$ are monotonic increasing continuous functions with respect to the product ordering on \mathbf{R}_+^2 for all $\alpha \in \mathbf{P}_d$. Therefore, there exists a simply connected open set \mathbb{S}_α such that $P_\alpha(T, V) < (1 - \phi_{\min})/C_{1,0}$ for all $(T, V) \in \mathbb{S}_\alpha$. Moreover, from Lemma 4.3 we deduce that $P_\alpha(0, 0) = \sum_{j \in \mathfrak{M}} \phi_{\alpha_j 0} < (1 - \phi_{\min})/C_{1,0}$ for all $\alpha \in \mathbf{P}_d$, which implies $(0, 0) \in \mathbb{S}_\alpha$ for all $\alpha \in \mathbf{P}_d$. Thus $\mathbb{S} = \bigcap_{\alpha \in \mathbf{P}_d} \mathbb{S}_\alpha$ is non-empty and satisfies all the desired inequalities. \square

A graphical representation of the determination of \mathbb{S} is given in Figure 4.1.

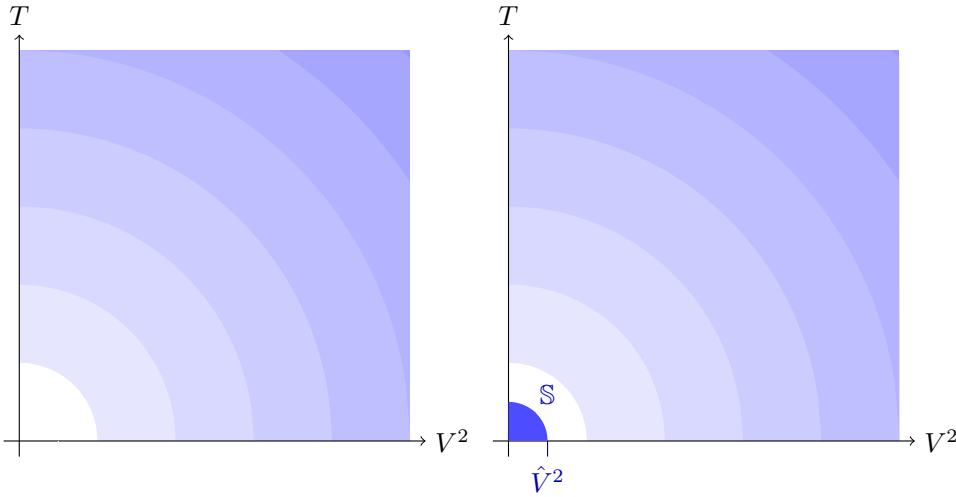


Figure 4.1: In both figures the circular shading represents an interval shading of the constant C in the identity $\max_{\alpha \in \mathbf{P}_d} P_\alpha(T, V) = C$. In the right figure the set \mathbb{S} is obtained for $C = (1 - \phi_{\min})/C_{1,0}$.

Lemma 4.6.

There exist a $\tau > 0$ such that for all $0 < \Delta t < \tau$ there exists an open simply connected region $\mathbb{R}_{\Delta t} \subset \mathbf{R}^2$ with the properties

$$(T, V) \in \mathbb{R}_{\Delta t} \Rightarrow Q_{\Delta t}(T, V) < V^2, \quad (4.24a)$$

$$(T, V) \in \partial \mathbb{R}_{\Delta t} \Rightarrow Q_{\Delta t}(T, V) = V^2, \quad (4.24b)$$

$$(T, V) \notin \overline{\mathbb{R}_{\Delta t}} \Rightarrow Q_{\Delta t}(T, V) > V^2, \quad (4.24c)$$

where $Q_{\Delta t}(T, V)$ denotes the upper bound of $\sum_{t_k \in [0, T]} \|\partial_z v^k\|_{L^2}^2 \Delta t$ obtained from applying the a-priori estimates of Lemma 4.3 to Equation (4.7b) and is

given by

$$\begin{aligned} Q_{\Delta t}(T, V) &= \tilde{Q}_0 \Delta t + \tilde{Q}_1 T + (\tilde{Q}_2 + \tilde{Q}_3 T) d_0(T, V) \\ &\quad + [\tilde{Q}_4(T) T + (\tilde{Q}_5 + \tilde{Q}_6 T) d_0(T, V)] d_1(T, V) e^{d_2(T, V)} \end{aligned} \quad (4.25)$$

with $\tilde{Q}_0, \tilde{Q}_1, \tilde{Q}_2, \tilde{Q}_3, \tilde{Q}_4, \tilde{Q}_5, \tilde{Q}_6 > 0$, if

$$\begin{aligned} 1 > Q_1 &:= \tilde{Q}_2(a_{11} + a_{12}) \\ &= \frac{7d - 5}{\Gamma_{\phi_{\min}}^2} \max_{m \in \mathfrak{M}} \left\{ \frac{H_{1m}^2}{a_{3m}(0) - a_{10m}} \right\} (a_{11} + a_{12}). \end{aligned} \quad (4.26)$$

Moreover, the limit $\lim_{\Delta t \downarrow 0} \mathbb{R}_{\Delta t}$ exists and is denoted by \mathbb{R}_0 .

Proof.

We assume that $\|\partial_z v^0\|_{L^2}^2 \Delta t \leq V^2$ holds for a not yet determined value of $V > 0$. By induction we will prove $\sum_{j=0}^k \|\partial_z v^j\|_{L^2}^2 \Delta t \leq V^2$ for the same value $V > 0$. By our assumption this identity holds for $k = 0$.

Note, for all $\Delta t \leq T$ we can choose any k such that $k\Delta t \in [0, T]$. Thus, there are sequences of Δt decreasing to 0 such that $T/\Delta t$ equals an integer for all Δt in these sequences. Hence, the induction is valid for all $k\Delta t = t_k \in [0, T]$ when $0 < \Delta t < \tau$, where τ has to be determined at a later stage. Remark, for $\Delta t > T$ we have $\sum_{t_k \in [0, T]} \|\partial_z v^k\|_{L^2}^2 \Delta t = \|\partial_z v^0\|_{L^2}^2 \Delta t \leq V^2$ by assumption. In this case, the induction ends immediately at $k = 0$, which is a reflection of the fact that the Δt -sized temporal discretization is too coarse and smaller Δt should be chosen.

Thus for our induction step, we take $0 < k = K \leq T/\Delta t$ for the case $\Delta t < T$ (a-priori assumed to be valid, since T is not yet determined, but only defined.). We integrate (4.7b) from 0 to z . This yields:

$$\begin{aligned} [\Gamma(\phi^{k-1})v^k]_0^z &= \int_0^z G_v(\phi^{k-1}) dz \\ &\quad - \left[\sum_{m \in \mathfrak{M}} (H_{0m}(\phi^{k-1})w_m^{k-1} + H_{1m}(\phi^{k-1})\mathcal{D}_{\Delta t}^k(w_m)) \right]_0^z. \end{aligned} \quad (4.27)$$

Inserting the boundary conditions (4.8b) and using $w_m^0 = 0$ gives:

$$\begin{aligned} \Gamma(\phi^{k-1})v^k &= \int_0^z G_v(\phi^{k-1})dz \\ &\quad - \sum_{m \in \mathfrak{M}} (H_{0m}(\phi^{k-1})w_m^{k-1} + H_{1m}(\phi^{k-1})\mathcal{D}_{\Delta t}^k(w_m)) \\ &\quad + \sum_{m \in \mathfrak{M}} \left(H_{0m}(\phi^{k-1}|_{z=0}) \sum_{j=1}^{k-1} \frac{\hat{J}_m \mathcal{L}(\phi_{m,res} - \phi_m^K|_{z=0})}{H_{1m}(\phi^j|_{z=0})} \Delta t \right. \\ &\quad \left. + \hat{J}_m \mathcal{L}(\phi_{m,res} - \phi_m^{k-1}|_{z=0}) \right). \end{aligned} \quad (4.28)$$

Dividing both sides by $\Gamma(\phi^{k-1})$ and then applying the derivative ∂_z to both sides, leads, with the use of (4.2), to the identity

$$\begin{aligned} \partial_z v^k &= -\frac{1}{\Gamma(\phi^{k-1})^2} \left(\sum_{i=1}^d \frac{\partial \Gamma_i(\phi_i^{k-1})}{\partial \phi_i^{k-1}} \frac{\partial \phi_i^{k-1}}{\partial z} \prod_{j \neq i} \Gamma_j(\phi_j^{k-1}) \right) \times \\ &\quad \times \left[\int_0^z G_v(\phi^{k-1})dz - \sum_{m \in \mathfrak{M}} (H_{0m}(\phi^{k-1})w_m^{k-1} + H_{1m}(\phi^{k-1})\mathcal{D}_{\Delta t}^k(w_m)) \right. \\ &\quad \left. + \sum_{m \in \mathfrak{M}} \left(H_{0m}(\phi^{k-1}|_{z=0}) \sum_{j=1}^{k-1} \frac{\hat{J}_m \mathcal{L}(\phi_{m,res} - \phi_m^K|_{z=0})}{H_{1m}(\phi^j|_{z=0})} \Delta t \right. \right. \\ &\quad \left. \left. + \hat{J}_m \mathcal{L}(\phi_{m,res} - \phi_m^{k-1}|_{z=0}) \right) \right] \\ &+ \frac{1}{\Gamma(\phi^{k-1})} \left[G_v(\phi^{k-1}) - \sum_{m \in \mathfrak{M}} (H_{0m}(\phi^{k-1})\partial_z w_m^{k-1} + H_{1m}(\phi^{k-1})\mathcal{D}_{\Delta t}^k(\partial_z w_m)) \right. \\ &\quad - \sum_{m \in \mathfrak{M}} \left(\sum_{i=1}^d \frac{\partial H_{0m,i}(\phi_i^{k-1})}{\partial \phi_i^{k-1}} \frac{\partial \phi_i^{k-1}}{\partial z} \prod_{j \neq i} H_{0m,j}(\phi_j^{k-1}) \right) w_m^{k-1} \\ &\quad \left. - \sum_{m \in \mathfrak{M}} \left(\sum_{i=1}^d \frac{\partial H_{1m,i}(\phi_i^{k-1})}{\partial \phi_i^{k-1}} \frac{\partial \phi_i^{k-1}}{\partial z} \prod_{j \neq i} H_{1m,j}(\phi_j^{k-1}) \right) \mathcal{D}_{\Delta t}^k(w_m) \right]. \end{aligned} \quad (4.29)$$

Recalling (4.2) for $f(\phi^{k-1})$ and the notation $\|f(\cdot)\|_{C^1([0,1])^d} \leq f$, using Minkowski's inequality, Hölder's inequality, the embedding $H^1(0,1) \hookrightarrow L^\infty(0,1)$ with optimal constant $C_{1,0}$, the definition of $\Gamma_{\phi_{\min}}$ and $H_{\phi_{\min}}$, and the inequality $|(x_1, \dots, x_n)|_1^2 \leq n|(x_1, \dots, x_n)|_2^2$ for $(x_1, \dots, x_n) \in \mathbf{R}^n$ with either $n = d$

or $n = 7d - 5$, we obtain

$$\begin{aligned}
\|\partial_z v^k\|_{L^2}^2 &\leq \frac{d(7d-5)\Gamma^2}{\Gamma_{\phi_{\min}}^4} \sum_{i=1}^d \|\partial_z \phi_i^{k-1}\|_{L^2}^2 \times \\
&\times \left[G_v^2 + C_{1,0}^2 \sum_{m \in \mathfrak{M}} \left(H_{0m}^2 \|w_m^{k-1}\|_{H^1}^2 + H_{1m}^2 \|\mathcal{D}_{\Delta t}^k(w_m)\|_{H^1}^2 \right) \right. \\
&\quad \left. + \sum_{m \in \mathfrak{M}} \left(H_{0m} \frac{\hat{J}_m \phi_{m,res}}{H_{\phi_{\min}}} T + \hat{J}_m \phi_{m,res} \right)^2 \right] \\
&+ \frac{7d-5}{\Gamma_{\phi_{\min}}^2} \left[G_v^2 + \sum_{m \in \mathfrak{M}} \left(H_{0m}^2 \|\partial_z w_m^{k-1}\|_{L^2}^2 + H_{1m}^2 \|\mathcal{D}_{\Delta t}^k(\partial_z w_m)\|_{L^2}^2 \right) \right. \\
&\quad + dC_{1,0}^2 \sum_{m \in \mathfrak{M}} H_{0m}^2 \sum_{i=1}^d \|\partial_z \phi_i^{k-1}\|_{L^2}^2 \|w_m^{k-1}\|_{H^1}^2 \\
&\quad \left. + dC_{1,0}^2 \sum_{m \in \mathfrak{M}} H_{1m}^2 \sum_{i=1}^d \|\partial_z \phi_i^{k-1}\|_{L^2}^2 \|\mathcal{D}_{\Delta t}^k(w_m)\|_{H^1}^2 \right]. \quad (4.30)
\end{aligned}$$

Summing over $k = 1$ to $k = K$ with $K\Delta t \leq T$, multiplying by Δt , and using the inequalities of Lemma 4.3, we obtain

$$\begin{aligned}
&\sum_{k=0}^K \|\partial_z v^k\|_{L^2}^2 \Delta t \\
&\leq \|\partial_z v^0\|_{L^2}^2 \Delta t + \frac{7d-5}{\Gamma_{\phi_{\min}}^2} G_v^2 T \\
&+ \frac{7d-5}{\Gamma_{\phi_{\min}}^2} \left[\max_{m \in \mathfrak{M}} \left\{ \frac{H_{1m}^2}{a_{3m}(0) - a_{10m}} \right\} + \max_{m \in \mathfrak{M}} \left\{ \frac{H_{0m}^2}{a_{1m}} \right\} T \right] d_0(T, V) \\
&+ \frac{d^2(7d-5)}{\Gamma_{\phi_{\min}}^2} \left[\frac{\Gamma^2}{\Gamma_{\phi_{\min}}^2} \left(G_v^2 + \sum_{m \in \mathfrak{M}} \left[H_{0m} \frac{\hat{J}_m \phi_{m,res}}{H_{\phi_{\min}}} T + \hat{J}_m \phi_{m,res} \right]^2 \right) T \right. \\
&\quad \left. + C_{1,0}^2 \left(1 + \frac{\Gamma^2}{\Gamma_{\phi_{\min}}^2} \right) \left(\max_{m \in \mathfrak{M}} \left\{ \frac{H_{1m}^2}{a_{2m}(0) - a_{9m}} + \frac{H_{1m}^2}{a_{3m}(0) - a_{10m}} \right\} \right. \right. \\
&\quad \left. \left. + \max_{m \in \mathfrak{M}} \left\{ H_{0m}^2 + \frac{H_{0m}^2}{a_{1m}} \right\} T \right) d_0(T, V) \right] d_1(T, V) e^{d_2(T, V)} \quad (4.31a) \\
&= Q_{\Delta t}(T, V). \quad (4.31b)
\end{aligned}$$

Hence, we can rewrite $Q_{\Delta t}(T, V)$ as

$$Q_{\Delta t}(T, V) = \tilde{Q}_0 \Delta t + \tilde{Q}_1 T + (\tilde{Q}_2 + \tilde{Q}_3 T) d_0(T, V) \\ + [\tilde{Q}_4(T) T + (\tilde{Q}_5 + \tilde{Q}_6 T) d_0(T, V)] d_1(T, V) e^{d_2(T, V)}. \quad (4.32)$$

This yields

$$Q_{\Delta t}(0, V) = \tilde{Q}_0 \Delta t + \tilde{Q}_2 d_0(0, V) + \tilde{Q}_5 d_0(0, V) d_1(0, V) e^{d_2(0, V)} \quad (4.33a)$$

$$= \|\partial_z v^0\|_{L^2}^2 \Delta t + \frac{7d-5}{\Gamma_{\phi_{\min}}^2} \max_{m \in \mathfrak{M}} \left\{ \frac{H_{1m}^2}{a_{3m}(0) - a_{10m}} \right\} (a_{11} + a_{12}) V^2 \\ + \frac{d^2(7d-5)C_{1,0}^2}{\Gamma_{\phi_{\min}}^2} \left(1 + \frac{\Gamma^2}{\Gamma_{\phi_{\min}}^2} \right) \max_{m \in \mathfrak{M}} \left\{ \frac{H_{1m}^2}{a_{2m}(0) - a_{9m}} + \frac{H_{1m}^2}{a_{3m}(0) - a_{10m}} \right\} \times \\ \times (a_{11} + a_{12}) \left(c_4 + \tilde{d}_{11}(a_{11} + a_{12}) \right) V^4 e^{(\sum_{l \in \mathcal{E}} c_{6l1} + \tilde{d}_{21}(a_{11} + a_{12})) V^2}. \quad (4.33b)$$

Hence, we have

$$Q_{\Delta t}(0, V) = Q_0 \Delta t + Q_1 V^2 + Q_2 V^4 e^{Q_3 V^2} \quad (4.34)$$

with

$$Q_1 = \frac{7d-5}{\Gamma_{\phi_{\min}}^2} \max_{m \in \mathfrak{M}} \left\{ \frac{H_{1m}^2}{a_{3m}(0) - a_{10m}} \right\} (a_{11} + a_{12}). \quad (4.35)$$

If $Q_1 < 1$, then by the Intermediate Value Theorem there is a $V^* \in \left(0, \sqrt[4]{\frac{1-Q_1}{Q_2 Q_3}}\right)$ for all $\Delta t > 0$ such that

$$\frac{\partial Q_{\Delta t}(0, V)}{\partial(V^2)} \Big|_{V=V^*} = 1 > Q_1 = \frac{\partial Q_{\Delta t}(0, V)}{\partial(V^2)} \Big|_{V=0}, \quad (4.36)$$

because $\partial Q_{\Delta t}(0, V)/\partial(V^2) = Q_1 + Q_2 V^2(2 + Q_3 V^2) e^{Q_3 V^2} \geq Q_1 + Q_2 Q_3 V^4$. Immediately we see that $Q_{\Delta t}(0, V^*) < (V^*)^2$ for $0 < \Delta t < \tau$ if we choose

$$\tau = \min \left\{ \frac{1-Q_1}{Q_0} \left(1 - \frac{1}{2 + Q_3 (V^*)^2} \right) (V^*)^2, H \right\} = \min \{ \hat{\tau}, H \}, \quad (4.37)$$

where H denotes the upper bound of $\Delta t > 0$ as found in Lemma 4.3. Moreover, for $0 < \Delta t < \tau$ we have the inequalities $Q_{\Delta t}(0, 0) > 0$, $Q_{\Delta t}(0, V^*) < (V^*)^2$, and $Q_{\Delta t}(0, \tilde{V}) > \tilde{V}^2 = (1 - Q_1)/Q_2 > (V^*)^2$ due to $Q_{\Delta t}(0, V) > Q_1 V^2 + Q_2 V^4$ for $V > 0$. Hence, by the Intermediate Value Theorem, there exist $V_{1, \Delta t} \in (0, V^*)$ and $V_{2, \Delta t} \in (V^*, \tilde{V})$ such that $Q_{\Delta t}(0, V_{1, \Delta t}) = V_{1, \Delta t}^2$ and $Q_{\Delta t}(0, V_{2, \Delta t}) = V_{2, \Delta t}^2$.

We see that $Q_{\Delta t}(T, V)$ is a monotonic increasing continuous function with respect to the product ordering on \mathbf{R}_+^2 for $0 < \Delta t < \tau$. Therefore, there exists a simply connected open set $\mathbb{R}_{\Delta t}$ such that $Q_{\Delta t}(T, V) < V^2$ for all $(T, V) \in \mathbb{R}_{\Delta t}$. Thus $\sum_{k=0}^K \|\partial_z v^k\|_{L^2}^2 \Delta t \leq V^2$ for $(T, V) \in \mathbb{R}_{\Delta t}$.

Hence, induction states that $\sum_{t_k \in [0, T]} \|\partial_z v^k\|_{L^2}^2 \Delta t \leq V^2$ for $(T, V) \in \mathbb{R}_{\Delta t}$.

Our assumption of $\|\partial_z v^0\|_{L^2}^2 \Delta t \leq V^2$ for some $V > 0$ can now be lifted for $\Delta t \leq T$. We have

$$\|\partial_z v^0\|_{L^2}^2 \Delta t = Q_0 \Delta t \leq Q_{\Delta t}(0, V_{1, \Delta t}) = V_{1, \Delta t}^2 \leq V^2 \quad (4.38)$$

for all $(0, V) \in \overline{\mathbb{R}_{\Delta t}}$ and, by monotonicity in T , this inequality holds for all $(T, V) \in \overline{\mathbb{R}_{\Delta t}}$. Do note that τ depends on $Q_0 = \|\partial_z v^0\|_{L^2}^2$. Thus for all $v^0 \in L^2(0, 1)$ with $v^0(0) = 0$ there exist a $\tau > 0$ such that our assumption and, therefore, our induction holds if $(T, V) \in \overline{\mathbb{R}_{\Delta t}}$.

Note, the region $\mathbb{R}_{\Delta t}$ contains the cylinder $[0, T) \times (\|\partial_z v^0\|_{L^2} \sqrt{\Delta t}, \infty)$ such that the case $\Delta t > T$ satisfies the assumption $\|\partial_z v^0\|_{L^2}^2 \Delta t \leq V^2$ and the three domain properties.

The limit set of $\mathbb{R}_{\Delta t}$ for $\Delta t \downarrow 0$, denoted by \mathbb{R}_0 , exists because the construction of $\mathbb{R}_{\Delta t}$ is only dependent on Δt when using the Intermediate Value Theorem to guarantee the existence of $V_{1, \Delta t}$ and $V_{2, \Delta t}$, which directly follows from the fact that $Q_{\Delta t}(T, V)$ is a right-continuous monotonic increasing function in $\Delta t \in \mathbf{R}_+$. Moreover, the cylinder $[0, T) \times (\|\partial_z v^0\|_{L^2} \sqrt{\Delta t}, \infty)$ becomes the empty set in the limit $\Delta t = 0$, since this cylinder represents the case $\Delta t > T$ and is, therefore, Δt -thick. Hence, \mathbb{R}_0 can be seen as the limit of the part of the set $\mathbb{R}_{\Delta t}$, where the case $\Delta t > T$ is satisfied. \square

A graphical representation of the determination of $\mathbb{R}_{\Delta t}$ and \mathbb{R}_0 is given in Figure 4.2.

Lemma 4.7.

Let $1 < d \leq C_{1,0}/(C_{1,0} - 1)$, $0 < \Delta t < \tau$, $0 < \phi_{\min} \leq 1 - C_{1,0}(d - 1)/d$ and $\phi^0 \in \Phi_d(\phi_{\min}, (1 - \phi_{\min})/C_{1,0})$, where the set $\Phi_d(s, r)$ is as defined in Lemma 4.5 and τ has the value as determined in the proof of Lemma 4.6. Then there exists a $\tau^* > 0$ such that

$$\{(\Delta t, \infty) \times \mathbf{R}_+\} \cap S \cap \mathbb{R}_{\Delta t} \neq \emptyset \quad \text{for all } 0 \leq \Delta t < \tau^*, \quad (4.39)$$

where S is the set as defined in Lemma 4.5 and $\mathbb{R}_{\Delta t}$ is the set as defined in Lemma 4.6.

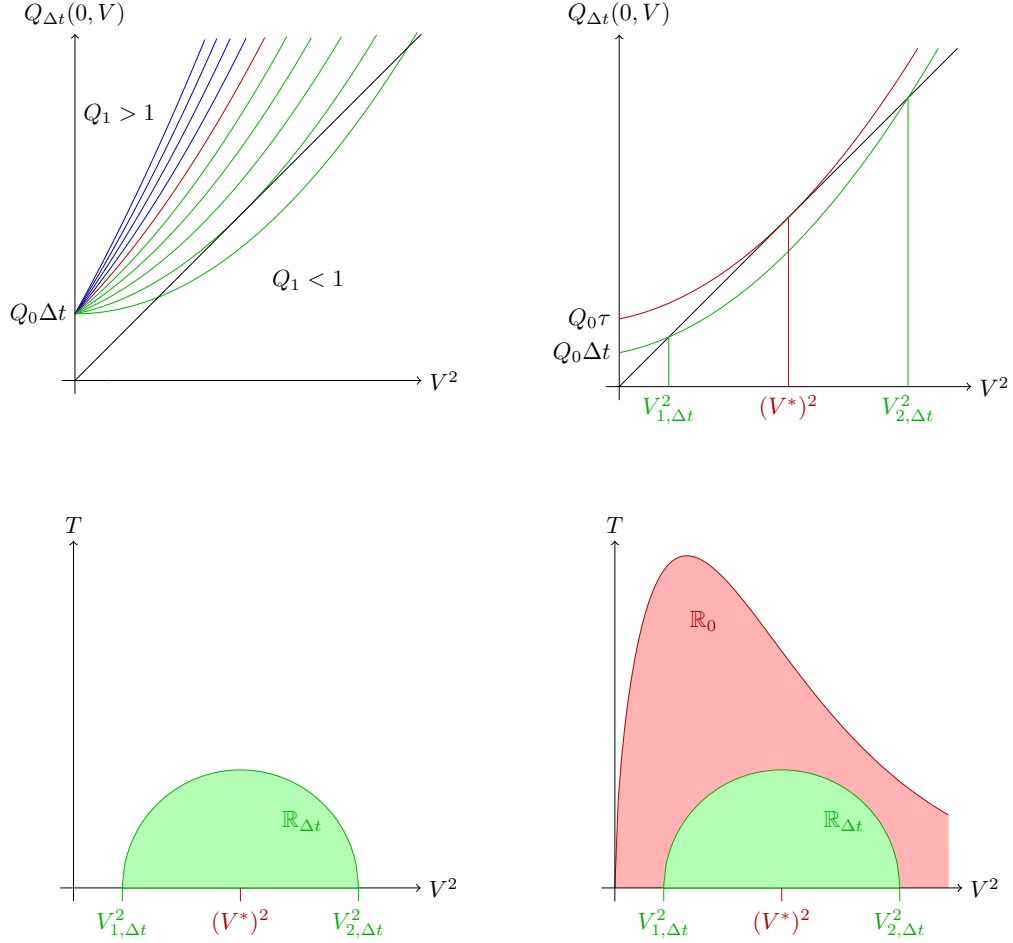


Figure 4.2: The top left figure shows in blue that for $Q_1 > 1$ the function $Q_{\Delta t}(0, V)$ cannot intersect/touch the black line V^2 (actually regardless of chosen $\Delta t > 0$), in green that for $Q_1 < 1$ the function $Q_{\Delta t}(0, V)$ is able to intersect/touch the black line twice (not for all chosen $\Delta t > 0$), and in red that for $Q_1 = 1$ the function $Q_{\Delta t}(0, V)$ is parallel but non-touching near the vertical axis.

The top right figure shows in red that for any $Q_1 < 1$ a single value τ can be found such that the function $Q_{\Delta t}(0, V)$ touches V^2 once at $(V^*)^2$, while for $\Delta t < \tau$ the black V^2 line is intersected twice by the green $Q_{\Delta t}(0, V)$ function at the intersection points $V_{1(2), \Delta t}^2$.

The bottom left picture shows that the function $Q_{\Delta t}(T, V)$ is equal to V^2 at the green boundary, which connects $V_{1(2), \Delta t}^2$ at the V^2 -axis, and smaller than V^2 in the green simply-connected inner region $\mathbb{R}_{\Delta t}$. The bottom right corner shows that the limit region \mathbb{R}_0 contains $\mathbb{R}_{\Delta t}$ for $\Delta t < \tau$ and touches the T -axis at the origin.

Proof.

Due to the monotonicity of both \mathbb{S} and $\mathbb{R}_{\Delta t}$ with respect to T , we only have to check for all $\alpha \in \mathbf{P}_d$ that there exists a $V_\alpha > 0$ such that $P_\alpha(0, V_\alpha) <$

$(1 - \phi_{\min})/C_{1,0}$. For $T = 0$ and using the equivalence of \mathbf{R}^n -norms, we obtain

$$\begin{aligned} P_{\alpha}(0, V) &\leq \sum_{j \in \mathfrak{M}} \phi_{\alpha_j 0} + \sum_{j \in \mathfrak{M}, \alpha_j \neq d-1} \sqrt{b_{4\alpha_j} + \tilde{e}_{21}(a_{11} + a_{12})} V \\ &\quad + e \left(\sum_{l \in \mathfrak{L}} c_{6l1} + \tilde{d}_{21}(a_{11} + a_{12}) \right)^{\frac{V^2}{2}} \sqrt{(d-1)(c_4 + \tilde{d}_{11}(a_{11} + a_{12}))} V. \end{aligned} \quad (4.40)$$

From Lemma 4.5 and condition (v) in Assumption 4.1, there exists an initial value $\phi^0 \in \Phi_d(\phi_{\min}, (1 - \phi_{\min})/C_{1,0})$ such that $\sum_{j \in \mathfrak{M}} \phi_{\alpha_j 0} < (1 - \phi_{\min})/C_{1,0}$ for all $\alpha \in \mathbf{P}_d$. Since $P_{\alpha}(0, V)$ is strictly increasing in V , there exists a $\hat{V}_{\alpha} > 0$ such that $P_{\alpha}(0, \hat{V}_{\alpha}) = (1 - \phi_{\min})/C_{1,0}$. Construct $\hat{V} = \min_{\alpha \in \mathbf{P}_d} \hat{V}_{\alpha}$.

Now we have two cases: either $\hat{V} \geq V_{1,\tau}$ or $0 < \hat{V} < V_{1,\tau}$, where $V_{1,\tau} = \lim_{\Delta t \uparrow \tau} V_{1,\Delta t}$ with $V_{1,\Delta t}$ and τ from the proof of Lemma 4.6. In the first case, we can introduce $\tau^{**} = \tau$, because $(\{0\} \times (0, \hat{V}]) \cap \overline{\mathbb{R}_{\tau}} \neq \emptyset$. In the second case, we have $(\{0\} \times (0, \hat{V}]) \cap \overline{\mathbb{R}_{\tau}} = \emptyset$. Fortunately, $V_{1,\Delta t}$ is a monotonically increasing function of Δt , because $Q_{\Delta t}(T, V)$ is monotonically increasing in Δt for all $(T, V) \in \mathbf{R}_+^2$ and $Q_0(0, 0) = 0$. Thus the Intermediate Value Theorem states there exists a $\tau^{**} < \tau$ such that $\hat{V} = V_{1,\tau^{**}}$ and thus $(\{0\} \times (0, \hat{V}]) \cap \overline{\mathbb{R}_{\tau^{**}}} \neq \emptyset$. Hence $\mathbb{S} \cap \mathbb{R}_{\Delta t} \neq \emptyset$ for all $0 \leq \Delta t < \tau^{**}$. However, $T < \Delta t$ is not allowed, as $k > 0$ integer such that $k\Delta t \leq T$ was implicitly used up to now in the proofs of Lemmas 4.3, 4.4, 4.5, and 4.6. Since $(0, V^*) \in \overline{\mathbb{R}_{\Delta t}}$, there are $(T, V) \in \mathbb{R}_{\Delta t}$ with $T < \Delta t$. Thus, even though $\mathbb{S} \cap \mathbb{R}_{\Delta t} \neq \emptyset$ for all $0 \leq \Delta t < \tau^{**}$, we still need to prove $\{(\Delta t, \infty) \times \mathbf{R}_+\} \cap \mathbb{S} \cap \mathbb{R}_{\Delta t} \neq \emptyset$.

For all $0 \leq \Delta t < \tau$, we have $Q_{\Delta t}(0, V^*) < (V^*)^2$ with V^* the unique value, independent of Δt , for which $\left. \frac{dQ_{\Delta t}(T, V)}{d(V^2)} \right|_{V=V^*} = 1$. Since $Q_{\Delta t}(T, V)$ is monotonic increasing in both Δt and T , we can define the new function $\mathcal{Q}(\Delta t) = Q_{\Delta t}(\Delta t, V^*) - (V^*)^2$. Due to $\overline{\mathbb{R}_{\tau}} = \{0\} \times \{V^*\}$ by construction, we find $\mathcal{Q}(\tau) > 0$, while $\mathcal{Q}(0) < 0$. Hence, by the Intermediate Value Theorem there exists a $0 < \tau^{***} < \tau$ such that $\mathcal{Q}(\tau^{***}) = 0$ and, therefore, $\{(\Delta t, \infty) \times \mathbf{R}_+\} \cap \mathbb{R}_{\Delta t} \neq \emptyset$ for all $0 \leq \Delta t < \tau^{***}$. Introduce $\tilde{V}_{\Delta t}$ as the minimal value of V such that $Q_{\Delta t}(\Delta t, V) \leq V^2$ if such a V exists. For $0 \leq \Delta t < \tau^{***}$, there exists a $(\Delta t, \tilde{V}_{\Delta t}) \in \{(\Delta t, \infty) \times \mathbf{R}_+\} \cap \mathbb{R}_{\Delta t}$. Introduce $\mathcal{P}(\Delta t) = \max_{\alpha \in \mathbf{P}_d} P_{\alpha}(\Delta t, \tilde{V}_{\Delta t})$. For $\tau^{***} \leq \tau^{**}$, if $\lim_{\Delta t \rightarrow \tau^{***}} \mathcal{P}(\Delta t) \leq \frac{1 - \phi_{\min}}{C_{1,0}}$, then $(\Delta t, \tilde{V}_{\Delta t}) \in \mathcal{S}$ for all $0 \leq \Delta t < \tau^* = \tau^{***} = \min\{\tau^{**}, \tau^{***}\}$. If $\lim_{\Delta t \rightarrow \tau^{***}} \mathcal{P}(\Delta t) > \frac{1 - \phi_{\min}}{C_{1,0}}$, which also occurs for $\tau^{**} \leq \tau^{***}$, then we recall $Q_0(0, 0) = 0$ and $P_{\alpha}(0, 0) < \frac{1 - \phi_{\min}}{C_{1,0}}$ for all $\alpha \in \mathbf{P}_d$. Hence, $\mathcal{P}(0) < \frac{1 - \phi_{\min}}{C_{1,0}}$. By continuity of $Q_{\Delta t}(T, V)$ and $P_{\alpha}(T, V)$ in the parameters Δt , T and V , follows the continuity of $\mathcal{P}(\Delta t)$. Thus by the Intermediate Value Theorem, there is a

$\tau^* \in (0, \tau^{**}) = (0, \min\{\tau^{**}, \tau^{***}\})$ such that $\mathcal{P}(\tau^*) = \frac{1-\phi_{\min}}{C_{1,0}}$. Thus there exists a $\tau^* \in (0, \min\{\tau^{**}, \tau^{***}\}]$ such that $(\Delta t, \tilde{V}_{\Delta t}) \in \overline{\{(\Delta t, \infty) \times \mathbf{R}_+\} \cap \mathbb{R}_{\Delta t} \cap \mathbb{S}}$ for all $0 \leq \Delta t < \tau^*$.

Hence, for all $0 \leq \Delta t < \tau^* \in (0, \min\{\tau^{**}, \tau^{***}\}]$, we have $\{(\Delta t, \infty) \times \mathbf{R}_+\} \cap \mathbb{R}_{\Delta t} \cap \mathbb{S} \neq \emptyset$ due to the monotonicity of $Q_{\Delta t}(T, V)$ and $P_{\alpha}(T, V)$ on the parameters $\Delta t, T$ and V . \square

In Figure 4.3 it is shown graphically why the intersection of \mathbb{R}_0 and \mathbb{S} is non-empty.

We have shown that the conditions $c_{5l} < c_{1l}$, $a_{9m} < 1$ and $a_{10m} < a_{3m}(0)$ are satisfied by the conditions (i), (viii) and (ix) in Assumption 4.1. Moreover, the conditions $\phi_{\min} \leq 1 - C_{1,0}(d-1)/d$ and $\phi^0 \in \Phi_d(\phi_{\min}, (1 - \phi_{\min})/C_{1,0})$ of Lemma 4.5 follows from (v), while the conditions (ii), (iii), (iv), (vi) and (vii) are needed for coercivity.

The condition $Q_1 < 1$ of Lemma 4.6 is equivalent to

$$1 > \frac{7d-5}{\Gamma_{\phi_{\min}}^2} \max_{m \in \mathfrak{M}} \left\{ \frac{H_{1m}^2}{a_{3m}(0) - a_{10m}} \right\} (a_{11} + a_{12}), \quad (4.41)$$

which can be satisfied if (x) in Assumption 4.1 is satisfied.

We finish the proof of Theorem 4.2 with remarking that we can choose any pair $(T, V) \in \mathbb{S} \cap \text{int}(\mathbb{R}_0)$ to satisfy the theorem, since $\lim_{\Delta t \downarrow 0} \{(\Delta t, \infty) \times \mathbf{R}_+\} \cap \mathbb{S} \cap \mathbb{R}_{\Delta t} = \mathbb{S} \cap \text{int}(\mathbb{R}_0)$.

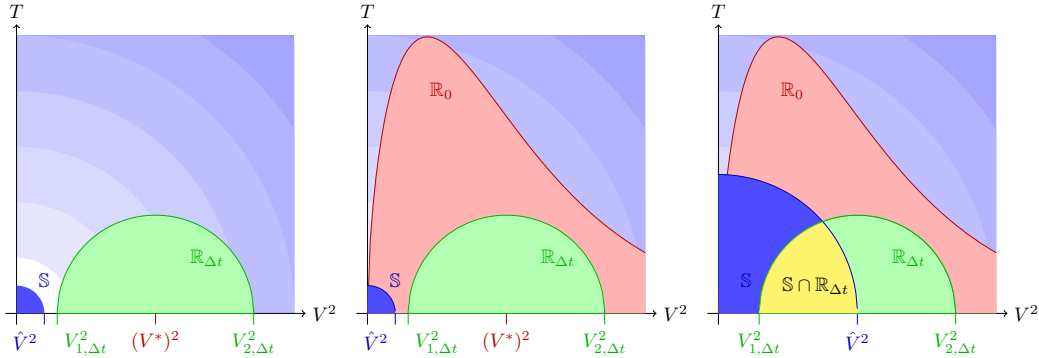


Figure 4.3: Again, in all three figures the circular shading indicates an interval shading of the constant C in the identity $\max_{\alpha \in \mathcal{P}_d} P_{\alpha}(T, V) = C$. Moreover, again in all three figures, the set \mathbb{S} is obtained for $C = (1 - \phi_{\min})/C_{1,0}$.

The left picture shows the general position of \mathbb{S} and $\mathbb{R}_{\Delta t}$ in (T, V^2) -space.

The middle picture shows that \mathbb{R}_0 always intersects with \mathbb{S} , even when $\mathbb{R}_{\Delta t}$ does not due to $0 < \hat{V} < V_{1,\Delta t}$. This is the case $\Delta t \geq \tau^*$.

The right picture shows that both \mathbb{R}_0 and $\mathbb{R}_{\Delta t}$ intersect \mathbb{S} due to $\hat{V} > V_{1,\Delta t}$. This is the case $\Delta t < \tau^*$.

4.5 Proof of Theorem 4.1

The proof of Theorem 4.1 is straightforward. We use an interpolation function $\hat{u}_{\Delta t}(t) := u^{k-1} + (t - t_{k-1})\mathcal{D}_{\Delta t}^k(u)$ on each interval $[t_{k-1}, t_k] \subset [0, T]$ for all functions $u \in \{\phi_l, v, w_m, W\}$ with $l \in \mathfrak{L}$ and $m \in \mathfrak{M}$ to extend the discrete-time solutions of Theorem 4.2 to $[0, T] \times [0, 1]$ and $[0, T]$. We see that $\hat{u}_{\Delta t}$ is measurable on $[0, T] \times [0, 1]$ for $u \in \{\phi_l, v, w_m\}$ and $[0, T]$ for $u = W$, has a time-derivative on $[0, T] \times [0, 1]$ a.e. for $u \in \{\phi_l, v, w_m\}$ and $[0, T]$ a.e. for $u = W$, and has a Δt -independent bound in an appropriate Bochner space (cf. Theorem 4.2). Hence, we obtain the following weak convergence results

$$(1) \quad \hat{\phi}_{l,\Delta t} \rightharpoonup \hat{\phi}_l \in H^1(0, T; L^2(0, 1)) \cap L^\infty(0, T; H^1(0, 1)) \\ \cap L^2(0, T; H^2(0, 1)), \quad (4.42a)$$

$$(2) \quad \hat{v}_{\Delta t} \rightharpoonup \hat{v} \in L^2(0, T; H^1(0, 1)), \quad (4.42b)$$

$$(3) \quad \hat{w}_{m,\Delta t} \rightharpoonup \hat{w}_m \in H^1(0, T; H^1(0, 1)) \cap L^\infty(0, T; H^2(0, 1)), \text{ and } (4.42c)$$

$$(4) \quad \hat{W}_{\Delta t} \rightharpoonup \hat{W} \in H^1(0, T) \quad (4.42d)$$

for $l \in \mathfrak{L}$ and $m \in \mathfrak{M}$.

As the time-continuous system has nonlinear terms, we need strong convergence of the $\hat{\phi}_{l,\Delta t}$ and $\hat{w}_{m,\Delta t}$ terms in order to pass to the limit $\Delta t \rightarrow 0$. The strong convergence is obtained here by combining two versions of the Lions-Aubin-Simon lemma, see [40, Theorem 1] for the version for piecewise constant functions and [129, Theorem 3] for the standard Lions-Aubin-Simon lemma, which is used for the piecewise linear functions.

Theorem 4.8 (Lions-Aubin-Simon lemma for piecewise constant functions).

Let \mathbb{X} , \mathbb{B} , and \mathbb{Y} be Banach spaces such that the embedding $\mathbb{X} \hookrightarrow \mathbb{B}$ is compact and the embedding $\mathbb{B} \hookrightarrow \mathbb{Y}$ is continuous. Furthermore, let either $1 \leq p < \infty$, $r = 1$ or $p = \infty$, $r > 1$, and let $(u_{\Delta t})$ be a sequence of functions, which are constant on each subinterval (t_{k-1}, t_k) , satisfying

$$\|\mathcal{D}_{\Delta t}(u_{\Delta t})\|_{L^r(\Delta t, T; \mathbb{Y})} + \|u_{\Delta t}\|_{L^p(0, T; \mathbb{X})} \leq C_0 \quad \text{for all } \Delta t \in (0, \tau), \quad (4.43)$$

where $C_0 > 0$ is a constant which is independent of Δt . If $p < \infty$, then $(u_{\Delta t})$ is relatively compact in $L^p(0, T; \mathbb{B})$. If $p = \infty$, there exists a subsequence of $(u_{\Delta t})$ which converges in each space $L^q(0, T; \mathbb{B})$, $1 \leq q < \infty$, to a limit which belongs to $C^0([0, T]; \mathbb{B})$.

Theorem 4.9 (Standard Lions-Aubin-Simon lemma). *Let \mathbb{X} and \mathbb{B} be Banach spaces, such that $\mathbb{X} \hookrightarrow \mathbb{B}$ is compact. Let $f \in \mathbb{F} \subset L^p(0, T; \mathbb{B})$ where $1 \leq p \leq \infty$, and assume*

(A) \mathbb{F} is bounded in $L^1_{loc}(0, T; X)$,

(B) $\|f(t + \Delta t) - f(t)\|_{L^p(0, T - \Delta t; \mathbb{B})} \rightarrow 0$ as $\Delta t \rightarrow 0$, uniformly for $f \in \mathbb{F}$.

Then \mathbb{F} is relatively compact in $L^p(0, T; \mathbb{B})$ (and in $C(0, T; \mathbb{B})$ if $p = \infty$).

We apply Theorem 4.8 and Theorem 4.9 with the triples

$$(\mathbb{X}, \mathbb{B}, \mathbb{Y}) = (H^2(0, 1), C^1([0, 1]), L^2(0, 1)) \quad (4.44)$$

or

$$(\mathbb{X}, \mathbb{B}, \mathbb{Y}) = (H^1(0, 1), C^0([0, 1]), L^2(0, 1)), \quad (4.45)$$

depending on the situation, together with the Rellich-Kondrachov theorem on $[0, 1]$, see [2, p.143] and [20], ensuing $\mathbb{X} \hookrightarrow \mathbb{B}$ compactly. We obtain the existence of a subsequence $\Delta t \downarrow 0$ for which we also have strong convergence next to the weak convergence:

$$\hat{\phi}_{l, \Delta t} \rightarrow \hat{\phi}_l \in C^0([0, T]; C^0[0, 1]) \quad \text{for } l \in \mathfrak{L}, \quad (4.46a)$$

$$\hat{w}_{m, \Delta t} \rightarrow \hat{w}_m \in C^0([0, T]; C^1[0, 1]) \quad \text{for } m \in \mathfrak{M}. \quad (4.46b)$$

The limit functions $\hat{\phi}_l$, \hat{v} and \hat{w}_m satisfy the weak formulation of the continuous-time equations (4.1a)-(4.1c).

Using the interpolation-trace inequality, $\|u\|_{C(\bar{\Omega})} \leq C \|u\|_{H^1(\Omega)}^{1-\theta} \|u\|_{L^2(\Omega)}^\theta$ (for $\theta = 1/2$, see [146, Example 21.62 on p.285]), we notice that the weak convergence for Theorem 4.2 applies up to the boundary, which together with the smoothness of the functions satisfying Equation (4.2) ensure the passage of the limit so that the boundary conditions are recovered. The initial conditions are satisfied by construction.

Hence, there exist $\phi_{\min} > 0$, $T > 0$, $V > 0$ such that $\phi_l := \hat{\phi}_l$, $v := \hat{v}$, $w_m := \hat{w}_m$ and $W := \hat{W}$ satisfy Theorem 4.1.

4.6 Numerical exploration of allowed parameter sets

In this section we simulate numerically the model (4.5), (4.7a)-(4.7c), (4.8a), and (4.8b). This model is already in a format that allows a straightforward numerical implementation next to allowing some analytical evaluation of observed (numerical) behaviors. The chosen model has $d = 3$ and is determined

by the following functions and constants, for all $l \in \mathfrak{L}$ and $m \in \mathfrak{M}$

$$\begin{aligned}
\delta_l &= \delta & \Gamma(\boldsymbol{\phi}) &= 4\phi_d \\
I_1(\boldsymbol{\phi}) &= 0 & I_3(\boldsymbol{\phi}) &= \epsilon \\
B_{l10l}(\boldsymbol{\phi}) &= \epsilon\phi_l & B_{lijm}(\boldsymbol{\phi}) &= 0 \text{ for } (i, j, m) \neq (1, 0, l) \\
H_{1m}(\boldsymbol{\phi}) &= \phi_m & H_{0m}(\boldsymbol{\phi}) &= 0 \\
E_{m10j}(\boldsymbol{\phi}) &= \frac{1}{2}D_j\phi_m & E_{minj}(\boldsymbol{\phi}) &= 0 \text{ for } (i, n) \neq (1, 0) \\
F_m(\boldsymbol{\phi}) &= 1 & \gamma_m &= \gamma \\
G_{\phi,l}(\boldsymbol{\phi}) &= \epsilon\kappa_l G_v(\boldsymbol{\phi}) & G_v(\boldsymbol{\phi}) &= \mathcal{L}(\phi_{1,sat} - \phi_1)\mathcal{L}(\phi_3 - \phi_{3,thr}) \\
G_{w,m}(\boldsymbol{\phi}) &= 0 & A_m &= A
\end{aligned} \tag{4.47}$$

The conditions of Assumption 4.1 have to be satisfied. To this end, we choose $\eta_m = \zeta\gamma|A|$ for $m \in \mathfrak{M}$ with $\zeta > 0$ in conditions (ix) and (x) of Assumption 4.1. This yields for $\phi_{\min} \in (0, 1 - 2\coth(1)/3) \approx (0, 0.124643143)$ the conditions

- (i) $\delta > 0$
- (ii) $|A| < 1$
- (iii) $\frac{1}{4}D_j^2\phi_m^2 < \frac{1}{9} \min\{3, \gamma(1-A)\} \min\{3/5, \gamma(1-A)\}$
- (iv) $64\phi_{d0}^2 > 36\phi_{l0}^2$ for all $l \in \mathfrak{L}$.
- (v) $\phi_{j0} \geq \phi_{\min}$, $\sum_{i \neq j} \phi_{i0} < \frac{1-\phi_{\min}}{\coth(1)}$ and $\sum_{i=1}^d \phi_{i0} = 1$ for all $1 \leq j \leq d$,
- (vi) $77\gamma A^2 < 1$,
- (vii) $\gamma > \frac{77\phi_m^2}{64\phi_d^2}$,
- (viii) $0 < \mathfrak{C}_{1m} = 1 - \sum_{j \in \mathfrak{M}} D_m \frac{\eta_{j01m1}}{4}$,
- (ix) $0 < \mathfrak{C}_{2m} = \gamma \left(1 - \left(1 + \frac{\zeta}{2} \right) |A| \right) - \frac{\eta_{m2}}{2} - \frac{1}{4} \sum_{j \in \mathfrak{M}} \left(\frac{D_j}{\eta_{m01j1}} + \frac{D_j}{\eta_{m01j2}} + D_m \eta_{j01m2} \right)$,
- (x) $1 > \frac{1}{2} \left(\frac{1-2\phi_{\min}}{\phi_{\min}} \right)^2 \max_{m \in \mathfrak{M}} \left\{ \frac{1}{\mathfrak{C}_{2m}} \right\} \sum_{m \in \mathfrak{M}} \left(\frac{\gamma|A|}{\zeta} + \frac{1}{\eta_{m2}} \right)$.

An upper bound for $|A|$ can be determined with (ix) and (x) by taking $D_m = 0$ and by removing both the η_{m2} terms and \mathfrak{C}_{1m} . This yields the conditions

$$|A| < \frac{2}{2 + \zeta} \text{ and } 1 > \left(\frac{1 - 2\phi_{\min}}{\phi_{\min}} \right)^2 \frac{|A|}{\zeta(2 - (2 + \zeta)|A|)}.$$

Using $\phi_{\min} < 1/8$, we obtain for $\zeta = 6$ the maximal value

$$|A| < \frac{2}{2 + \zeta + \frac{36}{\zeta}} \leq \frac{1}{7},$$

which is not even attainable due to the approximations made in the derivation. In any case, (x) is a stronger condition than (ii).

For γ , we need to first determine the values of η_{m01j1} and η_{m01j2} . For these we choose the values that are the square root of the product of their lower and upper limits obtained by letting all undetermined terms in (viii) and (ix) have an equal part such that $\mathfrak{C}_{1m} = 0$ and $\mathfrak{C}_{2m} = 0$ for $\zeta = 1$. This yields, for $|A| \leq \frac{1}{7}$, the positive numbers

$$\eta_{m01j1} = \sqrt{\frac{7d-5}{d-1} \frac{1}{\gamma(1-\frac{3}{2}|A|)}} \text{ and } \eta_{m01j2} = 1$$

and the inequality

$$1 > \left(\frac{1-2\phi_{\min}}{\phi_{\min}} \right)^2 \left(\gamma|A| + \frac{1}{\eta} \right) \max_{m \in \mathfrak{M}} \left\{ \frac{1}{1 - \frac{D_m}{2} \sqrt{\frac{8}{\gamma(1-\frac{3}{2}|A|)}}}} \right. \\ \left. + \frac{1}{\gamma(1-\frac{3}{2}|A|) - \frac{\eta}{2} - \frac{D_m}{2} - \frac{1}{4} \sum_{j \in \mathfrak{M}} \left(D_j \sqrt{\frac{\gamma(1-\frac{3}{2}|A|)}{8}} + D_j \right)} \right\}, \quad (4.48)$$

where we have chosen $\eta_{m2} = \eta$.

In the limit $|A| \downarrow 0$, choosing $D_m < 1$, we obtain the condition

$$1 > 2 \left(\frac{1-2\phi_{\min}}{\phi_{\min}} \right)^2 \frac{1}{\eta} \left(\frac{1}{2 - \sqrt{\frac{8}{\gamma}}} + \frac{1}{2\gamma - \eta - 2 - \sqrt{\frac{\gamma}{8}}} \right).$$

The second term yields a minimal value for $\eta = \gamma - 1 - \sqrt{\gamma/32}$, which leads to

$$1 > 2 \left(\frac{1-2\phi_{\min}}{\phi_{\min}} \right)^2 \frac{1}{\gamma - 1 - \sqrt{\frac{\gamma}{32}}} \left(\frac{1}{2 - \sqrt{\frac{8}{\gamma}}} + \frac{1}{\gamma - 1 - \sqrt{\frac{\gamma}{32}}} \right).$$

We obtain

$$\gamma > \gamma^* \approx 49.2186 \text{ with } \phi_{\min} < 0.124643143. \quad (4.49)$$

For a stricter upper bound of $|A|$, we take the parameter identification $D_j = \frac{2}{3}\sqrt{\min\{3, \gamma(1 - |A|)\} \min\{3/5, \gamma(1 - |A|)\}}$. With the γ^* of Equation (4.49) and the rough upper bound $|A| < 0.201$, we see that $D_j = 2/\sqrt{5}$. With this value of D_j , assuming $\gamma > \gamma^*$, $\eta = 1/(\gamma|A|)$, $\gamma \gg \sqrt{\gamma}$ and $1/\gamma \ll \gamma|A|$, we can remove some terms of Equation (4.48) and obtain

$$1 > 2 \left(\frac{1 - 2\phi_{\min}}{\phi_{\min}} \right)^2 |A| (1 + \gamma).$$

Hence, for $\phi_{\min} < 0.124643143$ we obtain

$$\frac{1}{\gamma^2} \ll |A| < A_\gamma^* = \frac{1}{2} \left(\frac{\phi_{\min}}{1 - 2\phi_{\min}} \right)^2 \frac{1}{1 + \gamma} \approx \frac{1}{72.55(1 + \gamma)}, \quad (4.50)$$

and additionally

$$\gamma \gg \gamma^{**} \approx 73.55, \quad \frac{1}{\gamma^2} \ll |A| < A_{\gamma^{**}}^* \approx \frac{1}{5409}. \quad (4.51)$$

Using the values of (4.51), we see that $D_j^2 < 4/5$ must hold and that (vi) and (vii) are also automatically satisfied. Hence, there exists a non-empty parameter region where all conditions of Assumption 4.1 are satisfied and, therefore, a continuous solution exists.

The analytically obtained parameter region is very restrictive due to the sometimes crude estimates used in the proofs of the theorems. The actual parameter region is expected to be much larger. Numerically, this region can be probed. Moreover, it allows us to probe the size T of the time-interval satisfying the physical constraints (I), (II) and (III).

A fixed set of reference parameter values has been chosen after a deliberate numerical search for parameter values around which T changes significantly. The reference parameter values are

$$\begin{array}{llll} A = 0.388 & \gamma = 10^4 & \delta = 1 & \epsilon = 0.0014 \\ D_1 = 0.38 & D_2 = 1 & \kappa_1 = 23.0 & \kappa_3 = -13.5 \\ J_1 = 0 & J_2 = 0.4 & J_3 = 2.0 & \phi_{\min} = 0.1 \\ \phi_{1,sat} = 1 & \phi_{3,thr} = 0 & \phi_{2,res} = 1 & \phi_{3,res} = 1 \\ \phi_{10} = 0.3 & \phi_{30} = 0.4 & & \end{array} \quad (4.52)$$

We solve the time-discrete system for the small time step $\Delta t = 0.001$. This value has been chosen arbitrarily, although it is large enough for keeping

the computational costs and duration of the simulation acceptable and small enough for showing continuous temporal behaviour.

Following the concept of Rothe method, we only need to solve numerically a 1D spatial problem at each time slice $\{t = t_k\}$. At $\{t = 0\}$ we still need to solve a different 1D spatial problem in order to obtain v^0 . We implemented the time-discrete system in MATLAB using the `bvp5c` solver, although one can also use the `bvp4c` solver. These solvers take a grid, a guess for the solution, and the boundary value problem (BVP) system as input. Then they automatically readjust the grid and interpolate the guess solution to obtain a starting point for the numerical scheme, controlling a certain error metric to determine the solution based on user-defined-convergence criteria. For an in depth description and performance analysis of the solvers, see [76, 126] for `bvp4c` and [77] for `bvp5c`.

Initially, we take a uniform grid of 300 intervals. As initial guess for the solution, we take the solution at time slice $\{t = t_{k-1}\}$ or the zero function.

Tests that check the conditions of Theorem 4.1 at each time slice, including $\{t = 0\}$, are incorporated in the numerical method. For these conditions, we use the value $V = 10^6$ and $\phi_{\min} = 0.1$. At the start of our numerical method additional tests are implemented to test the pseudo-parabolicity of the system. Failure to pass any of these tests ends the simulation.

To guarantee the end of any simulation, we incorporate an end time $T_{end} = 0.5$, which coincides with the time slice $\{t = t_{500}\}$.

The criteria for stopping a simulation in this numerical program allow one to probe the boundary of $\mathbb{S} \cap \text{int}(\mathbb{R}_{\Delta t})$ at fixed V -value lines and determine T in Δt increments for different parameter values. Smaller Δt will yield better approximations to T .

The simulation of the time-discrete system for the reference parameter values gives interesting results. All volume fractions ϕ_l are practically spatially constant functions at all time slices. Numerically, we expect a much larger area in (γ, A) -space for which Theorem 4.1 holds. As $(\gamma, A) = (10^4, 0.388)$ is well outside the analytically obtained existence region, we conclude that the conditions Assumption 4.1 are more restrictive than practically necessary. The simulation ends at time slice $\{t = t_{194}\}$ due to a violation of one of the condition of Theorem 4.1 with $\phi_3 < 0.1 = \phi_{\min}$ as shown in Figure 4.4. This indicates that $193\Delta t \leq T < 194\Delta t$ for these parameter values.

Next to the volume fraction conditions, we have the conditions on the velocity v as stated in Theorem 4.1. A clear supra-exponential growth of the

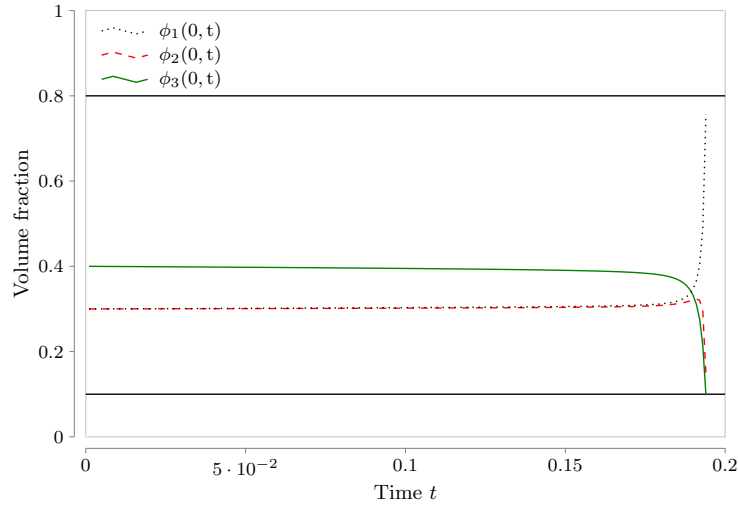


Figure 4.4: The time evolution of the volume fractions of the simulation at the reference values. The simulation automatically ended at time slice $\{t = t_{194}\}$ due to $\phi_3(0, t_{194}) < 0.1 = \phi_{\min}$. The other volume fractions stayed between the two black-lines, which indicates a guaranteed breach of $\phi_l < \phi_{\min}$ by one of the volume fractions.

$L^2(0, t; H_0^1(0, 1))$ norm of v is seen in Figure 4.5 in the region where in Figure 4.4 the volume fractions exhibited sudden drastic changes in value. Surprisingly the supra-exponential growth was not large enough to breach the $V = 10^6$ threshold of Theorem 4.1. Hence, the simulation was stopped only because the volume fraction condition was breached. The graph of $W(t)$ in Figure 4.5 looks similar to the graph of the norm, which is due to (4.4b) and the logarithmic scale of the axis.

We conclude that the reference parameter values allow a discrete solution that satisfies Theorem 4.2, even though the reference parameter values do not satisfy Assumption 4.1.

This result showed us a method of probing the parameter space dependence as the simulation was ended prematurely at $t = t_{194}$. From now on, we denote $t = t_{194}$ with $N_R = 194$, while a completed simulation is denoted by $N_R = 500$. By tracking the value of N_R at different parameter values, we indicate the dependence of T on the parameters, i.e. $(N_R - 1)\Delta t \leq T < N_R\Delta t$. We probed a grid in (γ, A) -space, a grid in ϵ -space and a grid in $(\phi_{10}, \phi_{20}, \phi_{30})$ -space. We restricted our attention to these parameters because ϵ should highly affect the volume fractions ϕ_l , and we have specific existence restrictions given by Assumption 4.1 for the other parameters.

It turns out that γ has a negligible effect on N_R in our (γ, A) -space grid. We

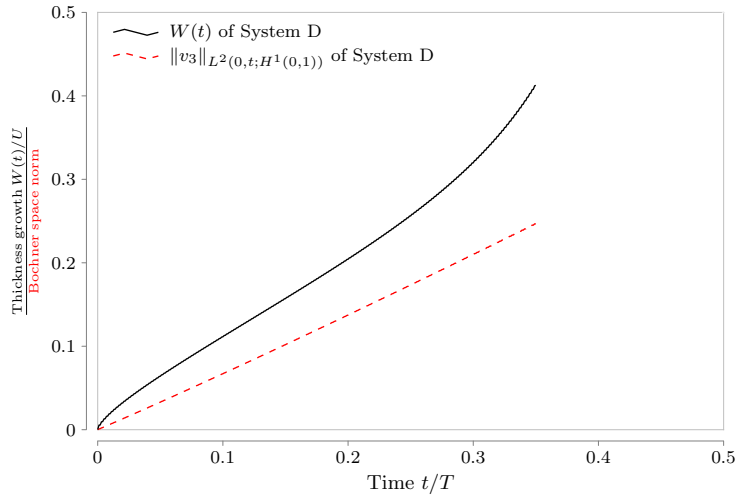


Figure 4.5: The time evolution of $W(t)$ and $\|v\|_{L^2(0,t;H^1_0(0,1))}$ of the simulation at the reference values. The simulation automatically ended at time slice $\{t = t_{194}\}$ due to $\phi_3(0, t_{194}) < 0.1 = \phi_{\min}$. The upper bound $V = 10^6$ was not yet reached. Both graphs show supra-exponential growth in the region where the volume fraction values changed dramatically.

choose the values $\gamma \in \{10^{3.5}, 10^4, 10^{4.5}, 10^5, 10^{5.5}, 10^6, 10^{6.5}, 10^7, 10^{7.5}, 10^8\}$ and $A \in \{0.376, 0.379, 0.382, 0.385, 0.388, 0.391, 0.394, 0.397, 0.400\}$.

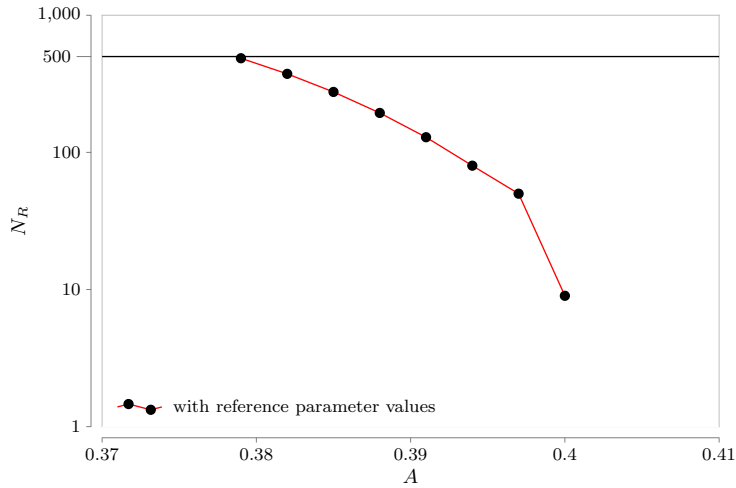


Figure 4.6: The dependence of N_R with respect to A with the other parameters taking their reference values. An approximately exponential dependence of N_R on A can be discerned. Note that A can be much larger than $\frac{1}{72.55(1+\gamma)}$ and still lead to a positive time T .

The dependence of A on N_R with $\gamma = 10^4$ is shown in Figure 4.6. An approx-

imately exponential dependence of N_R on A can be seen. Moreover, the values of N_R decrease rapidly to almost 0 for A approaching 0.4. This indicates that the actual threshold of A is much larger than $\frac{1}{72.55(1+\gamma)}$.

Since condition (viii) of Assumption 4.1 has been shown to be an underestimation of the actual existence region with respect to the parameter A , we expect a similar effect to happen for the initial conditions $(\phi_{10}, \phi_{20}, \phi_{30})$. The restriction $\phi_{10} + \phi_{20} + \phi_{30} = 1$ hints at the use of barycentric coordinates to represent the dependence of N_R on the initial conditions in the best way. In Figure 4.7 a grid, where the cells have edge size 0.1, has been placed on the region of nonnegative initial volume fractions. Additionally, the central gridpoint, where all volume fractions have the identical value $1/3$, has been added to the grid. At each gridpoint the actual value of N_R is shown for the simulation with that particular set of parameters. The inner shaded small triangle represents the region where Assumption 4.1 holds, while the shaded area between the two outer triangles represents the region where the initial conditions violate the condition of Theorem 4.1.

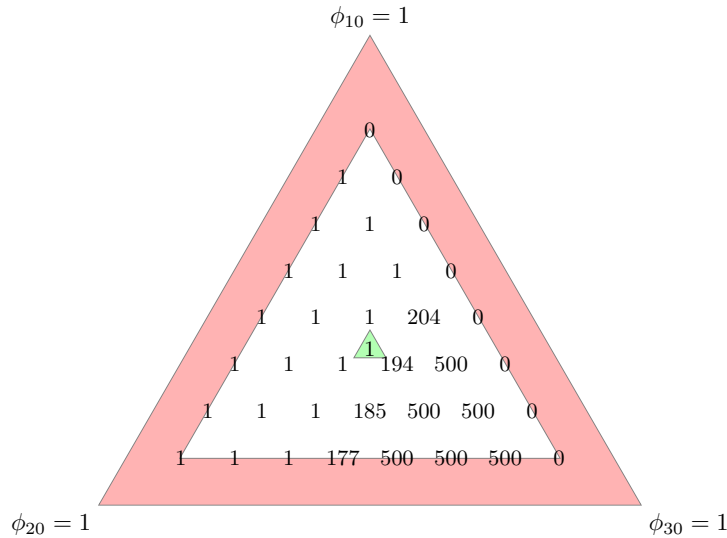


Figure 4.7: The dependence of N_R with respect to the initial conditions $(\phi_{10}, \phi_{20}, \phi_{30})$ with the other parameters taking their reference values. The inner triangle represents the region where Assumption 4.1 holds, while the shaded area between the two outer triangles represents the region where the initial conditions violate the condition of Theorem 4.1.

In Figure 4.7, the values of N_R increase with larger values of ϕ_{30} , which is expected since ϕ_3 is transformed in the reaction and can therefore decrease. Moreover, v is sensitive to the values of ϕ_3 and changes in v directly effect

ϕ_3 . Larger values of ϕ_{30} deminishes the influence of other terms on v and, therefore, the change in ϕ_3 itself. As it was shown in Figure 4.4 that ϕ_3 crossed the lower threshold set by Theorem 4.1, we expect N_R to increase with larger ϕ_{30} due to both the stabilizing effect and the higher starting value of the simulation.

Again, we see that the simulation gives $N_R > 1$ outside of the region defined by Assumption 4.1 indicating that the analytical condition in Assumption 4.1 is more restrictive than practically necessary. It is worth noting that the outer triangle of N_R values are on the boundary of the region where the condition of Theorem 4.1 holds. Due to machine-precision inaccuracies some simulations have $N_R = 0$, what indicates an unlawful starting value, or $N_R > 0$, what indicates that the starting values satisfied all conditions of Theorem 4.1.

The parameter ϵ indicates how strong certain terms influence the time-derivative of the volume fractions. In Figure 4.7, we see that there is a strong dependence between ϕ_3 and N_R . Therefore, we expect ϵ to have a significant effect on N_R as well. To this end we took a set of ϵ values and solved the time-discrete system for each of these values supplemented with the reference values of the other parameters. The used ϵ values here are: $\{1.4 \cdot 10^{-5}, 1.4 \cdot 10^{-4.5}, 1.4 \cdot 10^{-4}, \dots, 1.4 \cdot 10^{-0.5}, 1.4\}$. In Figure 4.8 a polynomial relation between N_R and ϵ can be discerned. This confirms our expectation that ϵ has a significant effect on N_R .

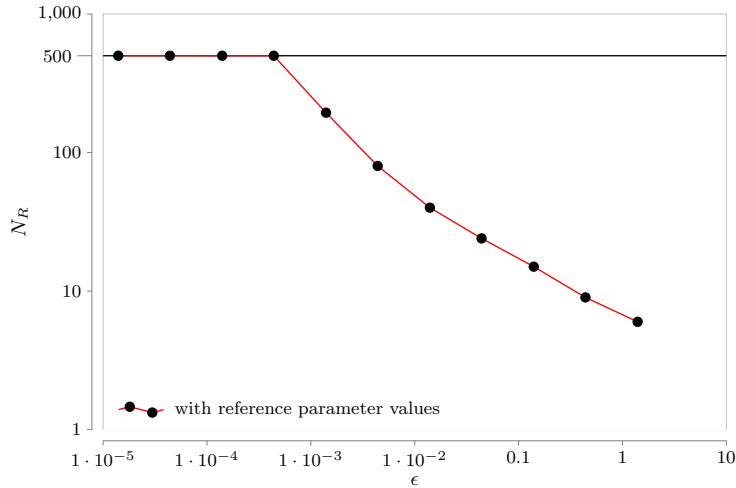


Figure 4.8: The dependence of N_R with respect to ϵ with the other parameters taking their reference values. A polynomial relation between N_R and ϵ can be discerned.

4.7 Conclusion

We have employed Rothe's method to prove Theorem 4.1, which essentially states that there exists a weak solution on $[0, T] \times (0, 1)$ of the continuous-time system given by Equations (4.1a)-(4.1c), (4.4a), (4.4b), and (4.5) for $(T, V) \in \mathbb{S} \cap \text{int}(\mathbb{R}_0)$ provided a suitable parameter regime is chosen (cf. Assumption 4.1).

Numerically, we have validated that the conditions of Theorem 4.1 can be violated for t large enough. Moreover, we have shown using numerical simulations that the parameter region for the existence of weak solutions as given by Assumption 4.1 is restrictive. Both in (γ, A) -space as in $(\phi_{10}, \phi_{20}, \phi_{30})$ -space the numerical simulations showed existence for points well outside the regions given by Assumption 4.1. Additionally, we have shown that A , ϕ_{30} and ϵ have a significant influence on T , as was expected. Moreover, we could indicate that γ has no significant effect on T in the numerical simulations. This was against the prediction of the shape of the existence region of Assumption 4.1.

This means that sharper inequality results probably hold, which would finally lead to a relaxation of conditions (v) and (viii) in Assumption 4.1.

Extensions to higher dimensional spatial domains lead to complications in the existence proof. The main difficulty lies in the a-priori absence of essential boundedness of ϕ^k for $k > 0$. The Rellich-Kondrachov Theorem (Theorem 2.6) states that for a d -dimensional spatial domain Ω more than $H^d(\Omega)$ -regularity is needed to obtain an embedding of $L^\infty(\Omega)$. Consequently, almost all non-linearities become intractable without obtaining much stronger regularity results for all unknowns. That is why we choose to decrease the complexity of the problem from quasi-linear to linear, so that we are allowed to look at domains of arbitrary dimensions in Chapter 5.

4.8 Appendix: Existence of solutions to discrete-time system

The subsystem (4.7a) with (4.8a) is a standard elliptic system in ϕ_l^k , which has a unique solution in $\phi_l^k \in H^1(0, 1)$ if $\phi_l^{k-1}, v^{k-1}, w_m^{k-1} \in H^1(0, 1)$ and $w_m^k \in H^1(0, 1)$. Similarly, by direct integration, the subsystem (4.7b) with (4.8b) has a unique solution $v^k \in L^2(0, 1)$ if there are unique $\phi_l^{k-1}, v^{k-1}, w_m^{k-1} \in L^2(0, 1)$,

$\phi_{\min} \leq \phi_l^{k-1} \leq 1$ almost everywhere, and $w_m^k \in L^2(0, 1)$. Moreover, this subsystem has a unique solution $v^k \in H^1(0, 1)$ if there are unique $\phi_l^{k-1}, v^{k-1}, w_m^{k-1} \in H^1(0, 1)$ and $w_m^k \in H^1(0, 1)$.

The existence of a unique $v^0 \in H^1(0, 1)$ is slightly more complicated. Even though any $v^0 \in H^1(0, 1)$ will give a unique solution, we do realize that the numerical method might be highly sensitive to the choice of $v^0 \in H^1(0, 1)$. Physically, we expect $v^0 \in H^1(0, 1)$ to be close to the solution of continuous-time system with the initial conditions filled in. Unfortunately, we do not have sufficient temporal regularity to extend the system to the $t = 0$ boundary. However, since any $v^0 \in H^1(0, 1)$ would suffice, we just choose the function $v^0 \in H^1(0, 1)$ that would be the solution if there was sufficient regularity.

To this end, we integrate (4.1b) from 0 to z and insert the initial conditions (4.5) in the continuous-time system. This yields, at $t = 0$, a system for v and $\partial_t w_m$.

$$\begin{aligned} \Gamma(\phi_0)v + \sum_{m \in \mathfrak{M}} H_{1m}(\phi_0)\partial_t w_m = G_v(\phi_0)z \\ + \sum_{m \in \mathfrak{M}} J_m \mathcal{L}(\phi_{m,res} - \phi_{m0}), \end{aligned} \quad (4.53a)$$

$$\begin{aligned} \partial_t w_m - \gamma_m \partial_z^2 \partial_t w_m + F_m(\phi_0)v \\ + \sum_{j \in \mathfrak{M}} E_{m01j}(\phi_0)\partial_z \partial_t w_j = G_{w,m}(\phi_0), \end{aligned} \quad (4.53b)$$

with boundary conditions

$$v|_{z=0} = 0, \quad (4.54a)$$

$$\partial_t w_m|_{z=0} = \frac{J_m}{H_{1m}(\phi_0)} \mathcal{L}(\phi_{m,res} - \phi_{m0}), \quad (4.54b)$$

$$\begin{aligned} \partial_z \partial_t w_m|_{z=1} = A_m \left(\partial_t w_m|_{z=1} + \sum_{j \in \mathfrak{M}} \frac{H_{1j}(\phi_0)}{\Gamma(\phi_0)} \partial_t w_j|_{z=1} \right) \\ - \frac{A_m}{\Gamma(\phi_0)} \left[G_v(\phi_0) + \sum_{j \in \mathfrak{M}} J_j \mathcal{L}(\phi_{j,res} - \phi_{j0}) + J_d \mathcal{L}(\phi_{d,res} - \phi_{d0}) \right] \Big|_{z=1}. \end{aligned} \quad (4.54c)$$

Inserting Equation (4.53a) in Equation (4.53b), testing with ψ_m and summing over $m \in \mathfrak{M}$, we obtain

$$\mathcal{B}(\partial_t \mathbf{w}, \boldsymbol{\psi}) = \sum_{m \in \mathfrak{M}} \mathcal{B}_m(\partial_t \mathbf{w}, \psi_m) = \sum_{m \in \mathfrak{M}} \mathfrak{G}_m(\psi_m), \quad (4.55)$$

where

$$\begin{aligned} \mathcal{B}_m(\mathbf{u}, \psi_m) &= \int_0^1 \gamma_m \partial_z u_m \partial_z \psi_m + \sum_{j \in \mathfrak{M}} E_{m01j}(\phi_0) (\partial_z u_j) \psi_m \\ &\quad - \sum_{j \in \mathfrak{M}} \frac{F_m(\phi_0) H_{1j}(\phi_0)}{\Gamma(\phi_0)} u_j \psi_m + u_m \psi_m \\ &\quad - \gamma_m A_m \left[\partial_z (u_m \psi_m) + \sum_{j \in \mathfrak{M}} \frac{H_{1j}(\phi_0)}{\Gamma(\phi_0)} \partial_z (u_j \psi_m) \right] dz \end{aligned} \quad (4.56)$$

and

$$\begin{aligned} \mathfrak{G}_m(\psi_m) &= \int_0^1 G_{w,m}(\phi_0) \psi_m - \frac{F_m(\phi_0)}{\Gamma(\phi_0)} \left[G_v(\phi_0) z + \sum_{j \in \mathfrak{M}} J_j \mathcal{L}(\phi_{j,res} - \phi_{j0}) \right] \psi_m dz \\ &\quad - \left[\frac{\gamma_m A_m}{\Gamma(\phi_0)} \left(G_v(\phi_0) + \sum_{j \in \mathfrak{M}} J_j \mathcal{L}(\phi_{j,res} - \phi_{j0}) + J_d \mathcal{L}(\phi_{d,res} - \phi_{d0}) \right) \psi_m \right]^{z=1}. \end{aligned} \quad (4.57)$$

Clearly, $\mathcal{B}(\cdot, \cdot) = \sum_{m \in \mathfrak{M}} \mathcal{B}_m(\cdot, \cdot)$ is a bilinear form on $H_{0,free}^1(0, 1)^{d-1}$, which is defined as $H_{0,free}^1(0, 1)^{d-1} = \{f \in H^1(0, 1)^d \mid f(0) = 0\}$. This bilinear form and $\sum_{m \in \mathfrak{M}} \mathfrak{G}_m(\cdot)$ are obviously continuous. However, $\mathcal{B}(\cdot, \cdot)$ is only coercive if the following conditions are satisfied for all $j, m \in \mathfrak{M}$:

$$E_{m01j}(\phi_0)^2 < \frac{4\gamma_j}{(3d-2)(5d-4)}, \quad (4.58a)$$

$$4\Gamma(\phi_0)^2 > (5d-4)^2 F_m(\phi_0)^2 H_{1j}(\phi_0)^2. \quad (4.58b)$$

$$\gamma_j A_j^2 < \frac{1}{(3d-2)(5d-4)}, \quad (4.58c)$$

$$\frac{H_{1m}(\phi_0)^2}{\Gamma(\phi_0)^2} < \frac{4\gamma_j}{(3d-2)(5d-4)}. \quad (4.58d)$$

Condition (4.58a) follows from condition (iii) in Assumption 4.1, while conditions (4.58b), (4.58c), (4.58d) are exactly conditions (iv), (vi) and (vii) in Assumption 4.1, respectively.

Unfortunately, due to the boundary conditions, $\partial_t w_m$ is not an element of $H_{0,free}^1(0, 1)^{d-1}$. However, using the decomposition

$$\partial_t w_m = \tilde{w}_m + \tilde{a}_m(1-z)^2 + \tilde{b}z^{A_m} \sin\left(\frac{\pi}{2}z\right) = \tilde{w}_m + \tilde{c}_m(z) \quad (4.59)$$

with

$$\tilde{\mathbf{w}} \in \left\{ f \in H^2(0,1)^{d-1} \left| f_m(0) = 0, (\partial_z f)_m(1) = A_m \left(f_m(1) + \sum_{j \in \mathfrak{M}} \frac{H_{1j}(\phi_0)}{\Gamma(\phi_0)^2} f_j(1) \right) \right. \right\} = \tilde{\mathfrak{W}}$$

and the bounded values

$$\tilde{a}_m = \frac{J_m}{H_{1m}(\phi_0)} \mathcal{L}(\phi_{m,res} - \phi_{m0}), \quad (4.60a)$$

$$\tilde{b} = \frac{G_v(\phi_0) + \sum_{j \in \mathfrak{M}} J_j \mathcal{L}(\phi_{j,res} - \phi_{j0}) + J_d \mathcal{L}(\phi_{d,res} - \phi_{d0})}{\sum_{j \in \mathfrak{M}} H_{1j}(\phi_0)}, \quad (4.60b)$$

which follow from the identities

$$\begin{aligned} \partial_t w_m(0) &= \tilde{w}_m(0) + \tilde{a}_m - \lim_{z \rightarrow 0} \tilde{b} \frac{\pi}{2A_m} \frac{\cos(\frac{\pi}{2}z)}{z^{-A_m-1}} \\ &= \begin{cases} \tilde{w}_m(0) + \tilde{a}_m & \text{for } A_m > -1, \\ \tilde{w}_m(0) + \tilde{a}_m + \frac{\pi}{2} \tilde{b} & \text{for } A_m = -1, \\ \infty & \text{for } A_m < -1, \end{cases} \end{aligned} \quad (4.61a)$$

$$\partial_t w_m(1) = \tilde{w}_m(1) + \tilde{b}, \quad (4.61b)$$

$$\partial_z \partial_t w_m(1) = \partial_z \tilde{w}_m(1) + A_m \tilde{b}, \quad (4.61c)$$

we see that $\tilde{\mathfrak{W}} \subset H_{0,free}^1(0,1)^{d-1}$ for all $A_m > -1$, which contains $|A_m| < 1$ of condition (ii) in Assumption 4.1.

Via Lax-Milgram we obtain a unique solution $\tilde{\mathbf{w}}$ in $H_{0,free}^1(0,1)^{d-1}$ that satisfies

$$\mathcal{B}(\tilde{\mathbf{w}}, \boldsymbol{\psi}) = -\mathcal{B}(\tilde{\mathbf{c}}(z), \boldsymbol{\psi}) + \sum_{m \in \mathfrak{M}} \mathfrak{G}_m(\psi_m). \quad (4.62)$$

Since, $\mathcal{B}(\cdot, \cdot)$ is a coercive bilinear form, there exists a constant $C > 0$ such that the inequality $\left| \sum_{m \in \mathfrak{M}} \int_0^1 \partial_z \tilde{w}_m \partial_z \psi_m dz \right| \leq C \|\boldsymbol{\psi}\|_{C_c^1(0,1)^{d-1}}$ holds for $\psi_m \in C_c^1(0,1)$, the space of C^1 functions with compact support on $(0,1)$. Hence, by Proposition 8.3 of [20], we have $\tilde{\mathbf{w}} \in H^2(0,1)^{d-1}$.

Applying a partial integration to (4.62), we see that $\tilde{\mathbf{w}} + \tilde{\mathbf{c}}(z)$ can only satisfy (4.53a)-(4.54c) if $\tilde{\mathbf{w}} \in \tilde{\mathfrak{W}}$. Hence, there exists a unique solution $\partial_t w_m \in H^2(0,1)$ and, therefore, a unique solution $v^0 \in H_{0,free}^1(0,1)$ satisfying (4.53a)-(4.54c).

For the existence of a unique weak solution $\mathbf{w}^k \in H^2(0,1)^{d-1}$, we follow

a similar procedure and use induction on k . Of course, $k = 0$ is satisfied by $\mathbf{w} = 0$. For the induction step we use $0 < k = K \leq T/\Delta t$ and assume that $\mathbf{w}^{k-1} \in H^2(0, 1)^{d-1}$. We test Equation (4.7c) with $\boldsymbol{\psi} \in H^1(0, 1)^{d-1}$. Using the decomposition

$$w_m^k = \hat{w}_m^k + \hat{a}_m^k (1-z)^2 + \hat{b}^k z^{A_m/2} \sin^{3/2}\left(\frac{\pi}{2}z\right) = \hat{w}_m^k + \hat{c}_m^k(z) \quad (4.63)$$

with

$$\hat{\mathbf{w}}^k \in \{f \in H^2(0, 1)^{d-1} \mid f_m(0) = 0, (\partial_z f)_m(1) = A_m(f_m(1))\} = \hat{\mathfrak{W}} \subset H_{0,free}^1(0, 1)^{d-1}$$

and

$$\hat{a}_m^k = w_m^{k-1}(0) + \frac{J_m \Delta t}{H_{1m}(\phi^{k-1})} \mathcal{L}(\phi_{m,res} - \phi_m^{k-1}), \quad (4.64a)$$

$$\hat{b}^k = 2W^k, \quad (4.64b)$$

which are straightforwardly derived from (4.8b), we obtain a bilinear form $\mathcal{A}_{\Delta t}(\hat{\mathbf{w}}, \boldsymbol{\psi})$ on $H_{0,free}^1(0, 1)^{d-1}$:

$$\begin{aligned} \mathcal{A}_{\Delta t}^k(\hat{\mathbf{w}}^k, \boldsymbol{\psi}) = & \sum_{m \in \mathfrak{M}} \int_0^1 (\gamma_m + D_m \Delta t) \partial_z \hat{w}_m^k \partial_z \psi_m + \hat{w}_m^k \psi_m \\ & - \sum_{j \in \mathfrak{M}} E_{m0j}(\phi^{k-1}) \hat{w}_j^k \partial_z \psi_m dz. \end{aligned} \quad (4.65)$$

Unfortunately, this bilinear form is used in the equation

$$\begin{aligned}
\mathcal{A}_{\Delta t}^k(\hat{\mathbf{w}}^k, \boldsymbol{\psi}) &= \mathcal{A}_{\Delta t}^k(\mathbf{w}^{k-1}, \boldsymbol{\psi}) - \mathcal{A}_{\Delta t}^k(\hat{\mathbf{c}}^k(z), \boldsymbol{\psi}) \\
&+ \sum_{m \in \mathfrak{M}} \left[(\gamma_m + D_m \Delta t) (\partial_z \hat{w}_m^k) \psi_m - \sum_{j \in \mathfrak{M}} E_{m01j}(\phi^{k-1}) \hat{w}_j^k \psi_m \right]_0^1 \\
&+ \sum_{m \in \mathfrak{M}} \left[(\gamma_m + D_m \Delta t) (\partial_z \hat{c}_m^k) \psi_m - \sum_{j \in \mathfrak{M}} E_{m01j}(\phi^{k-1}) \hat{c}_j^k \psi_m \right]_0^1 \\
&- \sum_{m \in \mathfrak{M}} \left[\gamma_m (\partial_z w_m^{k-1}) \psi_m - \sum_{j \in \mathfrak{M}} E_{m01j}(\phi^{k-1}) w_m^{k-1} \psi_m \right]_0^1 \\
&+ \Delta t \sum_{m \in \mathfrak{M}} \int_0^1 G_{w,m}(\phi^{k-1}) \psi_m - F_m(\phi^{k-1}) v^{k-1} \psi_m \\
&\quad + \sum_{j \in \mathfrak{M}} \sum_{i=0}^1 E_{mi0j} \partial_z^i w_j^{k-1} \partial_z \psi_m dz \\
&- \Delta t \sum_{m \in \mathfrak{M}} \left[\sum_{j \in \mathfrak{M}} \sum_{i=0}^1 E_{mi0j} \partial_z^i w_j^{k-1} \psi_m \right]_0^1 \tag{4.66a} \\
&= \sum_{m \in \mathfrak{M}} \left[(\gamma_m + D_m \Delta t) (\partial_z \hat{w}_m^k) \psi_m - \sum_{j \in \mathfrak{M}} E_{m01j}(\phi^{k-1}) \hat{w}_j^k \psi_m \right]_0^1 + \mathfrak{F}^k(\boldsymbol{\psi}), \tag{4.66b}
\end{aligned}$$

which has a right-hand-side that violates the conditions of Lax-Milgram. However, we can create a new bilinear form $a_{\Delta t}^k(\hat{\mathbf{w}}^k, \boldsymbol{\psi})$ on $H_{0,free}^1(0, 1)^{d-1}$ such that we can apply Lax-Milgram. Due to the behaviour of elements of $\hat{\mathfrak{M}}$ on the boundary of $(0, 1)$, we obtain

$$\begin{aligned}
a_{\Delta t}^k(\hat{\mathbf{w}}^k, \boldsymbol{\psi}) &= \mathcal{A}_{\Delta t}^k(\hat{\mathbf{w}}^k, \boldsymbol{\psi}) - \sum_{m \in \mathfrak{M}} (\gamma_m + D_m \Delta t) A_m \int_0^1 \partial_z (\hat{w}_m^k \psi_m) dz \\
&+ \sum_{m \in \mathfrak{M}} \sum_{j \in \mathfrak{M}} E_{m01j}(\phi^{k-1}(1)) \int_0^1 \partial_z (\hat{w}_j^k \psi_m) dz = \mathfrak{F}^k(\boldsymbol{\psi}). \tag{4.67}
\end{aligned}$$

Remark that the trace $\phi^{k-1}(1)$ exists due to $\phi^{k-1} \in H^1(0, 1)^d$. The continuity of $a_{\Delta t}^k(\hat{\mathbf{w}}, \boldsymbol{\psi})$ and $\mathfrak{F}^k(\boldsymbol{\psi})$ is straightforward. The coercivity of

$a_{\Delta t}^k(\hat{\mathbf{w}}, \psi)$ is equivalent to the conditions

$$0 < 1 - \sum_{j \in \mathfrak{M}} E_{j01m} \frac{\eta_{j01m1}}{2}, \quad (4.68a)$$

$$0 < \gamma_m(1 - |A_m|) - \frac{1}{2} \sum_{j \in \mathfrak{M}} \left(\frac{E_{m01j}}{\eta_{m01j1}} + \frac{E_{m01j}}{\eta_{m01j2}} + E_{j01m} \eta_{j01m2} \right), \quad (4.68b)$$

for $\eta_{m01j1}, \eta_{m01j2} > 0$, which follow from conditions (ii), (viii) and (ix) in Assumption 4.1 if E_{m01j} , γ_m and A_m satisfy condition (iii) in Assumption 4.1.

Thus Lax-Milgram gives a unique solution $\hat{\mathbf{w}}^k \in H_{0,free}^1(0,1)^{d-1}$. By the coercivity, we obtain again via proposition 8.3 of [20] that $\hat{\mathbf{w}}^k \in H^2(0,1)^{d-1}$. Applying a partial integration to (4.67), we see that equation (4.7c) with boundary conditions (4.4b) can only be satisfied if $\hat{\mathbf{w}}^k \in \hat{\mathfrak{W}}$. Hence, there is a unique weak solution $\mathbf{w}^k \in H^2(0,1)^{d-1}$. Thus induction gives us that there is a unique weak solution $\mathbf{w}^k \in H^2(0,1)^{d-1}$ for all $t_k \in [0, T]$.

4.9 Appendix: Derivation of discrete-time quadratic inequalities

In the derivation of the quadratic inequalities (4.11), (4.12), (4.10), we use the following identities

$$2(a-b)a = a^2 - b^2 + (a-b)^2, \quad (4.69a)$$

$$2(a-b)b = a^2 - b^2 - (a-b)^2, \quad (4.69b)$$

which are valid for all $a, b \in \mathbf{R}$.

The quadratic inequality (4.11) is obtained by testing Equation (4.7a) with ϕ_l , partially integrating the Laplacian terms, and using Young's inequality, leading to the following identities for the "b"-coefficients, where we use the

extra parameters $\eta_1, \eta_2, \eta_{3n}, \eta_{ijm}, \eta_{l1jmn} > 0$.

$$\begin{aligned}
b_{1l} &= 2\delta_l, & b_{6ln} &= \eta_{3n} + \sum_{m \in \mathfrak{M}} \sum_{j=0}^1 \eta_{l1jmn}, \\
b_{2l}(\Delta t) &= \Delta t, & b_{7l0m} &= \frac{B_{i00m}^2}{\eta_{i00m}} + \sum_{n \in \mathcal{L}} \frac{4B_{i10m}^2}{\eta_{i10mn}}, \\
b_{3l} &= \frac{G_{\phi,l}^2}{\eta_1}, & b_{7l1m} &= \frac{B_{i10m}^2}{\eta_{i10m}}, \\
b_{4l} &= \frac{4I_l^2 \Gamma^2}{\eta_2} + I_l^2 \Gamma^2 \sum_{n \in \mathcal{L}} \frac{1}{\eta_{3n}}, & b_{8l0m} &= \frac{B_{i01m}^2}{\eta_{i01m}} + \sum_{n \in \mathcal{L}} \frac{4B_{i11m}^2}{\eta_{i11mn}}, \\
b_{5l} &= \eta_1 + \eta_2 + \sum_{m \in \mathfrak{M}} \sum_{i,j=0}^1 \eta_{ijm}, & b_{8l1m} &= \frac{B_{i11m}^2}{\eta_{i11m}}.
\end{aligned} \tag{4.70}$$

Similarly, the quadratic inequality (4.12) is obtained by testing Equation (4.7a) with $\mathcal{D}_{\Delta t}^k(\phi_l)$, partially integrating the Laplacian terms, and using Young's inequality, leading to the following identities for the “c”-coefficients, where $\eta_1, \eta_2, \eta_{3n}, \eta_{ijm}, \eta_{l1jmn} > 0$.

$$\begin{aligned}
c_{1l} &= \frac{2}{\delta_l}, & c_{5l} &= \frac{2}{\delta_l} \left(\eta_1 + \eta_2 + \sum_{n \in \mathcal{L}} \eta_{3n} \right. \\
& & & \left. + \sum_{m \in \mathfrak{M}} \sum_{j=0}^1 \left[\sum_{n \in \mathcal{L}} \eta_{l1jmn} + \sum_{i=0}^1 \eta_{ijm} \right] \right), \\
c_{2l}(\Delta t) &= \Delta t, & c_{6l}^k &= \sum_{n \in \mathcal{L}} \left(\frac{2I_l^2 \Gamma^2}{\delta_l \eta_{3n}} \|\partial_z v^{k-1}\|_{L^2}^2 \right. \\
& & & \left. + \sum_{m \in \mathfrak{M}} \left[\frac{2B_{i10m}^2 C_{1,0}^2}{\delta_l \eta_{i10mn}} \|w_m^{k-1}\|_{H^1}^2 \right. \right. \\
& & & \left. \left. + \frac{2B_{i11m}^2 C_{1,0}^2}{\delta_l \eta_{i11mn}} \|\mathcal{D}_{\Delta t}^k(w_m)\|_{H^1}^2 \right] \right), \\
c_3 &= \frac{G_{\phi,l}^2}{2\delta_l \eta_1}, & c_{7im} &= \frac{B_{i10m}^2}{2\delta_l \eta_{i10m}}, \\
c_4 &= \frac{I_l^2 \Gamma^2}{2\delta_l \eta_2}, & c_{8im} &= \frac{B_{i11m}^2}{2\delta_l \eta_{i11m}}.
\end{aligned} \tag{4.71}$$

Note that

$$\begin{aligned}
\sum_{t_k \in [0, T]} c_{6l}^k \Delta t &\leq \sum_{n \in \mathcal{L}} \left[\frac{2I_l^2 \Gamma^2}{\delta_l \eta_{3n}} V^2 + \sum_{m \in \mathfrak{M}} \left[\frac{2B_{i10m}^2 C_{1,0}^2}{\delta_l \eta_{i10mn}} \left(\sum_{t_k \in [0, T]} \|w_m^{k-1}\|_{H^1}^2 \Delta t \right) \right. \right. \\
& & & \left. \left. + \frac{2B_{i11m}^2 C_{1,0}^2}{\delta_l \eta_{i11mn}} \left(\sum_{t_k \in [0, T]} \|\mathcal{D}_{\Delta t}^k(w_m)\|_{H^1}^2 \Delta t \right) \right] \right] \\
&= c_{6l1} V^2 + \sum_{m \in \mathfrak{M}} \sum_{t_k \in [0, T]} \left(c_{6l2m} \|w_m^{k-1}\|_{H^1}^2 + c_{6l3m} \|\mathcal{D}_{\Delta t}^k(w_m)\|_{H^1}^2 \right) \Delta t. \tag{4.72}
\end{aligned}$$

The quadratic inequality (4.10) is not so easy to obtain. First, we rewrite Equation (4.7c) into a more structured form:

$$\mathcal{D}_{\Delta t}^k(w_m) - \partial_z \mathcal{S}_m^k = G_{w,m}(\phi^{k-1}) - F_m(\phi^{k-1})v^{k-1}, \quad (4.73)$$

where $\mathcal{S}_m^k = \mathcal{S}_{m0}^k + \mathcal{S}_{m1}^k$ is given by

$$\mathcal{S}_{m0}^k = - \sum_{j \in \mathfrak{M}} [E_{m00j}(\phi^{k-1})w_j^{k-1} + E_{m01j}(\phi^{k-1})\mathcal{D}_{\Delta t}^k(w_j)], \quad (4.74a)$$

$$\mathcal{S}_{m1}^k = D_m \partial_z w_m^k + \gamma_m \mathcal{D}_{\Delta t}^k(\partial_z w_m) - \sum_{j \in \mathfrak{M}} E_{mi0j}(\phi^{k-1})\partial_z w_j^{k-1}, \quad (4.74b)$$

with \mathcal{S}_{m0}^k , a term with boundary evaluations at only $z = 0$, and, \mathcal{S}_{m1}^k , a term with boundary evaluations at only $z = 1$. Second, we test Equation (4.73) with both w_m^k and $\mathcal{D}_{\Delta t}^k(w_m)$, apply a partial integration to the $\partial_z \mathcal{S}_m^k$ term, obtain two quadratic inequalities and sum them. The partial integration of the $\partial_z \mathcal{S}_m^k$ term yields a boundary evaluation, which we can bound:

$$\begin{aligned} \left| [\mathcal{S}_m^k \psi]_0^1 \right| &\leq |\mathcal{S}_m^k(1) - \mathcal{S}_m^k(0)| |\psi(0)| \\ &\quad + [|\mathcal{S}_{m0}^k(0)| + |\mathcal{S}_{m1}^k(1)| + |\mathcal{S}_{m0}^k(1) - \mathcal{S}_{m0}^k(0)|] \|\partial_z \psi\|_{L^2}, \end{aligned} \quad (4.75)$$

where we use the following bounds

$$|\mathcal{S}_m^k(1) - \mathcal{S}_m^k(0)| \leq \|\mathcal{D}_{\Delta t}^k(w_m)\|_{L^2} + G_{w,m} + F_m \|v^{k-1}\|_{L^2}, \quad (4.76a)$$

$$|\mathcal{S}_{m0}^k(0)| \leq \sum_{j \in \mathfrak{M}} \frac{J_j \phi_{j,res}}{H_{\phi_{\min}}} [E_{m00j}T + E_{m01j}], \quad (4.76b)$$

$$\begin{aligned} |\mathcal{S}_{m1}^k(1)| &\leq |A_m|(\gamma_m + D_m T) \left[\frac{J_m \phi_{m,res}}{H_{\phi_{\min}}} + \frac{J_d \phi_{d,res}}{\Gamma_{\phi_{\min}}} \right] \\ &\quad + D_m |A_m| \left[|\mathcal{W}^0| + V\sqrt{T} \right] \\ &\quad + \gamma_m |A_m| \left[\|\mathcal{D}_{\Delta t}^k(\partial_z w_m)\|_{L^2} + \|\partial_z v^{k-1}\|_{L^2} \right], \end{aligned} \quad (4.76c)$$

$$\begin{aligned} |\mathcal{S}_{m0}^k(1) - \mathcal{S}_{m0}^k(0)| &\leq \sum_{j \in \mathfrak{M}} \left[E_{m00j} \|\partial_z w_j^{k-1}\|_{L^2} + E_{m01j} \|\mathcal{D}_{\Delta t}^k(\partial_z w_j)\|_{L^2} \right. \\ &\quad \left. + \frac{J_j \phi_{j,res}}{H_{\phi_{\min}}} (E_{m00j}T + E_{m01j}) \right]. \end{aligned} \quad (4.76d)$$

With the above bounds, we can test Equation (4.73) with both w_m^k and $\mathcal{D}_{\Delta t}^k(w_m)$, apply Young's inequality and sum the two inequalities. This leads

to the following identities for the “a”-coefficients with all η 's positive:

$$\begin{aligned}
a_{1m} &= \gamma_m + D_m, \\
a_{2m}(\Delta t) &= 2 + \Delta t, \\
a_{3m}(\Delta t) &= 2\gamma_m + (\gamma_m + D_m)\Delta t, \\
a_4 &= D_m^2 |A_m|^2 |\mathcal{W}^0|^2 \left(\frac{1}{\eta_{m8}} + \frac{1}{\eta_{am8}} \right) + D_m^2 |A_m|^2 V^2 T \left(\frac{1}{\eta_{m9}} + \frac{1}{\eta_{am9}} \right) \\
&\quad + G_{w,m}^2 \left(\frac{1}{\eta_{m1}} + \frac{1}{\eta_{am1}} \right) + \left(\frac{J_m \phi_{m,res} T}{H_{\phi_{\min}}} \right)^2 \left(\frac{1}{\eta_{m3}} + \eta_0 + \frac{1}{\eta_{am3}} + \eta_{a0} \right) \\
&\quad + \left(\sum_{j \in \mathfrak{M}} \frac{J_j \phi_{j,res}}{H_{\phi_{\min}}} (E_{m00j} T + E_{m01j}) \right)^2 \left(\frac{4}{\eta_{m4}} + \frac{4}{\eta_{am4}} \right) \\
&\quad + \left(\frac{J_m \phi_{m,res}}{H_{\phi_{\min}}} + \frac{J_d \phi_{d,res}}{\Gamma_{\phi_{\min}}} \right)^2 (D_m T + \gamma_m)^2 |A_m|^2 \left(\frac{1}{\eta_{m5}} + \frac{1}{\eta_{am5}} \right) \\
&\quad + 2G_{w,m} \frac{J_m \phi_{m,res}}{H_{\phi_{\min}}} (T + 1), \\
a_{5m} &= \eta_{m1} + \eta_{m2}, \\
a_{6m} &= \max \left\{ 0, \sum_{i=4}^9 \eta_{mi} - 2D_m(1 - |A_m|) + \frac{D_m^2 |A_m|^2}{\eta_{am6}} \right. \\
&\quad \left. + \sum_{j \in \mathcal{M}} (\eta_{m00j} + \eta_{m10j} + \eta_{m01j} + \eta_{m00j1} + \eta_{m01j1}) \right\}, \\
a_{7m} &= \sum_{j \in \mathfrak{M}} E_{j00m}^2 \left(\frac{1}{\eta_{j00m}} + \frac{1}{\eta_{aj00m}} \right), \\
a_{8m} &= \sum_{j \in \mathfrak{M}} \left[E_{j10m}^2 \left(\frac{1}{\eta_{j10m}} + \frac{1}{\eta_{aj10m}} \right) + E_{j00m}^2 \left(\frac{1}{\eta_{j00m1}} + \frac{1}{\eta_{aj00m1}} \right) \right], \\
a_{9m} &= \eta_{m3} + \eta_{am3} + \sum_{j \in \mathfrak{M}} \left(\frac{E_{j01m}^2}{\eta_{j01m}} + E_{j01m} \eta_{aj01m} \right), \\
a_{10m} &= \frac{\gamma_m^2 |A_m|^2}{\eta_{m6}} + 2\gamma_m |A_m| + \eta_{am1} + \eta_{am2} + \sum_{i=4}^9 \eta_{ami} \\
&\quad + \sum_{j \in \mathfrak{M}} \left(\frac{E_{j01m}^2}{\eta_{j01m1}} + \eta_{am00j1} + \eta_{am00j} + \eta_{am10j} \right) \\
&\quad + \sum_{j \in \mathfrak{M}} \left(\frac{E_{m01j}}{\eta_{am01j}} + \frac{E_{j01m}}{\eta_{aj01m1}} + E_{m01j} \eta_{am01j1} \right), \\
a_{11} &= F_m^2 \left(\frac{1}{\eta_0} + \frac{1}{\eta_{m2}} + \frac{1}{\eta_{a0}} + \frac{1}{\eta_{am2}} \right), \\
a_{12} &= \gamma_m^2 |A_m|^2 \left(\frac{1}{\eta_{m7}} + \frac{1}{\eta_{am7}} \right).
\end{aligned} \tag{4.77}$$

Homogenization and Corrector Estimates

Based on:

A.J. Vromans, A.A.F. van de Ven, and A. Muntean, “Periodic homogenization of a pseudo-parabolic equation via a spatial-temporal decomposition”, accepted to *Progress in Industrial Mathematics at ECMI 2018*, (I. Faragó, F. Izsák, and P. Simon, eds.), vol. 20 of *The European Consortium for Mathematics in Industry Series in Mathematics in Industry*, Scientific Committee of The 20th European Conference on Mathematics for Industry, Springer, Berlin.

A.J. Vromans, A.A.F. van de Ven, and A. Muntean, “Periodic homogenization of pseudo-parabolic equation structures”, 2018, CASA-report **18-06**

A.J. Vromans, A.A.F. van de Ven, and A. Muntean, “Homogenization of a pseudo-parabolic system via a spatial-temporal decoupling: upscaling and corrector estimates for perforated domains”, 2019, accepted to *Mathematics in Engineering*

A.J. Vromans, A.A.F. van de Ven, and A. Muntean, “Homogenization of a pseudo-parabolic system via a spatial-temporal decoupling: upscaling and corrector estimates for perforated domains”, 2019, CASA-report **19-01**

In this chapter, we determine corrector estimates quantifying the convergence speed of the upscaling of a pseudo-parabolic system containing drift terms incorporating the separation of length scales with relative size $\epsilon \ll 1$. To achieve this goal, we exploit a natural spatial-temporal decomposition, which splits the pseudo-parabolic system into an elliptic partial differential equation and an ordinary differential equation coupled together. We obtain upscaled model equations, explicit equations for effective transport coefficients, as well as corrector estimates delimitating the quality of the upscaling. Finally, for special cases we show convergence speeds for global times, i.e. $t \in \mathbf{R}_+$, by using time intervals expanding to the whole of \mathbf{R}_+ simultaneously with passing to the homogenization limit $\epsilon \downarrow 0$.

5.1 Introduction

Corrosion of concrete by acidic compounds is a problem for construction as corrosion can lead to erosion and degradation of the structural integrity of concrete structures [118], [123]. Structural failures and collapse as a result of concrete corrosion [42], [69], [132] is detrimental to society as it often impacts crucial infrastructure, typically leading to high costs [45], [134]. From a more positive side, these failures can be avoided with a sufficiently smart monitoring and timely repairs based on *a priori* calculations of the maximal lifespan of the concrete. These calculations have to take into account the heterogeneous nature of the concrete [104], the physical properties of the concrete [94], the corrosion reaction [131], and the expansion/contraction behaviour of corroded concrete mixtures, see [14], [32], [56]. For example, the typical length scale of the concrete heterogeneities is much smaller than the typical length scale used in concrete construction [104]. Moreover, concrete corrosion has a characteristic time that is many orders of magnitude smaller than the typical expected lifespan of concrete structures [131]. Hence, it is computationally expensive to use the heterogeneity length scale for detailed simulations of concrete constructions such as bridges. However, using averaging techniques in order to obtain effective properties on the typical length scale of concrete constructions, one can significantly decrease computational costs with the potential of preserving accuracy and precision.

Real-life problems usually involve a hierarchy of separated scales: from a microscale via intermediate scales to a macroscale. With averaging techniques one can obtain effective behaviours at a higher scale from the underlying lower scale. For example, Ern and Giovangigli used averaging techniques on statistical distributions in kinetic chemical equilibrium regimes to obtain continuous

macroscopic equations for mixtures, see [47] or see Chapter 4 of [62] for a variety of effective macroscopic equations obtained with this averaging technique. Of course, the use of averaging techniques to obtain effective macroscopic equations in mixture theory is by itself not new, see Fig 7.2 in [35] for an early application from 1934. The main problem with averaging techniques is choosing the right averaging methodology for the problem at hand. In this respect, periodic homogenization can be regarded as a successful method, since it expresses conditions under which macroscale behaviour can be obtained in a natural way from microscale behaviour. Furthermore, the homogenization method has been successfully used to derive not only equations for capturing macroscale behaviours but also the convergence/corrector speed depending on the scale separation between the macroscale and the microscale.

To obtain the macroscopic behaviour, we perform the homogenization by employing the concept of two-scale convergence as an averaging technique to obtain the macroscopic behaviour. Moreover, we use formal asymptotic expansions to determine the speed of convergence via so-called corrector estimates, see [75] for both thorough explanation of corrector estimates and applications of corrector estimates to selected parabolic chemical reaction systems. These estimates follow a procedure similar to those used by Cioranescu and Saint Jean-Paulin in Chapter 2 of [30]. Derivation via homogenization of constitutive laws, such as those arising from mixture theory, is a classical subject in homogenization, see [122]. Homogenization methods, upscaling, and corrector estimates are active research subjects due to the interdisciplinary nature of applying these mathematical techniques to real world problems and the complexities arising from the problem-specific constraints.

The microscopic equations of our concrete corrosion model are conservation laws for mass and momentum for an incompressible mixture, see [137] and [136] for details. The existence of weak solutions of this model was shown in [138] and Chapter 2 of [136]. The parameter space dependence of the existence region for this model was explored numerically in [137]. The two-scale convergence for a subsystem of these microscopic equations, a pseudo-parabolic system, was shown in [139]. This chapter handles the same pseudo-parabolic system as in [139] but posed on a perforated microscale domain.

In [107], Peszyńska, Showalter and Yi investigated the upscaling of a pseudo-parabolic system via two-scale convergence using a natural decomposition that splits the spatial and temporal behaviour. They looked at several different scale separation cases: classical case, highly heterogeneous case (also known as high-contrast case), vanishing time-delay case and Richards equation of

porous media. These cases were chosen to showcase the ease with which up-scaling could be done via this natural decomposition.

Similar decompositions are used in porous media flows, where they use a decomposition into pressure and saturation, see for example [37], [38]; or in solvent uptake in polymeric solids, see for example [41]; or in diffusion in fissured media, see for example [16].

In this chapter, we point out that this natural decomposition of [107] can also be applied to a pseudo-parabolic system with suitably scaled drift terms. Moreover, for such a pseudo-parabolic system with drift we determine the convergence speed via corrector estimates. This is in contrast with [107], where no convergence speed was derived for any pseudo-parabolic system they presented. Using this natural decomposition, the corrector estimates for the pseudo-parabolic equation follow straightforwardly from those of the spatially elliptic system with corrections due to the temporal first-order ordinary differential equation. Corrector estimates with convergence speeds have been obtained for the standard elliptic system, see [30], for a high-contrast coupled elliptic system of thermodiffusion, see [98], but also for coupled systems related to pseudo-parabolic equations such as the coupled elliptic-parabolic system with a mixed third order term describing thermoelasticity in [43]. The convergence speed we obtain, coincides for bounded spatial domains with known results for both elliptic systems and pseudo-parabolic systems on bounded temporal domains, see [117]. Finally, we apply our results to a concrete corrosion model, which describes the mechanics of concrete corrosion at a microscopic level with a perforated periodic domain geometry. Even though this model is linear, the main difficulty lies in determining effective macroscopic models for the mechanics of concrete corrosion based on the known microscopic mechanics model with such a complicated domain geometry. Obtaining these effective macroscopic models is difficult as the microscopic behavior is highly oscillatory due to the complicated domain geometry, while the macroscopic models need to encapsulate this behavior with a much less volatile effective behavior on a simple domain geometry without perforations or periodicity.

The remainder of this chapter is divided into six parts:

Section 5.2: Notation and problem statement,

Section 5.3: Main results,

Section 5.4: Upscaling procedure,

Section 5.5: Corrector estimates,

Section 5.6: Application to a concrete corrosion model,

Appendix 5.7: Exact forms of coefficients in corrector estimates.

5.2 Notation and problem statement

Geometry of the medium and related function spaces

We introduce the description of the geometry of the medium in question with a variant of the construction found in [97]. Let $(0, T)$, with $T > 0$, be a time-interval and $\Omega \subset \mathbf{R}^d$ for $d \in \{2, 3\}$ be a simply connected bounded domain with a C^2 -boundary $\partial\Omega$. Take $Y \subset \Omega$ a simply connected bounded domain, or more precisely there exists a diffeomorphism $\gamma : \mathbf{R}^d \rightarrow \mathbf{R}^d$ such that $\text{Int}(\gamma([0, 1]^d)) = Y$.

We perforate Y with a smooth open set $\mathcal{T} = \gamma(\mathcal{T}_0)$ for a smooth open set $\mathcal{T}_0 \subset (0, 1)^d$ such that $\overline{\mathcal{T}} \subset \overline{Y}$ with a C^2 -boundary $\partial\mathcal{T}$ that does not intersect the boundary of Y , $\partial\mathcal{T} \cap \partial Y = \emptyset$, and introduce $Y^* = Y \setminus \overline{\mathcal{T}}$. Remark that $\partial\mathcal{T}$ is assumed to be C^2 -regular.

Let G_0 be lattice¹ of the translation group \mathcal{T}_d on \mathbf{R}^d such that $[0, 1]^d = \mathcal{T}_d/G_0$. Hence, we have the following properties: $\bigcup_{g \in G_0} g([0, 1]^d) = \mathbf{R}^d$ and $(0, 1)^d \cap g((0, 1)^d) = \emptyset$ for all $g \in G_0$ not the identity-mapping. Moreover, we demand that the diffeomorphism γ allows $G_\gamma := \gamma \circ G_0 \circ \gamma^{-1}$ to be a discrete subgroup of \mathcal{T}_d with $\overline{Y} = \mathcal{T}_d/G_\gamma$.

Assume that there exists a sequence $(\epsilon_h)_h \subset (0, \epsilon_0)$ such that $\epsilon_h \rightarrow 0$ as $h \rightarrow \infty$ (we omit the subscript h when it is obvious from context that this sequence is mentioned). Moreover, we assume that for all $\epsilon_h \in (0, \epsilon_0)$ there is a set $G_\gamma^{\epsilon_h} = \{\epsilon_h g \text{ for } g \in G_\gamma\}$ with which we introduce $\mathcal{T}^{\epsilon_h} = \Omega \cap G_\gamma^{\epsilon_h}(\mathcal{T})$, the set of all holes and parts of holes inside Ω . Hence, we can define the domain $\Omega^{\epsilon_h} = \Omega \setminus \mathcal{T}^{\epsilon_h}$ and we demand that Ω^{ϵ_h} is connected for all $\epsilon_h \in (0, \epsilon_0)$. We introduce for all $\epsilon_h \in (0, \epsilon_0)$ the boundaries $\partial_{int}\Omega^{\epsilon_h}$ and $\partial_{ext}\Omega^{\epsilon_h}$ as $\partial_{int}\Omega^{\epsilon_h} = \bigcup_{g \in G_\gamma^{\epsilon_h}} \{\partial g(\overline{\mathcal{T}}) \mid g(\overline{\mathcal{T}}) \subset \Omega\}$ and $\partial_{ext}\Omega^{\epsilon_h} = \partial\Omega^{\epsilon_h} \setminus \partial_{int}\Omega^{\epsilon_h}$. The first boundary contains all the boundaries of the holes fully contained in Ω , while the second contains the remaining boundaries of the perforated region Ω . In Figure 5.1 a schematic representation of the domain components is shown.

Note, \mathcal{T} does not depend on ϵ , since this could give rise to unwanted complicating effects such as treated in [89].

Having the domains specified, we focus on defining the needed function spaces.

¹A lattice of a locally compact group \mathbb{G} is a discrete subgroup \mathbb{H} with the property that the quotient space \mathbb{G}/\mathbb{H} has a finite invariant (under \mathbb{G}) measure. A discrete subgroup \mathbb{H} of \mathbb{G} is a group $\mathbb{H} \subsetneq \mathbb{G}$ under group operations of \mathbb{G} such that there is (an open cover) a collection \mathbb{C} of open sets $C \subsetneq \mathbb{G}$ satisfying $\mathbb{H} \subset \bigcup_{C \in \mathbb{C}} C$ and for all $C \in \mathbb{C}$ there is a unique element $h \in \mathbb{H}$ such that $h \in C$.

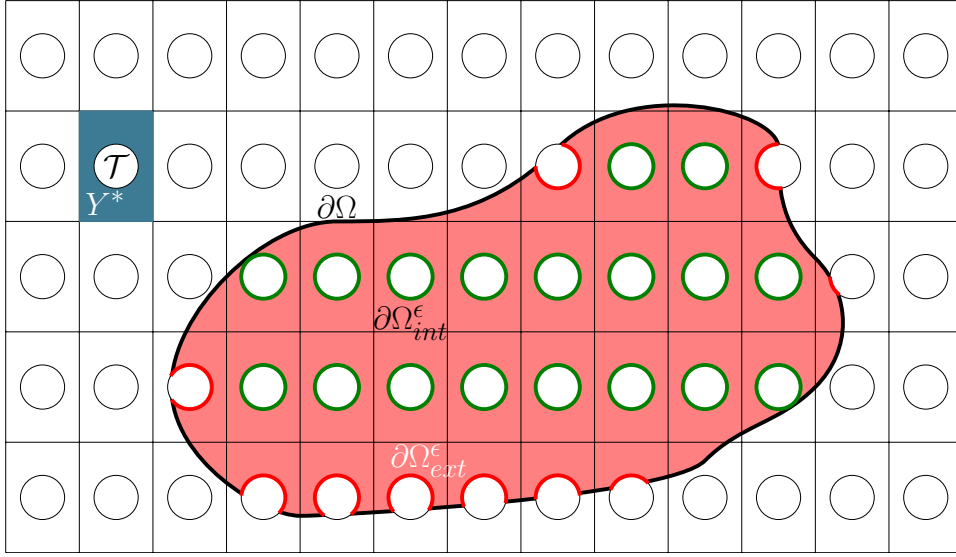


Figure 5.1: A domain Ω with the thick black boundary $\partial\Omega$ on an ϵ -sized periodic grid with grid cells Y , which contains a white circular perforation \mathcal{T} and the blue bulk Y^* yields the light-red coloured domain Ω^ϵ with thick red and black boundary $\partial\Omega_{ext}^\epsilon$ and the green internal perforation boundaries $\partial\Omega_{int}^\epsilon$. The thick red boundary parts of the perforations are locations where a choice will have to be made between the boundary condition of the perforation edges and the boundary condition of $\partial\Omega$.

We start by introducing $C_\#(Y)$, the space of continuous function defined on Y and periodic with respect to Y under G_γ . To be precise:

$$C_\#(Y) = \{f \in C(\mathbf{R}^d) \mid f \circ g = f \text{ for all } g \in G_\gamma\}. \quad (5.1)$$

Therefore, we introduce the nomenclature “ Y -periodic” for “invariant under G_γ ” for functions defined on Y . Similarly, we call a function “ Y^* -periodic” if it is “invariant under G_γ ” and defined on Y^* .

With $C_\#(Y)$ at hand, we construct Bochner spaces like $L^p(\Omega; C_\#(Y))$ for $p \geq 1$ integer. For a detailed explanation of Bochner spaces, see Section 2.19 of [79]. These types of Bochner spaces exhibit properties that hint at two-scale convergence, as is defined in Section 2.4. Similar function spaces are constructed for Y^* in an analogous way.

Introduce the space

$$\mathbb{V}_\epsilon = \{v \in H^1(\Omega^\epsilon) \mid v = 0 \text{ on } \partial_{ext}\Omega^\epsilon\} \quad (5.2)$$

equipped with the seminorm

$$\|v\|_{\mathbb{V}_\epsilon} = \|\nabla v\|_{L^2(\Omega^\epsilon)^d}. \quad (5.3)$$

Remark 5.1. *The seminorm in (5.3) is equivalent to the usual H^1 -norm by the Poincaré inequality, see Lemma 2.1 on page 14 of [30]. Moreover, according to [30] this equivalence of norms is uniform in ϵ .*

For correct use of functions spaces over Y and Y^* , we need an embedding result, which is based on an extension operator. The following theorem and corollary are Theorem 2.10 and Corollary 2.11 in Chapter 2 of [30].

Theorem 5.1. *Suppose that the domain Ω^ϵ is such that $\mathcal{T} \subset Y$ is a smooth open set with a C^2 -boundary that does not intersect the boundary of Y and such that the boundary of \mathcal{T}^ϵ does not intersect the boundary of Ω . Then there exists an extension operator \mathcal{P}^ϵ and a constant C independent of ϵ such that*

$$\mathcal{P}^\epsilon \in \mathcal{L}(L^2(\Omega^\epsilon); L^2(\Omega)) \cap \mathcal{L}(\mathbb{V}_\epsilon; H_0^1(\Omega)), \quad (5.4)$$

and for any $v \in \mathbb{V}_\epsilon$, we have the bounds

$$\|\mathcal{P}^\epsilon v\|_{L^2(\Omega)} \leq C\|v\|_{L^2(\Omega_\epsilon)}, \quad \|\nabla \mathcal{P}^\epsilon v\|_{L^2(\Omega)^d} \leq C\|\nabla v\|_{L^2(\Omega_\epsilon)^d}. \quad (5.5)$$

Corollary 5.2. *There exists a constant C independent of ϵ such that for all $v \in \mathbb{V}_\epsilon$*

$$\|\mathcal{P}^\epsilon v\|_{H_0^1(\Omega)} \leq C\|v\|_{\mathbb{V}_\epsilon}. \quad (5.6)$$

Introduce the notation $\hat{\cdot}$, a hat symbol, to denote extension via the extension operator \mathcal{P}^ϵ .

The Neumann problem (5.8a)-(5.9c)

The notation $\nabla = (\frac{d}{dx_1}, \dots, \frac{d}{dx_d})$ denotes the vectorial total derivative with respect to the components of $\mathbf{x} = (x_1, \dots, x_d)^\top$ for functions depending on both \mathbf{x} and \mathbf{x}/ϵ . Spatial vectors have d components, while variable vectors have N components. Tensors have $d^i N^j$ components for i, j nonnegative integers. Furthermore, the notation

$$c^\epsilon(t, \mathbf{x}) = c(t, \mathbf{x}, \mathbf{x}/\epsilon) \quad (5.7)$$

is used for the ϵ -independent functions $c(t, \mathbf{x}, \mathbf{y})$ in assumption (A1) further on. Moreover, the spatial inner product is denoted with \cdot , while the variable inner product is just seen as a product or operator acting on a variable vector or tensor.

Let $T > 0$. We consider the following Neumann problem for unknown functions $V_\alpha^\epsilon, U_\alpha^\epsilon$ with $\alpha \in \{1, \dots, N\}$ posed on $(0, T) \times \Omega^\epsilon$:

$$\begin{aligned} (\mathcal{A}^\epsilon \mathbf{V}^\epsilon)_\alpha &:= \sum_{\beta=1}^N M_{\alpha\beta}^\epsilon V_\beta^\epsilon - \sum_{i,j=1}^d \frac{d}{dx_i} \left(E_{ij}^\epsilon \frac{dV_\alpha^\epsilon}{dx_j} + \sum_{\beta=1}^N D_{i\alpha\beta}^\epsilon V_\beta^\epsilon \right) \\ &= \mathcal{H}_\alpha^\epsilon + \sum_{\beta=1}^N \left(K_{\alpha\beta}^\epsilon U_\beta^\epsilon + \sum_{i=1}^d \tilde{J}_{i\alpha\beta}^\epsilon \frac{dU_\beta^\epsilon}{dx_i} \right) =: (\mathcal{H}^\epsilon \mathbf{U}^\epsilon)_\alpha, \end{aligned} \quad (5.8a)$$

$$(\mathcal{L} \mathbf{U}^\epsilon)_\alpha := \frac{\partial U_\alpha^\epsilon}{\partial t} + \sum_{\beta=1}^N L_{\alpha\beta} U_\beta^\epsilon = \sum_{\beta=1}^N G_{\alpha\beta} V_\beta^\epsilon, \quad (5.8b)$$

with the boundary conditions

$$U_\alpha^\epsilon = U_\alpha^* \quad \text{in } \{0\} \times \Omega^\epsilon, \quad (5.9a)$$

$$V_\alpha^\epsilon = 0 \quad \text{on } (0, T) \times \partial_{ext} \Omega^\epsilon, \quad (5.9b)$$

$$\frac{dV_\alpha^\epsilon}{d\nu_{D^\epsilon}} := \sum_{i=1}^d \left(\sum_{j=1}^d E_{ij}^\epsilon \frac{dV_\alpha^\epsilon}{dx_j} + \sum_{\beta=1}^N D_{i\alpha\beta}^\epsilon V_\beta^\epsilon \right) n_i^\epsilon = 0 \quad \text{on } (0, T) \times \partial_{int} \Omega^\epsilon, \quad (5.9c)$$

for $\alpha \in \{1, \dots, N\}$ or, in short-hand notation, this reads:

$$\left\{ \begin{array}{l} \mathcal{A}^\epsilon \mathbf{V}^\epsilon := \mathbf{M}^\epsilon \mathbf{V}^\epsilon - \operatorname{div} (\mathbf{E}^\epsilon \cdot \nabla \mathbf{V}^\epsilon + \mathbf{D}^\epsilon \mathbf{V}^\epsilon) \\ \quad = \mathbf{H}^\epsilon + \mathbf{K}^\epsilon \mathbf{U}^\epsilon + \tilde{\mathbf{J}}^\epsilon \cdot \nabla \mathbf{U}^\epsilon =: \mathcal{H}^\epsilon \mathbf{U}^\epsilon \quad \text{in } (0, T) \times \Omega^\epsilon, \\ \mathcal{L} \mathbf{U}^\epsilon := \frac{\partial \mathbf{U}^\epsilon}{\partial t} + \mathbf{L} \mathbf{U}^\epsilon = \mathbf{G} \mathbf{V}^\epsilon \quad \text{in } (0, T) \times \Omega^\epsilon, \\ \mathbf{U}^\epsilon = \mathbf{U}^* \quad \text{in } \{0\} \times \Omega^\epsilon, \\ \mathbf{V}^\epsilon = \mathbf{0} \quad \text{on } (0, T) \times \partial_{ext} \Omega^\epsilon, \\ \frac{d\mathbf{V}^\epsilon}{d\nu_{D^\epsilon}} = (\mathbf{E}^\epsilon \cdot \nabla \mathbf{V}^\epsilon + \mathbf{D}^\epsilon \mathbf{V}^\epsilon) \cdot \mathbf{n}^\epsilon = 0 \quad \text{on } (0, T) \times \partial_{int} \Omega^\epsilon. \end{array} \right. \quad (5.10)$$

Assumptions

Consider the following technical requirements for the coefficients arising in the Neumann problem (5.8a) - (5.9c).

(A1) For all $\alpha, \beta \in \{1, \dots, N\}$ and for all $i, j \in \{1, \dots, d\}$, we assume:

$$\begin{aligned} M_{\alpha\beta}, H_\alpha, K_{\alpha\beta}, J_{i\alpha\beta} &\in L^\infty(\mathbf{R}_+; W^{2,\infty}(\Omega; C_\#^2(Y^*))), \\ E_{ij}, D_{i\alpha\beta} &\in L^\infty(\mathbf{R}_+; W^{3,\infty}(\Omega; C_\#^3(Y^*))), \\ L_{\alpha\beta}, G_{\alpha\beta} &\in L^\infty(\mathbf{R}_+; W^{4,\infty}(\Omega)), \\ U_\alpha^* &\in W^{4,\infty}(\Omega), \end{aligned} \quad (5.11)$$

with $\tilde{J}^\epsilon = \epsilon J^\epsilon$; see Remark 5.2 further on.

(A2) The tensors \mathbf{M} and \mathbf{E} have a linear sum decomposition² with a skew-symmetric matrix and a diagonal matrix with the diagonal elements of \mathbf{M} and \mathbf{E} denoted by $M_\alpha, E_i \in L^\infty(\mathbf{R}_+ \times \Omega; C_\#(Y^*))$, respectively, satisfying $M_\alpha > 0$, $E_i > 0$ and $1/M_\alpha, 1/E_i \in L^\infty(\mathbf{R}_+ \times \Omega \times Y^*)$.

(A3) The inequality

$$\|D_{i\beta\alpha}^\epsilon\|_{L^\infty(\mathbf{R}_+ \times \Omega^\epsilon; C_\#(Y^*))}^2 < \frac{4m_\alpha e_i}{dN^2} \quad (5.12)$$

holds with

$$\frac{1}{m_\alpha} = \left\| \frac{1}{M_\alpha} \right\|_{L^\infty(\mathbf{R}_+ \times \Omega \times Y^*)} \quad \text{and} \quad \frac{1}{e_i} = \left\| \frac{1}{E_i} \right\|_{L^\infty(\mathbf{R}_+ \times \Omega \times Y^*)} \quad (5.13)$$

for all $\alpha, \beta \in \{1, \dots, N\}$, for all $i \in \{1, \dots, d\}$, and for all $\epsilon \in (0, \epsilon_0)$.

(A4) The perforation holes do not intersect the boundary of Ω :

$$\partial\mathcal{T}^\epsilon \cap \partial\Omega = \emptyset \text{ for a given sequence } \epsilon \in (0, \epsilon_0).$$

Remark 5.2. *The dependence $\tilde{J}^\epsilon = \epsilon J^\epsilon$ was chosen to simplify both existence and uniqueness results and arguments for bounding certain terms. The case $\tilde{J}^\epsilon = J^\epsilon$ can be treated with the proofs outlined in this chapter if additional cell functions are introduced and special inequalities similar to the Poincaré-Wirtinger inequality are used. See (5.58) onward in Section 5.4 for the introduction of cell functions.*

²For real symmetric matrices \mathbf{M} and \mathbf{E} , the finite dimensional version of the spectral theorem states that they are diagonalizable by orthogonal matrices. Since \mathbf{M} acts on the variable space \mathbf{R}^N , while \mathbf{E} acts on the spatial space \mathbf{R}^d , one can simultaneously diagonalize both real symmetric matrices. For general real matrices \mathbf{M} and \mathbf{E} the linear sum decomposition in symmetric and skew-symmetric matrices allows for a diagonalization of the symmetric part. The orthogonal matrix transformations necessary to diagonalize the symmetric part does not modify the regularity of the domain Ω , of the perforated periodic cell Y^* or of the coefficients of \mathbf{D} , \mathbf{H} , \mathbf{K} , \mathbf{J} , \mathbf{L} , or \mathbf{G} . Hence, we are allowed to assume a linear sum decomposition of \mathbf{M} and \mathbf{E} in a diagonal and a skew-symmetric matrix.

Remark 5.3. *Satisfying inequality (5.12) implies that the same inequality is satisfied for the Y^* -averaged functions $\overline{D}_{i\beta\alpha}^\epsilon$, $\overline{M}_{\beta\alpha}^\epsilon$, and $\overline{E}_{ij}^\epsilon$ in $L^\infty(\mathbf{R}_+ \times \Omega)$, where we used the following notion of Y^* -averaged functions*

$$\overline{f}(t, \mathbf{x}) = \frac{1}{|Y|} \int_{Y^*} f(t, \mathbf{x}, \mathbf{y}) d\mathbf{y}. \quad (5.14)$$

Remark 5.4. *Assumption (A4) implies the following identities for the given sequence $\epsilon \in (0, \epsilon_0)$:*

$$\partial_{int}\Omega^\epsilon = \partial\mathcal{T}^\epsilon \cap \Omega, \quad \partial_{ext}\Omega^\epsilon = \partial\Omega. \quad (5.15)$$

Without (A4) perforations would intersect $\partial\Omega$. One must then decide which parts of the boundary of the intersected cell Y^ satisfies which boundary condition: (5.9b) or (5.9c). This leads to non-trivial situations, that ultimately affects the corrector estimates in non-trivial ways.*

Theorem 5.3. *Under assumptions (A1)-(A4), there exist a solution pair $(\mathbf{U}^\epsilon, \mathbf{V}^\epsilon) \in H^1((0, T) \times \Omega^\epsilon)^N \times L^\infty((0, T); \nabla_\epsilon \cap H^2(\Omega^\epsilon))^N$ satisfying the Neumann problem (5.8a)-(5.9c).*

Proof. For non-perforated domains the result follows by either Theorem 1 in [139] or Theorem 7 in Chapter 4 of [136].

For perforated domains, the result follows similarly. An outline of the proof is as follows. First, time-discretization is applied such that $\mathcal{A}^\epsilon \mathbf{V}^\epsilon$ at $t = k\Delta t$ equals $\mathcal{H}^\epsilon \mathbf{U}^\epsilon$ at $t = (k-1)\Delta t$ and $\mathcal{L}\mathbf{U}^\epsilon$ transformed after discretizing the time derivative and evaluating other terms at $t = k\Delta t$ equals $\mathbf{G}\mathbf{V}^\epsilon$ at $t = (k-1)\Delta t$. This is an application of the Rothe method. Under assumptions (A1)-(A4), testing $\mathcal{A}^\epsilon \mathbf{V}^\epsilon$ with a function ϕ yields a continuous and coercive bilinear form on $H^1(\Omega^\epsilon)^N$, while testing the discretized $\mathcal{L}\mathbf{U}^\epsilon$ with a function ψ yields a continuous and coercive bilinear form on $L^2(\Omega^\epsilon)^N$. Hence, Lax-Milgram leads to the existence of a solution at each time slice $t = k\Delta t$.

Choosing the right functions for ϕ and ψ and using a discrete version of Gronwall's inequality we obtain upper bounds of \mathbf{U}^ϵ and \mathbf{V}^ϵ independent of Δt . Linearly interpolating the time slices, we find that the Δt -independent time slices guarantee the existence of continuous weak limits. Due to sufficient regularity, we even obtain strong convergence and existence of boundary traces. Then the continuous weak limits are actually weak solutions of our Neumann problem (5.8a)-(5.9c). The uniqueness follows by the linearity of our Neumann problem (5.8a)-(5.9c). \square

5.3 Main results

Two special length scales are involved in the Neumann problem (5.8a)-(5.9c): The variable \mathbf{x} is the “macroscopic” scale, while \mathbf{x}/ϵ represents the “microscopic” scale. This leads to a double dependence of parameter functions (and, hence, of the solutions to the model equations), on both the macroscale and the microscale. For example, if $\mathbf{x} \in \Omega^\epsilon$, by the definition of Ω^ϵ , there exists $g \in G_\gamma^\epsilon$ such that $\mathbf{x}/\epsilon = g(\mathbf{y})$ with $\mathbf{y} \in Y^*$. This suggests that we look for a formal asymptotic expansion of the form

$$\mathbf{V}^\epsilon(t, \mathbf{x}) = \mathbf{V}^0\left(t, \mathbf{x}, \frac{\mathbf{x}}{\epsilon}\right) + \epsilon \mathbf{V}^1\left(t, \mathbf{x}, \frac{\mathbf{x}}{\epsilon}\right) + \epsilon^2 \mathbf{V}^2\left(t, \mathbf{x}, \frac{\mathbf{x}}{\epsilon}\right) + \dots, \quad (5.16a)$$

$$\mathbf{U}^\epsilon(t, \mathbf{x}) = \mathbf{U}^0\left(t, \mathbf{x}, \frac{\mathbf{x}}{\epsilon}\right) + \epsilon \mathbf{U}^1\left(t, \mathbf{x}, \frac{\mathbf{x}}{\epsilon}\right) + \epsilon^2 \mathbf{U}^2\left(t, \mathbf{x}, \frac{\mathbf{x}}{\epsilon}\right) + \dots \quad (5.16b)$$

with $\mathbf{V}^j(t, \mathbf{x}, \mathbf{y})$, $\mathbf{U}^j(t, \mathbf{x}, \mathbf{y})$ defined for $t \in \mathbf{R}_+$, $\mathbf{x} \in \Omega^\epsilon$ and $\mathbf{y} \in Y^*$ and Y^* -periodic (i.e. \mathbf{V}^j , \mathbf{U}^j are periodic with respect to G_γ^ϵ).

Theorem 5.4. *Let assumptions (A1)-(A4) hold. For all $T \in \mathbf{R}_+$ there exists a unique pair $(\mathbf{U}^\epsilon, \mathbf{V}^\epsilon) \in H^1((0, T) \times \Omega^\epsilon)^N \times L^\infty((0, T); \mathbb{V}_\epsilon)^N$ satisfying the Neumann problem (5.8a)-(5.9c). Moreover, for $\epsilon \downarrow 0$*

$$\hat{\mathbf{U}}^\epsilon \xrightarrow{2} \mathbf{U}^0 \text{ in } H^1(0, T; L^2(\Omega \times Y^*))^N \text{ and} \quad (5.17a)$$

$$\hat{\mathbf{V}}^\epsilon \xrightarrow{2} \mathbf{V}^0 \text{ in } L^\infty(0, T; L^2(\Omega \times Y^*))^N. \quad (5.17b)$$

This implies

$$\hat{\mathbf{U}}^\epsilon \rightharpoonup \frac{1}{|Y|} \int_{Y^*} \mathbf{U}^0(t, \mathbf{x}, \mathbf{y}) d\mathbf{y} \text{ in } H^1((0, T) \times \Omega)^N \text{ and} \quad (5.18a)$$

$$\hat{\mathbf{V}}^\epsilon \rightharpoonup \frac{1}{|Y|} \int_{Y^*} \mathbf{V}^0(t, \mathbf{x}, \mathbf{y}) d\mathbf{y} \text{ in } L^\infty((0, T); H_0^1(\Omega))^N \quad (5.18b)$$

for $\epsilon \downarrow 0$.

Proof. See Section 5.4 for the full details and [139] for a short proof of the two-scale convergence for a non-perforated setting. \square

Additionally, we are interested in deriving the speed of convergence of the formal asymptotic expansion. Boundary effects are expected to occur due to intersection of the external boundary with the perforated periodic cells. Hence, a cut-off function is introduced to remove this part from the analysis.

Let \mathcal{M}_ϵ be the cut-off function defined by

$$\begin{cases} \mathcal{M}_\epsilon \in \mathcal{D}(\Omega), \\ \mathcal{M}_\epsilon = 0 & \text{if } \text{dist}(\mathbf{x}, \partial\Omega) \leq \epsilon \text{diam}(Y), \\ \mathcal{M}_\epsilon = 1 & \text{if } \text{dist}(\mathbf{x}, \partial\Omega) \geq 2\epsilon \text{diam}(Y), \\ \epsilon \left| \frac{d\mathcal{M}_\epsilon}{dx_i} \right| \leq C \quad i \in \{1, \dots, d\}. \end{cases} \quad (5.19)$$

We refer to

$$\Phi^\epsilon = \mathbf{V}^\epsilon - \mathbf{V}^0 - \mathcal{M}_\epsilon(\epsilon \mathbf{V}^1 + \epsilon^2 \mathbf{V}^2), \quad (5.20a)$$

$$\Psi^\epsilon = \mathbf{U}^\epsilon - \mathbf{U}^0 - \mathcal{M}_\epsilon(\epsilon \mathbf{U}^1 + \epsilon^2 \mathbf{U}^2) \quad (5.20b)$$

as error functions. Now, we are able to state our convergence speed result.

Theorem 5.5. *Let assumptions (A1)-(A4) hold. There exist constants $l \geq 0$, $\kappa \geq 0$, $\tilde{\kappa} \geq 0$, $\lambda \geq 0$ and $\mu \geq 0$ all independent of ϵ such that*

$$\|\Phi^\epsilon\|_{\mathbb{V}^N}(t) \leq \mathcal{C}(\epsilon, t), \quad (5.21a)$$

$$\|\Psi^\epsilon\|_{H^1(\Omega^\epsilon)^N}(t) \leq \mathcal{C}(\epsilon, t) \sqrt{t_l e^{lt}} \quad (5.21b)$$

with

$$\mathcal{C}(\epsilon, t) = C(\epsilon^{\frac{1}{2}} + \epsilon^{\frac{3}{2}}) \left[1 + \epsilon^{\frac{1}{2}}(1 + \tilde{\kappa}e^{\lambda t})(1 + \kappa(1 + t_l e^{lt})) \right] \exp(\mu t_l e^{lt}) \quad (5.22)$$

where C is a constant independent of ϵ and t , and $t_l = \min\{1/l, t\}$.

Remark 5.5. *The upper bounds in (5.21a) and (5.21b) are $\mathcal{O}(\epsilon^{\frac{1}{2}})$ for ϵ -independent finite time intervals. We call this type of bounds corrector estimates.*

The corrector estimate of Φ^ϵ in Theorem 5.5 becomes that of the classic linear elliptic system for $\mathbf{K} = \mathbf{0}$ and $\mathbf{J} = 0$. This is because $\mathbf{K} = \mathbf{0}$ and $\mathbf{J} = 0$ imply $\tilde{\kappa} = \kappa = \mu = 0$, see Section 5.7. See [30] for the classical approach to corrector estimates of elliptic systems in perforated domains and [90] for a spectral approach in non-perforated domains.

Corollary 5.6. *Under the assumptions of Theorem 5.5,*

$$\|\hat{\mathbf{V}}^\epsilon - \mathbf{V}^0\|_{H_0^1(\Omega)^N}(t) \leq \mathcal{C}(\epsilon, t), \quad (5.23a)$$

$$\|\hat{\mathbf{U}}^\epsilon - \mathbf{U}^0\|_{H^1(\Omega)^N}(t) \leq \mathcal{C}(\epsilon, t) \sqrt{t_l e^{lt}} \quad (5.23b)$$

hold, where C is a constant independent of ϵ and t .

According to Remark 5.5, ϵ -independent finite time intervals yield $\mathcal{O}(\epsilon^{\frac{1}{2}})$ corrector estimates. Is it, then, possible to have a converging corrector estimate for diverging time intervals in the limit $\epsilon \downarrow 0$? The next theorem answers this question positively.

Theorem 5.7. *If $l > 0$, we introduce the rescaled time $\tau \ln(\frac{1}{\epsilon}) = \exp(lt) \geq 1$ satisfying $0 < \mu\tau/l < \frac{1}{2}$. Then, for $0 < \epsilon < \exp(-\frac{2\mu}{l})$, we have the corrector bounds*

$$\|\Phi^\epsilon\|_{\mathbb{V}_\epsilon^N}(t) = \mathcal{O}\left(\epsilon^{\frac{1}{2} - \frac{\mu}{l}\tau}\right) = o(1) = \omega\left(\epsilon^{\frac{1}{2}}\right), \quad (5.24a)$$

$$\|\Psi^\epsilon\|_{H^1(\Omega^\epsilon)^N}(t) = \mathcal{O}\left(\epsilon^{\frac{1}{2} - \frac{\mu}{l}\tau} \sqrt{\ln \frac{1}{\epsilon}}\right) = o(1) = \omega\left(\epsilon^{\frac{1}{2}}\right) \quad (5.24b)$$

as $\epsilon \downarrow 0$, where $f = \omega(g)$ means $\lim_{n \rightarrow \infty} |f(n)/g(n)| = \infty$.

Hence, the size of the time interval $(0, T)$ is allowed to depend in a diverging way on ϵ without destroying the convergence of $(\hat{U}^\epsilon, \hat{V}^\epsilon)$ to (\mathbf{u}, \mathbf{v}) .

If $l = 0$, we introduce the rescaled time $\tau \ln(\frac{1}{\epsilon}) = t \geq 0$ satisfying $0 < \max\{\mu\tau, (\lambda + \mu)\tau - \frac{1}{2}\} < \frac{1}{2}$. Then, for $0 < \epsilon < 1$, we have the corrector bounds

$$\|\Phi^\epsilon\|_{\mathbb{V}_\epsilon^N}(t) = \mathcal{O}\left(\epsilon^{\frac{1}{2} - \mu\tau}\right) + \mathcal{O}\left(\epsilon^{1 - (\lambda + \mu)\tau} \ln \frac{1}{\epsilon}\right), \quad (5.25a)$$

$$\|\Psi^\epsilon\|_{H^1(\Omega^\epsilon)^N}(t) = \left[\mathcal{O}\left(\epsilon^{\frac{1}{2} - \mu\tau}\right) + \mathcal{O}\left(\epsilon^{1 - (\lambda + \mu)\tau} \ln \frac{1}{\epsilon}\right) \right] \mathcal{O}\left(\sqrt{\ln \frac{1}{\epsilon}}\right) \quad (5.25b)$$

as $\epsilon \downarrow 0$. If, additionally, $\kappa = 0$ holds, then the bounds change to

$$\|\Phi^\epsilon\|_{\mathbb{V}_\epsilon^N}(t) = \mathcal{O}\left(\epsilon^{\min\{\frac{1}{2}, 1 - \lambda\tau\}}\right), \quad (5.26a)$$

$$\|\Psi^\epsilon\|_{H^1(\Omega^\epsilon)^N}(t) = \mathcal{O}\left(\epsilon^{\min\{\frac{1}{2}, 1 - \lambda\tau\}} \sqrt{\ln \frac{1}{\epsilon}}\right). \quad (5.26b)$$

Proof. Insert the definition of the rescaled time into (5.21a) and (5.21b), use $t_l = \min\{1/l, t\} = t$ for $l = 0$ and $t_l \leq 1/l$ for $l > 0$. The minimum function is needed since $\mathcal{O}(\epsilon^r) + \mathcal{O}(\epsilon^s) = \mathcal{O}(\epsilon^{\min\{r, s\}})$. The small o and small ω orders are upper and lower asymptotic convergence speeds, respectively, for $\epsilon \downarrow 0$. The upper bound for ϵ is needed to guarantee that the interval for τ corresponds to $t \geq 0$. \square

Note, all logarithms $\ln(\epsilon)$ can be changed into a power law of form ϵ^{-q}/q for any $q > 0$ because the product $\epsilon^q \ln(1/\epsilon)$ has a single maximal value of $\frac{1}{qe}$ at $\ln\left(\frac{1}{\epsilon}\right) = \frac{1}{q}$ for $q > 0$.

Theorem 5.7 indicates that convergence can be retained for certain diverging sequences of time-intervals. Consequently, appropriate rescalings of the time variable yield upscaled systems and convergence rates for systems with regularity conditions different from those in assumptions (A1) - (A3).

Remark 5.6. *The tensors \mathbf{L} and \mathbf{G} are not dependent on ϵ nor are unbounded functions of t . If such a dependence or unbounded behaviour does exist, then bounds similar to those stated in Theorem 5.5 are still valid in a new time-variable $s \in I \subset \mathbf{R}_+$ if an invertible C^1 -map f_ϵ from $t \in \mathbf{R}_+$ to s exists such that tensors $(\mathbf{L}^\epsilon/f'_\epsilon) \circ f_\epsilon^{-1}$, $(\mathbf{G}^\epsilon/f'_\epsilon) \circ f_\epsilon^{-1}$, $\mathbf{M}^\epsilon \circ f_\epsilon^{-1}$, $\mathbf{E}^\epsilon \circ f_\epsilon^{-1}$, $\mathbf{D}^\epsilon \circ f_\epsilon^{-1}$, $\mathbf{H}^\epsilon \circ f_\epsilon^{-1}$, $\mathbf{K}^\epsilon \circ f_\epsilon^{-1}$, and $\mathbf{J}^\epsilon \circ f_\epsilon^{-1}$ satisfy (A1)-(A3). Moreover, if $f_\epsilon(\mathbf{R}_+) = \mathbf{R}_+$ for $\epsilon > 0$ small enough, then the bounds of Theorem 5.7 are valid as well with τ defined in terms of s .*

5.4 Upscaling procedure

Upscaling of the Neumann problem (5.8a)-(5.9c) can be done by many methods, e.g. via asymptotic expansions or two-scale convergence in suitable function spaces. We proceed in four steps:

1. **Existence and uniqueness of $(\mathbf{U}^\epsilon, \mathbf{V}^\epsilon)$.**

We rely on Theorem 5.3.

2. **Obtain ϵ -independent bounds for $(\mathbf{U}^\epsilon, \mathbf{V}^\epsilon)$.**

See Section 5.4.

a. Obtain *a priori* estimates for $(\mathbf{U}^\epsilon, \mathbf{V}^\epsilon)$. See Lemma 5.8.

b. Obtain ϵ -independent bounds for $(\mathbf{U}^\epsilon, \mathbf{V}^\epsilon)$. See Theorem 5.9.

3. **Upscaling via two-scale convergence.**

See Section 5.4.

a. Two-scale limit of $(\mathbf{U}^\epsilon, \mathbf{V}^\epsilon)$ for $\epsilon \downarrow 0$. See Lemma 5.10.

b. Two-scale limit of problem (5.8a)-(5.9c) for $\epsilon \downarrow 0$. See Theorem 5.11.

4. Upscaling via asymptotic expansions and relating to two-scale convergence.

See Section 5.4.

- a. Expand (5.8a) and $(\mathbf{U}^\epsilon, \mathbf{V}^\epsilon)$. See equations (5.44)-(5.56).
- b. Obtain existence & uniqueness of $(\mathbf{U}^0, \mathbf{V}^0)$. See Lemma 5.12 and Lemma 5.13
- c. Obtain the defining system of $(\mathbf{U}^0, \mathbf{V}^0)$. See equations (5.58)-(5.65) and Lemma 5.15.
- d. Statement of the upscaled system. See Theorem 5.16.

ϵ -independent bounds for $(\mathbf{U}^\epsilon, \mathbf{V}^\epsilon)$

In this section, we show ϵ -independent bounds for a weak solution $(\mathbf{U}^\epsilon, \mathbf{V}^\epsilon)$ to the Neumann problem (5.8a)-(5.9c). We define a weak solution to the Neumann problem (5.8a)-(5.9c) as a pair $(\mathbf{U}^\epsilon, \mathbf{V}^\epsilon) \in H^1((0, T) \times \Omega^\epsilon)^N \times L^\infty((0, T), \mathbb{V}_\epsilon)^N$ satisfying

$$(\mathbf{P}_w^\epsilon) \quad \begin{cases} \int_{\Omega^\epsilon} \phi^\top [\mathbf{M}^\epsilon \mathbf{V}^\epsilon - \mathbf{H}^\epsilon - \mathbf{K}^\epsilon \mathbf{U}^\epsilon - \mathbf{J}^\epsilon \cdot \nabla \mathbf{U}^\epsilon] \\ \quad + (\nabla \phi)^\top \cdot (\mathbf{E}^\epsilon \cdot \nabla \mathbf{V}^\epsilon + \mathbf{D}^\epsilon \mathbf{V}^\epsilon) \, d\mathbf{x} = 0, \\ \int_{\Omega^\epsilon} \psi^\top \left[\frac{\partial \mathbf{U}^\epsilon}{\partial t} + \mathbf{L} \mathbf{U}^\epsilon - \mathbf{G} \mathbf{V}^\epsilon \right] \, d\mathbf{x} = 0, \\ \mathbf{U}^\epsilon(0, \mathbf{x}) = \mathbf{U}^*(\mathbf{x}) \text{ for all } \mathbf{x} \in \overline{\Omega}^\epsilon, \end{cases}$$

for a.e. $t \in (0, T)$ and for all test-functions $\phi \in \mathbb{V}_\epsilon^N$ and $\psi \in L^2(\Omega^\epsilon)^N$.

The existence and uniqueness of solutions to system (\mathbf{P}_w^ϵ) can only hold when the parameters are well-balanced. The next lemma provides a set of parameters for which these parameters are well-balanced.

Lemma 5.8. *Assume assumptions (A1)-(A3) hold and we have $\epsilon \in (0, \epsilon_0)$ for $\epsilon_0 > 0$, then there exist positive constants \tilde{m}_α , \tilde{e}_i , \tilde{H} , \tilde{K}_α , $\tilde{J}_{i\alpha}$, for $\alpha \in \{1, \dots, N\}$ and $i \in \{1, \dots, d\}$ such that the a priori estimate*

$$\begin{aligned} \sum_{\alpha=1}^N \tilde{m}_\alpha \|V_\alpha^\epsilon\|_{L^2(\Omega)}^2 + \sum_{i=1}^d \sum_{\alpha=1}^N \tilde{e}_i \left\| \frac{dV_\alpha^\epsilon}{dx_i} \right\|_{L^2(\Omega)}^2 \\ \leq \tilde{H} + \sum_{\alpha=1}^N \tilde{K}_\alpha \|U_\alpha^\epsilon\|_{L^2(\Omega)}^2 + \sum_{i=1}^d \sum_{\alpha=1}^N \tilde{J}_{i\alpha} \left\| \frac{dU_\alpha^\epsilon}{dx_i} \right\|_{L^2(\Omega)}^2 \end{aligned} \quad (5.27)$$

holds for a.e. $t \in (0, T)$.

Proof. We test the first equation of (\mathbf{P}_w^ϵ) with $\phi = \mathbf{V}^\epsilon$ and apply Young's inequality wherever a product is not a square. A non-square product containing both \mathbf{V}^ϵ and $\nabla \mathbf{V}^\epsilon$ can only be found in the D-term. Hence, Young's inequality allows all other non-square product terms to have a negligible effect on the coercivity constants m_α and e_i , while affecting \tilde{H} , \tilde{K}_α , $\tilde{J}_{i\alpha}$. Therefore, we only need to enforce two inequalities to prove the lemma by guaranteeing coercivity, i.e.

$$e_i - \sum_{\alpha=1}^N \frac{\eta_{i\beta\alpha}}{2} \tilde{D}_{i\beta\alpha} \geq \tilde{e}_i > 0 \text{ for } \beta \in \{1, \dots, N\}, i \in \{1, \dots, d\}, \quad (5.28a)$$

$$m_\alpha - \sum_{i=1}^d \sum_{\beta=1}^N \frac{\tilde{D}_{i\beta\alpha}}{2\eta_{i\beta\alpha}} \geq \tilde{m}_\alpha > 0 \text{ for } \alpha \in \{1, \dots, N\}, \quad (5.28b)$$

where $\tilde{D}_{i\beta\alpha} = \|D_{i\beta\alpha}\|_{L^\infty(\mathbf{R}_+ \times \Omega; C^\#(Y^*))}$. We can choose $\eta_{i\beta\alpha} > 0$ satisfying

$$\frac{dN\tilde{D}_{i\beta\alpha}}{2m_\alpha} < \eta_{i\beta\alpha} < \frac{2e_i}{N\tilde{D}_{i\beta\alpha}}, \quad (5.29)$$

if inequality (5.12) in assumption (A3) is satisfied. For the exact definition of the constants \tilde{m}_α , \tilde{e}_i , \tilde{H} , \tilde{K}_α , $\tilde{J}_{i\alpha}$, see equations (5.127a)-(5.127e) in Section 5.7. \square

Theorem 5.9. *Assume (A1)-(A3) to hold, then there exist positive constants C , $\tilde{\kappa}$ and λ independent of ϵ such that*

$$\|\mathbf{U}^\epsilon\|_{H^1(\Omega^\epsilon)^N}(t) \leq Ce^{\lambda t}, \quad \|\mathbf{V}^\epsilon\|_{\mathbb{V}_\epsilon^N}(t) \leq C(1 + \tilde{\kappa}e^{\lambda t}) \quad (5.30)$$

hold for $t \geq 0$.

Proof. By (A1) - (A3) there exist positive numbers \tilde{m}_α , \tilde{e}_i , \tilde{H} , \tilde{K}_α , $\tilde{J}_{i\alpha}$ for $\alpha \in \{1, \dots, N\}$ and $i \in \{1, \dots, d\}$ such that the *a priori* estimate (5.27) stated in Lemma 5.8 holds. Moreover, what concerns system (\mathbf{P}_w^ϵ) there exist L_G , L_N , G_G , and G_N , see equations (5.126a)-(5.126d) in Section 5.7, such that

$$\frac{\partial}{\partial t} \|\mathbf{U}^\epsilon\|_{L^2(\Omega^\epsilon)^N}^2 \leq L_N \|\mathbf{U}^\epsilon\|_{L^2(\Omega^\epsilon)^N}^2 + G_N \|\mathbf{V}^\epsilon\|_{L^2(\Omega^\epsilon)^N}^2, \quad (5.31a)$$

$$\begin{aligned} \frac{\partial}{\partial t} \|\nabla \mathbf{U}^\epsilon\|_{L^2(\Omega^\epsilon)^{d \times N}}^2 &\leq L_G \|\mathbf{U}^\epsilon\|_{L^2(\Omega^\epsilon)^N}^2 + L_N \|\nabla \mathbf{U}^\epsilon\|_{L^2(\Omega^\epsilon)^{d \times N}}^2 \\ &\quad + G_G \|\mathbf{V}^\epsilon\|_{L^2(\Omega^\epsilon)^N}^2 + G_N \|\nabla \mathbf{V}^\epsilon\|_{L^2(\Omega^\epsilon)^{d \times N}}^2 \end{aligned} \quad (5.31b)$$

hold. Adding (5.31a) and (5.31b), and using (5.27), we obtain a positive constant I and a vector $\mathbf{J} \in \mathbf{R}_+^N$ such that

$$\frac{\partial}{\partial t} \|\mathbf{U}^\epsilon\|_{H^1(\Omega^\epsilon)^N}^2 \leq \mathbf{J} + I \|\mathbf{U}^\epsilon\|_{H^1(\Omega^\epsilon)^N}^2 \quad (5.32)$$

with

$$I = \max \left\{ 0, L_N + \max \left\{ L_G + G_M \max_{1 \leq \alpha \leq N} \{\tilde{K}_\alpha\}, G_M \max_{1 \leq \alpha \leq N, 1 \leq i \leq d} \{\tilde{J}_{i\alpha}\} \right\} \right\}, \quad (5.33a)$$

$$G_M = \max_{1 \leq \alpha < N, 1 \leq i \leq d} \left\{ \frac{G_N + G_G}{\tilde{m}_\alpha}, \frac{G_N}{\tilde{e}_i} \right\}. \quad (5.33b)$$

Applying Gronwall's inequality, see [39, Thm. 1], to (5.32) yields the existence of a constant λ defined as $\lambda = I/2$, such that

$$\|\mathbf{U}^\epsilon\|_{H^1(\Omega^\epsilon)^N}(t) \leq C e^{\lambda t}, \quad \|\mathbf{V}^\epsilon\|_{\mathbb{V}_\epsilon^N}(t) \leq C(1 + \tilde{\kappa} e^{\lambda t}) \quad (5.34)$$

with $\tilde{\kappa} = \max_{1 \leq \alpha \leq N, 1 \leq i \leq d} \{\tilde{K}_\alpha, \tilde{J}_{i\alpha}\}$. \square

Remark 5.7. *It is difficult to obtain exact expressions for optimal values of L_N , L_G , G_N and G_G such that a minimal positive value of λ is obtained. See Section 5.7 for the exact dependence of λ on the parameters involved in the Neumann problem (5.8a)-(5.9c).*

Remark 5.8. *The $(0, T) \times \Omega^\epsilon$ -measurability of \mathbf{U}^ϵ and \mathbf{V}^ϵ can be proven based on the Rothe-method (discretization in time) in combination with the convergence of piecewise linear functions to any function in the spaces $H^1((0, T) \times \Omega^\epsilon)$ or $L^\infty((0, T); \mathbb{V}_\epsilon)$. One can prove that both \mathbf{U}^ϵ and \mathbf{V}^ϵ are measurable and are weak solutions to (\mathbf{P}_w^ϵ) . See Chapter 2 in [136] for a pseudo-parabolic system for which the Rothe-method is used to show existence (and hence also measurability).*

Remark 5.9. *Since we have $\mathbf{G} \in L^\infty(\mathbf{R}_+; W^{1,\infty}(\Omega))^{N \times N}$ and $\mathbf{V}^\epsilon \in L^\infty((0, T); \mathbb{V}_\epsilon)^N$, we are allowed to differentiate equation (5.8b) with respect to \mathbf{x} and test the resulting identity with both $\nabla \mathbf{U}^\epsilon$ and $\frac{\partial}{\partial t} \nabla \mathbf{U}^\epsilon$. However, conversely, we are not allowed to differentiate equation (5.8a) with respect to t as all tensors have insufficient regularity: they are in $L^\infty(\mathbf{R}_+ \times \Omega^\epsilon)^{N \times N}$.*

Remark 5.10. *We cannot differentiate equation (5.8b) with respect to \mathbf{x} when \mathbf{L} or \mathbf{G} has decreased spatial regularity, for example $L^\infty((0, T) \times \Omega)^{N \times N}$. One can still obtain unique solutions of (\mathbf{P}_w^ϵ) if and only if $\mathbf{J}^\epsilon = \mathbf{0}$ holds, since it removes the $\nabla \mathbf{U}^\epsilon$ term from equation (5.8a). Consequently, Theorem 5.9 holds with $\mathbf{U}^\epsilon \in H^1((0, T); L^2(\Omega^\epsilon))$ and $\mathbf{J}^\epsilon = \mathbf{0}$ under the additional relaxed regularity assumption $\mathbf{L}, \mathbf{G} \in L^\infty((0, T) \times \Omega)^{N \times N}$ and with λ modified by taking $L_G = \tilde{J}_{i\alpha} = 0$ and by replacing G_M with $G_N / \min_{1 \leq \alpha \leq N} \tilde{m}_\alpha$.*

Upscaling the system (\mathbf{P}_w^ϵ) via two-scale convergence

We recall the notation \hat{f}^ϵ to denote the extension on Ω via the operator \mathcal{P}^ϵ for f^ϵ defined on Ω^ϵ . This extension operator \mathcal{P}^ϵ , as defined in Theorem 5.1, is well-defined if both $\partial\mathcal{T}$ and $\partial\Omega$ are C^2 -regular, assumption (A4) holds, and $\partial\mathcal{T} \cap \partial Y = \emptyset$, see [30]. Hence, the extension operator is well-defined in our setting.

Lemma 5.10. *Assume (A1)-(A4) to hold. For each $\epsilon \in (0, \epsilon_0)$, let the pair of sequences $(\mathbf{U}^\epsilon, \mathbf{V}^\epsilon) \in H^1((0, T) \times \Omega^\epsilon)^N \times L^\infty((0, T); \mathbb{V}_\epsilon)^N$ be the unique weak solution to (\mathbf{P}_w^ϵ) . Then this sequence of weak solutions satisfies the estimates*

$$\|\mathbf{U}^\epsilon\|_{H^1((0, T) \times \Omega^\epsilon)^N} + \|\mathbf{V}^\epsilon\|_{L^\infty((0, T); \mathbb{V}_\epsilon)^N} \leq C, \quad (5.35)$$

for all $\epsilon \in (0, \epsilon_0)$ and there exist vector functions

$$\mathbf{u} \text{ in } H^1((0, T) \times \Omega)^N, \quad (5.36a)$$

$$\mathcal{U} \text{ in } H^1((0, T); L^2(\Omega; H_{\#}^1(Y^*)/\mathbf{R}))^N, \quad (5.36b)$$

$$\mathbf{v} \text{ in } L^\infty((0, T); H_0^1(\Omega))^N, \quad (5.36c)$$

$$\mathcal{V} \text{ in } L^\infty((0, T) \times \Omega; H_{\#}^1(Y^*)/\mathbf{R})^N, \quad (5.36d)$$

and a subsequence $\epsilon' \subset \epsilon$, for which the following two-scale convergences

$$\hat{\mathbf{U}}^{\epsilon'} \xrightarrow{2} \mathbf{u} \quad (5.37a)$$

$$\frac{\partial}{\partial t} \hat{\mathbf{U}}^{\epsilon'} \xrightarrow{2} \frac{\partial}{\partial t} \mathbf{u} \quad (5.37b)$$

$$\nabla \hat{\mathbf{U}}^{\epsilon'} \xrightarrow{2} \nabla \mathbf{u} + \nabla_{\mathbf{y}} \mathcal{U} \quad (5.37c)$$

$$\frac{\partial}{\partial t} \nabla \hat{\mathbf{U}}^{\epsilon'} \xrightarrow{2} \frac{\partial}{\partial t} \nabla \mathbf{u} + \frac{\partial}{\partial t} \nabla_{\mathbf{y}} \mathcal{U} \quad (5.37d)$$

$$\hat{\mathbf{V}}^{\epsilon'} \xrightarrow{2} \mathbf{v} \quad (5.37e)$$

$$\nabla \hat{\mathbf{V}}^{\epsilon'} \xrightarrow{2} \nabla \mathbf{v} + \nabla_{\mathbf{y}} \mathcal{V} \quad (5.37f)$$

hold.

Proof. For all $\epsilon > 0$, Theorem 5.9 gives the bounds (5.35) independent of the choice of ϵ . Hence, $\hat{\mathbf{U}}^\epsilon \rightharpoonup \mathbf{u}$ in $H^1((0, T) \times \Omega)^N$ and $\hat{\mathbf{V}}^\epsilon \rightharpoonup \mathbf{v}$ in $L^\infty((0, T); H_0^1(\Omega))^N$ as $\epsilon \rightarrow 0$. By Proposition 2.15 in Section 2.4, we obtain a subsequence $\epsilon' \subset \epsilon$ and functions $\mathbf{u} \in H^1((0, T) \times \Omega)^N$, $\mathbf{v} \in L^2((0, T); H_0^1(\Omega))^N$, $\mathcal{U}, \mathcal{V} \in L^2((0, T) \times \Omega; H_{\#}^1(Y^*)/\mathbf{R})^N$ such that (5.37a), (5.37b), (5.37c), (5.37e),

and (5.37f) hold for a.e. $t \in (0, T)$. Moreover, there exists a vector function $\tilde{\mathcal{U}} \in L^2((0, T) \times \Omega; H_{\#}^1(Y^*)/\mathbf{R})^N$ such that the following two-scale convergence

$$\frac{\partial}{\partial t} \nabla \hat{\mathcal{U}}^{\epsilon'} \xrightarrow{2} \frac{\partial}{\partial t} \nabla \mathbf{u} + \nabla_{\mathbf{y}} \tilde{\mathcal{U}} \quad (5.38)$$

holds for the same subsequence ϵ' . Using two-scale convergence, Fubini's Theorem and partial integration in time, we obtain an increased regularity for \mathcal{U} , i.e. $\mathcal{U} \in H^1((0, T); L^2(\Omega; H_{\#}^1(Y^*)/\mathbf{R}))^N$, with $\frac{\partial}{\partial t} \nabla_{\mathbf{y}} \mathcal{U} = \nabla_{\mathbf{y}} \tilde{\mathcal{U}}$. \square

By Lemma 5.10, we can determine the macroscopic version of (\mathbf{P}_w^ϵ) , which we denote by (\mathbf{P}_w^0) . This is as stated in Theorem 5.11.

Theorem 5.11. *Assume the hypotheses of Lemma 5.10 to be satisfied. Then the two-scale limits $\mathbf{u} \in H^1((0, T) \times \Omega)^N$ and $\mathbf{v} \in L^\infty((0, T); H_0^1(\Omega))^N$ introduced in Lemma 5.10 form a weak solution to*

$$(\mathbf{P}_w^0) \quad \begin{cases} \int_{\Omega} \phi^\top [\overline{\mathbf{M}}\mathbf{v} - \overline{\mathbf{H}} - \overline{\mathbf{K}}\mathbf{u}] \\ \quad + (\nabla \phi)^\top \cdot (\mathbf{E}^* \cdot \nabla \mathbf{v} + \mathbf{D}^* \mathbf{v}) \, d\mathbf{x} = 0, \\ \int_{\Omega} \psi^\top \left[\frac{\partial \mathbf{u}}{\partial t} + \mathbf{L}\mathbf{u} - \mathbf{G}\mathbf{v} \right] \, d\mathbf{x} = 0, \\ \mathbf{u}(0, \mathbf{x}) = \mathbf{U}^*(\mathbf{x}) \quad \text{for } \mathbf{x} \in \Omega, \end{cases}$$

for a.e. $t \in (0, T)$ for all test functions $\phi \in H_0^1(\Omega)^N$, and $\psi \in L^2(\Omega)^N$, where the barred tensors and vectors are Y^* averaged functions as introduced in (A2). Furthermore,

$$\mathbf{E}^* = \frac{1}{|Y|} \int_{Y^*} \mathbf{E} \cdot (1 + \nabla_{\mathbf{y}} \mathbf{W}) \, d\mathbf{y}, \quad \mathbf{D}^* = \frac{1}{|Y|} \int_{Y^*} \mathbf{D} + \mathbf{E} \cdot \nabla_{\mathbf{y}} \mathbf{Z} \, d\mathbf{y} \quad (5.39)$$

are the wanted effective coefficients. The auxiliary tensors $\mathbf{Z}_{\alpha\beta}, \mathbf{W}_i \in L^\infty(0, T; W^{2,\infty}(\Omega; H_{\#}^1(Y^*)/\mathbf{R}))$ satisfy the cell problems

$$\mathbf{0} = \int_{Y^*} \Phi^\top \cdot (\nabla_{\mathbf{y}} \cdot [\mathbf{E} \cdot (1 + \nabla_{\mathbf{y}} \mathbf{W})]) \, d\mathbf{y} = \int_{Y^*} \Phi^\top \cdot (\nabla_{\mathbf{y}} \cdot \hat{\mathbf{E}}) \, d\mathbf{y}, \quad (5.40a)$$

$$\mathbf{0} = \int_{Y^*} \Psi^\top (\nabla_{\mathbf{y}} \cdot [\mathbf{D} + \mathbf{E} \cdot \nabla_{\mathbf{y}} \mathbf{Z}]) \, d\mathbf{y} = \int_{Y^*} \Psi^\top (\nabla_{\mathbf{y}} \cdot \hat{\mathbf{D}}) \, d\mathbf{y} \quad (5.40b)$$

for all $\Phi \in C_{\#}(Y^*)^d$, $\Psi \in C_{\#}(Y^*)^N$.

Proof. The solution to system (\mathbf{P}_w^ϵ) is extended to Ω by taking $\hat{\mathbf{H}}^\epsilon, \hat{\mathbf{V}}^\epsilon, \hat{\mathbf{U}}^\epsilon$ for $\mathbf{H}^\epsilon, \mathbf{V}^\epsilon, \mathbf{U}^\epsilon$, respectively. The extended system is satisfied on $\mathcal{T}^\epsilon \cap \Omega$ and

it satisfies the boundary conditions on $\partial_{int}\Omega^\epsilon$ of system (\mathbf{P}_w^ϵ) . Hence, it is sufficient to look at (\mathbf{P}_w^ϵ) only. In (\mathbf{P}_w^ϵ) , we choose $\boldsymbol{\psi} = \boldsymbol{\psi}^\epsilon = \boldsymbol{\Psi}(t, \mathbf{x}, \frac{\mathbf{x}}{\epsilon})$ for the test function $\boldsymbol{\Psi} \in L^2((0, T); \mathcal{D}(\Omega^\epsilon; C_\#^\infty(Y^*)))^N$, and $\boldsymbol{\phi} = \boldsymbol{\phi}^\epsilon = \boldsymbol{\Phi}(t, \mathbf{x}) + \epsilon\boldsymbol{\varphi}(t, \mathbf{x}, \frac{\mathbf{x}}{\epsilon})$ for the test function $\boldsymbol{\Phi} \in L^2((0, T); C_0^\infty(\Omega^\epsilon))^N$, $\boldsymbol{\varphi} \in L^2((0, T); \mathcal{D}(\Omega^\epsilon; C_\#^\infty(Y^*)))^N$. Corollary 2.17 and Theorem 2.18 of Section 2.4 in combination with (2.33) lead to $\mathbb{T}^\epsilon \xrightarrow{2} \mathbb{T}$, where \mathbb{T}^ϵ is an arbitrary tensor or vector in (\mathbf{P}_w^ϵ) other than \mathbf{L} and \mathbf{G} . Moreover, by Corollary 2.17, Proposition 2.15 and Proposition 2.16 of Section 2.4 we have $\boldsymbol{\psi}^\epsilon \xrightarrow{2} \boldsymbol{\Psi}(t, \mathbf{x}, \mathbf{y})$, $\boldsymbol{\phi}^\epsilon \xrightarrow{2} \boldsymbol{\Phi}(t, \mathbf{x})$, and $\nabla\boldsymbol{\phi}^\epsilon \xrightarrow{2} \nabla\boldsymbol{\Phi}(t, \mathbf{x}) + \nabla_{\mathbf{y}}\boldsymbol{\varphi}(t, \mathbf{x}, \mathbf{y})$. By Corollary 2.17 and Theorem 2.18 of Section 2.4, there is a two-scale limit of (\mathbf{P}_w^ϵ) , reading

$$\begin{aligned} \int_{\Omega} \frac{1}{|Y|} \int_{Y^*} \boldsymbol{\Phi}^\top [\mathbf{M}\mathbf{v} - \mathbf{H} - \mathbf{K}\mathbf{u}] \\ + (\nabla\boldsymbol{\Phi} + \nabla_{\mathbf{y}}\boldsymbol{\varphi})^\top \cdot [\mathbf{E} \cdot (\nabla\mathbf{v} + \nabla_{\mathbf{y}}\mathcal{V}) + \mathbf{D}\mathbf{v}] \\ + \boldsymbol{\Psi}^\top \left[\frac{\partial\mathbf{u}}{\partial t} + \mathbf{L}\mathbf{u} - \mathbf{G}\mathbf{v} \right] d\mathbf{y}d\mathbf{x} = 0. \end{aligned} \quad (5.41)$$

Similarly, the initial condition

$$\mathbf{u}(0, \mathbf{x}) = \mathbf{U}^*(\mathbf{x}), \quad \mathbf{x} \in \bar{\Omega}, \quad (5.42)$$

is satisfied by \mathbf{u} as $\nabla_{\mathbf{y}}\mathbf{u} = 0$ holds.

For $\boldsymbol{\Phi} = \boldsymbol{\Psi} = \mathbf{0}$, we can take $\mathcal{V} = \mathbf{W} \cdot \nabla\mathbf{v} + \mathbf{Z}\mathbf{v} + \tilde{\mathcal{V}}$, where \mathbf{W} and \mathbf{Z} satisfy the cell problems (5.40a) and (5.40b), respectively, and $\nabla_{\mathbf{y}}\tilde{\mathcal{V}} = 0$. The existence and uniqueness of \mathbf{W} and \mathbf{Z} follows from Lax-Milgram as cell problems (5.40a) and (5.40b) are linear elliptic systems by (A2) for the Hilbert space $H_\#^1(Y^*)$. The regularity of \mathbf{W} and \mathbf{Z} in $t \in (0, T)$ and $\mathbf{x} \in \Omega$ follows from the regularity of \mathbf{E} and \mathbf{D} as stated in (A1), (A2) and (A3). Moreover, we obtain $\mathbf{v} \in L^\infty((0, T); H^2(\Omega))$ due to (A1). Then Proposition 2.15, Theorem 2.18 of Section 2.4 and the embedding $H^{1/2}(Y^*) \hookrightarrow L^2(\partial\mathcal{T})$ yields $0 = \frac{\partial\mathbf{v}^\epsilon}{\partial\nu_{\mathbf{D}^\epsilon}} \xrightarrow{2} (\hat{\mathbf{E}}\nabla\mathbf{v} + \hat{\mathbf{D}}\mathbf{v}) \cdot \mathbf{n} = 0$ on ∂Y^* , which is automatically guaranteed by (5.40a) and (5.40b). \square

Hence, (\mathbf{P}_w^0) yields the strong form system

$$(\mathbf{P}_s^0) \quad \begin{cases} \overline{\mathbf{M}}\mathbf{v} - \operatorname{div}(\mathbf{E}^* \cdot \nabla\mathbf{v} + \mathbf{D}^*\mathbf{v}) = \overline{\mathbf{H}} + \overline{\mathbf{K}}\mathbf{u} & \text{in } (0, T) \times \Omega, \\ \frac{\partial\mathbf{u}}{\partial t} + \mathbf{L}\mathbf{u} = \mathbf{G}\mathbf{v} & \text{in } (0, T) \times \Omega, \\ \mathbf{v} = \mathbf{0} & \text{on } (0, T) \times \partial\Omega, \\ \mathbf{u} = \mathbf{U}^* & \text{on } \{0\} \times \bar{\Omega}, \end{cases}$$

when, next to the regularity of (A1), the following regularity holds:

$$M_{\alpha\beta}, H_{\alpha}, K_{\alpha\beta} \in C(0, T; C^1(\Omega; C^1_{\#}(Y^*))), \quad (5.43a)$$

$$E_{ij}, D_{i\alpha\beta} \in C(0, T; C^2(\Omega; C^2_{\#}(Y^*))), \quad (5.43b)$$

$$L_{\alpha\beta}, G_{\alpha\beta} \in C(0, T; C^1(\Omega)), \quad (5.43c)$$

$$U^* \in C(\bar{\Omega}), \quad (5.43d)$$

for all $T \in \mathbf{R}_+$, when both $\partial\Omega$ and $\partial\mathcal{T}$ are C^3 -boundaries.

Upscaling via asymptotic expansions

Even though the previous section showed that there is a two-scale limit (\mathbf{u}, \mathbf{v}) , it is necessary to show the relation between (\mathbf{u}, \mathbf{v}) and (U^ϵ, V^ϵ) . To this end, we first rewrite the Neumann problem (5.8a)-(5.9c) and then use asymptotic expansions such that we are lead to the two-scale limit, including the cell-functions, in a natural way.

The Neumann problem (5.8a)-(5.9c) can be written in operator form as

$$\begin{cases} \mathcal{A}^\epsilon \mathbf{V}^\epsilon = \mathcal{H}^\epsilon \mathbf{U}^\epsilon & \text{on } (0, T) \times \Omega^\epsilon, \\ \mathcal{L} \mathbf{U}^\epsilon = \mathbf{G} \mathbf{V}^\epsilon & \text{on } (0, T) \times \Omega^\epsilon, \\ \mathbf{U}^\epsilon = \mathbf{U}^* & \text{in } \{0\} \times \Omega^\epsilon, \\ \mathbf{V}^\epsilon = 0 & \text{on } (0, T) \times \partial_{ext} \Omega^\epsilon, \\ \frac{d\mathbf{V}^\epsilon}{d\nu_{D^\epsilon}} = 0 & \text{on } (0, T) \times \partial_{int} \Omega^\epsilon. \end{cases} \quad (5.44)$$

as indicated in Section 5.2.

We postulate the following asymptotic expansions in ϵ of \mathbf{U}^ϵ and \mathbf{V}^ϵ :

$$\mathbf{V}^\epsilon(t, \mathbf{x}) = \mathbf{V}^0\left(t, \mathbf{x}, \frac{\mathbf{x}}{\epsilon}\right) + \epsilon \mathbf{V}^1\left(t, \mathbf{x}, \frac{\mathbf{x}}{\epsilon}\right) + \epsilon^2 \mathbf{V}^2\left(t, \mathbf{x}, \frac{\mathbf{x}}{\epsilon}\right) + \dots, \quad (5.45a)$$

$$\mathbf{U}^\epsilon(t, \mathbf{x}) = \mathbf{U}^0\left(t, \mathbf{x}, \frac{\mathbf{x}}{\epsilon}\right) + \epsilon \mathbf{U}^1\left(t, \mathbf{x}, \frac{\mathbf{x}}{\epsilon}\right) + \epsilon^2 \mathbf{U}^2\left(t, \mathbf{x}, \frac{\mathbf{x}}{\epsilon}\right) + \dots \quad (5.45b)$$

Note that a rigorous argument for using formal asymptotic expansions needs corrector estimates, which we obtain in the next section.

Let $\Phi = \Phi(t, \mathbf{x}, \mathbf{y}) \in L^\infty(0, T; C^2(\Omega; C^2_{\#}(Y^*)))^N$ be a vector function depending on two spatial variables \mathbf{x} and \mathbf{y} , and introduce $\Phi^\epsilon(t, \mathbf{x}) = \Phi(t, \mathbf{x}, \mathbf{x}/\epsilon)$. Then the total spatial derivatives in \mathbf{x} become two partial derivatives, one in

\mathbf{x} and one in \mathbf{y} :

$$\nabla \Phi^\epsilon(t, \mathbf{x}) = \frac{1}{\epsilon} (\nabla_{\mathbf{y}} \Phi) \left(t, \mathbf{x}, \frac{\mathbf{x}}{\epsilon} \right) + (\nabla_{\mathbf{x}} \Phi) \left(t, \mathbf{x}, \frac{\mathbf{x}}{\epsilon} \right), \quad (5.46a)$$

$$\operatorname{div} \Phi^\epsilon(t, \mathbf{x}) = \frac{1}{\epsilon} (\nabla_{\mathbf{y}} \cdot \Phi) \left(t, \mathbf{x}, \frac{\mathbf{x}}{\epsilon} \right) + (\nabla_{\mathbf{x}} \cdot \Phi) \left(t, \mathbf{x}, \frac{\mathbf{x}}{\epsilon} \right). \quad (5.46b)$$

Do note, the evaluation $\mathbf{y} = \mathbf{x}/\epsilon$ is suspended as is common in formal asymptotic expansions, leading to the use of $\mathbf{y} \in Y^*$ and $\mathbf{x} \in \Omega$.

Hence, $\mathcal{A}^\epsilon \Phi^\epsilon$ can be formally expanded:

$$\mathcal{A}^\epsilon \Phi^\epsilon = \left[\left(\frac{1}{\epsilon^2} \mathcal{A}^0 + \frac{1}{\epsilon} \mathcal{A}^1 + \mathcal{A}^2 \right) \Phi \right] \left(t, \mathbf{x}, \frac{\mathbf{x}}{\epsilon} \right), \quad (5.47)$$

where

$$\mathcal{A}^0 \Phi = -\nabla_{\mathbf{y}} \cdot (\mathbf{E} \cdot \nabla_{\mathbf{y}} \Phi), \quad (5.48a)$$

$$\mathcal{A}^1 \Phi = -\nabla_{\mathbf{y}} \cdot (\mathbf{E} \cdot \nabla_{\mathbf{x}} \Phi) - \nabla_{\mathbf{x}} \cdot (\mathbf{E} \cdot \nabla_{\mathbf{y}} \Phi) - \nabla_{\mathbf{y}} \cdot (\mathbf{D} \Phi), \quad (5.48b)$$

$$\mathcal{A}^2 \Phi = \mathbf{M} \Phi - \nabla_{\mathbf{x}} \cdot (\mathbf{E} \cdot \nabla_{\mathbf{x}} \Phi) - \nabla_{\mathbf{x}} \cdot (\mathbf{D} \Phi). \quad (5.48c)$$

Moreover, $\mathcal{H}^\epsilon \Phi^\epsilon$ can be written as $\mathbf{H} + (\mathcal{H}^0 + \epsilon \mathcal{H}^1) \Phi$, where

$$\mathcal{H}^0 = \mathbf{K} + \mathbf{J} \cdot \nabla_{\mathbf{y}}, \quad (5.49a)$$

$$\mathcal{H}^1 = \mathbf{J} \cdot \nabla_{\mathbf{x}}. \quad (5.49b)$$

Since the outward normal \mathbf{n} on $\partial \mathcal{T}$ depends only on \mathbf{y} and the outward normal \mathbf{n}^ϵ on $\partial_{int} \Omega^\epsilon = \partial \mathcal{T}^\epsilon \cap \Omega$ is defined as the Y -periodic function $\mathbf{n}|_{\mathbf{y}=\mathbf{x}/\epsilon}$, one has

$$\begin{aligned} \frac{\partial \Phi^\epsilon}{\partial \nu_{\mathbf{D}^\epsilon}} &= \left(\mathbf{E}^\epsilon \cdot \frac{d\Phi^\epsilon}{d\mathbf{x}} + \mathbf{D}^\epsilon \Phi^\epsilon \right) \cdot \mathbf{n}^\epsilon \\ &= \left(\frac{1}{\epsilon} \mathbf{E} \cdot \nabla_{\mathbf{y}} \Phi + \mathbf{E} \cdot \nabla_{\mathbf{x}} \Phi + \mathbf{D} \Phi \right) \cdot \mathbf{n}^\epsilon \\ &=: \frac{1}{\epsilon} \frac{\partial \Phi^\epsilon}{\partial \nu_{\mathbf{E}}} + \frac{\partial \Phi^\epsilon}{\partial \nu_{\mathbf{D}}}. \end{aligned} \quad (5.50)$$

Inserting (5.45a), (5.45b), (5.47) - (5.50) into the Neumann problem (5.44) and expanding the full problem into powers of ϵ , we obtain the following auxilliary systems:

$$\begin{cases} \mathcal{A}^0 \mathbf{V}^0 = 0 & \text{in } (0, T) \times \Omega \times Y^*, \\ \frac{\partial \mathbf{V}^0}{\partial \nu_{\mathbf{E}}} = 0 & \text{on } (0, T) \times \Omega \times \partial \mathcal{T}, \\ \mathbf{V}^0 = 0 & \text{on } (0, T) \times \partial \Omega \times Y^*, \\ \mathbf{V}^0 \text{ } Y\text{-periodic,} \end{cases} \quad (5.51)$$

$$\begin{cases} \mathcal{A}^0 \mathbf{V}^1 = -\mathcal{A}^1 \mathbf{V}^0 & \text{in } (0, T) \times \Omega \times Y^*, \\ \frac{\partial \mathbf{V}^1}{\partial \nu_{\mathbf{E}}} = -\frac{\partial \mathbf{V}^0}{\partial \nu_{\mathbf{D}}} & \text{on } (0, T) \times \Omega \times \partial \mathcal{T}, \\ \mathbf{V}^1 = 0 & \text{on } (0, T) \times \partial \Omega \times Y^*, \\ \mathbf{V}^1 \text{ } Y\text{-periodic,} \end{cases} \quad (5.52)$$

$$\begin{cases} \mathcal{A}^0 \mathbf{V}^2 = -\mathcal{A}^1 \mathbf{V}^1 - \mathcal{A}^2 \mathbf{V}^0 + \mathbf{H} + \mathcal{H}^0 \mathbf{U}^0 & \text{in } (0, T) \times \Omega \times Y^*, \\ \frac{\partial \mathbf{V}^2}{\partial \nu_{\mathbf{E}}} = -\frac{\partial \mathbf{V}^1}{\partial \nu_{\mathbf{D}}} & \text{on } (0, T) \times \Omega \times \partial \mathcal{T}, \\ \mathbf{V}^2 = 0 & \text{on } (0, T) \times \partial \Omega \times Y^*, \\ \mathbf{V}^2 \text{ } Y\text{-periodic.} \end{cases} \quad (5.53)$$

For $i \geq 3$, we have

$$\begin{cases} \mathcal{A}^0 \mathbf{V}^i = -\mathcal{A}^1 \mathbf{V}^{i-1} - \mathcal{A}^2 \mathbf{V}^{i-2} & \text{in } (0, T) \times \Omega \times Y^*, \\ \quad \quad \quad + \mathcal{H}^0 \mathbf{U}^{i-2} + \mathcal{H}^1 \mathbf{U}^{i-3} & \\ \frac{\partial \mathbf{V}^i}{\partial \nu_{\mathbf{E}}} = -\frac{\partial \mathbf{V}^{i-1}}{\partial \nu_{\mathbf{D}}} & \text{on } (0, T) \times \Omega \times \partial \mathcal{T}, \\ \mathbf{V}^i = 0 & \text{on } (0, T) \times \partial \Omega \times Y^*, \\ \mathbf{V}^i \text{ } Y\text{-periodic.} \end{cases} \quad (5.54)$$

Furthermore, we have

$$\begin{cases} \mathcal{L} \mathbf{U}^0 = \mathbf{G} \mathbf{V}^0 & \text{in } (0, T) \times \Omega \times Y^*, \\ \mathbf{U}^0 = \mathbf{U}^* & \text{in } \{0\} \times \Omega \times Y^*, \\ \mathbf{U}^0 \text{ } Y\text{-periodic,} \end{cases} \quad (5.55)$$

and, for $j \geq 1$,

$$\begin{cases} \mathcal{L} \mathbf{U}^j = \mathbf{G} \mathbf{V}^j & \text{in } (0, T) \times \Omega \times Y^*, \\ \mathbf{U}^j = 0 & \text{in } \{0\} \times \Omega \times Y^*, \\ \mathbf{U}^j \text{ } Y\text{-periodic.} \end{cases} \quad (5.56)$$

The existence and uniqueness of weak solutions of the systems (5.51) - (5.54) is stated in the following Lemma:

Lemma 5.12. *Let $F \in L^2(Y^*)$ and $g \in L^2(\partial\mathcal{T})$ be Y -periodic. Let $\mathbf{A}(\mathbf{y}) \in L^\infty_\#(Y^*)^{N \times N}$ satisfy $\sum_{i,j=1}^n \mathbf{A}_{ij}(\mathbf{y}) \xi_i \xi_j \geq a \sum_{i=1}^n \xi_i^2$ for all $\boldsymbol{\xi} \in \mathbf{R}^n$ for some $a > 0$. Consider the following boundary value problem for $\omega(\mathbf{y})$:*

$$\begin{cases} -\nabla_{\mathbf{y}} \cdot (\mathbf{A}(\mathbf{y}) \cdot \nabla_{\mathbf{y}} \omega) = F(\mathbf{y}) & \text{on } Y^*, \\ -[\mathbf{A}(\mathbf{y}) \nabla_{\mathbf{y}} \omega] \cdot \mathbf{n} = g(\mathbf{y}) & \text{on } \partial\mathcal{T}, \\ \omega \text{ is } Y\text{-periodic.} \end{cases} \quad (5.57)$$

Then the following statements hold:

- (i) *There exists a weak Y -periodic solution $\omega \in H^1_\#(Y^*)/\mathbf{R}$ to (5.57) if and only if $\int_{Y^*} F(\mathbf{y}) d\mathbf{y} = \int_{\partial\mathcal{T}} g(\mathbf{y}) d\sigma_{\mathbf{y}}$.*
- (ii) *If (i) holds, then the uniqueness of weak solutions is ensured up to an additive constant.*

See Lemma 2.1 in [97].

Existence and uniqueness of the solutions of the systems (5.55) and (5.56) can be handled via the application of Rothe's method, see [120] for details on Rothe's method, and Gronwall's inequality, and see [39] for various different versions of useful discrete Gronwall's inequalities.

Lemma 5.13. *The function \mathbf{V}^0 depends only on $(t, \mathbf{x}) \in (0, T) \times \Omega$.*

Proof. Applying Lemma 5.12 to system (5.51) yields the weak solution $\mathbf{V}^0(t, x, y) \in H^1_\#(Y^*)/\mathbf{R}$ pointwise in $(t, \mathbf{x}) \in (0, T) \times \Omega$ with uniqueness ensured up to an additive function depending only on $(t, \mathbf{x}) \in (0, T) \times \Omega$. Direct testing of (5.51) with \mathbf{V}^0 yields $\|\nabla_{\mathbf{y}} \mathbf{V}^0\|_{L^2_\#(Y^*)} = 0$. Hence, $\nabla_{\mathbf{y}} \mathbf{V}^0 = 0$ a.e. in Y^* . \square

Corollary 5.14. *The function \mathbf{U}^0 depends only on $(t, \mathbf{x}) \in (0, T) \times \Omega$.*

Proof. Apply the gradient $\nabla_{\mathbf{y}}$ to system (5.55). The independence of \mathbf{y} follows directly from (A1) and Lemma 5.13. \square

The application of Lemma 5.12 to system (5.52) yields, due to the divergence theorem, again a weak solution $\mathbf{V}^1(t, \mathbf{x}, \mathbf{y}) \in H^1_\#(Y^*)/\mathbf{R}$ pointwise in $(t, \mathbf{x}) \in (0, T) \times \Omega$ with uniqueness ensured up to an additive function depending only on $(t, \mathbf{x}) \in (0, T) \times \Omega$. One can determine \mathbf{V}^1 from \mathbf{V}^0 with the use

of a decomposition of V^1 into products of \mathbf{V}^0 derivatives and so-called cell functions:

$$\mathbf{V}^1 = \mathbf{W} \cdot \nabla_{\mathbf{x}} \mathbf{V}^0 + Z \mathbf{V}^0 + \tilde{\mathbf{V}}^1 \quad (5.58)$$

with $\tilde{\mathbf{V}}^1$ the Y^* -average of \mathbf{V}^1 satisfying $\nabla_{\mathbf{y}} \tilde{\mathbf{V}}^1 = 0$ and for $\alpha, \beta \in \{1, \dots, N\}$ and $i \in \{1, \dots, d\}$ with cell functions

$$Z_{\alpha\beta}, W_i \in L^\infty(\mathbf{R}_+; W^{2,\infty}(\Omega; C_{\#}^2(Y^*)/\mathbf{R})) \quad (5.59)$$

with vanishing Y^* -average. Insertion of (5.58) into system (5.52) leads to systems for the cell-functions \mathbf{W} and Z :

$$\begin{cases} \mathcal{A}^0 \mathbf{W} = -\nabla_{\mathbf{y}} \cdot \mathbf{E} & \text{in } Y^*, \\ \frac{\partial \mathbf{W}}{\partial \nu_{\mathbf{E}}} = -\mathbf{n} \cdot \mathbf{E} & \text{on } \partial \mathcal{T}, \\ \mathbf{W} & Y\text{-periodic,} \\ \frac{1}{|Y|} \int_{Y^*} \mathbf{W} \, d\mathbf{y} = \mathbf{0}. \end{cases} \quad (5.60)$$

and

$$\begin{cases} \mathcal{A}^0 Z = -\nabla_{\mathbf{y}} \cdot \mathbf{D} & \text{in } Y^*, \\ \frac{\partial Z}{\partial \nu_{\mathbf{E}}} = -\mathbf{n} \cdot \mathbf{D} & \text{on } \partial \mathcal{T}, \\ Z_{\alpha\beta} & Y\text{-periodic,} \\ \frac{1}{|Y|} \int_{Y^*} Z \, d\mathbf{y} = 0. \end{cases} \quad (5.61)$$

Again the existence and uniqueness up to an additive constant of the cell functions in systems (5.60) and (5.61) follow from Lemma 5.12 and convenient applications of the divergence theorem. The regularity of solutions follows from Theorem 9.25 and Theorem 9.26 in [20].

The existence and uniqueness for \mathbf{V}^2 follows from applying Lemma 5.12 to system (5.53), which states that a solvability condition has to be satisfied. Using the divergence theorem, this solvability condition becomes

$$\begin{aligned} \int_{Y^*} \mathcal{A}^2 \mathbf{V}^0 + \mathcal{A}^1 [(\mathbf{W} \cdot \nabla_{\mathbf{x}} + Z) \mathbf{V}^0] + \nabla_{\mathbf{y}} \cdot [(\mathbf{E} \cdot \nabla_{\mathbf{x}} + \mathbf{D})(\mathbf{W} \cdot \nabla_{\mathbf{x}} + Z) \mathbf{V}^0] \, d\mathbf{y} \\ = \int_{Y^*} \mathbf{H} \, d\mathbf{y} + \int_{Y^*} \mathcal{H}^0 \, d\mathbf{y} \, U^0. \end{aligned} \quad (5.62)$$

Inserting (5.48b), (5.48c), and (5.49a) and using both $\nabla_{\mathbf{y}} \mathbf{V}^0 = \mathbf{0}$ and $\nabla_{\mathbf{y}} U^0 = 0$, we find

$$\begin{aligned} & \int_{Y^*} \mathbf{M} \mathbf{V}^0 d\mathbf{y} - \int_{Y^*} \nabla_{\mathbf{x}} \cdot (\mathbf{D} \mathbf{V}^0) d\mathbf{y} - \int_{Y^*} \nabla_{\mathbf{x}} \cdot (\mathbf{E} \cdot \nabla_{\mathbf{x}} \mathbf{V}^0) d\mathbf{y} \\ & - \int_{Y^*} \nabla_{\mathbf{x}} \cdot (\mathbf{E} \cdot [\nabla_{\mathbf{y}} (\mathbf{W} \cdot \nabla_{\mathbf{x}} + \mathbf{Z})] \mathbf{V}^0) d\mathbf{y} = \int_{Y^*} \mathbf{H} d\mathbf{y} + \int_{Y^*} \mathbf{K} d\mathbf{y} U^0, \end{aligned} \quad (5.63)$$

which after rearrangement looks like

$$\begin{aligned} & \int_{Y^*} \mathbf{M} d\mathbf{y} \mathbf{V}^0 - \nabla_{\mathbf{x}} \cdot \left(\int_{Y^*} \mathbf{E} + \mathbf{E} \cdot \nabla_{\mathbf{y}} \mathbf{W} d\mathbf{y} \cdot \nabla_{\mathbf{x}} \mathbf{V}^0 \right) \\ & - \nabla_{\mathbf{x}} \cdot \left(\int_{Y^*} \mathbf{D} + \mathbf{E} \cdot \nabla_{\mathbf{y}} \mathbf{Z} d\mathbf{y} \mathbf{V}^0 \right) = \int_{Y^*} \mathbf{H} d\mathbf{y} + \int_{Y^*} \mathbf{K} d\mathbf{y} U^0. \end{aligned} \quad (5.64)$$

Dividing all terms by $|Y|$, we realize that this solvability condition is an up-scaled version of (5.8a), the spatial partial differential equation for \mathbf{V}^0 :

$$\overline{\mathbf{M}} \mathbf{V}^0 - \nabla_{\mathbf{x}} \cdot (\mathbf{E}^* \cdot \nabla_{\mathbf{x}} \mathbf{V}^0 + \mathbf{D}^* \mathbf{V}^0) = \overline{\mathbf{H}} + \overline{\mathbf{K}} U^0, \quad (5.65)$$

where we have used (5.58), the cell function decomposition, and the new short-hand notation

$$\mathbf{E}^* = \frac{1}{|Y|} \int_{Y^*} \mathbf{E} \cdot (1 + \nabla_{\mathbf{y}} \mathbf{W}) d\mathbf{y}, \quad (5.66a)$$

$$\mathbf{D}^* = \frac{1}{|Y|} \int_{Y^*} \mathbf{D} + \mathbf{E} \cdot \nabla_{\mathbf{y}} \mathbf{Z} d\mathbf{y}. \quad (5.66b)$$

Lemma 5.15. *The pair $(\mathbf{U}^0, \mathbf{V}^0) \in H^1((0, T) \times \Omega) \times L^\infty((0, T); H_0^1(\Omega))$ are weak solutions to the following system*

$$\begin{cases} \overline{\mathbf{M}} \mathbf{V}^0 - \nabla_{\mathbf{x}} \cdot (\mathbf{E}^* \cdot \nabla_{\mathbf{x}} \mathbf{V}^0 + \mathbf{D}^* \mathbf{V}^0) = \overline{\mathbf{H}} + \overline{\mathbf{K}} U^0 & \text{in } (0, T) \times \Omega, \\ \frac{\partial \mathbf{U}^0}{\partial t} + \mathbf{L} \mathbf{U}^0 = \mathbf{G} \mathbf{V}^0 & \text{in } (0, T) \times \Omega, \\ \mathbf{V}^0 = \mathbf{0} & \text{on } (0, T) \times \partial \Omega, \\ \mathbf{U}^0 = U^* & \text{on } \{0\} \times \Omega. \end{cases} \quad (5.67)$$

Proof. From system (5.51), equation (5.65), $\nabla_{\mathbf{y}} \mathbf{V}^0 = \mathbf{0}$, assumption (A3) and system (5.55), we see that $\nabla_{\mathbf{y}} U^0 = 0$. This leads automatically to system (5.67), since there is no \mathbf{y} -dependence and $\Omega^\epsilon \subset \Omega$, $\Omega^\epsilon \rightarrow \Omega$, $\partial_{ext} \Omega^\epsilon = \partial \Omega$. Analogous to the proof of Theorem 5.9 we obtain the required spatial regularity. Moreover, by testing the second line with $\frac{\partial}{\partial t} U^0$, applying a gradient to the second line and testing it with $\frac{\partial}{\partial t} \nabla U^0$, we obtain the required temporal regularity as well. \square

Combining two-scale convergence and asymptotic expansions

Theorem 5.16. *Let (A1)-(A3) be valid, then $(\mathbf{u}, \mathbf{v}) = (\mathbf{U}^0, \mathbf{V}^0)$.*

Proof. From (\mathbf{P}_s^0) and Lemma 5.15, we see that (\mathbf{u}, \mathbf{v}) and $(\mathbf{U}^0, \mathbf{V}^0)$ satisfy the same linear boundary value problem. We only have to prove the uniqueness for this boundary value problem.

From testing (5.61) with \mathbf{W} and (5.60) with Z , we obtain the identity

$$\int_{Y^*} (\nabla_{\mathbf{y}} \mathbf{W})^\top \cdot \mathbf{D} d\mathbf{y} = \int_{Y^*} \mathbf{E} \cdot \nabla_{\mathbf{y}} Z d\mathbf{y}. \quad (5.68)$$

Hence, from (5.66b) we get

$$\mathbf{D}^* = \frac{1}{|Y|} \int_{Y^*} (1 + (\nabla_{\mathbf{y}} \mathbf{W}))^\top \cdot \mathbf{D} d\mathbf{y}. \quad (5.69)$$

Moreover, testing system (5.60) with \mathbf{W} yields the identity

$$\mathbf{E}^* = \frac{1}{|Y|} \int_{Y^*} (1 + (\nabla_{\mathbf{y}} \mathbf{W}))^\top \cdot \mathbf{E} \cdot (1 + (\nabla_{\mathbf{y}} \mathbf{W})) d\mathbf{y}. \quad (5.70)$$

We subtract (\mathbf{P}_s^0) from (5.67) and introduce $\tilde{\mathbf{U}}, \tilde{\mathbf{V}}$ as

$$\tilde{\mathbf{U}} = \mathbf{U}^0 - \mathbf{u} \quad \text{and} \quad \tilde{\mathbf{V}} = \mathbf{V}^0 - \mathbf{v}. \quad (5.71)$$

Testing with $\tilde{\mathbf{V}}$, we obtain the equation

$$0 = \int_{\Omega} \frac{1}{|Y|} \int_{Y^*} \left[\tilde{\mathbf{V}}^\top \mathbf{M} \tilde{\mathbf{V}} + \zeta^\top \cdot (\mathbf{E} \cdot \zeta + \mathbf{D} \tilde{\mathbf{V}}) - \tilde{\mathbf{V}}^\top \mathbf{K} \tilde{\mathbf{U}} \right] d\mathbf{y} d\mathbf{x}, \quad (5.72)$$

where

$$\zeta = (1 + (\nabla_{\mathbf{y}} \mathbf{W})) \cdot \nabla_{\mathbf{x}} \tilde{\mathbf{V}}. \quad (5.73)$$

This equation is identical to the Neumann problem (5.8a)-(5.9c) with $\mathbf{H} = \mathbf{0}$, $\mathbf{J} = \mathbf{0}$, and replacements $\nabla_{\mathbf{x}} \mathbf{V} \rightarrow \zeta$, $\mathbf{U} \rightarrow \tilde{\mathbf{U}}$ and $\mathbf{V} \rightarrow \tilde{\mathbf{V}}$ in (5.8a). Moreover, (5.8a) is coercive due to assumption (A3). Therefore, we can follow the argument of the proof of Theorem 5.9, but we only use equations (5.27) and (5.31a) with constants \tilde{H} and $\tilde{J}_{i\alpha}$ set to 0. For some $R > 0$, this leads to

$$\frac{\partial}{\partial t} \|\tilde{\mathbf{U}}\|_{L^2(\Omega; L^2_{\#}(Y^*))^N}^2 \leq R \|\tilde{\mathbf{U}}\|_{L^2(\Omega; L^2_{\#}(Y^*))^N}^2. \quad (5.74)$$

Applying Gronwall inequality and using the initial value $\tilde{\mathbf{U}} = \mathbf{U}^* - \mathbf{U}^* = \mathbf{0}$, we obtain $\|\tilde{\mathbf{U}}\|_{L^2(\Omega; L^2_{\#}(Y^*))^N} = 0$ a.e. in $(0, T)$. By the coercivity, we obtain

$\|\tilde{\mathbf{V}}\|_{L^2(\Omega; L^2_{\#}(Y^*))^N} = 0$ and $\|\zeta\|_{L^2(\Omega; L^2_{\#}(Y^*))^N} = 0$.

From the proof of Proposition 6.12 in [29], we see that $1 + \nabla_{\mathbf{y}}W$ does not have a kernel that contains non-zero Y -periodic solutions. Therefore, $\zeta = \mathbf{0}$ yields $\nabla_{\mathbf{y}}\tilde{\mathbf{V}} = 0$. Thus, we have $\tilde{\mathbf{U}} = \mathbf{0}$ in $L^\infty((0, T); L^2(\Omega))^N$ and $\tilde{\mathbf{V}} = \mathbf{0}$ in $L^\infty((0, T); H_0^1(\Omega))^N$. Hence, $(\mathbf{u}, \mathbf{v}) = (\mathbf{U}^0, \mathbf{V}^0)$. \square

Corollary 5.17. *Let $\lambda \geq 0$ and $\tilde{\kappa} \geq 0$ be as in Theorem 5.9. Then there exists a positive constant C independent of ϵ such that*

$$\|\mathbf{U}^0\|_{H^1(\Omega^\epsilon)^N}(t) \leq Ce^{\lambda t}, \quad \|\mathbf{V}^0\|_{\mathbb{V}_\epsilon^N}(t) \leq C(1 + \tilde{\kappa}e^{\lambda t}) \quad (5.75)$$

holds for $t \geq 0$.

Proof. Bochner's Theorem states that $\|\hat{\mathbf{U}}^\epsilon\|_{H^1(\Omega)^N}(t)$, $\|\hat{\mathbf{V}}^\epsilon\|_{H_0^1(\Omega)^N}(t)$, $\|\mathbf{U}^\epsilon\|_{H^1(\Omega^\epsilon)^N}(t)$, and $\|\mathbf{V}^\epsilon\|_{\mathbb{V}_\epsilon^N}(t)$ are Lebesgue integrable, and, therefore, elements of $L^1(0, T)$. Since Ω does not depend on t , Theorem 5.1 is applicable for a.e. $t \in (0, T)$. From Theorem 5.9 we obtain that both $\|\hat{\mathbf{U}}^\epsilon\|_{H^1(\Omega)^N}(t)$ and $\|\hat{\mathbf{V}}^\epsilon\|_{H_0^1(\Omega)^N}(t)$ have ϵ -independent upper bounds for a.e. $t \in (0, T)$. Hence, the Eberlein-Šmuljan Theorem states that there is a subsequence $\epsilon' \subset \epsilon$ such that $\hat{\mathbf{U}}^{\epsilon'}$ and $\hat{\mathbf{V}}^{\epsilon'}$ converge weakly in $H^1(\Omega)^N$ and $H_0^1(\Omega)^N$, respectively, for a.e. $t \in (0, T)$. Moreover, Lemma 5.10 states that $\hat{\mathbf{U}}^{\epsilon'}$ and $\hat{\mathbf{V}}^{\epsilon'}$ two scale converge (and therefore weakly) to $\mathbf{u} \in H^1(0, T; L^2(\Omega))^N$ and $\mathbf{v} \in L^\infty(0, T; L^2(\Omega))^N$, respectively. Limits of weak convergences are unique. Hence, $\hat{\mathbf{U}}^{\epsilon'}(t) \rightharpoonup \mathbf{u}(t)$ in $H^1(\Omega)^N$ and $\hat{\mathbf{V}}^{\epsilon'}(t) \rightharpoonup \mathbf{v}(t)$ in $H_0^1(\Omega)^N$ for a.e. $t \in (0, T)$ as $\epsilon' \downarrow 0$. Using these weak convergences, (5.5) and (5.6) in Theorem 5.1, Theorem 5.9, and the limit inferior property of weakly convergent sequences, we obtain

$$\begin{aligned} \|\mathbf{U}^0\|_{H^1(\Omega^\epsilon)^N}(t) &\leq \|\mathbf{U}^0\|_{H^1(\Omega)^N}(t) = \liminf_{\epsilon \rightarrow 0} \|\hat{\mathbf{U}}^\epsilon\|_{H^1(\Omega)^N}(t) \\ &\leq \liminf_{\epsilon \rightarrow 0} C\|\mathbf{U}^\epsilon\|_{H^1(\Omega^\epsilon)^N}(t) \leq Ce^{\lambda t}, \end{aligned} \quad (5.76a)$$

$$\begin{aligned} \|\mathbf{V}^0\|_{\mathbb{V}_\epsilon^N}(t) &\leq \|\mathbf{V}^0\|_{H_0^1(\Omega)^N}(t) = \liminf_{\epsilon \rightarrow 0} \|\hat{\mathbf{V}}^\epsilon\|_{H_0^1(\Omega)^N}(t) \\ &\leq \liminf_{\epsilon \rightarrow 0} C\|\mathbf{V}^\epsilon\|_{\mathbb{V}_\epsilon^N}(t) \leq C(1 + \tilde{\kappa}e^{\lambda t}). \end{aligned} \quad (5.76b)$$

Hence, the bounds of Theorem 5.9 hold for \mathbf{U}^0 and \mathbf{V}^0 as well. \square

This concludes the proof of Theorem 5.4.

5.5 Corrector estimates via asymptotic expansions

It is natural to determine the speed of convergence of the weak solutions $(\mathbf{U}^\epsilon, \mathbf{V}^\epsilon)$ to $(\mathbf{U}^0, \mathbf{V}^0)$. However, certain boundary effects are expected due to intersection of the external boundary with the perforated periodic cells. It is clear that $\Omega^\epsilon \rightarrow \Omega$ for $\epsilon \downarrow 0$, but the boundary effects impact the periodic behavior, which can lead to $\mathbf{V}^j \neq \mathbf{0}$ at $\partial_{ext}\Omega^\epsilon$ for $j > 0$. Hence, a cut-off function is introduced to remove this potentially problematic part of the domain. The use of a cut-off function is a standard technique in corrector estimates for periodic homogenization. See [30] for a similar introduction of a cut-off function.

Let us again introduce the cut-off function \mathcal{M}_ϵ defined by

$$\begin{cases} \mathcal{M}_\epsilon \in \mathcal{D}(\Omega), \\ \mathcal{M}_\epsilon = 0 & \text{if } \text{dist}(\mathbf{x}, \partial\Omega) \leq \epsilon, \\ \mathcal{M}_\epsilon = 1 & \text{if } \text{dist}(\mathbf{x}, \partial\Omega) \geq 2\epsilon, \\ \epsilon \left| \frac{d\mathcal{M}_\epsilon}{dx_i} \right| \leq C \quad i \in \{1, \dots, d\}. \end{cases} \quad (5.77)$$

With this cut-off function defined, we introduce again the error functions

$$\Phi^\epsilon = \mathbf{V}^\epsilon - \mathbf{V}^0 - \mathcal{M}_\epsilon(\epsilon\mathbf{V}^1 + \epsilon^2\mathbf{V}^2), \quad (5.78a)$$

$$\Psi^\epsilon = \mathbf{U}^\epsilon - \mathbf{U}^0 - \mathcal{M}_\epsilon(\epsilon\mathbf{U}^1 + \epsilon^2\mathbf{U}^2), \quad (5.78b)$$

where the \mathcal{M}_ϵ terms are the so-called corrector terms.

Preliminaries

The solvability condition for system (5.53) naturally leads to the fact that $(\mathbf{U}^0, \mathbf{V}^0)$ has to satisfy system (5.67). Similar to solving system (5.52) for \mathbf{V}^1 , we handle system (5.53) for \mathbf{V}^2 with a decomposition into cell-functions:

$$\mathbf{V}^2 = \mathbf{P} + \mathbf{Q}^0\mathbf{V}^0 + \mathbf{R}^0\mathbf{U}^0 + \mathbf{Q}^1 \cdot \nabla_{\mathbf{x}}\mathbf{V}^0 + \mathbf{R}^1 \cdot \nabla_{\mathbf{x}}\mathbf{U}^0 + \mathbf{Q}^2 : \mathbf{D}_{\mathbf{x}}^2\mathbf{V}^0 \quad (5.79)$$

where we have the cell-functions

$$\begin{aligned} P_\alpha, R_{\alpha\beta}^0, R_{i\alpha\beta}^1 &\in L^\infty(\mathbf{R}_+; W^{2,\infty}(\Omega^\epsilon; C_{\#}^3(Y^*))), \\ Q_{\alpha\beta}^0, Q_{i\alpha\beta}^1 &\in L^\infty(\mathbf{R}_+; W^{2,\infty}(\Omega^\epsilon; C_{\#}^2(Y^*))), \\ Q_{ij}^2 &\in L^\infty(\mathbf{R}_+; W^{2,\infty}(\Omega^\epsilon; C_{\#}^2(Y^*))) \end{aligned} \quad (5.80)$$

for $\alpha, \beta \in \{1, \dots, N\}$ and for $i, j \in \{1, \dots, d\}$, and where

$$(\mathbf{Q}^2 : \mathbf{D}_{\mathbf{x}}^2 \mathbf{V}^0)_{\alpha} := \sum_{i,j=1}^d Q_{ij} \frac{\partial^2 V_{\alpha}^0}{\partial x_i \partial x_j}. \quad (5.81)$$

The cell-functions \mathbf{P} , \mathbf{Q}^0 , \mathbf{R}^0 , \mathbf{Q}^1 , \mathbf{R}^1 , \mathbf{Q}^2 satisfy the following systems of partial differential equations, obtained from subtracting (5.65) from (5.53) and inserting (5.79):

$$\begin{cases} \mathcal{A}^0 \mathbf{P} = \mathbf{H} - \overline{\mathbf{H}} & \text{in } Y^*, \\ \frac{\partial \mathbf{P}}{\partial \nu_{\mathbf{E}}} = \mathbf{0} & \text{on } \partial \mathcal{T}, \\ \mathbf{P} \text{ } Y\text{-periodic,} \end{cases} \quad (5.82)$$

$$\begin{cases} \mathcal{A}^0 \mathbf{Q}^0 = \nabla_{\mathbf{y}} \cdot (\mathbf{E} \cdot \nabla_{\mathbf{x}} \mathbf{Z}) + \nabla_{\mathbf{x}} \cdot (\mathbf{E} \cdot \nabla_{\mathbf{y}} \mathbf{Z}) + \nabla_{\mathbf{y}} \cdot (\mathbf{D} \mathbf{Z}) \\ \quad + \nabla_{\mathbf{x}} \cdot (\mathbf{D} - \mathbf{D}^*) + \overline{\mathbf{M}} - \mathbf{M} & \text{in } Y^*, \\ \frac{\partial \mathbf{Q}^0}{\partial \nu_{\mathbf{E}}} = -(\mathbf{D} \mathbf{Z} + \mathbf{E} \cdot \nabla_{\mathbf{x}} \mathbf{Z}) \cdot \mathbf{n} & \text{on } \partial \mathcal{T}, \\ \mathbf{Q}^0 \text{ } Y\text{-periodic,} \end{cases} \quad (5.83)$$

$$\begin{cases} \mathcal{A}^0 \mathbf{R}^0 = \mathbf{K} - \overline{\mathbf{K}} & \text{in } Y^*, \\ \frac{\partial R_{\alpha\beta}^0}{\partial \nu_{\mathbf{E}}} = 0 & \text{on } \partial \mathcal{T}, \\ \mathbf{R}^0 \text{ } Y\text{-periodic,} \end{cases} \quad (5.84)$$

$$\begin{cases} \mathcal{A}^0 \mathbf{Q}^1 = \nabla_{\mathbf{y}} \cdot (\mathbf{E} \cdot \nabla_{\mathbf{x}} \mathbf{W}) \otimes \mathbf{1} + \nabla_{\mathbf{y}} \cdot (\mathbf{E} \otimes \mathbf{Z}) \\ \quad + \nabla_{\mathbf{x}} \cdot (\mathbf{E} \cdot \nabla_{\mathbf{y}} \mathbf{W}) \otimes \mathbf{1} + \mathbf{E} \cdot \nabla_{\mathbf{y}} \mathbf{Z} \\ \quad + \nabla_{\mathbf{y}} \cdot (\mathbf{D} \otimes \mathbf{W}) + \nabla_{\mathbf{x}} \cdot (\mathbf{E} - \mathbf{E}^*) \otimes \mathbf{1} + \mathbf{D} - \mathbf{D}^* & \text{in } Y^*, \\ \frac{\partial \mathbf{Q}^1}{\partial \nu_{\mathbf{E}}} = \mathbf{W} \otimes (\mathbf{D} \cdot \mathbf{n}) + \mathbf{n} \cdot (\mathbf{E} \otimes \mathbf{Z} + \mathbf{E} \cdot \nabla_{\mathbf{x}} \mathbf{W} \otimes \mathbf{1}) & \text{on } \partial \mathcal{T}, \\ \mathbf{Q}^1 \text{ } Y\text{-periodic,} \end{cases} \quad (5.85)$$

$$\begin{cases} \mathcal{A}^0 \mathbf{R}^1 = 0 & \text{in } Y^*, \\ \frac{\partial \mathbf{R}^1}{\partial \nu_{\mathbf{E}}} = 0 & \text{on } \partial \mathcal{T}, \\ \mathbf{R}^1 \text{ } Y\text{-periodic,} \end{cases} \quad (5.86)$$

$$\begin{cases} \mathcal{A}^0 \mathbf{Q}^2 = \nabla_{\mathbf{y}} \cdot (\mathbf{E} \otimes \mathbf{W}) + \mathbf{E} \cdot \nabla_{\mathbf{y}} \mathbf{W} + \mathbf{E} - \mathbf{E}^* & \text{in } Y^*, \\ \frac{\partial \mathbf{Q}^2}{\partial \nu_{\mathbf{E}}} = -\mathbf{n} \cdot \mathbf{E} \otimes \mathbf{W} & \text{on } \partial \mathcal{T}, \\ \mathbf{Q}^2 & Y\text{-periodic.} \end{cases} \quad (5.87)$$

The well-posedness of the cell-problems (5.60) - (5.87) is given by Lemma 5.12, while the regularity follows from Theorem 9.25 and Theorem 9.26 in [20]. Note that cell-problem (5.86) yields $\mathbf{R}^1 = 0$.

Proof of Theorem 5.5

Let C denote a constant independent of ϵ , \mathbf{x} , \mathbf{y} and t .

We rewrite the error-function Φ^ϵ as

$$\Phi^\epsilon = \mathbf{V}^\epsilon - \mathbf{V}^0 - \mathcal{M}_\epsilon(\epsilon \mathbf{V}^1 + \epsilon^2 \mathbf{V}^2) = \phi^\epsilon + (1 - \mathcal{M}_\epsilon)(\epsilon \mathbf{V}^1 + \epsilon^2 \mathbf{V}^2), \quad (5.88)$$

where

$$\phi^\epsilon = \mathbf{V}^\epsilon - (\mathbf{V}^0 + \epsilon \mathbf{V}^1 + \epsilon^2 \mathbf{V}^2). \quad (5.89)$$

Similarly, we make use of the error-function Ψ^ϵ

$$\Psi^\epsilon = \mathbf{U}^\epsilon - \mathbf{U}^0 - \mathcal{M}_\epsilon(\epsilon \mathbf{U}^1 + \epsilon^2 \mathbf{U}^2). \quad (5.90)$$

The goal is to estimate both Φ^ϵ and Ψ^ϵ uniformly in ϵ .

Even though our problem for $(\mathbf{U}^\epsilon, \mathbf{V}^\epsilon)$ is defined on Ω^ϵ , while the asymptotic expansion terms $(\mathbf{U}^i, \mathbf{V}^i)$ are defined on $\Omega \times Y^*$, we are still able to use spaces defined on Ω^ϵ such as \mathbb{V}_ϵ^N since the evaluation $\mathbf{y} = \mathbf{x}/\epsilon$ transfers the zero-extension on \mathcal{T} to \mathcal{T}^ϵ .

Introduce the coercive bilinear form $a_\epsilon : \mathbb{V}_\epsilon^N \times \mathbb{V}_\epsilon^N \rightarrow \mathbf{R}$ defined as

$$a_\epsilon(\psi, \phi) = \int_{\Omega^\epsilon} \phi^\top \mathcal{A}^\epsilon \psi d\mathbf{x} \quad (5.91)$$

pointwise in $t \in \mathbf{R}_+$, on which it depends implicitly.

By construction, Φ^ϵ vanishes on $\partial_{ext} \Omega^\epsilon$, which allows for the estimation of $\|\Phi^\epsilon\|_{\mathbb{V}_\epsilon^N}$. This estimation follows the standard approach, see [30] for the details.

First the inequality $|a_\epsilon(\Phi^\epsilon, \phi)| \leq \mathcal{C}(\epsilon, t) \|\phi\|_{\mathbb{V}_\epsilon^N}$, where $\mathcal{C}(\epsilon, t)$ is a constant depending on ϵ and $t \in \mathbf{R}_+$, is obtained for any $\phi \in \mathbb{V}_\epsilon^N$. Second, we take $\phi = \Phi^\epsilon$ and using the coercivity, one immediately obtains $\|\Phi^\epsilon\|_{\mathbb{V}_\epsilon^N}$.

Our pseudo-parabolic system complicates this approach. Instead of $\mathcal{C}(\epsilon, t)$, one gets $C\|\Psi^\epsilon\|_{H_0^1(\Omega^\epsilon)^N}$. Via an ordinary differential equation for Ψ^ϵ , we obtain a temporal inequality for $\|\Psi^\epsilon\|_{H_0^1(\Omega^\epsilon)^N}$ that contains $\|\Phi^\epsilon\|_{\mathbb{V}_\epsilon^N}$. The upper bound for $\|\Phi^\epsilon\|_{\mathbb{V}_\epsilon^N}$ now follows from applying Gronwall's inequality, leading to an upper bound for $\|\Psi^\epsilon\|_{H_0^1(\Omega^\epsilon)^N}$.

From equation (5.88), we have

$$a_\epsilon(\Phi^\epsilon, \phi) = a_\epsilon(\phi^\epsilon, \phi) + a_\epsilon((1 - \mathcal{M}_\epsilon)(\epsilon \mathbf{V}^1 + \epsilon^2 \mathbf{V}^2), \phi) \quad (5.92)$$

for $\phi \in \mathbb{V}_\epsilon^N$.

Do note that \mathcal{M}_ϵ vanishes in a neighbourhood of the boundary $\partial_{ext}\Omega^\epsilon$, see (5.77), because of which the second term in (5.92) vanishes outside this neighbourhood.

We start by estimating the first term of (5.92), $a_\epsilon(\phi^\epsilon, \phi)$. From the asymptotic expansion of \mathcal{A}^ϵ , we obtain

$$\begin{aligned} \mathcal{A}^\epsilon \phi^\epsilon &= (\epsilon^{-2} \mathcal{A}^0 + \epsilon^{-1} \mathcal{A}^1 + \mathcal{A}^2) \phi^\epsilon \\ &= \mathcal{A}^\epsilon \mathbf{V}^\epsilon - \epsilon^{-2} \mathcal{A}^0 \mathbf{V}^0 - \epsilon^{-1} (\mathcal{A}^0 \mathbf{V}^1 + \mathcal{A}^1 \mathbf{V}^0) - (\mathcal{A}^0 \mathbf{V}^2 + \mathcal{A}^1 \mathbf{V}^1 + \mathcal{A}^2 \mathbf{V}^0) \\ &\quad - \epsilon (\mathcal{A}^1 \mathbf{V}^2 + \mathcal{A}^2 \mathbf{V}^1) - \epsilon^2 \mathcal{A}^2 \mathbf{V}^2. \end{aligned} \quad (5.93)$$

Using the definitions of $\mathcal{A}^0, \mathcal{A}^1, \mathcal{A}^2, \mathbf{V}^0, \mathbf{V}^1, \mathbf{V}^2$, we have

$$\mathcal{A}^\epsilon \phi^\epsilon = \mathbf{K}^\epsilon \mathbf{U}^\epsilon - \mathbf{K}|_{\mathbf{y}=\mathbf{x}/\epsilon} \mathbf{U}^0 + \epsilon \mathbf{J}^\epsilon \nabla \mathbf{U}^\epsilon - \epsilon (\mathcal{A}^2 \mathbf{V}^1 + \mathcal{A}^1 \mathbf{V}^2) - \epsilon^2 \mathcal{A}^2 \mathbf{V}^2. \quad (5.94)$$

The function ϕ^ϵ satisfies the following boundary condition on $\partial\mathcal{T}^\epsilon$

$$\frac{\partial \phi^\epsilon}{\partial \nu_{\mathcal{D}^\epsilon}} = -\epsilon^2 \frac{\partial \mathbf{V}^2}{\partial \nu_{\mathcal{D}}}, \quad (5.95)$$

as a consequence of the boundary conditions for the \mathbf{V}^i -terms. Hence, ϕ^ϵ satisfies the following system:

$$\begin{cases} \mathcal{A}^\epsilon \phi^\epsilon = \mathbf{f}^\epsilon - \epsilon \mathbf{g}^\epsilon & \text{in } \Omega^\epsilon, \\ \frac{\partial \phi^\epsilon}{\partial \nu_{\mathcal{D}^\epsilon}} = \epsilon^2 \mathbf{h}^\epsilon \cdot \mathbf{n}^\epsilon & \text{on } \partial\mathcal{T}^\epsilon, \\ \phi^\epsilon = -\epsilon \mathbf{V}^1 - \epsilon^2 \mathbf{V}^2 & \text{on } \partial\Omega. \end{cases} \quad (5.96)$$

Testing with $\phi^\top \in \mathbb{V}_\epsilon^N$ and performing a partial integration, we obtain

$$a_\epsilon(\phi^\epsilon, \phi) = \int_{\Omega^\epsilon} \phi^\top \mathbf{f}^\epsilon \, d\mathbf{x} - \int_{\Omega^\epsilon} \epsilon \phi^\top \mathbf{g}^\epsilon \, d\mathbf{x} + \int_{\partial\mathcal{T}^\epsilon} \epsilon^2 \phi^\top \mathbf{h}^\epsilon \cdot \mathbf{n}^\epsilon \, d\mathbf{s}, \quad (5.97)$$

where \mathbf{f}^ϵ , \mathbf{g}^ϵ and \mathbf{h}^ϵ are given by

$$\mathbf{f}^\epsilon = \mathbf{K}^\epsilon \mathbf{U}^\epsilon - \mathbf{K}|_{\mathbf{y}=\mathbf{x}/\epsilon} \mathbf{U}^0 \quad (5.98)$$

$$\begin{aligned} \mathbf{g}^\epsilon = & \mathcal{A}^1 [\mathbf{P} + \mathbf{Q}^0 \mathbf{V}^0 + \mathbf{R}^0 \mathbf{U}^0 + \mathbf{Q}^1 \cdot \nabla_{\mathbf{x}} \mathbf{V}^0 + \mathbf{R}^1 \cdot \nabla_{\mathbf{x}} \mathbf{U}^0 + \mathbf{Q}^2 : \mathbf{D}_{\mathbf{x}}^2 \mathbf{V}^0] \\ & + \mathcal{A}^2 [\mathbf{W} \cdot \nabla_{\mathbf{x}} \mathbf{V}^0 + \mathbf{Z} \mathbf{V}^0] - \mathbf{J}^\epsilon \cdot \nabla_{\mathbf{x}} \mathbf{U}^\epsilon \\ & + \epsilon \mathcal{A}^2 [\mathbf{P} + \mathbf{Q}^0 \mathbf{V}^0 + \mathbf{R}^0 \mathbf{U}^0 + \mathbf{Q}^1 \cdot \nabla_{\mathbf{x}} \mathbf{V}^0 + \mathbf{R}^1 \cdot \nabla_{\mathbf{x}} \mathbf{U}^0 + \mathbf{Q}^2 : \mathbf{D}_{\mathbf{x}}^2 \mathbf{V}^0], \quad (5.99) \end{aligned}$$

$$\mathbf{h}^\epsilon = -\frac{\partial}{\partial \nu_{\mathcal{D}}} [\mathbf{P} + \mathbf{Q}^0 \mathbf{V}^0 + \mathbf{R}^0 \mathbf{U}^0 + \mathbf{Q}^1 \cdot \nabla_{\mathbf{x}} \mathbf{V}^0 + \mathbf{R}^1 \cdot \nabla_{\mathbf{x}} \mathbf{U}^0 + \mathbf{Q}^2 : \mathbf{D}_{\mathbf{x}}^2 \mathbf{V}^0]. \quad (5.100)$$

Estimates for \mathbf{f}^ϵ , \mathbf{g}^ϵ and \mathbf{h}^ϵ follow from estimates on \mathbf{V}^0 , \mathbf{U}^0 , \mathbf{P} , \mathbf{Q}^0 , \mathbf{R}^0 , \mathbf{Q}^1 , \mathbf{R}^1 , \mathbf{Q}^2 , and \mathbf{W} . Due to the regularity of $\bar{\mathbf{H}}$, $\bar{\mathbf{K}}$, \mathbf{J} , \mathbf{G} , classical regularity results for elliptic systems, see Theorem 8.12 and Theorem 8.13 in [61], guarantee that all spatial derivatives up to the fourth order of $(\mathbf{U}^0, \mathbf{V}^0)$ are in $L^\infty(\mathbf{R}_+ \times \Omega)$. Similarly, from Theorem 9.25 and Theorem 9.26 in [20], the cell-functions \mathbf{W} , \mathbf{P} , \mathbf{Q}^0 , \mathbf{R}^0 , \mathbf{Q}^1 , \mathbf{R}^1 and \mathbf{Q}^2 have higher regularity, than given by Lemma 5.12: $W_i, P_\alpha, Q_{\alpha\beta}^0, R_{\alpha\beta}^0, Q_{i\alpha\beta}^1, R_{\alpha\beta}^1, Q_{ij}^2$ are in $L^\infty(\mathbf{R}_+; W^{2,\infty}(\Omega; H_{\#}^3(Y^*)/\mathbf{R}))$. We denote with κ the time-independent bound

$$\kappa = \sup_{1 \leq \alpha, \beta \leq N} \|K_{\alpha\beta}\|_{L^\infty(\mathbf{R}_+; W^{1,\infty}(\Omega; C_{\#}^1(Y^*)))}. \quad (5.101)$$

Note that $\|\mathbf{R}^0\|_{L^\infty(\mathbf{R}_+ \times \Omega; C_{\#}^1(Y^*))}^{N \times N} \leq C\kappa$ by the Poincaré-Wirtinger inequality.

Bounding \mathbf{g}^ϵ follows now directly from equation (5.99) and Corollary 5.17:

$$\|g_\alpha^\epsilon\|_{L^2(\Omega^\epsilon)^N} \leq C(1 + \epsilon)(1 + (\kappa + \tilde{\kappa})e^{\lambda t}), \quad (5.102)$$

where C is independent of ϵ .

Bounding \mathbf{h}^ϵ is more difficult as it is defined on the boundary $\partial\mathcal{T}^\epsilon$. The following result, see Lemma 2.31 on page 47 in [30], gives a trace inequality, which shows that \mathbf{h}^ϵ is properly defined.

Lemma 5.18. *Let $\psi \in H^1(\Omega^\epsilon)$. Then*

$$\|\psi\|_{L^2(\partial\mathcal{T}^\epsilon)} \leq C\epsilon^{-1/2} \|\psi\|_{\mathbb{V}_\epsilon}, \quad (5.103)$$

where C is independent of ϵ .

By (5.100), the regularity of the cell-functions, the regularity of the normal at the boundary, Corollary 5.17 and using Lemma 5.18 twice, we have

$$\left| \int_{\partial\mathcal{T}^\epsilon} \epsilon^2 \boldsymbol{\phi}^\top \mathbf{h}^\epsilon \cdot \mathbf{n}^\epsilon ds(\mathbf{x}) \right| \leq C\epsilon(1 + (\kappa + \tilde{\kappa})e^{\lambda t}) \|\boldsymbol{\phi}\|_{\mathbb{V}_\epsilon^N}. \quad (5.104)$$

We estimate \mathbf{f}^ϵ in $L^2(\Omega^\epsilon)^N$ from the standard inequality $|a_1b_1 - a_2b_2| \leq |a_1 - a_2||b_2| + |a_1||b_1 - b_2|$ for all $a_1, a_2, b_1, b_2 \in \mathbf{R}$. This leads to

$$\begin{aligned} \|\mathbf{f}^\epsilon\|_{L^2(\Omega^\epsilon)^N} &\leq \|\mathbf{K}^\epsilon - \mathbf{K}\|_{L^2(\Omega^\epsilon)^{N \times N}} \|\mathbf{U}^\epsilon\|_{L^\infty(\Omega^\epsilon)^N} \\ &\quad + \|\mathbf{K}\|_{L^\infty(\Omega^\epsilon)^{N \times N}} \|\mathbf{U}^\epsilon - \mathbf{U}^0\|_{L^2(\Omega^\epsilon)^N}. \end{aligned} \quad (5.105)$$

With this inequality, the estimation depends on the convergence of \mathbf{K}^ϵ and \mathbf{U}^ϵ to \mathbf{K} and \mathbf{U}^0 , respectively, but with the notation according to (5.7) we have $\mathbf{K}^\epsilon - \mathbf{K}|_{\mathbf{y}=\mathbf{x}/\epsilon} = \mathbf{0}$ a.e.

From the definition of $\boldsymbol{\Psi}^\epsilon$, we obtain

$$\begin{aligned} \|\mathbf{U}^\epsilon - \mathbf{U}^0\|_{L^2(\Omega^\epsilon)^N} &= \|\boldsymbol{\Psi}^\epsilon + \mathcal{M}_\epsilon(\epsilon\mathbf{U}^1 + \epsilon^2\mathbf{U}^2)\|_{L^2(\Omega^\epsilon)^N} \\ &\leq \|\boldsymbol{\Psi}^\epsilon\|_{L^2(\Omega^\epsilon)^N} + \epsilon\|\mathbf{U}^1\|_{L^2(\Omega^\epsilon)^N} + \epsilon^2\|\mathbf{U}^2\|_{L^2(\Omega^\epsilon)^N}. \end{aligned} \quad (5.106)$$

Introduce the notations $l = L_N$ and $t_l = \min\{1/l, t\}$. Using system (5.56), the bounds $C(1 + (\kappa + \tilde{\kappa})e^{\lambda t})$ for $\|\mathbf{V}^1\|_{H^1(\Omega^\epsilon)^N}$ and $\|\mathbf{V}^2\|_{H^1(\Omega^\epsilon)^N}$ obtained via the cell-function decompositions (5.58) and (5.79), respectively, the inequalities (5.31a) and (5.31b), and by employing Gronwall's inequality, we obtain

$$\|\mathbf{U}^1\|_{H^1(\Omega^\epsilon)^N} \leq C(1 + (\kappa + \tilde{\kappa})e^{\lambda t}) \sqrt{t_l e^{lt} + t_l^2 e^{2lt}}, \quad (5.107a)$$

$$\|\mathbf{U}^2\|_{H^1(\Omega^\epsilon)^N} \leq C(1 + (\kappa + \tilde{\kappa})e^{\lambda t}) \sqrt{t_l e^{lt} + t_l^2 e^{2lt}}, \quad (5.107b)$$

$$\begin{aligned} \|\mathbf{U}^\epsilon - \mathbf{U}^0\|_{L^2(\Omega^\epsilon)^N} &\leq \|\boldsymbol{\Psi}^\epsilon\|_{L^2(\Omega^\epsilon)^N} \\ &\quad + C(\epsilon + \epsilon^2)(1 + (\kappa + \tilde{\kappa})e^{\lambda t}) \sqrt{t_l e^{lt} + t_l^2 e^{2lt}}. \end{aligned} \quad (5.107c)$$

Thus from identity (5.105) we obtain

$$\begin{aligned} \|\mathbf{f}^\epsilon\|_{L^2(\Omega^\epsilon)^N} &\leq \kappa \|\boldsymbol{\Psi}^\epsilon\|_{L^2(\Omega^\epsilon)^N} \\ &\quad + C(\epsilon + \epsilon^2)\kappa(1 + (\kappa + \tilde{\kappa})e^{\lambda t}) \sqrt{t_l e^{lt} + t_l^2 e^{2lt}}, \end{aligned} \quad (5.108)$$

We now have all the ingredients to estimate $a_\epsilon(\boldsymbol{\phi}^\epsilon, \boldsymbol{\phi})$. Inserting estimates (5.102), (5.104) and (5.108) into (5.97), we find

$$\begin{aligned} |a_\epsilon(\boldsymbol{\phi}^\epsilon, \boldsymbol{\phi})| &\leq [\kappa \|\boldsymbol{\Psi}^\epsilon\|_{L^2(\Omega^\epsilon)^N} \\ &\quad C(\epsilon + \epsilon^2)(1 + (\kappa + \tilde{\kappa})e^{\lambda t})(1 + \kappa(1 + t_l e^{lt}))] \|\boldsymbol{\phi}\|_{\mathbb{V}_\epsilon^N}. \end{aligned} \quad (5.109)$$

Next, we need to estimate the second right-hand term of (5.92), $a_\epsilon((1 - \mathcal{M}_\epsilon)(\epsilon \mathbf{V}^1 + \epsilon^2 \mathbf{V}^2), \phi)$. Trusting [30] (see pages 48 and 49 in the reference) and using the bounds $C(1 + (\kappa + \tilde{\kappa})e^{\lambda t})$ for $\|\mathbf{V}^1\|_{H^1(\Omega^\epsilon)^N}$ and $\|\mathbf{V}^2\|_{H^1(\Omega^\epsilon)^N}$, we obtain

$$\begin{aligned} & |a_\epsilon((1 - \mathcal{M}_\epsilon)(\epsilon \mathbf{V}^1 + \epsilon^2 \mathbf{V}^2), \phi)| \\ & \leq \left[C(\epsilon^{\frac{1}{2}} + \epsilon^{\frac{3}{2}}) + C(\epsilon + \epsilon^2) (1 + (\kappa + \tilde{\kappa})e^{\lambda t}) \right] \|\phi\|_{\mathbb{V}_\epsilon^N}. \end{aligned} \quad (5.110)$$

The combination of (5.109) and (5.110) yields

$$\begin{aligned} |a_\epsilon(\Phi^\epsilon, \phi)| & \leq \left[\kappa \|\Psi^\epsilon\|_{L^2(\Omega^\epsilon)^N} \right. \\ & \left. + C(\epsilon^{\frac{1}{2}} + \epsilon^{\frac{3}{2}}) \left(1 + \epsilon^{\frac{1}{2}} (1 + (\kappa + \tilde{\kappa})e^{\lambda t}) (1 + \kappa(1 + t_l e^{lt})) \right) \right] \|\phi\|_{\mathbb{V}_\epsilon^N}. \end{aligned} \quad (5.111)$$

Since $\mathcal{L}\Psi^\epsilon = \mathbf{G}\Phi^\epsilon$, we obtain an identity similar to (5.31a) to which we apply Gronwall's inequality, leading to

$$\|\Psi^\epsilon\|_{L^2(\Omega^\epsilon)^N}^2(t) \leq \int_0^t e^{l(t-s)} G_N \|\Phi^\epsilon\|_{L^2(\Omega^\epsilon)^N}^2(s) ds. \quad (5.112)$$

Choosing $\phi = \Phi^\epsilon$ and with m denoting the coercivity constant $\min_{1 \leq i \leq n, 1 \leq \alpha \leq N} \{\tilde{m}_\alpha, \tilde{e}_i\}$, we obtain

$$m \|\Phi^\epsilon\|_{\mathbb{V}_\epsilon^N}^2 \leq \left[\kappa \sqrt{\int_0^t e^{l(t-s)} G_N \|\Phi^\epsilon\|_{L^2(\Omega^\epsilon)^N}^2(s) ds} + \mathcal{B}(\epsilon, t) \right] \|\Phi^\epsilon\|_{\mathbb{V}_\epsilon^N}, \quad (5.113)$$

where

$$\mathcal{B}(\epsilon, t) = C(\epsilon^{\frac{1}{2}} + \epsilon^{\frac{3}{2}}) \left(1 + \epsilon^{\frac{1}{2}} (1 + (\kappa + \tilde{\kappa})e^{\lambda t}) (1 + \kappa(1 + t_l e^{lt})) \right). \quad (5.114)$$

Applying Young's inequality twice, once with $\eta > 0$ and once with $\eta_1 > 0$, using the Poincaré inequality (see Remark 5.1) and Gronwall's inequality to (5.113), we arrive at

$$\begin{aligned} \|\Phi^\epsilon\|_{\mathbb{V}_\epsilon^N}^2 & \leq \frac{\mathcal{B}(\epsilon, t)^2}{\eta_1(2m - \eta_1 - \eta)} \\ & + \int_0^t \frac{\kappa^2 G_N e^{l(t-s)} \mathcal{B}(\epsilon, s)^2}{\eta(2m - \eta_1 - \eta)^2 \eta_1} \exp \left(\int_s^t \frac{\kappa G_N}{\eta(2m - \eta_1 - \eta)} e^{l(t-u)} du \right) ds. \end{aligned} \quad (5.115)$$

Since $0 < \mathcal{B}(\epsilon, s) \leq \mathcal{B}(\epsilon, t)$ for $s \leq t$, we can use the Leibniz rule to obtain

$$\|\Phi^\epsilon\|_{\mathbb{V}_\epsilon^N}^2 \leq \frac{\mathcal{B}(\epsilon, t)^2}{\eta_1(2m - \eta_1 - \eta)} \exp \left(\frac{\kappa^2 G_N}{\eta(2m - \eta_1 - \eta)} t_l e^{lt} \right). \quad (5.116)$$

Minimizing the two fractions separately leads us to $\eta_1 = m - \frac{\eta}{2}$ and $\eta = m - \frac{\eta_1}{2}$, whence $\eta = \eta_1 = \frac{2}{3}m$. Hence, we obtain

$$\begin{aligned} \|\Phi^\epsilon\|_{\mathbb{V}_\epsilon^N} &\leq C(\epsilon^{\frac{1}{2}} + \epsilon^{\frac{3}{2}}) \left(1 + \epsilon^{\frac{1}{2}}(1 + (\kappa + \tilde{\kappa})e^{\lambda t})(1 + \kappa(1 + t_l e^{lt}))\right) \exp(\mu t_l e^{lt}), \\ &= \mathcal{C}(\epsilon, t) \end{aligned} \tag{5.117}$$

and from (5.112), we arrive at

$$\|\Psi^\epsilon\|_{H^1(\Omega^\epsilon)^N} \leq \mathcal{C}(\epsilon, t) \sqrt{t_l e^{lt}} \tag{5.118}$$

with

$$\mu = \frac{9\kappa^2 G_N}{8m^2}. \tag{5.119}$$

This completes the proof of Theorem 5.5.

5.6 Upscaling and convergence speeds for a concrete corrosion model

In [137] a concrete corrosion model has been derived from first principles. This model combines mixture theory with balance laws, while incorporating chemical reaction effects, mechanical deformations, incompressible flow, diffusion, and moving boundary effects. The model represents the onset of concrete corrosion by representing the corroded part as a layer of cement (the mixture) on top of a concrete bed and below an acidic fluid. The mixture contains three components $\phi = (\phi_1, \phi_2, \phi_3)$, which react chemically via $3 + 2 \rightarrow 1$. For simplification, we work in volume fractions. Hence, the identity $\phi_1 + \phi_2 + \phi_3 = 1$

holds. The model equations on a domain Ω become for $\alpha \in \{1, 2, 3\}$

$$\frac{\partial \phi_\alpha}{\partial t} + \epsilon \operatorname{div}(\phi_\alpha \mathbf{v}_\alpha) - \epsilon \delta_\alpha \Delta \phi_\alpha = \epsilon \kappa_\alpha F(\phi_1, \phi_3), \quad (5.120a)$$

$$\operatorname{div} \left(\sum_{\alpha=1}^3 \phi_\alpha \mathbf{v}_\alpha \right) - \sum_{\alpha=1}^3 \delta_\alpha \Delta \phi_\alpha = \sum_{\alpha=1}^3 \kappa_\alpha F(\phi_1, \phi_3), \quad (5.120b)$$

$$\nabla(-\phi_\alpha p + [\lambda_\alpha + \mu_\alpha] \operatorname{div}(\mathbf{u}_\alpha)) + \mu_\alpha \Delta \mathbf{u}_\alpha = \chi_\alpha (\mathbf{v}_\alpha - \mathbf{v}_3) - \sum_{\beta=1}^3 \gamma_{\alpha\beta} \Delta \mathbf{v}_\beta, \quad (5.120c)$$

$$\nabla \left(-p + \sum_{\alpha=1}^2 (\lambda_\alpha + \mu_\alpha) \operatorname{div}(\mathbf{u}_\alpha) \right) + \sum_{\alpha=1}^2 \mu_\alpha \Delta \mathbf{u}_\alpha + \sum_{\alpha=1}^3 \sum_{\beta=1}^3 \gamma_{\alpha\beta} \Delta \mathbf{v}_\beta = 0, \quad (5.120d)$$

where \mathbf{u}_α and $\mathbf{v}_\alpha = \partial \mathbf{u}_\alpha / \partial t$ are the displacement and velocity of component α , respectively, and ϵ is a small positive number independent of any spatial scale. Equation (5.120a) denotes a mass balance law, (5.120b) denotes the incompressibility condition, (5.120c) the partial (for component α) momentum balance law, and (5.120d) the total momentum balance.

For $t = \mathcal{O}(\epsilon^0)$, we can treat ϕ as constant, which removes some nonlinearities from the model. Moreover, with equation (5.120b) we can eliminate \mathbf{v}_3 in favor of \mathbf{v}_1 and \mathbf{v}_2 , while with equation (5.120d) we can eliminate p . This leads to a final expression for $\mathbf{u} = (\mathbf{u}_1, \mathbf{u}_2)$:

$$\tilde{\mathbf{M}} \partial_t \mathbf{u} - \tilde{\mathbf{A}} \mathbf{u} - \operatorname{div} \left(\tilde{\mathbf{B}} \mathbf{u} + \tilde{\mathbf{D}} \partial_t \mathbf{u} + \mathbf{E} \cdot \nabla \left(\mathbf{F} \mathbf{u} + \tilde{\mathbf{G}} \partial_t \mathbf{u} \right) \right) = \mathbf{H}, \quad (5.121)$$

with

$$\tilde{\mathbf{M}} = \begin{pmatrix} \chi_1 \frac{\phi_1 + \phi_3}{\phi_3} & \chi_1 \frac{\phi_2}{\phi_3} \\ \chi_2 \frac{\phi_1}{\phi_3} & \chi_2 \frac{\phi_2 + \phi_3}{\phi_3} \end{pmatrix}, \quad \tilde{\mathbf{A}} = \tilde{\mathbf{B}} = \tilde{\mathbf{D}} = 0, \quad (5.122a)$$

$$\mathbf{F} = \begin{pmatrix} \mu_1(\phi_2 + \phi_3) & -\mu_2 \phi_1 \\ -\mu_1 \phi_2 & \mu_2(\phi_1 + \phi_3) \end{pmatrix}, \quad \mathbf{E} = \mathbf{I}, \quad (5.122b)$$

$$\tilde{\mathbf{G}}_{\alpha\beta} = -\gamma_{\alpha\beta} + \phi_\alpha \sum_{\lambda=1}^3 \gamma_{\lambda\beta}, \quad H_\alpha = \frac{\chi_\alpha}{\phi_3} F(\phi_1, \phi_3) \sum_{\lambda=1}^3 \kappa_\lambda. \quad (5.122c)$$

According to [137], there are several options for $\gamma_{\alpha\beta}$, but all these options lead to non-invertible $\tilde{\mathbf{G}}$. Suppose we take $\gamma_{11} = \gamma_{22} = \gamma_1 < 0$ and $\gamma_{12} = \gamma_{21} =$

$\gamma_2 < 0$ with $\gamma_1 > \gamma_2$. Then $\tilde{\mathbf{G}}$ is invertible and positive definite for $\phi_3 > 0$, since the determinant of $\tilde{\mathbf{G}}$ equals $(\gamma_1^2 - \gamma_2^2)\phi_3$.

According to Section 4.3 of [136], we obtain the Neumann problem (5.8a), (5.8b) with

$$\mathbf{M} = \tilde{\mathbf{M}}\tilde{\mathbf{G}}^{-1}, \mathbf{D} = \mathbf{0}, \mathbf{L} = \tilde{\mathbf{G}}^{-1}\mathbf{F}, \mathbf{G} = \tilde{\mathbf{G}}^{-1}, \mathbf{K} = -\tilde{\mathbf{M}}\tilde{\mathbf{G}}^{-1}\mathbf{F}, \mathbf{J} = \mathbf{0}. \quad (5.123)$$

Note, that both \mathbf{E} and \mathbf{H} do not change in this transformation. Moreover, \mathbf{M} is positive definite, since both $\tilde{\mathbf{M}}$ and $\tilde{\mathbf{G}}$ are positive definite.

Suppose the cement mixture has a periodic microstructure, satisfying assumption (A4), inherited from the concrete microstructure if corroded. Assume the constants χ_α , μ_α , κ_α , and $\gamma_{\alpha\beta}$ are actually functions of both the macroscopic scale \mathbf{x} and the microscopic scale \mathbf{y} , such that Assumptions (A1)-(A3) are satisfied. Note that (A3) is trivially satisfied.

From the main results we see that a macroscale limit $(\mathbf{U}^0, \mathbf{V}^0)$ of this microscale corrosion problem exists, which satisfies system (\mathbf{P}_w^0) , and that the convergence speed is given by Theorem 5.5 with constants l , κ , λ and μ given by Section 5.7.

5.7 Appendix: Determining κ , $\tilde{\kappa}$ and exponents l , λ and μ .

In Theorem 5.5, the three constants l , λ and μ are introduced as exponents indicating the exponential growth in time of the corrector bounds. Moreover, there was also a constant κ that indicated whether additional exponential growth occurs or not. For brevity it was not stated how these constants depend on the given matrices and tensors. Here we will give an exact determination procedure of these constants.

The constant κ denotes the maximal operator norm of the tensor \mathbf{K} .

$$\kappa = \sup_{1 \leq \alpha, \beta \leq N} \|K_{\alpha\beta}\|_{L^\infty(\mathbf{R}_+; W^{1,\infty}(\Omega; C_\#^1(Y^*)))}. \quad (5.124)$$

The constants l , λ , $\tilde{\kappa}$ and μ were obtained via Young's inequality, which make them a coupled system via several additional positive constants: η , η_1 , η_2 , η_3 .

The obtained expressions are

$$l = \max\{0, L_N\}, \quad (5.125a)$$

$$\lambda = \frac{1}{2} \max\left\{0, L_N + \max\left\{L_G + G_M \max_{1 \leq \alpha \leq N} \tilde{K}_\alpha, G_M \max_{1 \leq \alpha \leq N} \max_{1 \leq i \leq d} \tilde{J}_{i\alpha}\right\}\right\}, \quad (5.125b)$$

$$\mu = \frac{9\kappa^2}{8m^2} G_N, \quad (5.125c)$$

$$\tilde{\kappa} = \max_{1 \leq \alpha \leq N, 1 \leq i \leq d} \{\tilde{K}_\alpha, \tilde{J}_{i\alpha}\} \quad (5.125d)$$

with the values

$$L_N = 2\mathcal{L}_{\min} + \eta G_{\max} + \eta_1 dN \mathcal{L}_G, \quad (5.126a)$$

$$L_G = 2\mathcal{L}_{\min} + \frac{dN}{\eta_1} \mathcal{L}_G + \eta_2 G_{\max} + \eta_3 dN G_G, \quad (5.126b)$$

$$G_N = \frac{1}{\eta} G_{\max} + \frac{dN}{\eta_3} G_G, \quad (5.126c)$$

$$G_G = \frac{1}{\eta_2} G_{\max}, \quad (5.126d)$$

$$G_M = \max_{1 \leq \alpha \leq N} \max_{1 \leq i \leq d} \left\{ \frac{G_N + G_G}{\tilde{m}_\alpha}, \frac{G_N}{\tilde{e}_i} \right\}, \quad (5.126e)$$

$$m = \min_{1 \leq \alpha \leq N} \min_{1 \leq i \leq d} \{\tilde{m}_\alpha, \tilde{e}_i\}, \quad (5.126f)$$

where we have the positive values

$$\tilde{m}_\alpha = m_\alpha - \eta_\alpha - \sum_{\beta=1}^N \left(\eta_{\alpha\beta} + \sum_{i=1}^d \left[\frac{\|D_{i\beta\alpha}\|_{L^\infty(\mathbf{R}_+ \times \Omega; C_\#(Y^*))}}{2\eta_{i\beta\alpha}} + \tilde{\eta}_{i\alpha\beta} \right] \right), \quad (5.127a)$$

$$\tilde{e}_i = e_i - \sum_{\alpha, \beta=1}^N \frac{\eta_{i\beta\alpha}}{2} \|D_{i\beta\alpha}\|_{L^\infty(\mathbf{R}_+ \times \Omega; C_\#(Y^*))}, \quad (5.127b)$$

$$\tilde{H} = \sum_{\alpha=1}^N \frac{1}{4\eta_\alpha} \|\mathbf{H}_\alpha\|_{L^\infty(\mathbf{R}_+ \times \Omega; C_\#(Y^*))}^2, \quad (5.127c)$$

$$\tilde{K}_\alpha = \sum_{\beta=1}^N \frac{1}{4\eta_{\beta\alpha}} \|K_{\beta\alpha}\|_{L^\infty(\mathbf{R}_+ \times \Omega; C_\#(Y^*))}^2, \quad (5.127d)$$

$$\tilde{J}_{i\alpha} = \sum_{\beta=1}^N \frac{\epsilon_0^2}{4\tilde{\eta}_{i\beta\alpha}} \|J_{i\beta\alpha}\|_{L^\infty(\mathbf{R}_+ \times \Omega; C_\#(Y^*))}^2 \quad (5.127e)$$

for $\eta_{i\beta\alpha} > 0$, $\eta_\beta > 0$, $\eta_{\alpha\beta} > 0$, $\tilde{\eta}_{i\alpha\beta} > 0$ and ϵ_0 the supremum of allowed ϵ values (which is 1 for Theorem 5.7). Moreover, we have

- \mathcal{L}_{\min} as the $L^\infty(\mathbf{R}_+ \times \Omega)$ -norm of the absolute value of the largest negative eigenvalue or it is -1 times the smallest positive eigenvalue of L if no negative or 0 eigenvalues exist,
- \mathcal{L}_G as the $L^\infty(\mathbf{R}_+ \times \Omega)$ -norm of the largest absolute value of the ∇L components,
- G_{\max} as the $L^\infty(\mathbf{R}_+ \times \Omega)$ -norm of the largest eigenvalue of G ,
- G_G as the $L^\infty(\mathbf{R}_+ \times \Omega)$ -norm of the largest absolute value of the ∇G components.

Remark 5.11. *Remark that smaller l and μ yield longer times τ in Theorem 5.7 and faster convergence rates in ϵ . However, l and μ are only coupled via λ . Hence, l and μ can be made as small as needed as long as λ remains finite and independent of ϵ .*

Remark 5.12. *Note that $\mathcal{L}_{\min} < 0$ allows for a hyperplane of positive values of η and η_1 in $(\eta, \eta_1, \eta_2, \eta_3)$ -space such that $l = L_N = 0$. In this case not λ or μ should be minimized. Instead τ_{end} should be maximized, the time τ for which the bounds of Theorem 5.7 equal $\mathcal{O}(1)$ for $p = q = 0$. For $\mu \geq \lambda$ this yields a minimization of μ , while for $\mu < \lambda$ a minimization of $\mu + \lambda$. Due to the use of maximums in the definition of λ and τ_{end} , we refrain from maximizing τ_{end} as any attempt leads to a large tree of cases for which an optimization problem has to be solved.*

**Upscaling Non-linear
Pseudoparabolic-like Systems on
Vanishing Thin Multidomains**

Blanchard and Gaudiello [12] showed the convergence of a nonlinear elliptic system on a bed-of-nails-like domain. This domain is characterized by a “forest” of cylinders of thickness ϵ and periodicity of size $\mathcal{O}(\epsilon)$ on a substrate of thickness h_ϵ that vanishes as $\epsilon \downarrow 0$. In this chapter, the Blanchard-Gaudiello system is extended by adding a nonlinear ordinary differential equation in time and by adding nonlinear couplings between the two equations. The convergence as $\epsilon \downarrow 0$ is shown for the extended system on the same bed-of-nails-like domain. Additionally, several convergence rates for this extended system are related to the convergence speed of h_ϵ and the ϵ -dependence of known data.

6.1 Introduction

Upscaling is heavily dependent on the size of the scale length and of their separation when considering microstructures scale and macro domains. One field where such a scale separation is physically almost at its maximum is in semiconductors production. The electronic components are close to the nanometer level, while the finished product is still centimeter sized. This yields a scale separation of $\epsilon \sim 10^{-6}$. Disregarding the effects of quantum mechanics, which in principle becomes noticeable at the nanometer level, we focus on a specific subfield of semiconductor industry: the production of photo-voltaic cells as they are used in harvesting solar energy [63]. The everlasting race for higher efficiency has relatively recently created novel domain topologies. One of these topologies are best characterized as a “forest” of periodically spaced narrow columns with respect to their height placed on a thin substrate [7]. The aspect ratio of these columns (height over width) is dependent on the duration of the etching process. More etching yields longer columns with the same width [7]. Moreover, the substrate becomes smaller, as the columns are etched out of the substrate. See Figure 6.1 for electron microscopy images of an actual photo-voltaic cell with this nanostructure.

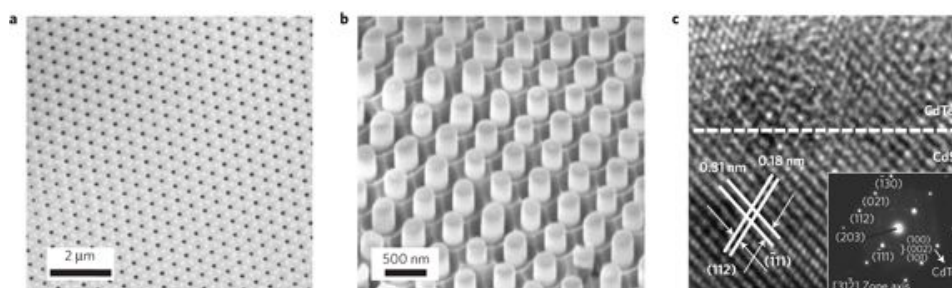


Figure 6.1: An example of a “forest” of periodically spaced columns on a substrate at a nanometer level. [51] ©Nature Materials

On this domain of silicon, shown in Figure 6.1, light is adsorbed and transformed into a different energy type, which creates heat as a byproduct. The distribution and flow of heat throughout this domain is described by the heat conduction equation. We have chosen to use a generalized version of this process by taking a system similar to the decomposed pseudo-parabolic system of Chapter 5, which is an elliptic spatial partial differential equation and a temporal ordinary differential equation, and generalizing it further by allowing for non-linear operators. In this way our system encompasses the (non-linear) heat diffusion systems, but also allows for drift effects.

In Chapter 5 the target porous domain was perforated, while this silicon domain consists of just the “perforations”, which are glued by a connected non-perforated substrate. As the substrate is rather thin, we expect difficulties to appear in transporting heat from one column to the other. Our expectation is, therefore, that the macroscopic system will be dominated by the direction in which the columns are pointing and that the transversal transmission coefficients will be rather small. This expected result is in some respect incorporated by the macroscopic system shown as one of the main results in Section 6.3.

These main results, reported in Sections 6.4, 6.5, and 6.6, extend the results of [11] and [12], which treat the same microscopic geometry, to our model equations. Furthermore, we obtain several corrector estimates for this problem. In [5] corrector estimates are obtained for a similar system, but without a vanishing substrate. Moreover, in [13] our system is again treated but with the focus on a different vanishing speed for the substrate. Twice more, the system has been treated by Gaudiello: in [60] the focus was on a high-contrast version of the diffusion operator in the vanishing cylinders, while in [59] the focus was on different regularity for the data with focus on entropy-like a-priori bounds. Hence, corrector estimates for the system with a vanishing substrate was still a missing element in the work of Gaudiello. In this chapter, we try to fill this knowledge gap.

Related work concerning homogenization of coupled systems of partial differential equations posed in $W^{1,p}(\Omega)$ has been done by H. Matano and M. Böhm, see [87], [88]. Similar work regarding homogenization of pseudo-parabolic systems in a monotone operator setting has been reported in [135], but without the vanishing domain components and without the corrector estimates.

The remaining part of this chapter has five sections: a preliminary section for introducing basic notions, a main results section, a well-posedness section, an upscaling section, and a convergence speed section.

The mathematical description of the domain consisting of a “forest” of columns on a thin substrate together with a description of the system on this domain and the associated assumptions are found in Section 6.2. The major results discussed in the different sections are summarized in Section 6.3. Using the theory of monotone operators, we show in Section 6.8 the existence and uniqueness of a solution to our system. We upscale directly within the monotone operator framework with a minor help of identifying limit functions via two-scale convergence. This is in contrast to Chapter 5, where either two-scale asymptotic expansions or two-scale convergence are the main upscaling techniques. We present convergence bounds to the upscaled solution in Section 6.5. We end with a drift term extension of our problem in the Hilbert space setting in Section 6.6.

For a detailed account of techniques on homogenization methods, we refer the reader to the classical monographs of e.g. [29], [85].

6.2 Preliminaries

Domain

Let $(0, T)$, with $T > 0$, be a time-interval and $\omega \subset \mathbf{R}^{d-1}$ for $d \in \mathbf{N}$ with $d \geq 2$ a simply connected bounded domain with a C^2 -boundary $\partial\omega$. Take $Y \subset \mathbf{R}^{d-1}$ a simply connected bounded domain, such that there exists a diffeomorphism $\gamma : \mathbf{R}^{d-1} \rightarrow \mathbf{R}^{d-1}$ such that $\text{Int}(\gamma([0, 1]^{d-1})) = Y$. Introduce $\mathcal{B} \subset Y$, a $(d - 1)$ -dimensional ball such that $\partial\mathcal{B} \cap \partial Y = \emptyset$.

We tile \mathbf{R}^{d-1} periodically with Y -tiles: Let G_0 be a lattice¹ of the translation group \mathcal{T}_{d-1} on \mathbf{R}^{d-1} such that $[0, 1]^{d-1} = \mathcal{T}_{d-1}/G_0$. Hence, we have the following properties: $\bigcup_{g \in G_0} g([0, 1]^{d-1}) = \mathbf{R}^{d-1}$ and $(0, 1)^d \cap g((0, 1)^{d-1}) = \emptyset$ for all $g \in G_0$ different than the identity-mapping. Moreover, we demand that the diffeomorphism γ allows the representation $G_\gamma := \gamma \circ G_0 \circ \gamma^{-1}$ to be a discrete subgroup of \mathcal{T}_{d-1} with $\bar{Y} = \mathcal{T}_{d-1}/G_\gamma$.

After introducing a Y -tiling of \mathbf{R}^{d-1} , we rescale the tiling to a periodicity of size ϵ : Take a sequence $(\epsilon) \subset (0, \epsilon_0)$ such that $\epsilon \rightarrow 0$ and assume that for all $\epsilon \in (0, \epsilon_0)$ there is a set $G_\gamma^\epsilon = \{\epsilon g \mid g \in G_\gamma\}$. Hence, we can define $\omega_\epsilon = \bigcup_{g \in G_\gamma^\epsilon} \{g(\mathcal{B}) \mid g(\bar{\mathcal{B}}) \subset \bar{\omega}\}$, the set of $(d - 1)$ -dimensional “balls” (shifted \mathcal{B} of size ϵ) fully inside ω with centers mapped onto each other by elements of G_γ^ϵ .

¹A lattice of a locally compact group \mathbb{G} is a discrete subgroup \mathbb{H} with the property that the quotient space \mathbb{G}/\mathbb{H} has a finite invariant (under \mathbb{G}) measure. A discrete subgroup \mathbb{H} of \mathbb{G} is a group $\mathbb{H} \subseteq \mathbb{G}$ under group operations of \mathbb{G} such that there is (an open cover) a collection \mathbb{C} of open sets $C \subseteq \mathbb{G}$ satisfying $\mathbb{H} \subset \bigcup_{C \in \mathbb{C}} C$ and for all $C \in \mathbb{C}$ there is a unique element $h \in \mathbb{H}$ such that $h \in C$.

Relying on ω_ϵ , we create a “forest” of periodically spaced cylinders with base shape \mathcal{B} and place this “forest” onto a thin substrate: Introduce the domains $\Omega_\epsilon^+ = \omega_\epsilon \times (0, l_d)$ for $l_d \in \mathbf{R}_+$, $\Omega_\epsilon^- = \omega \times (-h_\epsilon, 0)$ for a sequence of positive values $h_\epsilon \in (0, 1)$ satisfying $h_\epsilon \downarrow 0$ as $\epsilon \downarrow 0$, and hence, $\Omega_\epsilon = \text{int}(\overline{\Omega_\epsilon^- \cup \Omega_\epsilon^+})$.

See Figure 6.2 for a schematic representation of the sets Ω_ϵ^+ and Ω_ϵ^- .

Moreover, we introduce the domains $\Omega^+ = \omega \times (0, l_d)$, $\Omega^- = \omega \times (-1, 0)$ and $\Omega = \text{int}(\overline{\Omega^- \cup \Omega^+})$. Hence, Ω^+ is the smallest block containing Ω_ϵ^+ for all $\epsilon > 0$. Hence, $\Omega_\epsilon^+ \subset \Omega^+$ and $\Omega_\epsilon^- \subset \Omega^-$ for all $\epsilon \in (0, \epsilon_0)$.

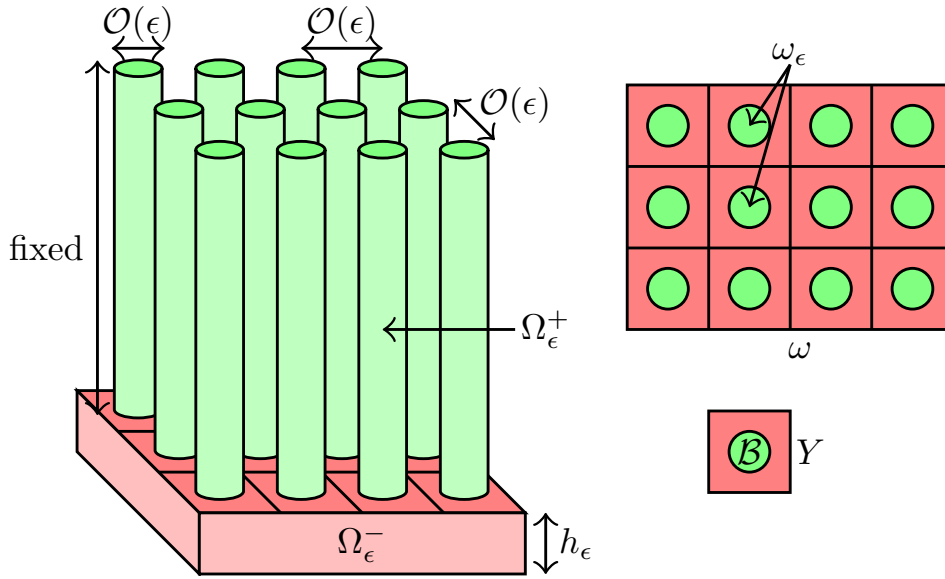


Figure 6.2: Schematic representation of the ϵ -dependent domain Ω_ϵ . Left: Side view of Ω_ϵ , which shows Ω_ϵ^+ as a collection of green $\mathcal{O}(\epsilon)$ -thick, $\mathcal{O}(\epsilon)$ -spaced “forest” of columns and Ω_ϵ^- as a red h_ϵ -thick substrate. Right: Top view of Ω_ϵ , which shows ω as the red domain on which the “forest” of green columns with base shape ω_ϵ is located. In general, ω is an arbitrary domain with smooth boundary $\partial\omega$ and not the rectangle as depicted here. The domain ω is depicted here as being completely tiled with Y -tiles, each containing \mathcal{B} -balls.

Setting of the model equations and assumptions

We are interested in the asymptotic behaviour, $\epsilon \downarrow 0$, of the weak solutions to the following Neumann problem: Find (U_ϵ, V_ϵ) satisfying

$$\begin{cases} \mathcal{M}(V_\epsilon) - \text{div}(\mathcal{E}(\nabla V_\epsilon)) = F_\epsilon + \mathcal{K}(U_\epsilon) & \text{in } \Omega_\epsilon \times (0, T), \\ \frac{\partial U_\epsilon}{\partial t} + \mathcal{L}(U_\epsilon) = \mathcal{G}(V_\epsilon) & \text{in } \Omega_\epsilon \times (0, T), \\ \mathcal{E}(\nabla V_\epsilon) \cdot \mathbf{n}_\epsilon = 0 & \text{on } \partial\Omega_\epsilon \times (0, T), \\ U_\epsilon = U^* & \text{in } \overline{\Omega_\epsilon} \times \{0\}, \end{cases} \quad (6.1)$$

where \mathbf{n}_ϵ denotes the exterior unit normal on $\partial\Omega_\epsilon$. This choice of microscopic system is motivated by our previous work on modeling, analysis, simulation and upscaling of reactive flow through deformable chemically-active porous media, see [136] and [137].

Fix $p \geq 2$ and take $q = \frac{p}{p-1}$, such that $\frac{1}{p} + \frac{1}{q} = 1$. We assume the following properties:

(A1) $\mathcal{E} = (\mathcal{E}_1, \dots, \mathcal{E}_d) : \mathbf{R}^d \rightarrow \mathbf{R}^d$ and $\mathcal{M} : \mathbf{R} \rightarrow \mathbf{R}$ are monotone continuous functions satisfying the following growth conditions:

$$\exists e_i \in \mathbf{R}_+ : e_i |\boldsymbol{\xi}|^p \leq \mathcal{E}(\boldsymbol{\xi}) \boldsymbol{\xi} \quad \text{for all } \boldsymbol{\xi} \in \mathbf{R}^d, \quad (6.2a)$$

$$\exists m_i \in \mathbf{R}_+ : m_i |\zeta|^p \leq \mathcal{M}(\zeta) \zeta \quad \text{for all } \zeta \in \mathbf{R}, \quad (6.2b)$$

$$\exists e_s \in \mathbf{R}_+ : |\mathcal{E}(\boldsymbol{\xi})| \leq e_s |\boldsymbol{\xi}|^{p-1} \quad \text{for all } \boldsymbol{\xi} \in \mathbf{R}^d, \quad (6.2c)$$

$$\exists m_s \in \mathbf{R}_+ : |\mathcal{M}(\zeta)| \leq m_s |\zeta|^{p-1} \quad \text{for all } \zeta \in \mathbf{R}. \quad (6.2d)$$

(A2) The mappings $\mathcal{K} : \mathbf{R} \rightarrow \mathbf{R}$, $\mathcal{L} : \mathbf{R} \rightarrow \mathbf{R}$, $\mathcal{G} : \mathbf{R} \rightarrow \mathbf{R}$ are bounded and continuous.

(A3) For given $F_\epsilon \in L^q(\Omega_\epsilon)$, there exists $F \in L^q(\Omega^+)$ such that $F_\epsilon \rightarrow F$ strongly in $L^q(\Omega^+)$ as $\epsilon \rightarrow 0$.

(A4) $\exists c \in \mathbf{R}_+$ independent of ϵ such that $\|F_\epsilon(\mathbf{x}', h_\epsilon x_d)\|_{L^q(\Omega^-)} \leq c$ for all ϵ , where we used the decomposition $\mathbf{x} = (x_1, \dots, x_d) = (\mathbf{x}', x_d) \in \mathbf{R}^d$.

(A5) $\lim_{\epsilon \downarrow 0} \frac{\epsilon^p}{h_\epsilon} = 0$, which can also be written as $\epsilon^p = o(h_\epsilon)$.

(A6) \mathcal{E} and \mathcal{M} are strictly monotone.

(A7) \mathcal{L} , \mathcal{G} , and \mathcal{K} are monotone, continuous functions on $L^p(\Omega)$ satisfying

$$\exists l_i \in \mathbf{R}_+ : l_i \|\zeta\|^p \leq \mathcal{L}(\zeta) \zeta \quad \text{for all } \zeta \in \mathbf{R}, \quad (6.3a)$$

$$\exists l_s \in \mathbf{R}_+ : |\mathcal{L}(\zeta)| \leq l_s |\zeta|^{p-1} \quad \text{for all } \zeta \in \mathbf{R}, \quad (6.3b)$$

$$\exists g_s \in \mathbf{R}_+ : |\mathcal{G}(\zeta)| \leq g_s |\zeta|^{p-1} \quad \text{for all } \zeta \in \mathbf{R}, \quad (6.3c)$$

$$\exists k_s \in \mathbf{R}_+ : |\mathcal{K}(\zeta)| \leq k_s |\zeta|^{p-1} \quad \text{for all } \zeta \in \mathbf{R}. \quad (6.3d)$$

(A8) $U^* \in L^2(\Omega)$.

(A9) For $p \geq 2$, the functions \mathcal{E} , \mathcal{M} , \mathcal{L} have positive constants E , M , L respectively, such that they satisfy

$$(\mathcal{E}(\boldsymbol{\xi}_1) - \mathcal{E}(\boldsymbol{\xi}_2))(\boldsymbol{\xi}_1 - \boldsymbol{\xi}_2) \geq E |\boldsymbol{\xi}_1 - \boldsymbol{\xi}_2|^p \quad \text{for all } \boldsymbol{\xi}_1, \boldsymbol{\xi}_2 \in \mathbf{R}^d, \quad (6.4a)$$

$$(\mathcal{M}(\zeta_1) - \mathcal{M}(\zeta_2))(\zeta_1 - \zeta_2) \geq M |\zeta_1 - \zeta_2|^p \quad \text{for all } \zeta_1, \zeta_2 \in \mathbf{R}, \quad (6.4b)$$

$$(\mathcal{L}(\zeta_1) - \mathcal{L}(\zeta_2))(\zeta_1 - \zeta_2) \geq L |\zeta_1 - \zeta_2|^p \quad \text{for all } \zeta_1, \zeta_2 \in \mathbf{R}. \quad (6.4c)$$

Note, assumption (A9) implies assumption (A6).

(A10) The operators \mathcal{G} and \mathcal{K} satisfy for $p \in (1, 2)$ a $(p-1)$ -Hölder condition

$$\exists G \in \mathbf{R}_+ : |\mathcal{G}(\zeta_1) - \mathcal{G}(\zeta_2)| \leq G|\zeta_1 - \zeta_2|^{p-1} \text{ for all } \zeta_1, \zeta_2 \in \mathbf{R}, \quad (6.5a)$$

$$\exists K \in \mathbf{R}_+ : |\mathcal{K}(\zeta_1) - \mathcal{K}(\zeta_2)| \leq K|\zeta_1 - \zeta_2|^{p-1} \text{ for all } \zeta_1, \zeta_2 \in \mathbf{R}, \quad (6.5b)$$

and for $p \geq 2$ a Lipschitz condition

$$\exists G \in \mathbf{R}_+ : |\mathcal{G}(\zeta_1) - \mathcal{G}(\zeta_2)| \leq G|\zeta_1 - \zeta_2| \text{ for all } \zeta_1, \zeta_2 \in \mathbf{R}, \quad (6.6a)$$

$$\exists K \in \mathbf{R}_+ : |\mathcal{K}(\zeta_1) - \mathcal{K}(\zeta_2)| \leq K|\zeta_1 - \zeta_2| \text{ for all } \zeta_1, \zeta_2 \in \mathbf{R}. \quad (6.6b)$$

Moreover, if (A9) holds, then we also have the bound

$$\frac{GK}{L} < \beta_i = \min \{M, E\}. \quad (6.7)$$

Rescaled behaviour

What concerns the asymptotic behaviour as $\epsilon \downarrow 0$, it is natural to rescale the plate Ω_ϵ^- by linearly mapping Ω^- bijectively onto Ω_ϵ^- , i.e. $x_d \mapsto h_\epsilon x_d$ for $\mathbf{x} = (\mathbf{x}', x_d) \in \Omega^-$. We adapt to our setting here the working ideas from [11] and [12]. The next object introduces a new gradient on $\Omega_\epsilon^+ \cup \Omega^-$:

$$\nabla = \begin{cases} D_{\mathbf{x}} & \text{for } \mathbf{x} \in \Omega_\epsilon^+, \\ \left(\frac{\partial}{\partial x_1}, \dots, \frac{\partial}{\partial x_{d-1}}, \frac{1}{h_\epsilon} \frac{\partial}{\partial x_d} \right) = \left(D_{\mathbf{x}'}, \frac{1}{h_\epsilon} \frac{\partial}{\partial x_d} \right) & \text{for } \mathbf{x} \in \Omega^-. \end{cases} \quad (6.8)$$

In a similar manner as in 6.8, we redefine the unknowns U_ϵ and V_ϵ as well as the functions F_ϵ , U^* , viz.

$$u_\epsilon(\mathbf{x}) := \begin{cases} U_\epsilon(\mathbf{x}) & \text{for } \mathbf{x} \in \Omega_\epsilon^+, \\ U_\epsilon(\mathbf{x}', h_\epsilon x_d) & \text{for } \mathbf{x} \in \Omega^-, \end{cases} \quad (6.9a)$$

$$v_\epsilon(\mathbf{x}) := \begin{cases} V_\epsilon(\mathbf{x}) & \text{for } \mathbf{x} \in \Omega_\epsilon^+, \\ V_\epsilon(\mathbf{x}', h_\epsilon x_d) & \text{for } \mathbf{x} \in \Omega^-, \end{cases} \quad (6.9b)$$

$$f_\epsilon(\mathbf{x}) := \begin{cases} F_\epsilon(\mathbf{x}) & \text{for } \mathbf{x} \in \Omega_\epsilon^+, \\ F_\epsilon(\mathbf{x}', h_\epsilon x_d) & \text{for } \mathbf{x} \in \Omega^-, \end{cases} \quad (6.9c)$$

$$u_\epsilon^*(\mathbf{x}) := \begin{cases} U^*(\mathbf{x}) & \text{for } \mathbf{x} \in \Omega_\epsilon^+, \\ U^*(\mathbf{x}', h_\epsilon x_d) & \text{for } \mathbf{x} \in \Omega^-. \end{cases} \quad (6.9d)$$

Definition 6.1. *The pair $(u_\epsilon, v_\epsilon) \in L^p((0, T) \times \Omega_\epsilon^+ \cup \Omega^-) \cap H^1(0, T; L^2(\Omega_\epsilon^+ \cup \Omega^-)) \times L^p(0, T; W^{1,p}(\Omega_\epsilon^+ \cup \Omega^-))$ given by (6.9a) and (6.9b) is a weak solution of (6.1) if the following identities*

$$\left\{ \begin{array}{l} \int_{\Omega_\epsilon^+} \mathcal{M}(v_\epsilon)\phi + \mathcal{E}(Dv_\epsilon) \cdot D\phi d\mathbf{x} \\ + h_\epsilon \int_{\Omega^-} \mathcal{M}(v_\epsilon)\phi + \mathcal{E} \left(D_{\mathbf{x}'}v_\epsilon, \frac{1}{h_\epsilon} \frac{\partial v_\epsilon}{\partial x_d} \right) \cdot \left(D_{\mathbf{x}'}\phi, \frac{1}{h_\epsilon} \frac{\partial \phi}{\partial x_d} \right) d\mathbf{x} \\ = \int_{\Omega_\epsilon^+} (f_\epsilon + \mathcal{K}(u_\epsilon)) \phi d\mathbf{x} + h_\epsilon \int_{\Omega^-} (f_\epsilon + \mathcal{K}(u_\epsilon)) \phi d\mathbf{x} \quad \text{for a.e. } t \in (0, T), \\ \int_{\Omega_\epsilon^+} \left(\frac{\partial u_\epsilon}{\partial t} + \mathcal{L}(u_\epsilon) \right) \psi d\mathbf{x} + h_\epsilon \int_{\Omega^-} \left(\frac{\partial u_\epsilon}{\partial t} + \mathcal{L}(u_\epsilon) \right) \psi d\mathbf{x} \\ = \int_{\Omega_\epsilon^+} \mathcal{G}(v_\epsilon)\psi d\mathbf{x} + h_\epsilon \int_{\Omega^-} \mathcal{G}(v_\epsilon)\psi d\mathbf{x} \quad \text{for a.e. } t \in (0, T), \end{array} \right. \quad (6.10)$$

hold for all $\phi \in W^{1,p}(\Omega_\epsilon^+ \cup \Omega^-)$ and $\psi \in L^p(\Omega_\epsilon^+ \cup \Omega^-)$ while satisfying the boundary condition

$$\mathcal{E}(Dv_\epsilon) \cdot \mathbf{n} = 0 \quad \text{on } \partial(\Omega_\epsilon^+ \cup \Omega^-) \text{ for a.e. } t \in (0, T), \quad (6.11)$$

and initial condition

$$u_\epsilon = u_\epsilon^* \quad \text{on } \overline{\Omega_\epsilon^+ \cup \Omega^-} \text{ for } t = 0. \quad (6.12)$$

6.3 Main results

In this section, we present our main results concerning problem (6.1). The proofs of these results are the subject of the next sections.

Our main results are subdivided into three categories: well-posedness, upscaling, and convergence bounds. First, the existence and uniqueness of a solution pair in the sense of Definition 6.1 to system (6.1) is shown.

Theorem 6.2 (Well-posedness). *Assume (A1), (A2), (A7)-(A10). Let $U^* \in L^2(\Omega)$. Then there exists a unique solution pair $U_\epsilon \in L^p((0, T) \times \Omega_\epsilon) \cap H^1(0, T; L^2(\Omega_\epsilon))$ and $V_\epsilon \in L^p(0, T; W^{1,p}(\Omega_\epsilon))$ satisfying*

$$\left\{ \begin{array}{l} \int_{\Omega_\epsilon} \left(\frac{dU_\epsilon}{dt} + \mathcal{L}(U_\epsilon) \right) \psi d\mathbf{x} = \int_{\Omega_\epsilon} \mathcal{G}(V_\epsilon)\psi d\mathbf{x} \quad \text{in } \Omega_\epsilon \times (0, T), \\ U_\epsilon = U^* \quad \text{on } \overline{\Omega_\epsilon} \times \{0\}. \end{array} \right. \quad (6.13)$$

for all $\psi \in L^q((0, T) \times \Omega_\epsilon)$, and

$$\begin{cases} \langle \phi, \mathcal{T}V_\epsilon \rangle = \int_{\Omega_\epsilon^+} (F_\epsilon + \mathcal{K}(U_\epsilon)) \phi d\mathbf{x} & \text{in } \Omega_\epsilon \times (0, T), \\ \mathcal{E}(\nabla V_\epsilon) \cdot \mathbf{n} = 0 & \text{on } \partial\Omega_\epsilon \times (0, T) \end{cases} \quad (6.14)$$

for all $\phi \in L^p(0, T; W^{1,p}(\Omega_\epsilon))$, where

$$\langle \phi, \mathcal{T}V_\epsilon \rangle = \int_{\Omega_\epsilon^+} \mathcal{E}(\nabla V_\epsilon) \cdot \nabla \phi + \mathcal{M}(V_\epsilon) \phi d\mathbf{x}. \quad (6.15)$$

Proof. The existence of solutions in the sense of Definition 6.1 follow by standard results on monotone evolution equations [58], [85], [127]. Alternatively, due to the strong similarity of our problem setting with diffusion scenarios in partially fissured media, the working methodology from [15] is also applicable in our case. The uniqueness of solutions as well as the structural stability of the solution with respect to model parameters follows by standard arguments. \square

Theorem 6.25 follows by standard results, which have already been applied to similar pseudo-parabolic equations with more complicated non-linear behaviour such as hysteresis in porous media models with dynamic capillary, see [36], [38], [78], [82], [124]. One way to approximate the weak solution (U_ϵ, V_ϵ) is to use a linear decoupled scheme as stated in Theorem 6.25 in Section 6.8. This procedure works fine for $p \geq 2$ and it is similar to the procedure used in [37].

Accepting the well-posedness of system (6.1), we now seek the limit system for $\epsilon \downarrow 0$, i.e. we perform our upscaling/homogenization procedure.

Theorem 6.3 (Upscaling). *Assume (A1)-(A10), let $U^* \in L^2(\Omega)$, and let $B_Y = \frac{|B|}{|Y|}$. Let (u_ϵ, v_ϵ) be the unique solution pair of system (6.10), then there*

exists a unique solution triple (u, v, \mathbf{d}') of

$$\left\{ \begin{array}{ll} \mathcal{M}(v) - \frac{\partial}{\partial x_d} \left(\mathcal{E}_d \left(\frac{\mathbf{d}'}{B_Y}, \frac{\partial v}{\partial x_d} \right) \right) = f + \mathcal{K}(u) & \text{in } \Omega^+ \times (0, T), \\ \frac{\partial u}{\partial t} + \mathcal{L}(u) = \mathcal{G}(v) & \text{in } \Omega^+ \times [0, T], \\ \mathcal{E}_i \left(\frac{\mathbf{d}'}{B_Y}, \frac{\partial v}{\partial x_d} \right) = 0 & \text{in } \overline{\Omega^+} \times (0, T), \text{ for } i \neq d, \\ \mathcal{E}_d \left(\frac{\mathbf{d}'}{B_Y}, \frac{\partial v}{\partial x_d} \right) = 0 & \text{on } \omega \times \{0, 1\} \times (0, T), \\ u = U^* & \text{in } \Omega^+ \times \{0\} \end{array} \right. \quad (6.16)$$

such that

$\chi_{\Omega_\epsilon^+} u_\epsilon \rightharpoonup B_Y u$ in $H^1(0, T; L^2(\Omega^+))$, $\chi_{\Omega_\epsilon^+} v_\epsilon \rightharpoonup B_Y v$ in $L^p(0, T; \mathbb{V}^p(\Omega^+))$,
 $\chi_{\Omega_\epsilon^+} D_{\mathbf{x}'} v_\epsilon \rightharpoonup \mathbf{d}'$ in $L^p((0, T) \times \Omega^+)^{d-1}$, $\chi_{\Omega_\epsilon^+} u_\epsilon \rightarrow B_Y u$ in $L^p((0, T) \times \Omega^+)$,
and $\chi_{\Omega_\epsilon^+} v_\epsilon \rightarrow B_Y v$ in $L^p((0, T) \times \Omega^+)$, where $\mathbb{V}^p(\Omega^+) = L^p(\omega; W^{1,p}(0, l_d))$.

With the limit system derived, we are now interested in convergence rates for the upscaling process - the so called corrector estimates. First, we show these convergence rates for the interior of the parabolic cylinders. Second, we show the convergence on the entire domain Ω^+ up to its top and bottom boundaries.

Theorem 6.4 (Interior Convergence Estimates). *Assume (A1)-(A10). There exists a subsequence $\epsilon' \subset \epsilon$ such that $\chi_{\Omega_{\epsilon'}^+} \xrightarrow{*} B_Y$ in $L^\infty(\Omega^+)$. Let (u_ϵ, v_ϵ) be the unique solution pair of system (6.10) and let (u, v) be the unique solution pair of system (6.16), as shown in Theorem 6.3, then there exists a constant $C > 0$ independent of ϵ such that the convergence error between $(u_{\epsilon'}, v_{\epsilon'})$ and (u, v) on the cylinders $\Omega_{\epsilon'}^+$ is given by*

$$\|u_{\epsilon'} - u\|_{L^p((0, T) \times \Omega_{\epsilon'}^+)}^p \leq C \|f_{\epsilon'} - f\|_{L^q((0, T) \times \Omega^+)}^q, \quad (6.17a)$$

$$\|v_{\epsilon'} - v\|_{L^p(0, T; W^{1,p}(\Omega_{\epsilon'}^+))}^p \leq C \|f_{\epsilon'} - f\|_{L^q((0, T) \times \Omega^+)}^q, \quad (6.17b)$$

$$\|u_{\epsilon'} - u\|_{L^\infty(0, T; L^2(\Omega_{\epsilon'}^+))}^2 \leq C \|f_{\epsilon'} - f\|_{L^q((0, T) \times \Omega^+)}^q. \quad (6.17c)$$

Theorem 6.5 (Convergence Estimates up to the Boundary). *Assume (A1)-(A10). Introduce $\psi_\epsilon(\mathbf{x}) = \chi_{\Sigma_\epsilon}(\mathbf{x}', 0)$, then there exists a subsequence $\epsilon' \subset \epsilon$ such that $\psi_{\epsilon'} \xrightarrow{*} B_Y$ in $L^\infty(\Omega^+)$. Let (u_ϵ, v_ϵ) be the unique solution pair of system (6.10) and let (u, v) be the unique solution pair of system (6.16), as*

shown in Theorem 6.3, then there exists a constant $C > 0$ independent of ϵ such that the convergence error between $(u_{\epsilon'}, v_{\epsilon'})$ and (u, v) on Ω is given by

$$\left\| \frac{\partial v_{\epsilon'}}{\partial x_d} \right\|_{L^p((0,T) \times \Omega^-)} \leq Ch_{\epsilon}^{\frac{1}{q}}. \quad (6.18)$$

Additionally, for $d = 3$ and $p \in (\frac{3}{2}, 2]$, we also have

$$\|\psi_{\epsilon'} v_{\epsilon'} - B_Y v\|_{L^1((0,T) \times \Omega^+)} \leq C \|f_{\epsilon} - f\|_{L^q((0,T) \times \Omega^+)}^{\frac{1}{p-1}} + C\epsilon. \quad (6.19)$$

Furthermore, if $v \in L^p(0, T; W^{3,p}(\Omega^+))$ then it yields

$$\|\psi_{\epsilon'} v_{\epsilon'} - B_Y v|_{\Sigma}\|_{L^1((0,T) \times \Omega^-)} \leq Ch_{\epsilon}^{\frac{1}{q}} + C \|f_{\epsilon} - f\|_{L^q((0,T) \times \Omega^+)}^{\frac{1}{p-1}} + C\epsilon. \quad (6.20)$$

For $p = 2$, (6.18) in Theorem 6.5 has a form similar to error bounds in the literature, e.g. Lemma 9 and Lemma 12 in [111].

6.4 Simultaneous homogenization and dimension reduction for (6.1)

Theorem 6.25 states the existence of a solution pair

$$(U_{\epsilon}, V_{\epsilon}) \in H^1(0, T; L^2(\Omega_{\epsilon}^+)) \cap L^p((0, T) \times \Omega_{\epsilon}^+) \times L^p(0, T; W^{1,p}(\Omega_{\epsilon}^+))$$

to problem (6.1). In this section, we apply periodic homogenization techniques to perform the upscaling of system (6.1) as the microstructure parameter ϵ vanishes. To this end, we use the two-scale convergence approach, see [4], [99]. Firstly, we obtain a-priori estimates to obtain ϵ -independent upper bounds on suitable norms of the solution, secondly we obtain several weak limits, thirdly we connect the domains Ω_{ϵ}^+ and Ω_{ϵ}^- , and finally, we obtain the upscaled limit.

ϵ -independent a-priori estimates and corresponding weak limits

The domain Ω_{ϵ} splits into three parts: Ω_{ϵ}^+ , Ω_{ϵ}^- , and $\Sigma_{\epsilon} = \{\mathbf{x} \in \Omega_{\epsilon} \mid x_N = 0\} = \omega_{\epsilon} \times \{0\}$, which is part of $\Sigma = \omega \times \{0\}$. On $\Sigma_{\epsilon} = \Sigma \cap \text{int}(\Omega_{\epsilon})$, we have no condition as it is a null-set part of Ω_{ϵ} on which our system is defined. However, on $\Sigma_{\epsilon, \text{ext}} = \Sigma \setminus \Sigma_{\epsilon} = \Sigma \cap \partial\Omega_{\epsilon}$ we have the Neumann boundary condition $\mathcal{E}(\nabla V_{\epsilon}) \cdot \mathbf{n}_{\epsilon} = 0$. Such decomposition of the domain allows one to simultaneously do partial integration on Ω_{ϵ}^+ and Ω_{ϵ}^- for the expression

$$\int_{\Omega_{\epsilon}^+} \text{div} \mathcal{E}(\nabla V_{\epsilon}) d\mathbf{x} + \int_{\Omega_{\epsilon}^-} \text{div} \mathcal{E}(\nabla V_{\epsilon}) d\mathbf{x} = \int_{\Omega_{\epsilon} \setminus \Sigma_{\epsilon}} \text{div} \mathcal{E}(\nabla V_{\epsilon}) d\mathbf{x} \quad (6.21)$$

without obtaining boundary terms on Σ . On $\Sigma_{\epsilon,ext}$ the boundary term is 0, while on Σ_ϵ both partial integrations lead to identical boundary integrals with opposite pointing normal vectors, which cancel each other.²

This partial integration result is therefore also valid for v_ϵ after appropriate rescaling. This fact helps us to obtain ϵ -independent a-priori estimates in a straightforward manner. We state them in Proposition 6.6.

Proposition 6.6. *Assume (A1) - (A10). Let (u_ϵ, v_ϵ) be the unique weak solution pair of the problem (6.10), where (u_ϵ, v_ϵ) follow from (U_ϵ, V_ϵ) via (6.9a) and (6.9b). Then there exists a positive constant C independent of ϵ such that the following bounds*

$$\|u_\epsilon\|_{L^\infty(0,T;L^2(\Omega_\epsilon^+))} \leq C, \quad (6.22a)$$

$$\|v_\epsilon\|_{L^p((0,T)\times\Omega_\epsilon^+)} \leq C, \quad (6.22b)$$

$$\|Dv_\epsilon\|_{L^p((0,T)\times\Omega_\epsilon^+)^d} \leq C, \quad (6.22c)$$

$$\left\| h_\epsilon^{\frac{1}{2}} u_\epsilon \right\|_{L^\infty(0,T;L^2(\Omega^-))} \leq C, \quad (6.22d)$$

$$\left\| h_\epsilon^{\frac{1}{p}} v_\epsilon \right\|_{L^p((0,T)\times\Omega^-)} \leq C, \quad (6.22e)$$

$$\left\| h_\epsilon^{\frac{1}{p}} \left(D_{\mathbf{x}'} v_\epsilon, \frac{1}{h_\epsilon} \frac{\partial v_\epsilon}{\partial x_d} \right) \right\|_{L^p((0,T)\times\Omega^-)^d} \leq C, \quad (6.22f)$$

$$\|\mathcal{M}(v_\epsilon)\|_{L^q((0,T)\times\Omega_\epsilon^+)} \leq C, \quad (6.22g)$$

$$\left\| h_\epsilon^{\frac{1}{q}} \mathcal{M}(v_\epsilon) \right\|_{L^q((0,T)\times\Omega^-)} \leq C, \quad (6.22h)$$

$$\|\mathcal{E}(Dv_\epsilon)\|_{L^q((0,T)\times\Omega_\epsilon^+)^d} \leq C, \quad (6.22i)$$

$$\left\| h_\epsilon^{\frac{1}{q}} \mathcal{E} \left(D_{\mathbf{x}'} v_\epsilon, \frac{1}{h_\epsilon} \frac{\partial v_\epsilon}{\partial x_d} \right) \right\|_{L^q((0,T)\times\Omega^-)^d} \leq C, \quad (6.22j)$$

$$\|\mathcal{K}(u_\epsilon)\|_{L^q((0,T)\times\Omega_\epsilon^+)} \leq C, \quad (6.22k)$$

$$\left\| h_\epsilon^{\frac{1}{q}} \mathcal{K}(u_\epsilon) \right\|_{L^q((0,T)\times\Omega^-)} \leq C, \quad (6.22l)$$

$$(6.22m)$$

²A different argument states that the integrals are identical to integration over Ω_ϵ as a null-set like Σ_ϵ does not change the value of the integral. Then partial integration leads to a boundary term on $\partial\Omega_\epsilon$, which vanishes due to the boundary condition.

$$\left\| \frac{\partial u_\epsilon}{\partial t} \right\|_{L^2((0,T) \times \Omega_\epsilon^+)} \leq C, \quad (6.23a)$$

$$\left\| h_\epsilon^{\frac{1}{2}} \frac{\partial u_\epsilon}{\partial t} \right\|_{L^2((0,T) \times \Omega^-)} \leq C, \quad (6.23b)$$

$$\|\mathcal{L}(u_\epsilon)\|_{L^q((0,T) \times \Omega_\epsilon^+)} \leq C, \quad (6.23c)$$

$$\left\| h_\epsilon^{\frac{1}{q}} \mathcal{L}(u_\epsilon) \right\|_{L^q((0,T) \times \Omega^-)} \leq C, \quad (6.23d)$$

$$\|\mathcal{G}(v_\epsilon)\|_{L^q((0,T) \times \Omega_\epsilon^+)} \leq C, \quad (6.23e)$$

$$\left\| h_\epsilon^{\frac{1}{q}} \mathcal{G}(v_\epsilon) \right\|_{L^q((0,T) \times \Omega^-)} \leq C \quad (6.23f)$$

hold with $q = \frac{p}{p-1}$.

Proof. We test (6.10) with $\phi = v_\epsilon$ and $\psi = u_\epsilon$. This leads to two basic inequalities:

$$\begin{aligned} & \alpha \|v_\epsilon\|_{L^p(0,T;W^{1,p}(\Omega_\epsilon^+))}^p + \alpha \left\| h_\epsilon^{\frac{1}{p}} v_\epsilon \right\|_{L^p((0,T) \times \Omega^-)}^p + \alpha \left\| h_\epsilon^{\frac{1}{p}} \left(D_{\mathbf{x}'} v_\epsilon, \frac{1}{h_\epsilon} \frac{\partial v_\epsilon}{\partial x_d} \right) \right\|_{L^p((0,T) \times \Omega^-)}^p \\ & \leq \|f_\epsilon\|_{L^q((0,T) \times \Omega_\epsilon^+)} \|v_\epsilon\|_{L^p((0,T) \times \Omega_\epsilon^+)} + \left\| h_\epsilon^{\frac{1}{q}} f_\epsilon \right\|_{L^q((0,T) \times \Omega^-)} \left\| h_\epsilon^{\frac{1}{p}} v_\epsilon \right\|_{L^p((0,T) \times \Omega^-)} \\ & \quad + k_s \|u_\epsilon\|_{L^p((0,T) \times \Omega_\epsilon^+)}^{p-1} \|v_\epsilon\|_{L^p((0,T) \times \Omega_\epsilon^+)} \\ & \quad + k_s \left\| h_\epsilon^{\frac{1}{p}} u_\epsilon \right\|_{L^p((0,T) \times \Omega^-)} \left\| h_\epsilon^{\frac{1}{p}} v_\epsilon \right\|_{L^p((0,T) \times \Omega^-)}, \quad (6.24) \end{aligned}$$

and

$$\begin{aligned} & \|u_\epsilon\|_{L^2(\Omega_\epsilon^+)}^2(t) + \left\| h_\epsilon^{\frac{1}{2}} u_\epsilon \right\|_{L^2(\Omega^-)}^2(t) + l_i \|u_\epsilon\|_{L^p((0,t) \times \Omega_\epsilon^+)}^p + l_i \left\| h_\epsilon^{\frac{1}{p}} u_\epsilon \right\|_{L^p((0,t) \times \Omega^-)}^p \\ & \leq g_s \|v_\epsilon\|_{L^p((0,t) \times \Omega_\epsilon^+)}^{p-1} \|u_\epsilon\|_{L^p((0,t) \times \Omega_\epsilon^+)} \\ & \quad + g_s \left\| h_\epsilon^{\frac{1}{p}} v_\epsilon \right\|_{L^p((0,t) \times \Omega^-)}^{p-1} \left\| h_\epsilon^{\frac{1}{p}} u_\epsilon \right\|_{L^p((0,t) \times \Omega^-)}. \quad (6.25) \end{aligned}$$

The direct application of Young's inequality (see Inequality 3), of the inclusion inequality (see Lemma 2.1), of taking the supremum over $t \in (0, T)$, (A3),

(A4), and the Gronwall inequality (Inequality 11), we obtain all ϵ -independent bounds stated above except for (6.23a) and (6.23b). These last two inequalities follow from taking as test functions $\psi = \partial u_\epsilon / \partial t$ and $\phi = 0$ and by applying Young's inequality in a suitable way. \square

Corollary 6.7. *Assume (A1) - (A10). Let (u_ϵ, v_ϵ) be the unique weak solution pair of the problem (6.10). Then there exists a positive constant C independent of ϵ such that*

$$\|v_\epsilon\|_{L^p((0,T) \times \Sigma_\epsilon)} \leq C. \quad (6.26)$$

Proof. This is a direct application of the 1D trace inequality, see Proposition 2.11, combined with $\Sigma_\epsilon \subset \partial\Omega_\epsilon^+$ and the ϵ -independent bounds stated in Proposition 6.6. \square

Proposition 6.8. *Let $w_\epsilon \in L^p(0, T; W^{1,p}(\Omega^\epsilon))$ satisfy the inequalities*

$$\left\| h_\epsilon^{\frac{1}{p}} \left(D_{\mathbf{x}'} w_\epsilon, \frac{1}{h_\epsilon} \frac{\partial w_\epsilon}{\partial x_d} \right) \right\|_{L^p((0,T) \times \Omega^-)} \leq C, \quad \|w_\epsilon\|_{L^p((0,T) \times \Sigma_\epsilon)} \leq C \quad (6.27)$$

for some $C > 0$ independent of ϵ . Then, there exists a $c > 0$ independent of ϵ such that

$$\|w_\epsilon\|_{L^p((0,T) \times \Omega^-)} \leq c. \quad (6.28)$$

Proof. The proof of (6.27) is identical to the proof of Proposition 3.3 on page 455-456 of [12]. \square

Recall the notation B_Y for the volume fraction $|\mathcal{B}|/|Y|$. Moreover, introduce the space $\mathbb{V}^p(\Omega^+) = \left\{ v \in L^p(\Omega^+) : \frac{\partial v}{\partial x_d} \in L^p(\Omega^+) \right\}$ with norm $\|v\|_{\mathbb{V}^p(\Omega^+)} = \left(\int_{\Omega^+} |v|^p + \left| \frac{\partial v}{\partial x_d} \right|^p d\mathbf{x} \right)^{\frac{1}{p}}$. The a-priori estimates obtained in Proposition 6.6, Corollary 6.7, and Proposition 6.8, have several important consequences what concerns the wanted weak limits.

Proposition 6.9. *Assume (A1)-(A10) and let the pair (u_ϵ, v_ϵ) be the weak solution pair to (6.10) in the sense of Definition 6.1. Then the following convergence holds:*

$$\frac{\partial v_\epsilon}{\partial x_d} \rightarrow 0 \text{ in } L^p((0, T) \times \Omega^-). \quad (6.29)$$

Moreover, there exist a subsequence $\epsilon' \subset \epsilon$, and limit functions $u \in L^2((0, T) \times \Omega^+)$ and $v \in L^p(0, T; \mathbb{V}^p(\Omega^+))$ such that

$$\chi_{\Omega_{\epsilon'}^+} u_{\epsilon'} \rightharpoonup B_Y u \quad \text{in } L^2((0, T) \times \Omega^+), \quad (6.30a)$$

$$\chi_{\Omega_{\epsilon'}^+} v_{\epsilon'} \rightharpoonup B_Y v \quad \text{in } L^p((0, T) \times \Omega^+), \quad (6.30b)$$

$$\frac{\partial \chi_{\Omega_{\epsilon'}^+} v_{\epsilon'}}{\partial x_d} \rightharpoonup B_Y \frac{\partial v}{\partial x_d} \quad \text{in } L^p((0, T) \times \Omega^+). \quad (6.30c)$$

Furthermore, we have the convergence

$$v_{\epsilon'} \rightharpoonup v|_{\Sigma} \quad \text{in } L^p((0, T) \times \Omega^-). \quad (6.31)$$

Proof. Inequality (6.22f) yields

$$\left\| \frac{\partial v_{\epsilon}}{\partial x_d} \right\|_{L^p((0, T) \times \Omega^-)} \leq Ch_{\epsilon}^{\frac{1}{q}}. \quad (6.32)$$

This shows (6.29).

We recall that $\chi_{\Omega_{\epsilon}^+}$ denotes the indicator function corresponding to $\Omega_{\epsilon}^+ \subset \Omega^+$. Hence, $\|\chi_{\Omega_{\epsilon}^+}\|_{L^1(\Omega^+)} = |\Omega_{\epsilon}^+| \leq |\Omega^+| < \infty$ and $\|\chi_{\Omega_{\epsilon}^+}\|_{L^\infty(\Omega^+)} = 1$. Moreover, $\chi_{\Omega_{\epsilon}^+}$ is an almost everywhere constant function and it satisfies

$$\chi_{\Omega_{\epsilon}^+} \xrightarrow{*} B_Y \text{ in } L^\infty(\Omega^+) : \int_{\Omega^+} \chi_{\Omega_{\epsilon}^+} \phi d\mathbf{x} \rightarrow \int_{\Omega^+} B_Y \phi d\mathbf{x} \text{ for all } \phi \in L^1(\Omega^+). \quad (6.33)$$

Consequently, (6.30a)-(6.30c) are a direct consequence of the weak convergences of u_{ϵ} and v_{ϵ} due to the bounds (6.22a), (6.22b), and (6.22c).

By Proposition 6.8, due to inequalities (6.22f) and Corollary 6.7, we obtain a weak limit $\nu \in L^p(0, T; W^{1,p}(\Omega^-))$ of v_{ϵ} . Using (A5), we have

$\lim_{\epsilon \downarrow 0} \|\epsilon Dv_{\epsilon}\|_{L^p((0, T) \times \Omega^-)^d} = 0$. Consequently, we have $\epsilon Dv_{\epsilon} \rightarrow \mathbf{0}$ in $L^p((0, T) \times \Omega^-)$, and ϵDv_{ϵ} is bounded in $L^p((0, T) \times \Omega^-)$. For a subsequence ϵ' , we even have $v_{\epsilon'} \xrightarrow{2} n$ in $L^p((0, T) \times \Omega^-; W_{\#}^{1,p}(Y))$, and $\epsilon' Dv_{\epsilon'} \xrightarrow{2} D_{\mathbf{y}} n = \mathbf{0}$ in $L^p((0, T) \times \Omega^-; L_{\#}^p(Y))$. By Definition 2.13, we have $\nu = \frac{1}{|Y|} \int_Y n d\mathbf{y} = n$.

Realizing that the periodicity in Ω_{ϵ}^+ is in all directions in \mathbf{R}^d orthogonal to the x_d -direction, we are allowed to introduce a function $\psi_{\epsilon}(\mathbf{x})$ on $\Omega^+ \cup \Sigma \cup \Omega^-$ such that $\psi_{\epsilon}(\mathbf{x}) = \chi_{\Omega_{\epsilon}^+}(\mathbf{x}) = \chi_{\Sigma_{\epsilon}}(\mathbf{x}', 0)$ for $\mathbf{x} \in \Omega^+$ and $\psi_{\epsilon}(\mathbf{x}) = \chi_{\Sigma_{\epsilon}}(\mathbf{x}', 0)$ for $\mathbf{x} \in \Sigma \cup \Omega^-$. Hence, $\psi_{\epsilon} \xrightarrow{*} B_Y$ in $L^\infty(\Omega^+ \cup \Sigma \cup \Omega^-)$. Thus, $\psi_{\epsilon'} v_{\epsilon'} \rightharpoonup B_Y \nu$ in $L^p((0, T) \times \Omega^-)$. Using (6.33) and continuous representatives of $\frac{\partial(\psi_{\epsilon'} v_{\epsilon'} \phi)}{\partial x_d}$,

and $\frac{\partial(v\phi)}{\partial x_d}$ for which the fundamental theorem of calculus holds, we see

$$\begin{aligned} \lim_{\epsilon' \downarrow 0} \int_{\Sigma} \psi_{\epsilon'} v_{\epsilon'} \phi d\mathbf{x} &= \lim_{\epsilon' \downarrow 0} \left(\int_{\Omega^-} \frac{\partial(\psi_{\epsilon'} v_{\epsilon'})}{\partial x_d} \phi d\mathbf{x} + \int_{\Omega^-} \psi_{\epsilon'} v_{\epsilon'} \frac{\partial \phi}{\partial x_d} d\mathbf{x} \right) \\ &= \int_{\Omega^-} B_Y \nu \frac{\partial \phi}{\partial x_d} d\mathbf{x} = \int_{\Sigma} B_Y \nu \phi d\mathbf{x}', \end{aligned} \quad (6.34a)$$

$$\begin{aligned} \lim_{\epsilon' \downarrow 0} \int_{\Sigma} \psi_{\epsilon'} v_{\epsilon'} \phi d\mathbf{x} &= - \lim_{\epsilon' \downarrow 0} \left(\int_{\Omega^+} \frac{\partial(\chi_{\Omega_{\epsilon'}^+} v_{\epsilon'})}{\partial x_d} \phi d\mathbf{x} + \int_{\Omega^+} \chi_{\Omega_{\epsilon'}^+} v_{\epsilon'} \frac{\partial \phi}{\partial x_d} d\mathbf{x} \right) \\ &= - \int_{\Omega^+} B_Y \frac{\partial v}{\partial x_d} \phi d\mathbf{x} - \int_{\Omega^+} B_Y v \frac{\partial \phi}{\partial x_d} d\mathbf{x} \\ &= \int_{\Sigma} B_Y \nu \phi d\mathbf{x}' \end{aligned} \quad (6.34b)$$

for all $\phi \in C_0^\infty(\Omega^+ \cup \Sigma \cup \Omega^-)$. Due to (6.29) and (6.22b), we have that ν is independent of x_d . Hence, $\nu = \nu|_{\Sigma}$. \square

Passage to the homogenization limit

As a consequence of Proposition 6.6, we have the following weak limits available:

$$\chi_{\Omega_\epsilon^+} u_\epsilon \rightharpoonup u^+ \quad \text{in } L^\infty(0, T; L^2(\Omega^+)), \quad (6.35a)$$

$$\chi_{\Omega_\epsilon^+} v_\epsilon \rightharpoonup v^+ \quad \text{in } L^p((0, T) \times \Omega^+), \quad (6.35b)$$

$$\chi_{\Omega_\epsilon^+} Dv_\epsilon \rightharpoonup \mathbf{d} \quad \text{in } L^p((0, T) \times \Omega^+)^d, \quad (6.35c)$$

$$\chi_{\Omega_\epsilon^+} \mathcal{M}(v_\epsilon) \rightharpoonup m^+ \quad \text{in } L^q((0, T) \times \Omega^+), \quad (6.35d)$$

$$\chi_{\Omega_\epsilon^+} \mathcal{E}(Dv_\epsilon) \rightharpoonup \mathbf{e}^+ \quad \text{in } L^q((0, T) \times \Omega^+)^d, \quad (6.35e)$$

$$\chi_{\Omega_\epsilon^+} \mathcal{K}(u_\epsilon) \rightharpoonup k^+ \quad \text{in } L^q((0, T) \times \Omega^+), \quad (6.35f)$$

$$\chi_{\Omega_\epsilon^+} \mathcal{L}(u_\epsilon) \rightharpoonup l^+ \quad \text{in } L^q((0, T) \times \Omega^+), \quad (6.35g)$$

$$\chi_{\Omega_\epsilon^+} \mathcal{G}(v_\epsilon) \rightharpoonup g^+ \quad \text{in } L^q((0, T) \times \Omega^+), \quad (6.35h)$$

$$\chi_{\Omega_\epsilon^+} \frac{\partial u_\epsilon}{\partial t} \rightharpoonup \tau^+ \quad \text{in } L^2((0, T) \times \Omega^+). \quad (6.35i)$$

It is worth noting that, by Proposition 6.9, the identifications $u^+ = B_Y u$, $v^+ = B_Y v$, $d_d = B_Y \frac{\partial v}{\partial x_d}$, and $Dv^+ = \mathbf{d}$ hold. Consequently, the next result holds for the convergence of duality pairings of two specific weak sequences, we refer here to this as *the convergence of the energies*.

Lemma 6.10 (Convergence of the energies). *Assume (A1)-(A10).*

Let $\mathcal{T}_0\chi_{\Omega_\epsilon^+}v_\epsilon \rightharpoonup T^+$ in $(W^{1,p}(\Omega^+))^$. Then for any sequence $\chi_{\Omega_\epsilon^+}w_\epsilon \rightharpoonup w^+$ in $W^{1,p}(\Omega^+)$, the convergence*

$$\langle \chi_{\Omega_\epsilon^+}w_\epsilon, \mathcal{T}_0\chi_{\Omega_\epsilon^+}v_\epsilon - \mathcal{K}(u_\epsilon)\chi_{\Omega_\epsilon^+} \rangle \rightarrow \left\langle \frac{w^+}{B_Y}, T^+ - k^+ \right\rangle \quad (6.36)$$

holds as $\epsilon \rightarrow 0$.

Proof. By the strong convergence of f_ϵ , which via (6.9c) follows from (A3), we have

$$\begin{aligned} \lim_{\epsilon \downarrow 0} \langle \chi_{\Omega_\epsilon^+}w_\epsilon, \mathcal{T}_0\chi_{\Omega_\epsilon^+}v_\epsilon - \mathcal{K}(u_\epsilon)\chi_{\Omega_\epsilon^+} \rangle &= \lim_{\epsilon \downarrow 0} \langle \chi_{\Omega_\epsilon^+}w_\epsilon, f_\epsilon\chi_{\Omega_\epsilon^+} \rangle \\ &= \langle w^+, f \rangle = \lim_{\epsilon \downarrow 0} \left\langle \frac{w^+}{B_Y}, f_\epsilon\chi_{\Omega_\epsilon^+} \right\rangle \\ &= \lim_{\epsilon \downarrow 0} \left\langle \frac{w^+}{B_Y}, \mathcal{T}_0\chi_{\Omega_\epsilon^+}v_\epsilon - \mathcal{K}(u_\epsilon)\chi_{\Omega_\epsilon^+} \right\rangle = \left\langle \frac{w^+}{B_Y}, T^+ - k^+ \right\rangle. \end{aligned} \quad (6.37)$$

□

Corollary 6.11. *Lemma 6.10 holds for any sequence $\chi_{\Omega_\epsilon^+}w_\epsilon \rightharpoonup w^+$ in $\mathbb{V}^p(\Omega^+)$.*

Proof. Proposition 1.1 in [11] states that $W^{1,p}(\Omega^+)$ is dense in $\mathbb{V}^p(\Omega^+)$. □

We continue with the determination of the weak limits of the individual terms in (6.1) via a technique for identifying limits of hemicontinuous monotone operators; see the next lemma.

Lemma 6.12. *Let \mathbb{X} be a function space over a domain $\Omega^+ \subset \mathbf{R}^d$ for a $d > 0$ integer. Let $\mathcal{A}(\cdot) : \mathbb{X} \rightarrow \mathbb{X}^*$ be a hemicontinuous monotone operator satisfying $\mathcal{A}(z_\epsilon)\chi_{\Omega_\epsilon^+} \rightharpoonup a^+$ in \mathbb{X}^* , and let $\chi_{\Omega_\epsilon^+}z_\epsilon \rightharpoonup z^+$ in \mathbb{X} . If $C_c^\infty(\Omega^+)^n$ is a dense subset of \mathbb{X} for some $n \geq 1$ integer, and $\langle z_\epsilon\chi_{\Omega_\epsilon^+}, \mathcal{A}(z_\epsilon)\chi_{\Omega_\epsilon^+} \rangle \rightarrow \left\langle \frac{z^+}{B_Y}, a^+ \right\rangle$, then $a^+ = B_Y\mathcal{A}\left(\frac{z^+}{B_Y}\right)$.*

Proof. As $\epsilon \rightarrow 0$, we have

$$\langle \chi_{\Omega_\epsilon^+}(z_\epsilon - \zeta), \mathcal{A}(\chi_{\Omega_\epsilon^+}z_\epsilon) - \mathcal{A}(\chi_{\Omega_\epsilon^+}\zeta) \rangle \rightarrow \left\langle \frac{z^+}{B_Y} - \zeta, a^+ - B_Y\mathcal{A}(\zeta) \right\rangle, \quad (6.38)$$

where we used the fact that $\mathcal{A}(\chi_{\Omega_\epsilon^+}\xi) = \chi_{\Omega_\epsilon^+}\mathcal{A}(\xi)$ for all $\xi \in D(\mathcal{A})$. Note, that the right-hand side of (6.38) is non-negative, because the left-hand side

is non-negative for all ϵ by monotonicity of \mathcal{A} . Now, we choose $\zeta = \frac{z^+}{B_Y} - \lambda\phi$ for each $\phi \in C_c^\infty(\Omega^+)^n \cap D(\mathcal{A})$ and for all $\lambda > 0$. Hence, after dividing by λ , as $\lambda \rightarrow 0$ we have

$$\left\langle \phi, a^+ - B_Y \mathcal{A} \left(\frac{z^+}{B_Y} - \lambda\phi \right) \right\rangle \rightarrow \left\langle \phi, a^+ - B_Y \mathcal{A} \left(\frac{z^+}{B_Y} \right) \right\rangle \quad (6.39)$$

by the hemicontinuity of \mathcal{A} . Now, the right-hand side of (6.39) is zero, because the left-hand side is non-negative for all $\lambda > 0$ and for all $\phi \in C_c^\infty(\Omega^+)^n$, regardless of sign. The assertion follows as Equation (6.39) holds for all $\phi \in C_c^\infty(\Omega^+)^n \cap D(\mathcal{A})$. \square

Corollary 6.13. *Let (A1)-(A10) be satisfied and let $T < \infty$, then we have the weak limit $\mathcal{T}_0(v_\epsilon)\chi_{\Omega_\epsilon^+} \rightharpoonup B_Y \mathcal{T}_0 \left(\frac{v^+}{B_Y} \right)$ in $(W^{1,p}(\Omega^+))^*$.*

Proof. Lemma 6.27 and its proof show that $\mathcal{T}_0 : W^{1,p}(\Omega^+) \rightarrow (W^{1,p}(\Omega^+))^*$ is a hemicontinuous monotone operator. Proposition 6.9 together with the ϵ -independent bounds of Proposition 6.6, the uniqueness of weak limits and the fact, taken from Proposition 1.1 in [11], that $W^{1,p}(\Omega^+)$ is dense in $\mathbb{V}^p(\Omega^+)$, we have $v_\epsilon\chi_{\Omega_\epsilon^+} \rightharpoonup v^+$ in $W^{1,p}(\Omega^+) = D(\mathcal{T}_0)$ by (A1). Remark 18 on page 287 of [20] states that $C_c^\infty(\Omega)$ is a dense subset of $W_0^{1,p}(\Omega)$, which is a closed subset of $W^{1,p}(\Omega)$ for $p \in [1, \infty)$. From (A3), (A4), and Proposition 6.6 we obtain

$$\begin{aligned} \|\mathcal{T}_0 v_\epsilon \chi_{\Omega_\epsilon}\|_{(W^{1,p}(\Omega^+))^*} &= \sup_{\phi \in W^{1,p}(\Omega^+), \|\phi\|_{W^{1,p}(\Omega^+)}=1} |\langle \phi, \mathcal{T}_0 v_\epsilon \chi_{\Omega_\epsilon} \rangle| \\ &= \sup_{\phi \in W^{1,p}(\Omega^+), \|\phi\|_{W^{1,p}(\Omega^+)}=1} |\langle \phi, [f_\epsilon + \mathcal{K}(u_\epsilon)] \chi_{\Omega_\epsilon} \rangle| \\ &\leq \|f_\epsilon\|_{L^q(\Omega^+)} + \|\mathcal{K}(u_\epsilon)\|_{L^q(\Omega^+)} \leq C \end{aligned} \quad (6.40)$$

with C independent of ϵ . Thus there exists a $T^+ \in (W^{1,p}(\Omega^+))^*$ such that $\mathcal{T}_0 v_\epsilon \chi_{\Omega_\epsilon} \rightharpoonup T^+$ in $(W^{1,p}(\Omega^+))^*$. Moreover, by the Rellich-Kondrachov Theorem, we have $v_\epsilon \chi_{\Omega_\epsilon^+} \rightarrow v^+$ in $L^p(\Omega^+)$. Hence, we have

$$\langle v_\epsilon \chi_{\Omega_\epsilon^+}, \mathcal{K}(u_\epsilon) \chi_{\Omega_\epsilon^+} \rangle \rightarrow \left\langle \frac{v^+}{B_Y}, k^+ \right\rangle, \quad (6.41)$$

which with the convergence of the energies of Lemma 6.10 for $w_\epsilon = v_\epsilon$ yields the needed convergence $\langle v_\epsilon \chi_{\Omega_\epsilon^+}, \mathcal{T}_0(v_\epsilon) \chi_{\Omega_\epsilon^+} \rangle \rightarrow \left\langle \frac{v^+}{B_Y}, T^+ \right\rangle$. The result follows by application of Lemma 6.12. \square

Corollary 6.14. *Let (A1)-(A10) be satisfied, then*

$$\mathcal{M}(v_\epsilon)\chi_{\Omega_\epsilon^+} \rightharpoonup m^+ = B_Y \mathcal{M}(v) \quad \text{in } L^q(\Omega^+), \quad (6.42a)$$

$$\mathcal{E}(Dv_\epsilon)\chi_{\Omega_\epsilon^+} \rightharpoonup e^+ = B_Y \mathcal{E}\left(\frac{\mathbf{d}}{B_Y}\right) \quad \text{in } L^q(\Omega^+)^d. \quad (6.42b)$$

Proof. From the strong convergence $v_\epsilon\chi_{\Omega_\epsilon^+} \rightarrow v^+ = B_Y v$ in $L^p(\Omega^+)$ and the demicontinuity of \mathcal{M} follows (6.42a). Automatically, (6.42b) follows by subtracting (6.42a) from $\mathcal{T}_0(v_\epsilon)\chi_{\Omega_\epsilon^+} \rightarrow B_Y \mathcal{T}_0\left(\frac{v^+}{B_Y}\right)$. \square

Next to the determination of the weak limit of $\mathcal{T}_0 v_\epsilon \chi_{\Omega_\epsilon}$, there is a constraint on the sum e^+ , which is due to the vanishing thickness of the individual cylinders $g(\mathcal{B}) \times [0, l_d]$ for $g \in G_\gamma^\epsilon$.

Lemma 6.15. *Let (A1)-(A10) be satisfied. The identity $e_i^+ = 0$ holds a.e. in Ω^+ for all $i \in \{1, \dots, d-1\}$.*

Proof. Fix an $i \in \{1, \dots, d-1\}$. Since $\partial\mathcal{B} \cap \partial Y = \emptyset$, there is a $\delta > 0$ such that $\delta = \inf_{\mathbf{b} \in \partial\mathcal{B}, \mathbf{y} \in \partial Y} |\mathbf{b} - \mathbf{y}|$. Introduce the functions $w_\epsilon^i \in W^{1,\infty}(\Omega^+)$ such that $w_\epsilon^i(\mathbf{x})$ are constant on $\omega_\epsilon \times \{x_d\}$ with the value $\inf_{\mathbf{x}' \in g(\mathcal{B})} x_i$ on each g -mapped convex hull $g(\gamma(CH(\gamma^{-1}(\mathcal{B}))))$ of $g(\mathcal{B}) \subset \omega_\epsilon$, $w_\epsilon^i(\mathbf{x}) = x_i$ for all $\mathbf{x} \in \partial\Omega^+ \cup \left(\bigcup_{g \in G_\gamma^\epsilon, g(\mathcal{B}) \subset \omega_\epsilon} \partial(g(Y)) \times (0, l_d)\right)$, and on $\Omega^+ \cap g(Y)/g(\gamma(CH(\gamma^{-1}(\mathcal{B})))) \times (0, l_d)$ we have $w_\epsilon^i(\mathbf{x})$ as the linear interpolation between the values of w_ϵ^i of the pair $(\mathbf{p}_1, \mathbf{p}_2)$ in $(\partial g(\gamma(CH(\gamma^{-1}(\mathcal{B})))) \cup \partial g(Y))^2$, which are connected by a path through \mathbf{x}' that is the $g \circ \gamma$ -mapping of the shortest straight line through $(g \circ \gamma)^{-1}(\mathbf{x}')$ between $(g \circ \gamma)^{-1}(\mathbf{p}_1)$ and $(g \circ \gamma)^{-1}(\mathbf{p}_2)$. A schematic representation of the use of the convex hull method in the proof of Lemma 6.15 can be found in Figure 6.3.

By continuity of x_i , g and the convexity of both the convex hull and Y , we have indeed $w_\epsilon^i \in W^{1,\infty}(\Omega^+)$. Moreover, for $i \in \{1, \dots, d-1\}$ by construction, we have $Dw_\epsilon^i = 0$ a.e. on Ω_ϵ^+ for all $\epsilon > 0$, and $w_\epsilon^i \rightarrow x_i$ in $L^\infty(\Omega^+)$ as $\epsilon \downarrow 0$, because $\sup_{\mathbf{x}' \in g(Y)} |w_\epsilon^i - x_i| \leq \epsilon$ for all $g \in G_\gamma^\epsilon$ such that $g(\mathcal{B}) \subset \omega_\epsilon$ due to $\epsilon \lfloor \frac{x_i}{\epsilon} \rfloor \leq w_\epsilon^i \leq x_i$.

Take $\varphi \in C_c^\infty(\Omega^+)$ and use $\phi = \varphi w_\epsilon^i$, $\psi = 0$ as test functions in system (6.10).

This leads to

$$\begin{aligned}
 & \int_{\Omega^+} m^+ \varphi x_i + \mathbf{e}^+ \cdot (D\varphi)x_i - k^+ \varphi x_i \, d\mathbf{x} \\
 &= \lim_{\epsilon \downarrow 0} \int_{\Omega^+} [\mathcal{M}(v_\epsilon) \varphi w_\epsilon^i + \mathcal{E}(Dv_\epsilon) \cdot (D\varphi)w_\epsilon^i - \mathcal{K}(u_\epsilon) \varphi w_\epsilon^i] \chi_{\Omega_\epsilon^+} \, d\mathbf{x} \\
 &= \lim_{\epsilon \downarrow 0} \int_{\Omega^+} f_\epsilon \varphi w_\epsilon^i \chi_{\Omega_\epsilon^+} \, d\mathbf{x} = \int_{\Omega^+} B_Y f x_i \varphi \, d\mathbf{x} \quad (6.43)
 \end{aligned}$$

due to the strong convergence of f_ϵ as given by (A3) and due to the strong convergence of w_ϵ^i .

For the same $\varphi \in C_c^\infty(\Omega^+)$, use $\phi = \varphi x_i$, $\psi = 0$ as test functions in system (6.10). This leads to

$$\begin{aligned}
 & \int_{\Omega^+} m^+ \varphi x_i + \mathbf{e}^+ \cdot D(\varphi x_i) - k^+ \varphi x_i \, d\mathbf{x} \\
 &= \lim_{\epsilon \downarrow 0} \int_{\Omega^+} [\mathcal{M}(v_\epsilon) \varphi x_i + \mathcal{E}(Dv_\epsilon) \cdot D(\varphi x_i) - \mathcal{K}(u_\epsilon) \varphi x_i] \chi_{\Omega_\epsilon^+} \, d\mathbf{x} \\
 &= \lim_{\epsilon \downarrow 0} \int_{\Omega^+} f_\epsilon \varphi x_i \chi_{\Omega_\epsilon^+} \, d\mathbf{x} = \int_{\Omega^+} B_Y f x_i \varphi \, d\mathbf{x}. \quad (6.44)
 \end{aligned}$$

Subtracting (6.43) from (6.44) yields

$$\int_{\Omega^+} \mathbf{e}^+ \cdot D x_i \varphi \, d\mathbf{x} = 0. \quad (6.45)$$

This gives the desired result as $\varphi \in C_c^\infty(\Omega^+)$ was chosen arbitrarily. \square

Remark 6.1. *The result stated in Lemma 6.15 is not surprising since in the limit $\epsilon \rightarrow 0$, the cylinders become lines, which are dense in Ω^+ . Then at almost every point in Ω^+ , the cylinder boundary condition must be satisfied, which should be equal to $\mathbf{e}^+ \cdot \mathbf{n} = 0$ for all $\mathbf{n} \in S^{d-2} \times \{0\}$.*

Note, the proof of Lemma 6.15 cannot be extended to $i = d$, since $w_\epsilon^d = 0$. Moreover, we can not construct piecewise constant functions \tilde{w}_ϵ^d that strongly converge to x_i and are simultaneously elements of $W^{1,p}(\Omega^+)$ for $p \in (1, \infty]$, see line (ii) in Remark 2 on page 203 in [20]. Essentially, this is because the Rellich-Kondrachov Theorem states that \tilde{w}_ϵ^d must be continuous as an element of $W^{1,p}(\Omega^+)$.

For the coupled ordinary differential equation, we obtain similar limits.

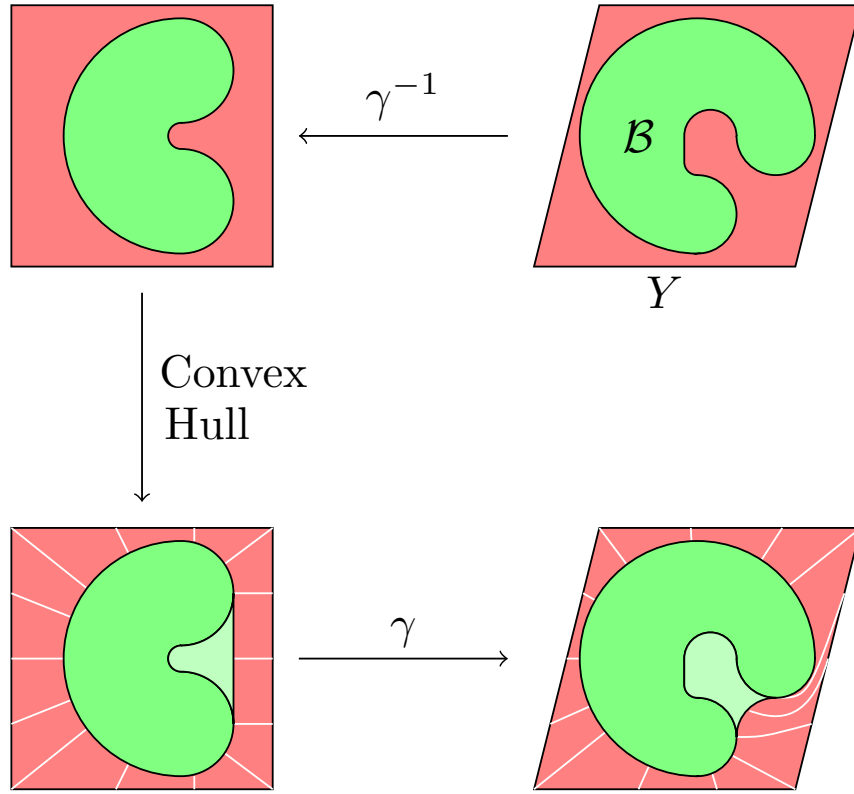


Figure 6.3: The domains Y (in red) and \mathcal{B} (in green) do not need to be convex (see top right). However, $\gamma^{-1}(Y)$ is convex by construction, and $\gamma^{-1}(\mathcal{B}) \subset \gamma^{-1}(Y)$ with non-touching boundaries (see top left). Therefore, we can take the convex hull of $\gamma^{-1}(\mathcal{B})$ (shown as the union of the green $\gamma^{-1}(\mathcal{B})$ and the light green set), which is now a convex subset of the convex set $\gamma^{-1}(Y)$. Thus we can connect the boundaries $\partial\gamma^{-1}(\mathcal{B})$ and $\gamma^{-1}(Y)$ with shortest distance straight line paths (shown in white, see bottom left). The γ mapping of this convex hull domain and the associated straight paths become the desired domains and paths by which we can create $w_\epsilon^i(\mathbf{x})$. These paths and the convex hull guarantee the continuity of $w_\epsilon^i(\mathbf{x})$, while preserving its properties on \mathcal{B} and ∂Y .

Proposition 6.16. *Let (A1)-(A10) be satisfied, then $\tau^+ = B_Y \frac{\partial u}{\partial t}$, $g^+ = B_Y \mathcal{G}(v)$, and $l^+ = B_Y \mathcal{L}(u)$.*

Proof. Note, we are allowed to apply Fubini to each function in $L^1((0, T) \times \Omega^+)$. Hence, we apply Fubini to $\chi_{\Omega_\epsilon^+} \frac{\partial u_\epsilon}{\partial t} \phi$ and then partially integrate with respect to time for all $\phi \in H^1(0, T; L^2(\Omega^+))$. Since $\chi_{\Omega_\epsilon^+} u_\epsilon \rightharpoonup u^+ \in L^\infty(0, T; L^2(\Omega^+))$, we obtain

$$\int_0^T \int_{\Omega^+} \chi_{\Omega_\epsilon^+} \frac{\partial u_\epsilon}{\partial t} \phi d\mathbf{x} dt \rightarrow \int_{\Omega^+} \left([u^+ \phi]_0^T - \int_0^T u^+ \frac{\partial \phi}{\partial t} dt \right) d\mathbf{x}. \quad (6.46)$$

Again the partial integration and the application of Fubini together with the determination $u^+ = B_Y u$ yield the result $\tau^+ = B_Y \frac{\partial u}{\partial t}$.

We recall that $\chi_{\Omega_\epsilon^+} v_\epsilon \rightarrow v^+ = B_Y v$ in $L^p((0, T) \times \Omega^+)$. Hence, the demicontinuity of \mathcal{G} yields $g^+ = B_Y \mathcal{G}(v)$.

We have $\chi_{\Omega_\epsilon^+} u_\epsilon \rightarrow u^+$ in $L^p((0, T) \times \Omega^+)$ due to the Rellich-Kondrachev Theorem. Hence, $\langle \chi_{\Omega_\epsilon^+} \mathcal{L}(u_\epsilon), \chi_{\Omega_\epsilon^+} u_\epsilon \psi \rangle \rightarrow \langle l^+, u \psi \rangle$. Thus Lemma 6.12 ensures $l^+ = B_Y \mathcal{L}(u)$. \square

The upscaled system, therefore, is

$$\begin{cases} \mathcal{M}(v) - \frac{\partial}{\partial x_d} \left(\mathcal{E}_d \left(\frac{\mathbf{d}'}{B_Y}, \frac{\partial v}{\partial x_d} \right) \right) = f + \mathcal{K}(u) & \text{in } \Omega^+ \times (0, T), \\ \frac{\partial u}{\partial t} + \mathcal{L}(u) = \mathcal{G}(v) & \text{in } \Omega^+ \times (0, T), \\ \mathcal{E}_i \left(\frac{\mathbf{d}'}{B_Y}, \frac{\partial v}{\partial x_d} \right) = 0 & \text{in } \overline{\Omega^+} \times (0, T), \text{ for } i \neq d, \\ \mathcal{E}_d \left(\frac{\mathbf{d}'}{B_Y}, \frac{\partial v}{\partial x_d} \right) = 0 & \text{on } \Sigma \times \{0, 1\} \times (0, T), \\ u = U^* & \text{in } \Omega^+ \times \{0\}, \end{cases} \quad (6.47)$$

with unknowns $v \in L^p(0, T; \mathbb{V}^p(\Omega^+))$, $u \in H^1(0, T; L^2(\Omega^+)) \cap L^p((0, T) \times \Omega^+)$, and $\mathbf{d}' \in L^p((0, T) \times \Omega^+)^{d-1}$. Note, the boundary conditions can be written as they are since $e_d^+ + d_d^+ \in L^p((0, T) \times \omega; W^{1,p}(0, l_d))$ and, consequently, $\mathbf{d}' \in L^p((0, T) \times \omega; W^{1,p}(0, l_d))^d$ and $\frac{\partial v}{\partial x_d} \in L^p((0, T) \times \omega; W^{1,p}(0, l_d))$. This concludes the proof of Theorem 6.3.

6.5 Corrector estimates

We are interested in the convergence rate of u_ϵ and v_ϵ to u and v and how this rate relates to the oscillating ω_ϵ , h_ϵ and f_ϵ .

Firstly, we study the convergence rate on Ω^- . Then we investigate what happens on Ω^+ . It appears that it is sufficient to learn what happens with v_ϵ versus v , and to recall fairly standard corrector estimates for elliptic equations what concerns u_ϵ versus u .

Recall $\psi_\epsilon(\mathbf{x}) = \chi_{\Sigma_\epsilon}(\mathbf{x}', 0) \in L^\infty(\Omega^+ \cup \Sigma \cup \Omega^-)$.

Lemma 6.17. *Assume (A1)-(A10). Let (u_ϵ, v_ϵ) be the weak solution pair of system (6.10), then there exists a constant $C > 0$ independent of ϵ such that the following estimates hold*

$$\|\psi_\epsilon(v_\epsilon - v_\epsilon|_\Sigma)\|_{L^p((0, T) \times \Omega^-)}^p \leq Ch_\epsilon^{p-1}, \quad (6.48a)$$

$$\|v_\epsilon - v_\epsilon|_\Sigma\|_{L^p((0, T) \times \Omega^-)}^p \leq Ch_\epsilon^{p-1} \quad (6.48b)$$

for $p \in (1, \infty)$.

Proof. Let $\omega_\epsilon \subset \omega$ for all $\epsilon > 0$. By Hölder's inequality, (6.32) leads to

$$\begin{aligned}
\|\psi_{\epsilon'}(v_{\epsilon'} - v_{\epsilon'}|_\Sigma)\|_{L^p((0,T)\times\Omega^-)}^p &= \int_0^T \int_{\Omega^-} |\psi_{\epsilon'}(v_{\epsilon'} - v_{\epsilon'}|_\Sigma)|^p \, d\mathbf{x}dt \\
&= \int_0^T \int_{\omega_{\epsilon'}} \int_{-1}^0 |v_{\epsilon'}(\mathbf{x}', x_d) - v_{\epsilon'}(\mathbf{x}', 0)|^p \, dx_d d\mathbf{x}' dt \\
&= \int_0^T \int_{\omega_{\epsilon'}} \int_{-1}^0 \left| \int_{x_d}^0 \frac{\partial v_{\epsilon'}}{\partial x_d}(\mathbf{x}', y) dy \right|^p \, dx_d d\mathbf{x}' dt \\
&\leq \left\| \frac{\partial v_{\epsilon'}}{\partial x_d} \right\|_{L^p((0,T)\times\Omega^-)}^p \leq Ch_{\epsilon'}^{p-1}. \tag{6.49}
\end{aligned}$$

The other bound for v_ϵ follows by removing ψ_ϵ , and changing ω_ϵ into ω . \square

Convergence bounds on Ω^+ cannot be obtained by applying the Poincaré-Wirtinger inequality to each cylinder in Ω_ϵ^+ because the resulting approximation of v_ϵ is constant in the \mathbf{x}' -directions on each cylinder and, therefore, we lose control on the difference of these constants between cylinders, which makes it difficult to relate it to v . To obtain the wanted corrector estimates we use the evolution systems solved by (u_ϵ, v_ϵ) and (u, v) .

Proposition 6.18. *Assume (A1)-(A10). Let (u_ϵ, v_ϵ) be the weak solution pair of system (6.10), and let (u, v) be the weak solution pair of system (6.47), then for $p \in (1, 2]$ there exists a subsequence $\epsilon' \subset \epsilon$ such that the following estimates hold:*

$$\|\psi_{\epsilon'}(u_{\epsilon'} - u)\|_{L^p((0,T)\times\Omega^+)}^p \leq \left(\frac{\frac{G}{L\beta_i}}{1 - \frac{GK}{L\beta_i}} \right)^q \|f_\epsilon - f\|_{L^q((0,T)\times\Omega^+)}^q, \tag{6.50a}$$

$$\|\psi_{\epsilon'}(v_{\epsilon'} - v)\|_{L^p(0,T;W^{1,p}(\Omega^+))}^p \leq \left(\frac{1}{\beta_i - \frac{GK}{L}} \right)^q \|f_\epsilon - f\|_{L^q((0,T)\times\Omega^+)}^q, \tag{6.50b}$$

$$\frac{1}{2} \|\psi_{\epsilon'}(u_{\epsilon'} - u)\|_{L^\infty(0,T;L^2(\Omega^+))}^2 \leq L \left(\frac{\frac{G}{L\beta_i}}{\beta_i - \frac{GK}{L}} \right)^q \|f_\epsilon - f\|_{L^q((0,T)\times\Omega^+)}^q. \tag{6.50c}$$

Proof. We notice that the systems (6.10) and (6.47) have the same structure on Ω^+ , except for the restriction to Ω_ϵ^+ which applies to system (6.10). Hence, we are allowed to exploit the properties (A9) and (A10). We subtract the

weak version of system (6.47) from (6.10) and test with $\phi = \psi_{\epsilon'} (v_{\epsilon'} - v)$ and $\psi = \psi_{\epsilon'} (u_{\epsilon'} - u)$. This leads for $p \in (1, 2]$ to

$$\begin{aligned} & \beta \|\psi_{\epsilon'} (v_{\epsilon'} - v)\|_{L^p(0,T;W^{1,p}(\Omega^+))}^{p-1} \\ & \leq \|f_{\epsilon} - f\|_{L^q((0,T)\times\Omega^+)} + K \|\psi_{\epsilon'} (u_{\epsilon'} - u)\|_{L^p((0,T)\times\Omega^+)}^{p-1}, \end{aligned} \quad (6.51a)$$

$$\begin{aligned} & \|\psi_{\epsilon'} (u_{\epsilon'} - u)\|_{L^\infty(0,T;L^2(\Omega^+))}^2 + L \|\psi_{\epsilon'} (u_{\epsilon'} - u)\|_{L^p((0,T)\times\Omega^+)}^p \\ & \leq G \|\psi_{\epsilon'} (v_{\epsilon'} - v)\|_{L^p(0,T;W^{1,p}(\Omega^+))}^{p-1} \|\psi_{\epsilon'} (u_{\epsilon'} - u)\|_{L^p((0,T)\times\Omega^+)}. \end{aligned} \quad (6.51b)$$

The bound (6.50b) follows from bounding $\|\psi_{\epsilon'} (u_{\epsilon'} - u)\|_{L^p((0,T)\times\Omega^+)}$ in (6.51a) with (6.51b). The bounds (6.50a) and (6.50c) follow from bounding the factor $\|\psi_{\epsilon'} (v_{\epsilon'} - v)\|_{L^p(0,T;W^{1,p}(\Omega^+))}$ in (6.51b) with (6.50b). \square

Since we are using the function ψ_{ϵ} , and knowing its weak-* convergence to B_Y , we wonder whether we can give error bounds on this convergence. The answer is given in the next result.

Lemma 6.19. *Let $\psi_{\epsilon} \in L^\infty(\Omega^+ \cup \Sigma \cup \Omega^-)$ be given as $\psi_{\epsilon}(\mathbf{x}) = \chi_{\Sigma_{\epsilon}}(\mathbf{x}', 0) = \chi_{\omega_{\epsilon}}(\mathbf{x}', 0)$, then there exists a constant C independent of ϵ such that*

$$\left| \int_{\Omega^+} (\psi_{\epsilon} - B_Y) \varphi d\mathbf{x} \right| \leq C\epsilon \|D_{\mathbf{x}'} \varphi\|_{L^1(\Omega^+)} + C\epsilon \|\varphi\|_{L^\infty(\Omega^+)} \quad (6.52)$$

for all $\varphi \in W^{1,1}(\Omega^+) \cap L^\infty(\Omega^+)$.

Proof. On each periodic cell with base $g(Y) \subset \omega$ and, therefore, $g(\mathcal{B}) \subset \omega$ for $g \in G_{\gamma}^{\epsilon}$, we have

$$\begin{aligned} & \left| \int_a^b \int_{g(\mathcal{B})} \varphi d\mathbf{x}' - B_Y \int_{g(Y)} \varphi d\mathbf{x}' dx_d \right| \\ & = \left| \int_a^b \int_{g(Y)} \frac{|g(\mathcal{B})|}{|g(Y)|} \frac{1}{|g(\mathcal{B})|} \int_{g(\mathcal{B})} \varphi d\mathbf{x}' - B_Y \varphi d\mathbf{x}' dx_d \right| \\ & \leq B_Y C \text{diam}(Y) \|D_{\mathbf{x}'} \varphi\|_{L^1(g(Y)\times(a,b))} \end{aligned} \quad (6.53)$$

by the Poincaré-Wirtinger inequality, see Theorem 2.9, for all $\varphi \in W^{1,1}(\Omega^+)$ and all $(a, b) \subset \mathbf{R}$ with C independent of ϵ and using the identity $\frac{|g(\mathcal{B})|}{|g(Y)|} = B_Y$. For the case that $g(y)$ is not entirely contained in ω , the same calculation will have $g(y)$ and $g(\mathcal{B})$ replaced with $g(y) \cap \omega$ and $g(\mathcal{B}) \cap \omega$, respectively. The fraction $\frac{|g(\mathcal{B}) \cap \omega|}{|g(y) \cap \omega|}$ is now not equal to B_Y , but falls into the range $[0, 1)$

as $(g(\mathcal{B}) \cap \omega) \subset (g(Y) \cap \omega)$ and $g(\mathcal{B}) \cap \omega = \emptyset$ might occur. Consequently, the Poincaré-Wirtinger inequality can not be used. However, Minkowski's inequality yields

$$\left| \int_a^b \int_{g(\mathcal{B}) \cap \omega} \varphi d\mathbf{x}' - B_Y \int_{g(Y) \cap \omega} \varphi d\mathbf{x}' dx_d \right| \leq (1 + B_Y) \|\varphi\|_{L^1(g(Y) \cap \omega \times (a,b))}. \quad (6.54)$$

Define a new set, $G_{\gamma,full}^\epsilon(Y)$, as the set of all mappings $g \in G_\gamma^\epsilon$ such that $g(Y) \subset \omega$. Moreover define a complementary set $G_{\gamma,part}^\epsilon(Y)$ as the set of all mappings $g \in G_\gamma^\epsilon$ such that $g(Y)$ is intersected by $\partial\omega$.

Hence, we obtain

$$\left| \int_{\Omega^+} (\psi_\epsilon - B_Y) \varphi d\mathbf{x} \right| \leq \sum_{g \in G_{\gamma,part}^\epsilon} (1 + B_Y) \|\varphi\|_{L^1(g(Y) \cap \omega \times (0,l_d))} + \sum_{g \in G_{\gamma,full}^\epsilon} B_Y C \text{diam}(Y) \|D_{\mathbf{x}'} \varphi\|_{L^1(g(Y) \times (0,l_d))}. \quad (6.55)$$

The first and second term on the right-hand side of (6.55) are bounded by $(1 + B_Y)C|\partial\omega|l_d\epsilon\|\varphi\|_{L^\infty(\Omega^+)}$ and $B_Y C\epsilon \|D_{\mathbf{x}'} \varphi\|_{L^1(\Omega^+)}$ respectively, because $\text{diam}(Y) \leq C\epsilon$ holds and $\bigcup_{g \in G_{\gamma,part}^\epsilon(Y)} g(Y)$ is at most a $\text{diam}(Y)$ -thick layer at the boundary $\partial\omega$. \square

Note that the upper bound in (6.52) holds for $\|(\psi_\epsilon - B_Y)\varphi\|_{L^1(\Omega^+)}$ as one can apply the Poincaré-Wirtinger inequality with respect to the $g(\mathcal{B})$ -average of φ inside the norm. This yields for $g(Y) \subset \omega$ a term similar to the second line of (6.53) with the absolute value inside the double integral. The triangle inequality then shows that the same line of reasoning can be followed to obtain the same upper bound as in (6.52).

In what follows, we give further corrector estimates for a specific case.

Theorem 6.20. *Assume (A1)-(A10). Assume $d = 3$ and $p \in (\frac{3}{2}, 2]$. Let (u_ϵ, v_ϵ) be the weak solution pair of system (6.10), and let (u, v) be the weak solution pair of system (6.47), then there exists a subsequence $\epsilon' \subset \epsilon$ and a constant C independent of ϵ such that the following corrector estimate holds:*

$$\|\psi_{\epsilon'} v_{\epsilon'} - B_Y v\|_{L^1((0,T) \times \Omega^+)} \leq C \|f_\epsilon - f\|_{L^q((0,T) \times \Omega^+)}^{\frac{1}{p-1}} + C\epsilon. \quad (6.56)$$

Proof. Note, for $d = 3$ and $p \in (\frac{3}{2}, 2]$, we have $d < 2p < 2d$. Hence, the Rellich-Kondrachov Theorem (Theorem 2.6) and the Sobolev inequality (Theorem 2.5) yield $W^{2,p}(\Omega^+) \subset L^\infty(\Omega^+) \cap W^{1,1}(\Omega^+)$. Proposition 9.3 in [20] gives $v \in L^p(0, T; W^{2,p}(\Omega^+))$. Hence, v has the right regularity for applying Lemma 6.19. From Proposition 6.18, Lemma 6.19, and the inclusion inequality (Lemma 2.1), we obtain

$$\begin{aligned} & \|\psi_{\epsilon'} v_{\epsilon'} - B_Y v\|_{L^1((0,T) \times \Omega^+)} \\ & \leq (|\Omega^+|T)^{\frac{1}{q}} \|\psi_{\epsilon'}(v_{\epsilon'} - v)\|_{L^p((0,T) \times \Omega^+)} + \|(\psi_{\epsilon'} - B_Y)v\|_{L^1((0,T) \times \Omega^+)} \\ & \leq C \|f_\epsilon - f\|_{L^q((0,T) \times \Omega^+)}^{\frac{1}{p-1}} + C\epsilon. \end{aligned} \quad (6.57)$$

□

Corollary 6.21. *Let the conditions of Theorem 6.20 be satisfied. Suppose $v \in L^p(0, T; W^{3,p}(\Omega^+))$, then*

$$\|\psi_{\epsilon'} v_{\epsilon'} - B_Y v|_\Sigma\|_{L^1((0,T) \times \Omega^-)} \leq Ch_\epsilon^{\frac{1}{2}} + C \|f_\epsilon - f\|_{L^q((0,T) \times \Omega^+)}^{\frac{1}{p-1}} + C\epsilon. \quad (6.58)$$

Proof. (6.58) follows from combining the inequalities stated in Lemma 6.17, Proposition 6.18 and Lemma 6.19 applied to

$$\begin{aligned} & \|\psi_{\epsilon'} v_{\epsilon'} - B_Y v|_\Sigma\|_{L^1((0,T) \times \Omega^-)} \\ & \leq \|\psi_{\epsilon'}(v_{\epsilon'} - v_\epsilon|_\Sigma)\|_{L^1((0,T) \times \Omega^-)} + \|\psi_{\epsilon'}(v_\epsilon|_\Sigma - v|_\Sigma)\|_{L^1((0,T) \times \Sigma)} \\ & \quad + \|(\psi_{\epsilon'} - B_Y)v|_\Sigma\|_{L^1((0,T) \times \Omega^-)} \\ & \leq (|\Omega^-|T)^{\frac{1}{q}} \|\psi_{\epsilon'}(v_{\epsilon'} - v_\epsilon|_\Sigma)\|_{L^p((0,T) \times \Omega^-)} + l_d \left\| \psi_{\epsilon'} \frac{\partial(v_\epsilon - v)}{\partial x_d} \right\|_{L^1((0,T) \times \Omega^+)} \\ & \quad + l_d \left\| (\psi_{\epsilon'} - B_Y) \frac{\partial v}{\partial x_d} \right\|_{L^1((0,T) \times \Omega^+)}, \end{aligned} \quad (6.59)$$

where we used the inclusion inequality (Lemma 2.1) and a combination of the Poincaré inequality (Theorem 2.8) and the Poincaré-Wirtinger inequality (Theorem 2.9), which in 1D is basically an application of the fundamental theorem of calculus applied to a continuous representative. □

Combining some corrector estimates, we obtain a comprehensive result for the convergence rate to the solution (u, v) .

Theorem 6.22. *Assume (A1)-(A10). Assume $d = 3$ and $p \in (\frac{3}{2}, 2]$. Let (u_ϵ, v_ϵ) be the weak solution pair of system (6.10), and let (u, v) be the weak*

solution pair of system (6.47), then there exists a subsequence $\epsilon' \subset \epsilon$ and a constant C independent of ϵ such that the following corrector estimate holds:

$$\|\psi_{\epsilon'} v_{\epsilon'} - B_Y v\|_{L^1((0,T) \times \Omega^+)} \leq C \|f_{\epsilon} - f\|_{L^q((0,T) \times \Omega^+)}^{\frac{1}{p-1}} + C\epsilon, \quad (6.60)$$

$$\|\psi_{\epsilon'} (u_{\epsilon'} - u)\|_{L^p((0,T) \times \Omega^+)}^p \leq \left(\frac{\frac{G}{L\beta_i}}{1 - \frac{GK}{L\beta_i}} \right)^q \|f_{\epsilon} - f\|_{L^q((0,T) \times \Omega^+)}^q, \quad (6.61a)$$

$$\frac{1}{2} \|\psi_{\epsilon'} (u_{\epsilon'} - u)\|_{L^\infty(0,T;L^2(\Omega^+))}^2 \leq L \left(\frac{\frac{G}{L\beta_i}}{\beta_i - \frac{GK}{L}} \right)^q \|f_{\epsilon} - f\|_{L^q((0,T) \times \Omega^+)}^q. \quad (6.61b)$$

6.6 A comment on the case $p = 2$.

For the case $p = 2$, the appearance of an additional drift term in the Neumann problem (6.1) does not significantly change the results from Sections 6.4 and 6.5 what concerns the asymptotic behaviour for $\epsilon \downarrow 0$ of the weak solutions or for the convergence rate results.

We state here a modification of (6.1), namely: Find (U_ϵ, V_ϵ) satisfying

$$\begin{cases} \mathcal{M}(V_\epsilon) - \operatorname{div}(\mathcal{E}(\nabla V_\epsilon) + \mathcal{D}(V_\epsilon)) = F_\epsilon + \mathcal{K}(U_\epsilon) & \text{in } \Omega_\epsilon \times (0, T), \\ \frac{\partial U_\epsilon}{\partial t} + \mathcal{L}(U_\epsilon) = \mathcal{G}(V_\epsilon) & \text{in } \Omega_\epsilon \times [0, T], \\ (\mathcal{E}(\nabla V_\epsilon) + \mathcal{D}(V_\epsilon)) \cdot \mathbf{n}_\epsilon = 0 & \text{on } \partial\Omega_\epsilon \times (0, T), \\ U_\epsilon = U^* & \text{in } \Omega_\epsilon \times \{0\}, \end{cases} \quad (6.62)$$

where \mathbf{n}_ϵ denotes the exterior unit normal on $\partial\Omega_\epsilon$.

We assume the following additional properties:

(A1*) $\mathcal{D} = (\mathcal{D}_1, \dots, \mathcal{D}_d) : \mathbf{R}^d \rightarrow \mathbf{R}^d$ is a monotone continuous function satisfying

$$\exists d_s \in \mathbf{R}_+ : |\mathcal{D}(\zeta)| \leq d_s |\zeta| \quad \text{for all } \zeta \in \mathbf{R}, \quad (6.63)$$

such that the following ellipticity condition holds true

$$d_s \leq 2m_i^{1/2} e_i^{1/2}. \quad (6.64)$$

(A9*) The operator \mathcal{D} satisfies the Lipschitz condition

$$\exists \mathfrak{D} \in \mathbf{R}_+ : |\mathcal{D}(\zeta_1) - \mathcal{D}(\zeta_2)| \leq \mathfrak{D} |\zeta_1 - \zeta_2| \quad \text{for all } \zeta_1, \zeta_2 \in \mathbf{R}. \quad (6.65)$$

Moreover, we have the strict monotonicity condition

$$\mathfrak{D} < 2M^{1/2}E^{1/2}. \quad (6.66)$$

(A10*) If (A9), (A10), and (A9*) holds, then the bound (6.7) is replaced by the stricter bound

$$\frac{GK}{L} < \beta_i = \min_{\left(\frac{\mathfrak{D}}{2E}\right)^{\frac{1}{2}} < \eta < \left(\frac{2M}{\mathfrak{D}}\right)^{\frac{1}{2}}} \left\{ M - \frac{\mathfrak{D}\eta^2}{2}, E - \frac{\mathfrak{D}}{2\eta^2} \right\}. \quad (6.67)$$

We employ the rescalings (6.8), (6.9a), (6.9b),(6.9c), and (6.9d). Hence, we are able to introduce the following concept of weak solutions to system (6.62).

Definition 6.23. *The pair $(u_\epsilon, v_\epsilon) \in L^2((0, T) \times \Omega_\epsilon^+ \cup \Omega^-) \cap H^1(0, T; L^2(\Omega_\epsilon^+ \cup \Omega^-)) \times L^2(0, T; W^{1,2}(\Omega_\epsilon^+ \cup \Omega^-))$ given by (6.9a) and (6.9b) is a weak solution of (6.62) if the following identities*

$$\left\{ \begin{array}{l} \int_{\Omega_\epsilon^+} \mathcal{M}(v_\epsilon)\phi + (\mathcal{E}(Dv_\epsilon) + \mathcal{D}(v_\epsilon)) \cdot D\phi d\mathbf{x} \\ + h_\epsilon \int_{\Omega^-} \mathcal{M}(v_\epsilon)\phi + \left(\mathcal{E} \left(D_{\mathbf{x}'} v_\epsilon, \frac{1}{h_\epsilon} \frac{\partial v_\epsilon}{\partial x_d} \right) + \mathcal{D}(v_\epsilon) \right) \cdot \left(D_{\mathbf{x}'} \phi, \frac{1}{h_\epsilon} \frac{\partial \phi}{\partial x_d} \right) d\mathbf{x} \\ = \int_{\Omega_\epsilon^+} (f_\epsilon + \mathcal{K}(u_\epsilon)) \phi d\mathbf{x} + h_\epsilon \int_{\Omega^-} (f_\epsilon + \mathcal{K}(u_\epsilon)) \phi d\mathbf{x} \quad \text{for a.e. } t \in (0, T), \\ \int_{\Omega_\epsilon^+} \left(\frac{\partial u_\epsilon}{\partial t} + \mathcal{L}(u_\epsilon) \right) \psi d\mathbf{x} + h_\epsilon \int_{\Omega^-} \left(\frac{\partial u_\epsilon}{\partial t} + \mathcal{L}(u_\epsilon) \right) \psi d\mathbf{x} \\ = \int_{\Omega_\epsilon^+} \mathcal{G}(v_\epsilon)\psi d\mathbf{x} + h_\epsilon \int_{\Omega^-} \mathcal{G}(v_\epsilon)\psi d\mathbf{x} \quad \text{for a.e. } t \in [0, T], \\ (\mathcal{E}(Dv_\epsilon) + \mathcal{D}(v_\epsilon)) \cdot \mathbf{n} = 0 \quad \text{on } \partial(\Omega_\epsilon^+ \cup \Omega^-) \text{ for a.e. } t \in (0, T), \\ u_\epsilon = u_\epsilon^* \quad \text{on } \overline{\Omega_\epsilon^+ \cup \Omega^-} \text{ for } t = 0 \end{array} \right. \quad (6.68)$$

hold for all $\phi \in H^1(\Omega_\epsilon^+ \cup \Omega^-)$ and $\psi \in L^2(\Omega_\epsilon^+ \cup \Omega^-)$.

We introduce the monotone operator $\mathcal{T}_D : W^{1,2}(\Omega_\epsilon) \rightarrow (W^{1,2}(\Omega_\epsilon))^*$ given by

$$\langle \phi, \mathcal{T}_D v \rangle = \int_{\Omega_\epsilon} \mathcal{M}(v)\phi + [\mathcal{E}(\nabla v) + \mathcal{D}(v)] \cdot \nabla \phi d\mathbf{x} \text{ for all } \phi \in W^{1,2}(\Omega_\epsilon). \quad (6.69)$$

It turns out that \mathcal{T}_D is maximal monotone operators.

Lemma 6.24. *Given (A1), then \mathcal{T}_0 is a coercive, maximal monotone operator. If additionally (A6) or (A9) is satisfied, then \mathcal{T}_0 is also strictly monotone.*

Given $p = 2$, (A1) and (A9), then \mathcal{T}_D is a coercive, strictly monotone, maximal monotone operator.

Proof. Choosing $\phi = v$, we see by (A1) and by applying Young's inequality that \mathcal{T}_D is coercive with the coercivity constant

$$\alpha = \min_{\sqrt{\frac{d_s}{2e_i}} < \eta < \sqrt{\frac{2m_i}{d_s}}} \left\{ e_i - \frac{d_s}{2\eta^2}, m_i - \frac{d_s\eta^2}{2} \right\} > 0. \quad (6.70)$$

By (A9) and Young's inequality, we obtain

$$\begin{aligned} \langle v_1 - v_2, \mathcal{T}_D v_1 - \mathcal{T}_D v_2 \rangle &\geq \left(M - \frac{\mathfrak{D}\eta^2}{2} \right) \|v_1 - v_2\|_{L^2(\Omega_\epsilon)}^2 \\ &\quad + \left(E - \frac{\mathfrak{D}}{2\eta^2} \right) \|\nabla v_1 - \nabla v_2\|_{L^2(\Omega_\epsilon)}^2 \\ &\geq \beta \|v_1 - v_2\|_{W^{1,2}(\Omega_\epsilon)}^2 \end{aligned} \quad (6.71)$$

for $\sqrt{\frac{\mathfrak{D}}{2E}} < \eta < \sqrt{\frac{2M}{\mathfrak{D}}}$ and with β as defined in (6.4c). Hence, \mathcal{T}_D is strictly monotone.

The remainder of the proof is identical to the proof of (6.84), since \mathcal{D} can be shown to be demicontinuous in the same way as \mathcal{E} was shown to be demicontinuous. \square

Introduce the $\epsilon \downarrow 0$ limit $\chi_{\Omega_\epsilon^+} \mathcal{D}(v_\epsilon) \rightharpoonup \mathbf{D}^+ = (D_1^+, \dots, D_d^+)$ in $L^2((0, T) \times \Omega^+)^d$. The ϵ -independent boundedness of $\chi_{\Omega_\epsilon^+} \mathcal{D}(v_\epsilon)$ follows from Lemma 6.24. All convergence and corrector results can now be extended to the $p = 2$ case with drift term $\mathcal{D}(v_\epsilon)$ by changing the assumptions into their starred versions, all e_i^+ into $e_i^+ + D_i^+$ and all $\mathcal{E}_i \left(\frac{\mathbf{d}'}{B_Y}, \frac{\partial v}{\partial x_d} \right)$ into $\mathcal{E}_i \left(\frac{\mathbf{d}'}{B_Y}, \frac{\partial v}{\partial x_d} \right) + \mathcal{D}_i(v)$ for all $i \in \{1, \dots, d\}$, and all \mathcal{T}_0 into \mathcal{T}_D .

6.7 Conclusions

The vanishing thickness of the non-touching cylinders as $\epsilon \downarrow 0$ implies that the boundary conditions valid on the cylinder boundaries must hold almost everywhere in the domain Ω^+ in the limit $\epsilon = 0$. The non-touching condition is essential as it guarantees the existence of continuous $W^{1,1}(\Omega^+)$ sequences of functions which are constant on Ω_ϵ^+ , but are approximating any chosen linear

function in Ω^+ from below as $\epsilon \downarrow 0$. Consequently, there is a loss of regularity of the solution (u, v) of the limit system on the directions \mathbf{x}' as only the $\partial/\partial x_d$ gradient remains in the elliptic part of the coupled limit system.

The simultaneous vanishing thickness of the substrate as $\epsilon \downarrow 0$ implies that the solution (u_ϵ, v_ϵ) on Ω^- converges to the constant function with value equal to the boundary value of (u, v) at the interface Σ .

The specific pseudoparabolic system of this paper yields a lower regularity for u_ϵ than for v_ϵ . As a direct consequence only a corrector estimate for v_ϵ in Ω^- can be obtained, but not for u_ϵ in Ω^- . Even in Ω^+ only corrector estimates far from the boundary can be obtained for u_ϵ due to the low regularity.

6.8 Appendix: An approximation scheme of (U_ϵ, V_ϵ)

Theorem 6.25 (Approximation result). *Assume (A1), (A2), (A7)-(A10). Let $U^* \in L^2(\Omega)$, and let $p \geq 2$. Introduce two sequences $\{U_\epsilon^N\}$ and $\{V_\epsilon^N\}$ for $N \geq 1$ with $V_\epsilon^0 = 0$, via $U_\epsilon^N \in L^p((0, T) \times \Omega_\epsilon) \cap H^1(0, T; L^2(\Omega_\epsilon))$ the unique weak solution of*

$$\begin{cases} \int_{\Omega_\epsilon} \left(\frac{dU_\epsilon^N}{dt} + \mathcal{L}(U_\epsilon^N) \right) \psi d\mathbf{x} = \int_{\Omega_\epsilon} \mathcal{G}(V_\epsilon^{N-1}) \psi d\mathbf{x} & \text{in } \Omega_\epsilon \times (0, T), \\ U_\epsilon^N = U^* & \text{on } \overline{\Omega_\epsilon} \times \{0\}. \end{cases} \quad (6.72)$$

for $V_\epsilon^{N-1} \in L^p((0, T) \times \Omega_\epsilon)$ for all $\psi \in L^q((0, T) \times \Omega_\epsilon)$, and $V_\epsilon^N \in L^p(0, T; W^{1,p}(\Omega_\epsilon))$ the unique weak solution of

$$\begin{cases} \langle \phi, \mathcal{T}V_\epsilon^N \rangle = \int_{\Omega_\epsilon^+} (F_\epsilon + \mathcal{K}(U_\epsilon^N)) \phi d\mathbf{x} & \text{in } \Omega_\epsilon \times (0, T), \\ \mathcal{E}(\nabla V_\epsilon^N) \cdot \mathbf{n} = 0 & \text{on } \partial\Omega_\epsilon \times (0, T) \end{cases} \quad (6.73)$$

for $U_\epsilon^N \in L^p((0, T) \times \Omega_\epsilon) \cap H^1(0, T; L^2(\Omega_\epsilon))$ for all $\phi \in L^p(0, T; W^{1,p}(\Omega_\epsilon))$, where

$$\langle \phi, \mathcal{T}V_\epsilon^N \rangle = \int_{\Omega_\epsilon^+} \mathcal{E}(\nabla V_\epsilon^N) \cdot \nabla \phi + \mathcal{M}(V_\epsilon^N) \phi d\mathbf{x}. \quad (6.74)$$

Then there are functions $U_\epsilon \in L^p((0, T) \times \Omega_\epsilon) \cap H^1(0, T; L^2(\Omega_\epsilon))$ and $V_\epsilon \in L^p(0, T; W^{1,p}(\Omega_\epsilon))$ such that

$$U_\epsilon^N \rightarrow U_\epsilon \text{ in } L^p((0, T) \times \Omega_\epsilon) \quad \text{and} \quad V_\epsilon^N \rightarrow V_\epsilon \text{ in } L^p(0, T; W^{1,p}(\Omega_\epsilon)) \quad (6.75)$$

as $N \rightarrow \infty$ and (U_ϵ, V_ϵ) is the unique solution pair of system (6.1).

In this section, we prove Theorem 6.25. We base our existence and uniqueness proof of weak solutions to (6.10) in the sense of Definition 6.1 on the theory of monotone operators, see [127].

Remark 6.2. *Our approach for showing existence and uniqueness consists of several steps. First, we show that the first equation of (6.1) can be written in terms of a maximal monotone coercive operator \mathcal{T} on the left-hand side. Hence, \mathcal{T} has a solution u_ϵ for any given v_ϵ . Second, we show that \mathcal{T} is a strictly monotone operator, implying that \mathcal{T} has a unique solution u_ϵ for any given v_ϵ . Third, we use a standard result of monotone operator theory to obtain a unique solution u_ϵ of the second equation of (6.1) for any given v_ϵ . Then, we create an iterated scheme in which we start with $v_\epsilon^0 = 0$ and proceed from $n = 1$ on with obtaining v_ϵ^n from u_ϵ^n , and u_ϵ^{n+1} from v_ϵ^n . This yields sequences of solutions $\{u_\epsilon^n\}$ and $\{v_\epsilon^n\}$ that converge both weakly and strongly to u_ϵ and v_ϵ , respectively. Moreover, we show that these limits form a valid solution pair for (6.1). Finally, we show that (6.1) has only a single solution pair.*

Firstly, we show that there exist monotone operators that satisfy (A1), (A6), (A7), and (A9) simultaneously.

Lemma 6.26. *Let $p > 1$ and $n \in \mathbf{N}$ given. Introduce $\mathcal{S} : \mathbf{R}^n \rightarrow \mathbf{R}^n$, defined by $\mathcal{S}(\zeta) = |\zeta|^{p-2}\zeta$ for $\zeta \in \mathbf{R}^n$. Then \mathcal{S} is a strictly monotone, continuous function satisfying*

$$\exists s_i \in \mathbf{R}_+ : s_i |\zeta|^p \leq \mathcal{S}(\zeta)\zeta \text{ for all } \zeta \in \mathbf{R}^n, \quad (6.76a)$$

$$\exists s_s \in \mathbf{R}_+ : |\mathcal{S}(\zeta)| \leq s_s |\zeta|^{p-1} \text{ for all } \zeta \in \mathbf{R}^n, \quad (6.76b)$$

for all $p > 1$, and satisfying

$$\exists S \in \mathbf{R}_+ : (\mathcal{S}(\zeta_1) - \mathcal{S}(\zeta_2))(\zeta_1 - \zeta_2) \geq S |\zeta_1 - \zeta_2|^p \text{ for all } \zeta_1, \zeta_2 \in \mathbf{R}^n \quad (6.77)$$

for all $p \geq 2$.

Proof. Properties (6.76a) and (6.76b) are straightforward and yield $s_i = s_s = 1$. To prove both the continuity of \mathcal{S} and property (6.77), we use the identity:

$$\begin{aligned} \mathcal{S}(\zeta_1) - \mathcal{S}(\zeta_2) &= \frac{1}{2} (|\zeta_1|^{p-2} + |\zeta_2|^{p-2}) (\zeta_1 - \zeta_2) \\ &\quad + \frac{1}{2} (|\zeta_1|^{p-2} - |\zeta_2|^{p-2}) (\zeta_1 + \zeta_2). \end{aligned} \quad (6.78)$$

The operator \mathcal{S} is continuous, since

$$\begin{aligned} |\mathcal{S}(\zeta_1) - \mathcal{S}(\zeta_2)| &\leq \max\{|\zeta_1|, |\zeta_2|\}^{p-2} |\zeta_1 - \zeta_2| \\ &\quad + |p-2| \max\{|\zeta_1|, |\zeta_2|\} \max\{|\zeta_1|^{p-3}, |\zeta_2|^{p-3}\} |\zeta_1 - \zeta_2| \end{aligned} \quad (6.79)$$

for $\zeta_1, \zeta_2 \in \mathbf{R}^n \setminus \{\mathbf{0}\}$, which follows by application of the Mean Value Theorem and from the fact that x^α is either monotonically increasing or monotonically decreasing for $\alpha \in \mathbf{R}$ and $x \in \mathbf{R}_+$. Note that property (6.76b) yields continuity for the cases $\zeta_1 = \mathbf{0}$ or $\zeta_2 = \mathbf{0}$ in (6.79).

As we will show next, property (6.77) now follows from the generalized mean inequality (see Inequality 8) and the triangle inequality (see Inequality 1). For $p \in \{2\} \cup [3, \infty)$, we have

$$\begin{aligned} &(\mathcal{S}(\zeta_1) - \mathcal{S}(\zeta_2))(\zeta_1 - \zeta_2) \\ &= \frac{1}{2} (|\zeta_1|^{p-2} + |\zeta_2|^{p-2}) |\zeta_1 - \zeta_2|^2 + \frac{1}{2} (|\zeta_1|^{p-2} - |\zeta_2|^{p-2}) (|\zeta_1|^2 - |\zeta_2|^2) \\ &\geq \frac{1}{2} (|\zeta_1|^{p-2} + |\zeta_2|^{p-2}) |\zeta_1 - \zeta_2|^2 = [\mathcal{M}_{p-2}(|\zeta_1|, |\zeta_2|)]^{p-2} |\zeta_1 - \zeta_2|^2 \\ &\geq \left(\frac{|\zeta_1| + |\zeta_2|}{2} \right)^{p-2} |\zeta_1 - \zeta_2|^2 = [\mathcal{M}_1(|\zeta_1|, |\zeta_2|)]^{p-2} |\zeta_1 - \zeta_2|^2 \\ &\geq \left(\frac{1}{2} \right)^{p-2} |\zeta_1 - \zeta_2|^p, \end{aligned} \quad (6.80)$$

due to convexity of x^{p-2} . For $p \in (2, 3)$, we have

$$\begin{aligned} &(\mathcal{S}(\zeta_1) - \mathcal{S}(\zeta_2))(\zeta_1 - \zeta_2) \\ &= \frac{1}{2} (|\zeta_1|^{p-2} + |\zeta_2|^{p-2}) |\zeta_1 - \zeta_2|^2 + \frac{1}{2} (|\zeta_1|^{p-2} - |\zeta_2|^{p-2}) (|\zeta_1|^2 - |\zeta_2|^2) \\ &\geq \frac{1}{2} (|\zeta_1|^{p-2} + |\zeta_2|^{p-2}) |\zeta_1 - \zeta_2|^2 \\ &\geq \frac{1}{2} (|\zeta_1| + |\zeta_2|)^{p-2} |\zeta_1 - \zeta_2|^2 \\ &\geq \frac{1}{2} |\zeta_1 - \zeta_2|^p, \end{aligned} \quad (6.81)$$

due to subadditivity of concave functions and because x^{p-2} is a monotonically increasing function. The strict monotonicity is for $p \geq 2$ a direct consequence of (6.77).

The strict monotonicity for $p \in (1, 2)$ is shown in two steps. First, for $|\zeta_1| = |\zeta_2|$, we have $0 = (\mathcal{S}(\zeta_1) - \mathcal{S}(\zeta_2))(\zeta_1 - \zeta_2) = |\zeta_1|^{p-2} |\zeta_1 - \zeta_2|^2$. Consequently,

$\zeta_1 = \zeta_2$, since $1/|\zeta_1| = 0$ is not allowed. Second, for $|\zeta_1| \neq |\zeta_2|$, we have

$$\begin{aligned}
& (\mathcal{S}(\zeta_1) - \mathcal{S}(\zeta_2))(\zeta_1 - \zeta_2) \\
&= \frac{1}{2}(|\zeta_1|^{p-2} + |\zeta_2|^{p-2})|\zeta_1 - \zeta_2|^2 + \frac{1}{2}(|\zeta_1|^{p-2} - |\zeta_2|^{p-2})(|\zeta_1|^2 - |\zeta_2|^2) \\
&= \frac{1}{2}|\zeta_1|^{p-1} \left[\frac{|\zeta_1 - \zeta_2|^2 - |\zeta_2|^2}{|\zeta_1|} + |\zeta_1| \right] + \frac{1}{2}|\zeta_2|^{p-1} \left[\frac{|\zeta_1 - \zeta_2|^2 - |\zeta_1|^2}{|\zeta_2|} + |\zeta_2| \right] \\
&\geq |\zeta_1|^{p-1}(|\zeta_1| - |\zeta_2|) + |\zeta_2|^{p-1}(|\zeta_2| - |\zeta_1|) \\
&= (|\zeta_1|^{p-1} - |\zeta_2|^{p-1})(|\zeta_1| - |\zeta_2|) \\
&> 0
\end{aligned} \tag{6.82}$$

due to the triangle inequality and because x^{p-1} is a monotonically increasing function. Hence, we have strict monotonicity as $0 = (\mathcal{S}(\zeta_1) - \mathcal{S}(\zeta_2))(\zeta_1 - \zeta_2)$ is equivalent to $\zeta_1 = \zeta_2$. \square

With the existence of monotone operators that satisfy both (A1) and (A6), we are able to introduce the monotone operator $\mathcal{T}_0 : W^{1,p}(\Omega_\epsilon) \rightarrow (W^{1,p}(\Omega_\epsilon))^*$ given by

$$\langle \phi, \mathcal{T}_0 v \rangle = \int_{\Omega_\epsilon} \mathcal{M}(v)\phi + \mathcal{E}(\nabla v) \cdot \nabla \phi d\mathbf{x}. \tag{6.83}$$

It turns out that \mathcal{T}_0 is a maximal monotone operator.

Lemma 6.27. *Given (A1), then \mathcal{T}_0 is a coercive, maximal monotone operator. If additionally (A6) or (A9) is satisfied, then \mathcal{T}_0 is also strictly monotone.*

Proof. Choosing $\phi = v$, we see via (A1) and Young's inequality that \mathcal{T}_0 is coercive with coercivity constant

$$\alpha = \min \{e_i, m_i\} > 0. \tag{6.84}$$

The operators \mathcal{M} and \mathcal{E} are monotone by (A1) and, by linearity, so is \mathcal{T}_0 . Since (A6) is implied by (A9), we only show the strict monotonicity with the additional assumption (A6). For the strict monotonicity, we need to ensure that $\langle v_1 - v_2, \mathcal{T}_0 v_1 - \mathcal{T}_0 v_2 \rangle = 0$ implies $v_1 = v_2$ in $W^{1,p}(\Omega_\epsilon)$. Due to the monotonicity of \mathcal{E} and \mathcal{M} and the respective linearity, we have $(\mathcal{E}(\nabla v_1) - \mathcal{E}(\nabla v_2))(\nabla v_1 - \nabla v_2) = 0$ and $(\mathcal{M}(v_1) - \mathcal{M}(v_2))(\nabla v_1 - \nabla v_2) = 0$. From (A6), the strict monotonicity of \mathcal{E} and \mathcal{M} yields $v_1 = v_2$ a.e. in Ω_ϵ and $\nabla v_1 = \nabla v_2$ a.e. in Ω_ϵ . Thus $v_1 = v_2$ in $W^{1,p}(\Omega_\epsilon)$. Hence, \mathcal{T}_0 is strictly monotone. Take a sequence $\{v_n\} \in W^{1,p}(\Omega_\epsilon)$ such that $v_n \rightarrow v$ in $W^{1,p}(\Omega_\epsilon)$. Then $\nabla v_n \rightarrow \nabla v$ in $L^p(\Omega_\epsilon)$. By continuity $\mathcal{E}(\nabla v_n) \rightarrow \mathcal{E}(\nabla v)$, and $\mathcal{M}(v_n) \rightarrow \mathcal{M}(v)$

a.e. on Ω_ϵ for a subsequence. Moreover, by (A1), $\{\mathcal{E}(\nabla v_n)\}$ is bounded in $L^q(\Omega_\epsilon)^d$, and $\{\mathcal{M}(v_n)\}$ is bounded in $L^q(\Omega_\epsilon)$. Thus $\mathcal{E}(\nabla v_n) \rightharpoonup \mathcal{E}(\nabla v)$ in $L^q(\Omega_\epsilon)^d$, and $\mathcal{M}(v_n) \rightharpoonup \mathcal{M}(v)$ in $L^q(\Omega_\epsilon)$. Hence, $\mathcal{T}_0 v_n \rightharpoonup \mathcal{T}_0 v$ in $(W^{1,p}(\Omega_\epsilon))^*$. Thus \mathcal{T}_0 is demicontinuous. The operator \mathcal{T}_0 is well-defined for all $W^{1,p}(\Omega_\epsilon)$. Therefore, [73] states that \mathcal{E} , \mathcal{M} , and \mathcal{T}_0 are hemicontinuous. Since $W^{1,p}(\Omega_\epsilon)$ is a reflexive Banach space, we find that \mathcal{E} , \mathcal{M} , and \mathcal{T}_0 are maximal monotone. \square

Lemma 6.28. *Assume (A1) and (A2) hold. Given $u \in W^{1,p}(\Omega_\epsilon)$, there exist weak solutions $v \in W^{1,p}(\Omega_\epsilon)$ of*

$$\langle \phi, \mathcal{T}_0 v \rangle = \int_{\Omega_\epsilon} (F_\epsilon + \mathcal{K}(u)) \phi d\mathbf{x} \quad (6.85)$$

for all $\phi \in W^{1,p}(\Omega_\epsilon)$.

Proof. By (A2), we see $F_\epsilon + \mathcal{K}(u) \in L^q(\Omega_\epsilon) \subset (W^{1,p}(\Omega_\epsilon))^*$. Then, since \mathcal{T}_0 is maximal monotone by Lemma 6.27, \mathcal{T}_0 is surjective on $(W^{1,p}(\Omega_\epsilon))^*$. Hence, there exist weak solutions to (6.85) for any given $v \in W^{1,p}(\Omega_\epsilon)$. \square

Lemma 6.29. *Assume (A1), (A2) and (A9) hold. Given $u \in W^{1,p}(\Omega_\epsilon)$, there exist a unique weak solution $v \in W^{1,p}(\Omega_\epsilon)$ of (6.85).*

Proof. Assume there are at least two solutions v_1 and v_2 of (6.85). Since the right-hand side of (6.85) is independent of v , we see that the difference of (6.85) for v_1 and v_2 yields $\langle v_1 - v_2, \mathcal{T}_0 v_1 - \mathcal{T}_0 v_2 \rangle = 0$. The operator \mathcal{T}_0 is strictly monotone. Hence, $v_1 = v_2$, which is a contradiction. Thus the weak solution to (6.85) is unique. \square

Lemma 6.30. *Assume (A2), (A7) and (A8).*

For $p \geq 2$ and $U^ \in L^2(\Omega)$, given $v \in L^p(0, T; W^{1,p}(\Omega_\epsilon))$, there exists a unique weak solution u of*

$$\begin{cases} \frac{du}{dt} + \mathcal{L}u = \mathcal{G}(v) & \text{in } (0, T) \times \Omega_\epsilon, \\ u(0) = U^* & \text{on } \{0\} \times \Omega_\epsilon. \end{cases} \quad (6.86)$$

with regularity $L^p((0, T) \times \Omega_\epsilon) \cap W^{1,q}(0, T; L^q(\Omega_\epsilon)) \cap C([0, T]; L^2(\Omega_\epsilon))$.

For $p \in (1, 2)$, assume additionally (A9). Given $v \in L^p(0, T; W^{1,p}(\Omega_\epsilon))$, there exists a unique weak solution u of (6.86) with regularity $L^p((0, T) \times \Omega_\epsilon) \cap L^\infty(0, T; L^2(\Omega_\epsilon)) \cap H^1(0, T; L^2(\Omega_\epsilon))$.

Proof. For $p \geq 2$, this is a standard result in [127]. By (A8), the initial function $u_0 = U^*$ satisfies the correct regularity. By (A7) and mimicking the proof of Lemma 6.27, the operator \mathcal{L} is monotone, hemicontinuous and has time-independent continuity and coercivity. So, pointwise in time, \mathcal{L} satisfies the desired continuity and coercivity properties. As the coercivity and continuity constants are time-independent, these properties even hold uniformly in time. Finally, by (A2), \mathcal{G} maps any function in $v \in L^p(0, T; W^{1,p}(\Omega_\epsilon))$ to a function in $L^q(0, T; W^{1,p}(\Omega_\epsilon))$. Hence, $\mathcal{G}(v)$ has the correct regularity.

For $p \in (1, 2)$, by strict monotonicity and linearity of the time-derivative, we obtain uniqueness in a straightforward manner:

$$\|u_1 - u_2\|_{L^\infty(0,T;L^2(\Omega_\epsilon))}^2 + 2L\|u_1 - u_2\|_{L^p((0,T)\times\Omega_\epsilon)}^p \leq 0. \quad (6.87)$$

Moreover, testing with $\frac{\partial u}{\partial t}$, applying Hölder's inequality, the inclusion inequality (Lemma 2.1), and Young's inequality yields

$$\begin{aligned} & \left\| \frac{\partial u}{\partial t} \right\|_{L^2((0,T)\times\Omega_\epsilon)}^2 \left(1 - \frac{\eta^2}{2} (|\Omega_\epsilon|T)^{2-p} \right) \\ & \leq \frac{g_s^{\frac{p}{p-1}} \|v\|_{L^p((0,T)\times\Omega_\epsilon)}^p + l_s^{\frac{p}{p-1}} \|u\|_{L^p((0,T)\times\Omega_\epsilon)}^p}{p/(p-1)} + \frac{1 - \frac{p}{2}}{p\eta^{\frac{2p}{2-p}}} |\Omega_\epsilon| \end{aligned} \quad (6.88)$$

for some $\eta \in (0, \sqrt{2} [|\Omega_\epsilon|T]^{\frac{p}{2}-1})$.

For the existence, we discretize in time via the Rothe method. Since the operator $\mathcal{A}_{\Delta t}(u) = u + \Delta t \mathcal{L}(u)$ is a coercive and hemicontinuous strictly monotone operator in $L^2(\Omega_\epsilon)$ for all $\Delta t \leq 1$ due to the inclusion inequality, and (A7) guarantees via the inclusion inequality that $\mathcal{G}(v) \in L^2(\Omega_\epsilon)$, we obtain a unique weak solution $u^k = u|_{t=k\Delta t} \in L^2(\Omega_\epsilon)$ of $\mathcal{A}_{\Delta t}(u^k) = u^{k-1} + \Delta t \mathcal{G}(v^k)$ at each time slice $\{t = k\Delta t\}$ for $k\Delta t \in (0, T]$. Moreover, we obtain $(u^k - u^{k-1})/\Delta t \in L^2(\Omega_\epsilon)$ for $k\Delta t \in [\Delta t, T]$. Due to Δt -independent bounds of $u^k \in L^2(\Omega_\epsilon)$ and due to the Lions-Aubin-Simon lemma, we obtain a family of piecewise constant on $(0, T]$ functions $u_{\Delta t} \rightarrow u \in L^2((0, T) \times \Omega_\epsilon)$ and $(u^k - u^{k-1})/\Delta t \chi_{[\Delta t, T]} \rightarrow \partial u / \partial t \in L^2((0, T) \times \Omega_\epsilon)$. Hence, by the demicontinuity of \mathcal{L} , u is a weak solution of (6.86) and it is the unique solution due to the previously shown uniqueness. \square

Even though separate solutions u_ϵ and v_ϵ can be found given v_ϵ and u_ϵ , respectively, it is not clear that a coupled (u_ϵ, v_ϵ) solution to (6.10) can be found.

We create the sequences $\{U_\epsilon^n\}$ and $\{V_\epsilon^n\}$ for $n \geq 1$ with $V_\epsilon^0 = 0$, and where

$U_\epsilon^N \in H^1(0, T; L^2(\Omega_\epsilon)) \cap L^p((0, T) \times \Omega_\epsilon)$ is the unique weak solution of

$$\begin{cases} \frac{dU_\epsilon^N}{dt} + \mathcal{L}(U_\epsilon^N) = \mathcal{G}(V_\epsilon^{N-1}) & \text{in } (0, T) \times \Omega_\epsilon, \\ U_\epsilon^N = U^* & \text{on } \{0\} \times \overline{\Omega_\epsilon}. \end{cases} \quad (6.89)$$

and $V_\epsilon^N \in L^p(0, T; W^{1,p}(\Omega_\epsilon))$ is the unique weak solution of

$$\begin{cases} \langle \phi, \mathcal{T}_0 V_\epsilon^N \rangle = \int_{\Omega_\epsilon^+} (F_\epsilon + \mathcal{K}(U_\epsilon^N)) \phi d\mathbf{x} & \text{in } (0, T) \times \Omega_\epsilon, \\ (\mathcal{E}(\nabla V_\epsilon^N) + \mathcal{D}(V_\epsilon^N)) \cdot n = 0 & \text{on } \partial\Omega_\epsilon \times (0, T). \end{cases} \quad (6.90)$$

Hence, we have a sequence of mappings

$$0 = V_\epsilon^0 \mapsto U_\epsilon^1 \mapsto V_\epsilon^1 \mapsto \dots \mapsto V_\epsilon^{N-1} \mapsto U_\epsilon^N \mapsto V_\epsilon^N \mapsto \dots \quad (6.91)$$

We are interested in the limit behaviour ($N \rightarrow \infty$) of this procedure, which is reminiscent of Picard iteration.

Proposition 6.31. *Assume (A1), (A2), (A7), (A8) and (A9). Then there are functions $U_\epsilon \in H^1(0, T; L^2(\Omega_\epsilon^+)) \cap L^p((0, T) \times \Omega_\epsilon)$, $V_\epsilon \in L^p(0, T; W^{1,p}(\Omega_\epsilon))$ such that*

$$U_\epsilon^N \rightharpoonup U_\epsilon \quad \text{and} \quad V_\epsilon^N \rightharpoonup V_\epsilon \quad \text{as } N \rightarrow \infty. \quad (6.92)$$

Proof. Take $N \in \mathbf{N}$ arbitrarily. Testing (6.89) with U_ϵ^N , integrating in time, taking supremum over $[0, T]$ and using (A7), we obtain

$$\begin{aligned} & \|U_\epsilon^N\|_{L^\infty(0, T; L^2(\Omega_\epsilon))}^2 + 2l_i \|U_\epsilon^N\|_{L^p((0, T) \times \Omega_\epsilon)}^p \\ & \leq \|U^*\|_{L^2(\Omega_\epsilon)}^2 + 2g_s \|V_\epsilon^{N-1}\|_{L^p((0, T) \times \Omega_\epsilon)}^{p-1} \|U_\epsilon^N\|_{L^p((0, T) \times \Omega_\epsilon)}. \end{aligned} \quad (6.93)$$

Taking $\phi = V_\epsilon^{N-1}$ in (6.90), integrating in time, and using (A2), we obtain

$$\begin{aligned} & \alpha \|V_\epsilon^{N-1}\|_{L^p(0, T; W^{1,p}(\Omega_\epsilon))}^p \\ & \leq \left[T^{1/q} \|F_\epsilon\|_{L^q(\Omega_\epsilon)} + k_s \|U_\epsilon^{N-1}\|_{L^p((0, T) \times \Omega_\epsilon)}^{p-1} \right] \|V_\epsilon^{N-1}\|_{L^p((0, T) \times \Omega_\epsilon)}. \end{aligned} \quad (6.94)$$

This is equivalent to

$$\|V_\epsilon^{N-1}\|_{L^p(0, T; W^{1,p}(\Omega_\epsilon))}^{p-1} \leq \frac{T^{1/q}}{\alpha} \|F_\epsilon\|_{L^q(\Omega_\epsilon)} + \frac{k_s}{\alpha} \|U_\epsilon^{N-1}\|_{L^p((0, T) \times \Omega_\epsilon)}^{p-1} \quad (6.95)$$

Moreover, combining (6.93) and (6.95) and applying Young's inequality, we obtain for any $n \in \mathbf{N}$ the recursive inequality

$$\begin{aligned} \|U_\epsilon^N\|_{L^p((0,T)\times\Omega_\epsilon)}^p &\leq \frac{1}{\left(l_i - \frac{g_s(\eta_1^p + \eta_2^p)}{p}\right)} \left[\frac{1}{2} \|U^*\|_{L^2(\Omega_\epsilon)}^2 + \frac{g_s T \|F_\epsilon\|_{L^q(\Omega_\epsilon)}^q}{q\alpha^q \eta_1^q} \right] \\ &\quad + \frac{g_s k_s^q}{q\alpha^q \eta_2^q \left(l_i - \frac{g_s(\eta_1^p + \eta_2^p)}{p}\right)} \|U_\epsilon^{N-1}\|_{L^p((0,T)\times\Omega_\epsilon)}^p \end{aligned} \quad (6.96)$$

for $\eta_1, \eta_2 \in \mathbf{R}_+$ with $\eta_1^p + \eta_2^p < pl_i/g_s$. Applying the discrete Gronwall inequality, see Inequality 13 of Section 2.2, we obtain the upper bound

$$\begin{aligned} \|U_\epsilon^N\|_{L^p((0,T)\times\Omega_\epsilon)}^p &\leq \frac{1}{\left(l_i - \frac{g_s(\eta_1^p + \eta_2^p)}{p}\right)} \left[\frac{1}{2} \|U^*\|_{L^2(\Omega_\epsilon)}^2 + \frac{g_s T \|F_\epsilon\|_{L^q(\Omega_\epsilon)}^q}{q\eta^q \alpha^q \eta_1^q q} \right] \\ &\quad \exp \left(\frac{g_s}{q\eta_2^q \left(l_i - \frac{g_s(\eta_1^p + \eta_2^p)}{p}\right)} \frac{k_s^q}{\alpha^q} \right). \end{aligned} \quad (6.97)$$

Note that the p -th root of (6.97) is finite for finite T and it is independent of N for all valid choices of η_1, η_2 . Hence, there is a weak limit of U_ϵ^N in $L^p((0, T) \times \Omega_\epsilon)$.

(6.95) yields a finite upper bound independent of N also for V_ϵ^N . Hence, there is a weak limit of V_ϵ^N in $L^p(0, T; W^{1,p}(\Omega_\epsilon))$. Moreover, testing (6.89) with $\frac{\partial U_\epsilon^N}{\partial t}$, we immediately obtain ϵ -independent bounds in $L^2((0, T) \times \Omega_\epsilon^+)$ by applying Young's inequality and the inclusion inequality (Lemma 2.1). \square

Before continuing with a strong convergence result, we need the following auxiliary lemma.

Lemma 6.32. *Let $\{x_i\}_{i=1}^\infty$ be a sequence of positive numbers satisfying the inequality $x_i \leq ax_{i-1}^b$ for positive numbers a and b , then the sum $\sum_{i=N}^\infty x_i$ converges to 0 as N goes to infinity, if $b = 1$ and $a < 1$ or $b < 1$ and $x_1^{1-b} < a$.*

Proof. We have

$$\begin{cases} x_N \leq a^{\frac{1-bN-1}{1-b}} x_1^{b^{N-1}} & \text{for } b \neq 1, \\ x_N \leq a^{N-1} x_1 & \text{for } b = 1. \end{cases} \quad (6.98)$$

This leads for $b = 1$ to a bound given by the geometric series if $a < 1$. For $b < 1$ and $x_1^{1-b} < a$, we have

$$\left(\frac{x_1^{1-b}}{a}\right)^{\frac{bN}{1-b}} < \frac{1-b}{(\ln b)((1-b)\ln x_1 - \ln a)} \frac{d}{dN} \left(\frac{x_1^{1-b}}{a}\right)^{\frac{bN}{1-b}}. \quad (6.99)$$

This inequality leads to a single upper bound expression via the integral test

$$\begin{aligned} \sum_{i=N}^{\infty} x_i &\leq \sum_{i=N}^{\infty} a^{\frac{1-b^{i-1}}{1-b}} x_1^{b^{i-1}} \leq a^{\frac{1}{1-b}} \int_{N-2}^{\infty} \left(\frac{x_1^{1-b}}{a}\right)^{\frac{bZ}{1-b}} dZ \\ &\leq \frac{(1-b)a^{\frac{1}{1-b}}}{(\ln b)((1-b)\ln x_1 - \ln a)} \int_{N-2}^{\infty} \frac{d}{dZ} \left(\frac{x_1^{1-b}}{a}\right)^{\frac{bZ}{1-b}} dZ \\ &\leq \frac{(1-b)a^{\frac{1}{1-b}}}{(\ln b)((1-b)\ln x_1 - \ln a)} \left[1 - \left(\frac{x_1^{1-b}}{a}\right)^{\frac{b(N-2)}{1-b}} \right]. \end{aligned} \quad (6.100)$$

This upper bound goes to 0 as N goes to infinity. \square

Now we are able to report the following strong convergence result.

Proposition 6.33. *Assume (A1), (A2), (A7) - (A10). The sequences $\{U_\epsilon^n\}$ and $\{V_\epsilon^n\}$ introduced at (6.89) and (6.90), respectively, are strongly convergent to their weak limits $U_\epsilon \in L^p((0, T) \times \Omega_\epsilon)$, $V_\epsilon \in L^p(0, T; W^{1,p}(\Omega_\epsilon))$.*

Proof. First, we show the case $p \in [2, \infty)$. Take $N \in \mathbf{N}$ arbitrarily. By the strict monotonicity of \mathcal{L} , we obtain

$$\begin{aligned} &\|U_\epsilon^N - U_\epsilon^{N+1}\|_{L^\infty(0, T; L^2(\Omega_\epsilon))}^2 + 2L\|U_\epsilon^N - U_\epsilon^{N+1}\|_{L^p((0, T) \times \Omega_\epsilon)}^p \\ &\leq 2G\|V_\epsilon^{N-1} - V_\epsilon^N\|_{L^p((0, T) \times \Omega_\epsilon)}\|U_\epsilon^N - U_\epsilon^{N+1}\|_{L^p((0, T) \times \Omega_\epsilon)}(|\Omega_\epsilon|T)^{\frac{p-2}{p}}. \end{aligned} \quad (6.101)$$

Similarly, by strict monotonicity of \mathcal{T}_0 and due to (A10), we have

$$\begin{aligned} &\beta\|V_\epsilon^{N-1} - V_\epsilon^N\|_{L^p(0, T; W^{1,p}(\Omega_\epsilon))}^p \\ &\leq K\|U_\epsilon^{N-1} - U_\epsilon^N\|_{L^p((0, T) \times \Omega_\epsilon)}\|V_\epsilon^{N-1} - V_\epsilon^N\|_{L^p((0, T) \times \Omega_\epsilon)}(|\Omega_\epsilon|T)^{\frac{p-2}{p}}. \end{aligned} \quad (6.102)$$

(6.90) yields

$$\|V_\epsilon^{N-1} - V_\epsilon^N\|_{L^p(0,T;W^{1,p}(\Omega_\epsilon))}^{p-1} \leq \frac{K}{\beta} \|U_\epsilon^{N-1} - U_\epsilon^N\|_{L^p((0,T)\times\Omega_\epsilon)} (|\Omega_\epsilon|T)^{\frac{p-2}{p}}. \quad (6.103)$$

Moreover, combining (6.101) and (6.103), we obtain the recursive inequality

$$\|U_\epsilon^N - U_\epsilon^{N+1}\|_{L^p((0,T)\times\Omega_\epsilon)}^{(p-1)^2} \leq \frac{K}{\beta} \left(\frac{G}{L}\right)^{p-1} (|\Omega_\epsilon|T)^{p-2} \|U_\epsilon^{N-1} - U_\epsilon^N\|_{L^p((0,T)\times\Omega_\epsilon)}. \quad (6.104)$$

Using Lemma 6.32 for $b = 1$ due to $p = 2$, we obtain strong convergence as the geometric series leads to an upper bound, stated below, that goes to zero as N goes to infinity if $KG < L\beta$, which is guaranteed by (A10).

$$\|U_\epsilon^N - U_\epsilon\|_{L^p((0,T)\times\Omega_\epsilon)} \leq \frac{\left(\frac{KG}{L\beta}\right)^{N-1}}{1 - \frac{KG}{L\beta}} \|U_\epsilon^1 - U_\epsilon^2\|_{L^p((0,T)\times\Omega_\epsilon)} \quad (6.105)$$

For $p > 2$ and using $V_\epsilon^0 = 0$, we have

$$\|U_\epsilon^1 - U_\epsilon^2\|_{L^p((0,T)\times\Omega_\epsilon)} \leq \left[\frac{G}{L} (|\Omega_\epsilon|T)^{\frac{p-2}{p}}\right]^{\frac{1}{p-1}} \|V_\epsilon^1\|_{L^p((0,T)\times\Omega_\epsilon)}^{\frac{1}{p-1}}. \quad (6.106)$$

An upper bound for $\|V_\epsilon^1\|_{L^p((0,T)\times\Omega_\epsilon)}$ follows from equations (6.95) and (6.97). Denote this upper bound by B .

Lemma 6.32 yields strong convergence for $p > 2$, which represents the case $b < 1$, if

$$B < \left(\frac{K}{\beta}\right)^{\frac{p-1}{p(p-2)}} \left(\frac{G}{L}\right)^{\frac{1}{p(p-2)}} (|\Omega_\epsilon|T)^{\frac{1}{p}}. \quad (6.107)$$

Similarly, we obtain from (6.103) the following upper bound

$$\begin{aligned} \|V_\epsilon^N - V_\epsilon\|_{L^p(0,T;W^{1,p}(\Omega_\epsilon))} &\leq \sum_{n=0}^{\infty} \|V_\epsilon^{N+n} - V_\epsilon^{N+n+1}\|_{L^p(0,T;W^{1,p}(\Omega_\epsilon))} \\ &\leq \left(\frac{K}{\beta} (|\Omega_\epsilon|T)^{\frac{p-2}{p}}\right)^{\frac{1}{p-1}} \sum_{n=0}^{\infty} \|U_\epsilon^{N+n} - U_\epsilon^{N+n+1}\|_{L^p((0,T)\times\Omega_\epsilon)}^{\frac{1}{p-1}}, \end{aligned} \quad (6.108)$$

which goes to zero as $N \rightarrow \infty$ due to Lemma 6.32 when taking $y_i = x_i^{\sqrt{b}}$ and identifying (6.108) with $\sum_{i=N}^{\infty} y_i$ if $KG < L\beta$ for $p = 2$ or if (6.107) holds for $p > 2$. \square

By the demicontinuity of \mathcal{T}_0 , \mathcal{K} , \mathcal{L} , and \mathcal{G} , the limit pair (U_ϵ, V_ϵ) satisfies system (6.1) on the interior $(0, T) \times \Omega_\epsilon$ due to the strong convergence, which automatically allows for satisfying the boundary conditions due to the trace theorems and the higher regularity obtained with Proposition 9.3 in [20]. This concludes a proof for Theorem 6.25.

Conclusions and recommendations

In this dissertation, we derived well-posed parabolic-pseudo-parabolic equations coupling chemical reactions, diffusion, flow and mechanics in a heterogeneous medium using the framework of mixture theory. Moreover, as an example, we showed how to upscale the microscopic mechanics of sewer pipe corrosion into macroscopic mechanics. As many different microscopic behaviors can lead to the same upscaled macroscopic behavior, upscaling *the* microscopic mechanics of a sewer pipe hints at a central problem of homogenization: What are correct microscopic behaviors to upscale? We answered this question in Chapter 3 and Chapter 4.

The model parameters of the model derived in Chapter 3 impact the existence of a solution for the model equations quite significantly as we showed that the time interval of existence is highly dependent on several parameters such as ϕ_{30} and ϵ , and on control parameters such as V . The ϵ -dependence of the size of this time-interval likely follows a power law relation, while other dependencies such as the dependence on the initial volume fractions show a more complicated relation.

In Chapter 4, we showed that more general models, than the ones derived in Chapter 3, are weakly solvable. Moreover, we showed that there exist time-intervals and parameter regions for which the solutions of these models do not violate elementary physical constraints, e.g. the positivity of volume fractions. These results were attained by assuming a product-like non-linearity in the unknowns such that for each unknown the system behaves like a semilinear system. Some of these non-linearities need a specific regularity, for instance $C^1(0, 1)$ in each of the product components. In the end the pseudo-parabolic

term turns out to be an advantage in our semilinear setting as it regularizes any potentially parabolicity breaking effects, while still maintaining properties of a parabolic problem as was observed in [128]. It is worth pointing out that if on top of coupling chemical reactions, mechanics, diffusion and flow, also thermal effects play a role, then porous media scenarios referencing to harvesting geothermal energy can be treated.

In Chapter 5, we upscaled model D of Chapter 3, which describes the microscopic behaviour of sewer pipe corrosion, for the situation that an equilibrium in the corrosion reaction has arisen, i.e. ϕ is a constant vector. We showed that a spatio-temporal decomposition, originally introduced in [107], allows for a straightforward upscaling of pseudo-parabolic equation structures, the class of systems to which our sewer pipe corrosion model belongs. We pointed out that the upscaling limit can be obtained by using the concept of two-scale convergence. Moreover, we showed that the pseudo-parabolic equation structures converge to their upscaling limit with a convergence rate given by a power-law relation on ϵ , even in the case of simultaneous divergence of the time domain.

In Chapter 6, we showed for a non-linear version of the pseudo-parabolic system containing monotone operators that both the upscaling and the convergence rate determination are possible. For the special bed-of-nails-like domain of Chapter 6, the upscaled system loses dependence on the planar direction, in which the microscopic system exhibited periodicity. The convergence rate behaves as a powerlaw in ϵ , the shrinking rate of the substrate thickness, and the convergence rate of the data in the cylinders.

The research presented in this dissertation allows for several natural continuations. We have shown that the spatio-temporal decomposition allows for a straightforward upscaling of pseudo-parabolic equation structures. An interesting direction, which has not been addressed in this dissertation, is the effect of ϵ -dependence of the different terms and parameters. Another interesting research direction looks at domain dependent descriptions of the parameters in the pseudo-parabolic equation structure, like in, for example, high-contrast porous media or periodic composites. Cases of upscaling systems with either the ϵ -dependence or the domain dependence of the parameters are discussed in [107], showing promising results for the application of the decoupling methodology to more complex pseudo-parabolic problems.

A major implicit assumption throughout this dissertation is the deterministic description of the parameters of the model as a function of the three

variables in a microscopic evolution model (time t , macro scale \mathbf{x} , and micro scale \mathbf{y}). This implicit assumption is a reflection of a deterministic approach in the underlying model creation. One can, however, argue that at small enough scales stochastic effects become noticeable if not dominant. Hence, a more stochastic approach to homogenization for upscaling a microscopic structure can be useful for modeling of semiconductor behaviour like is performed in Chapter 6. Note that the geometric scenario for Chapter 6 resembles also a scenario one obtains in steel production via additive manufacturing. In this context, defects often occur and weaken the material. A stochastic extension of homogenization that can handle defects exists and has been successfully applied to problems close to the periodic homogenization setting as was done in e.g. [84]. Investigating the effects of such stochastic homogenization handling defects on a (stochastic) pseudo-parabolic system on a (stochastic) domain seems a natural continuation of the research presented in this dissertation. Another line of thinking, which we have not exploited in Chapter 5 and Chapter 6, is how to perform the upscaling of our PDE systems when some spatial scales are not separated. We believe that the concept of very weak two-scale convergence, proposed by A. Holmbom and collaborators, can be very useful in this context; see e.g. [54], [65].

List of symbols

Notation within brackets is a rare or field-specific alternative

$a, 0, 1$	scalar, zero scalar, unit scalar
$\mathbf{a}, \mathbf{0}, \mathbf{1}$	vector, zero vector, unit vector
$\mathbb{T}, \mathbf{0}, \mathbf{1}$	tensor, zero tensor, unit tensor
$\mathbb{T}^\top, \mathbf{a}^\top$	tensor transpose, vector transpose
$\mathbf{R}^n, \mathbf{R}_+$	n -dimensional Euclidean space, set of positive real numbers
\mathbb{X}, \mathbb{X}^*	function space, dual space of \mathbb{X}
i, α	spatial index, component index
ϵ, ε	small positive number
$\mathbb{T} \cdot \mathbf{a}$	spatial inner product
$\mathbb{T} \mathbf{a}$	component inner product
$\mathbb{T} \otimes \mathbf{a}$	tensor product between spatial tensor and component vector
$t, \mathbf{x}, \mathbf{y}$	time, spatial vectors
x_i, y_i	spatial vector element
$T_{\alpha\beta}, T_{ij}, T_{i\alpha}$	component, spatial, mixed tensor element
\mathcal{A}	operator
$\frac{d}{dt} (d_t, \frac{D}{Dt})$	total derivative w.r.t. time
$\frac{\partial}{\partial t} (\partial_t), \frac{\partial}{\partial x_i} (\partial_{x_i})$	partial derivative w.r.t. time, i -th space direction
$\text{div} (\text{div}_{\mathbf{x}}), \text{div}_{\mathbf{y}}$	divergence w.r.t. \mathbf{x}, \mathbf{y}
$\nabla (\nabla_{\mathbf{x}}), \nabla_{\mathbf{y}}$	gradient w.r.t. \mathbf{x}, \mathbf{y}

D^α	$\frac{\partial^{ \alpha _1}}{\partial x_1^{\alpha_1} \partial x_2^{\alpha_2} \dots \partial x_n^{\alpha_n}}$, a specific $ \alpha _1$ -order partial derivative
$\Delta (\Delta_x), \Delta_y$	Laplacian w.r.t. \mathbf{x}, \mathbf{y}
$\Delta t, \Delta x$	discrete time step, discrete space step
$ \cdot $	Euclidean 2-norm (absolute value for scalars)
$ \cdot _p$	p -norm for $p \in [1, \infty]$ (both discrete and continuous versions)
$\ \cdot\ _{\mathbb{X}}$	norm of normed space \mathbb{X}
$\ \mathcal{A}\ $	operator norm
$\Omega, \partial\Omega, \bar{\Omega}$	spatial domain, boundary of Ω , closure of Ω
$L^p(\Omega)$	Lebesgue space of measurable finite p -norm functions on Ω
$W^{k,p}(\Omega)$	Sobolev space of functions with $l \in [0, k]$ order derivatives in $L^p(\Omega)$
$C^k(\Omega), C_c^k(\Omega)$	space of k -times differentiable functions on/with compact support in Ω
$C_{\#}(Y)$	space of continuous functions on Y that are Y -periodic
$H^k(\Omega), H_0^k(\Omega)$	$W^{k,2}(\Omega)$, functions in $W^{k,2}(\Omega)$ that are zero on $\partial\Omega$
$L^p(Y; W^{k,p}(\Omega))$	Bochner space of functions in $L^p(Y)$ that are pointwise in $W^{k,p}(\Omega)$
$H^1(\Omega)/\mathbf{R}$	Space of functions in $H^1(\Omega)$ with average value 0
$\langle f, g \rangle_{\mathbb{X}}$	duality pairing of $f \in \mathbb{X}$ and $g \in \mathbb{X}^*$
$\longrightarrow, \rightharpoonup, \xrightarrow{2}, \xrightarrow{*}$	strong, weak, two-scale, weak-* convergence
\hookrightarrow	continuous embedding
\emptyset	empty set
$f = \mathcal{O}(g), o(g), \omega(g)$	$\lim_{n \rightarrow \infty} \left \frac{f(n)}{g(n)} \right = 0, \limsup_{n \rightarrow \infty} \left \frac{f(n)}{g(n)} \right < \infty, \lim_{n \rightarrow \infty} \left \frac{f(n)}{g(n)} \right = \infty$
$u _{\partial\Omega}$	restriction of u to $\partial\Omega$
$\text{Tr}(u) (u _{\partial\Omega})$	Trace of u (operator $W^{1,p}(\Omega) \rightarrow L^p(\partial\Omega)$)
$\text{Tr}(\mathbf{T})$	Trace of \mathbf{T} (sum of all diagonal elements, i.e. $\sum_{\alpha=1}^n \mathbf{T}_{\alpha\alpha}$)
χ_{Ω}	indicator function on Ω

Remark: Deviations from this text are possible for avoiding cumbersome notation or for adhering to field-specific conventions.

Bibliography

- [1] Abels, H., and Liu, Y. Sharp interface limit for a Stokes/Allen-Cahn system. *Arch. Rational. Mech. Anal.* 229, 1 (2018), 417–502.
- [2] Adams, R. A. *Sobolev Spaces*. Academic Press, 1975.
- [3] Ali, G., Furuholt, V., Natalini, R., and Torcicollo, I. A mathematical model of sulphite chemical aggression of limestones with high permeability. part ii: Numerical approximation. *Transp. Porous Media* 69, 2 (2007), 175–188.
- [4] Allaire, G. Homogenization and two-scale convergence. *SIAM J. Math. Anal.* 23, 6 (1992), 1482–1518.
- [5] Amirat, Y., Bodart, O., Demaio, U., and Gaudiello, A. Asymptotic approximation of the solution of the laplace equation in a domain with highly oscillating boundary. *SIAM J. MATH. ANAL.* 35, 6 (2004), 1598–1616.
- [6] Arab, N., Zemskov, E. P., Muntean, A., and Fatima, T. Homogenization of a reaction-diffusion system modeling sulfate corrosion of concrete in locally periodic perforated domains. *J. Engrg. Math.* 69, 2 (2011), 261–276.
- [7] Balasundaram, K., Sadhu, J. S., Shin, J. C., Azeredo, B., Chanda, D., Malik, M., Hsu, K., Rogers, J. A., Ferreira, P., Sinha, S., and Li, X. Porosity control in metal-assisted chemical etching of degenerately doped silicon nanowires. *Nanotechnology* 23, 305304 (2012), 1–7.

- [8] Barbu, V. *Nonlinear Differential Equations of Monotone Types in Banach Spaces*. Springer Monographs in Mathematics. Springer Science+Business Media, 2010.
- [9] Basista, M., and Weglewski, W. Micromechanical modelling of sulphate corrosion in concrete: influence of ettringite forming reaction. *Theoret. Appl. Mech.* 35, 1-3 (2008), 29–52.
- [10] Bertsch, M., Smarrazzo, F., and Tesei, A. Pseudoparabolic regularization of forwardbackward parabolic equations: a logarithmic nonlinearity. *Anal. PDE* 6 (2013), 1719–1754.
- [11] Blanchard, D., Carbone, L., and Gaudiello, A. Homogenization of a monotone problem in a domain with oscillating boundary. *ESAIM: Modélisation mathématique et analyse numérique* 33, 5 (1999), 1057–1070.
- [12] Blanchard, D., and Gaudiello, A. Homogenization of highly oscillating boundaries and reduction of dimension for a monotone problem. *ESAIM: Control, Optimisation and Calculus of Variations* 9 (2003), 449–460.
- [13] Blanchard, D., Gaudiello, A., and Mossino, J. Highly oscillating boundaries and reduction of dimension: the critical case. *Analysis and Applications* 5, 2 (2007), 137–163.
- [14] Böhm, M., Deviny, J., Jahani, F., and Rosen, G. On a moving-boundary system modeling corrosion in sewer pipes. *Appl. Math. Comput.* 92 (1998), 247–269.
- [15] Böhm, M., and Showalter, R. E. Diffusion in fissured media. *SIAM J. Math. Anal.* 16, 3 (1985), 500–509.
- [16] Böhm, M., and Showalter, R. E. A nonlinear pseudoparabolic diffusion equation. *SIAM J. MATH. ANAL.* 16, 5 (1985), 980–999.
- [17] Bouchelaghem, F. A numerical and analytical study on calcite dissolution and gypsum precipitation. *Appl. Math. Model.* 34 (2010), 467–480.
- [18] Bowen, R. M. *Continuum Physics*, vol. 3. Academic Press, New York, NY, 1976, ch. 1. Theory of Mixtures.
- [19] Bowen, R. M. Incompressible porous media models by use of the theory of mixtures. *Int. J. Engng. Sci.* 18 (1980), 1129–1148.

- [20] Brezis, H. *Functional Analysis, Sobolev Spaces and Partial Differential Equations*. Springer, New York, NY, 2010.
- [21] Bulíček, M., Málek, J., and Rajagopal, R. On Kelvin-Voigt model and its generalizations. Tech. rep., Nečas Center for Mathematical Modeling, Mathematical Institute, Charles University, Prague, Czech Republic, 2010.
- [22] Cahn, R. W., Haasen, P., and Kramer, E. J. *Materials Science and Technology - A Comprehensive Treatment*, vol. 1 of *Corrosion and Environmental Degradation*. WILEY-VCH, Chichester, 2000. Volume Editor: Michael Schütze.
- [23] Cao, X., and Pop, I. S. Two-phase porous media flows with dynamic capillary effects and hysteresis: uniqueness of weak solutions. *Comput. Math. Appl.* 69 (2015), 688–695.
- [24] Cao, X., and Pop, I. S. Degenerate two-phase porous media flow model with dynamic capillarity. *J. Differential Equations* 260 (2016), 2418–2456.
- [25] Chabaud, B., and Calderer, M. C. Effects of permeability and viscosity in linear polymeric gels. *Math. Meth. Appl. Sci.* 39 (2016), 1395–1409.
- [26] Chalupecky, V., Fatima, T., Muntean, A., and Kruschwitz, J. Macroscopic corrosion front computations of sulfate attack in sewer pipes based on a micro-macro reaction-diffusion model. In *Multiscale Mathematics: Hierarchy of Collective Phenomena and Interrelations Between Hierarchical Structures* (Japan, 2011), F. I. of Mathematics for Industry, Ed., vol. 39 of *COE Lecture Note Series*, Collaborate Research Meeting of Institute of Mathematics for Industry & Next Collaborative Workshop of Mathematics and Mathematical Sciences with Various Sciences and Industrial Technologies, Fukuoka, Japan, December 8-11, 2011, Kyushu University, pp. 22–31.
- [27] Chen, X., Jüngel, A., and J.-G. Liu. A note on Aubin-Lions-Dubinskii lemmas. *Acta Appl. Math.* 133, 1 (2013), 33–43.
- [28] Chill, R. Quelques méthodes de résolution pour les équations non-linéaires. Tech. rep., Laboratoire de Mathématiques et Applications de Metz, 2007.
- [29] Ciorănescu, D., and Donato, P. *An Introduction to Homogenization*. No. 17 in Oxford Lecture Series in Mathematics and its Applications. Oxford University Press, 1999.

- [30] Ciorănescu, D., and Saint Jean Paulin, J. *Homogenization of Reticulated Structures*. No. 136 in Applied Mathematical Sciences. Springer-Verlag, 1998.
- [31] Claisse, P., Ganjian, E., and Adham, T. In situ measurement of the intrinsic permeability of concrete. *Magazine of Concrete Research* 55, 2 (2003), 125–132.
- [32] Clarelli, F., Fasano, A., and Natalini, R. Mathematics and monument conservation: free boundary models of marble sulfation. *SIAM J. Appl. Math.* 69, 1 (2008), 149–168.
- [33] Clark, G. W., and Showalter, R. E. Two-scale convergence of a model for flow in a partially fissured medium. *Electron. J. Diff. Eqns.* 1999, 2 (1999), 1–20.
- [34] Colli, P., and Hoffmann, K. A nonlinear evolution problem describing multi-component phase changes with dissipation. *Numer. Funct. Anal. and Optimiz.* 14, 3&4 (1993), 275–297.
- [35] Cowin, S. *Continuum Mechanics of Anisotropic Materials*. Springer, Berlin, 2013.
- [36] Cuesta, C., and Hulshof, J. A model problem for groundwater flow with dynamic capillary pressure: Stability of travelling waves. *Nonlinear Anal.* 52 (2003), 1199–1218.
- [37] Cuesta, C. M., and Pop, I. S. Numerical schemes for a pseudo-parabolic burgers equation: Discontinuous data and long-time behaviour. *J. Comp. Appl. Math* 224 (2009), 269–283.
- [38] Cuesta, C. M., van Duijn, C. J., and Hulshof, J. Infiltration in porous media with dynamic capillary pressure: Travelling waves. *European J. Appl. Math.* 11 (2004), 381–397.
- [39] Dragomir, S. S. *Some Gronwall Type Inequalities and Applications*. RGMIA Monographs. Nova Science, New York, 2003.
- [40] Dreher, M., and Jüngel, A. Compact families of piecewise constant functions in $L^p(0, T; B)$. *Nonlin. Anal.* 75 (2012), 3072–3077.
- [41] Düll, W.-P. Some qualitative properties of solutions to a pseudoparabolic equation modeling solvent uptake in polymeric solids. *Comm. Partial Differential Equations* 31 (2006), 1117–1138.

- [42] Durning, E. D. D. *Corrosion Atlas - A Collection of Illustrated Case Histories*, 3rd exp. rev. ed. Elsevier, Amsterdam, 1997.
- [43] Eden, M. *Homogenization of Thermoelasticity Systems Describing Phase Transformations*. PhD thesis, Universität Bremen, 2018.
- [44] Eden, M., and Muntean, A. Homogenization of a fully coupled thermoelasticity problem for a highly heterogeneous medium with a priori known phase transformations. *Math. Meth. Appl. Sci.* 40, 11 (2017), 3955–3972.
- [45] Elsener, B. *Materials Science and Technology - A Comprehensive Treatment*, vol. 2 of *Corrosion and Environmental Degradation*. WILEY-VCH, Chichester, 2000, ch. 8. Corrosion of Steel in Concrete. Volume Editor: Michael Schütze.
- [46] Emmerich, E. Discrete Versions of Gronwall’s Lemma and Their Application to the Numerical Analysis of Parabolic Problems. Tech. rep., TU Berlin, 1999.
- [47] Ern, A., and Giovangigli, V. The kinetic chemical equilibrium regime. *Physica A* 260 (1998), 49–72.
- [48] Evans, L. C. *Partial Differential Equations*, 2nd ed. American Mathematical Society, Providence, RI, 2010.
- [49] Fan, Y., and Pop, I. S. A class of degenerate pseudo-parabolic equations: existence, uniqueness of weak solutions, and error estimates for the euler-implicit discretization. *Math. Methods Appl. Sci.* 34 (2011), 2329–2339.
- [50] Fan, Y., and Pop, I. S. Equivalent formulations and numerical schemes for a class of pseudo-parabolic equations. *J. Comput. Appl. Math.* 246 (2013), 86–93.
- [51] Fan, Z., Razavi, H., won Do, J., Moriwaki, A., Ergen, O., Chueh, Y.-L., Leu, P. W., Ho, J. C., Takahashi, T., Reichertz, L. A., Neale, S., Yu, K., Wu, M., Ager, J. W., and Javey, A. Three-dimensional nanopillar-array photovoltaics on low-cost and flexible substrates. *Nature Materials* 8 (2009), 648–653.
- [52] Fasullo, G. T. *Sulphuric Acid: Use & Handling*. McGraw Hill, New York, New York, 1965.

- [53] Fatima, T., and Muntean, A. Sulfate attack in sewer pipes: Derivation of a concrete corrosion model via two-scale convergence. *Nonlinear Anal. Real World Appl.* 15 (2014), 326–344.
- [54] Flodén, L., Holmbom, A., Olsson Lindberg, M., and Persson, J. Homogenization of parabolic equations with an arbitrary number of scales in both space and time. *Journal of Applied Mathematics 2014*, Article ID 101685 (2014), 16 pages.
- [55] Ford, W. H. Galerkin approximations to non-linear pseudo-parabolic partial differential equations. *Aequationes Math.* 14 (1976), 271–291.
- [56] Fusi, L., Farina, A., and Primicerio, M. A free boundary problem for CaCO_3 neutralization of acid waters. *Nonlinear Anal. Real World Appl.* 15 (2014), 42–50.
- [57] Fusi, L., Primicerio, M., and Monti, A. A model for calcium carbonate neutralization in the presence of armoring. *Appl. Math. Modell.* 39 (2015), 348–362.
- [58] Gajewski, H., Gröger, K., and Zacharias, K. *Nichtlineare Operatorgleichungen und Operatordifferentialgleichungen, IV*. No. 281. Akademie-Verlag, Berlin, 1974.
- [59] Gaudiello, A., and Guibé, O. Homogenization of an evolution problem with $l \log(l)$ data in a domain with oscillating boundary. *Annali di Matematica* 197 (2018), 153–169.
- [60] Gaudiello, A., and Sili, A. Homogenization of highly oscillating boundaries with strongly contrasting diffusivity. *SIAM J. MATH. ANAL.* 47, 3 (2015), 1671–1692.
- [61] Gilbarg, D., and Trudinger, N. *Elliptic Partial Differential Equations of Second Order*, 1998 reprint ed. Springer, Berlin, 1977.
- [62] Giovangigli, V. *Multicomponent Flow Modeling*. Modeling and Simulation in Science, Engineering and Technology. Springer Science+Business Media, 1999.
- [63] Hansson, R., Ericsson, L. K. E., Holmes, N. P., Rysz, J., Opitz, A., Campoy-Quiles, M., Wang, E., Barr, M. G., Kilcoyne, A. L. D., Zhou, X., Dastoor, P., and Moons, E. Vertical and lateral morphology effects on solar cell performance for a thiophenequinoxaline copolymer:pc₇₀bm blend. *Journal of Materials Chemistry A* 3, 13 (2015), 6970–6979.

- [64] Haynes, W. M., Lide, D. R., and Bruno, T. J. *CRC Handbook of Chemistry and Physics*, 97th edition ed. CRC Press, Boca Raton, Florida, 2017.
- [65] Holmbom, A. Homogenization of parabolic equations an alternative approach and some corrector-type results. *Applications of Mathematics* 42, 5 (1997), 321–343.
- [66] Holmes, M. H. *Introduction to Perturbation Methods*, 2nd ed. No. 20 in Texts in Applied Mathematics. Springer, Berlin, 2013.
- [67] Holte, J. M. Discrete Gronwall lemma and applications. *Gustavus Adolphus College* <http://homepages.gac.edu/~holte/publications> (24 October 2009).
- [68] Hornung, U. *Homogenization and Porous Media*, softcover reprint of 1st ed. No. 6 in Interdisciplinary Applied Mathematics. Springer Science + Business Media, New York, 1997.
- [69] J.-D. Gu, Ford, T. E., and Mitchell, R. *Uhlig's Corrosion Handbook*, 3rd ed. John Wiley & Sons, Hoboken, New Jersey, 2011, ch. 32. Microbial Corrosion of Concrete.
- [70] Jäger, W., Mikelic, A., and Neuss-Radu, M. Analysis of differential equations modelling the reactive flow through a deformable system of cells. *Arch. Rational Mech. Anal.* 192 (2009), 331–374.
- [71] Jäger, W., Mikelic, A., and Neuss-Radu, M. Homogenization-limit of a model system for interaction of flow, chemical reactions and mechanics in cell tissues. *SIAM J. Math. Anal.* 43, 3 (2011), 1390–1435.
- [72] Jikov, V. V., Kozlov, S. M., and Oleinik, O. A. *Homogenization of Differential Operators and Integral Functionals*, softcover reprint of 1st ed. Springer-Verlag, Berlin, 1994. Based on the original Russian edition, translated from the original Russian by G.A. Yosifian.
- [73] Kato, T. Demicontinuity, hemicontinuity and monotonicity. *Bull. Amer. Math. Soc.* 70, 4 (1964), 548–550.
- [74] Kačur, J. *Method of Rothe in Evolution Equations*. Band 80, Teubner-Texte zur Mathematik, Leipzig, 1985.
- [75] Khoa, V. A. *Corrector Homogenization Estimates for PDE Systems with Coupled Fluxes posed in Media with Periodic Microstructures*. PhD thesis, Gran Sasso Science Institute, 2017.

- [76] Kierzenka, J., and Shampine, L. F. A BVP solver based on residual control and the MATLAB PSE. *ACM Trans. Math. Software* 27, 3 (2001), 299–316.
- [77] Kierzenka, J. A., and Shampine, L. F. A BVP solver that controls residual and error. *J. Num. Anal., Indus. & Appl. Math.* 3, 1-2 (2008), 27–41.
- [78] Koch, J., Rätz, A., and Schweizer, B. Two-phase flow equations with a dynamic capillary pressure. *European J. Appl. Math.* 24 (2013), 49–75.
- [79] Kufner, A., John, O., and Fučík, S. *Function Spaces*. Noordhoff International Publishing, Leyden, 1977.
- [80] Ladyženskaja, O. A., Solonnikov, V. A., and Ural'ceva, N. N. *Linear and Quasi-linear Equations of Parabolic Type*, reprint ed. American Mathematical Society, Providence, RI, 1988. Translated from the Russian 1967 version by S. Smith.
- [81] Lafhaj, Z., Richard, G., Kaczmarek, M., and Skoczylas, F. Experimental determination of intrinsic permeability of limestone and concrete: Comparison between in situ and laboratory results. *Building and Environment* 42, 8 (2007), 3042–3050.
- [82] Lamacz, A., Rätz, A., and Schweizer, B. A well-posed hysteresis model for flows in porous media and applications to fingering effects. *Advances in Mathematical Sciences and Applications* 21 (2011), 33–64.
- [83] Lax, P. D., and Milgram, A. Parabolic equations. In *Contributions to the Theory of Partial Differential Equations*, *Ann. Math. Studies*, vol. 33. Princeton University Press, 1954, pp. 167–190.
- [84] Le Bris, C., L egoll, F., and Thomin es, F. Rate of convergence of a two-scale expansion for some “weakly” stochastic homogenization problems. *Asymptot. Anal.* 80 (2012), 237–267.
- [85] Lions, J.-L. *Quelques m ethodes de r esolution des probl emes aux limites non lin eaires*.  tudes Math ematiques. Dunod Gauthier-Villars, Paris, 1969.
- [86] Lukkassen, D., Nguetseng, G., and Wall, P. Two-scale convergence. *Int. J. of Pure and Appl. Math.* 2, 1 (2002), 35–62.

- [87] Mahato, H. S. *Homogenization of a System of Nonlinear Multi-Species Diffusion-Reaction Equations in an $H^{1,p}$ Setting*. PhD thesis, Universität Bremen, 2013.
- [88] Mahato, H. S., and Böhm, M. Homogenization of a system of semilinear diffusion-reaction equations in an $h^{1,p}$ setting. *Electronic Journal of Differential Equations* 2013, 210 (2013), 1–22.
- [89] Marchenko, V. A., and Krushlov, E. *Homogenization of Partial Differential Equations*. No. 46 in Progress in Mathematical Physics. Birkhäuser, Boston, Basel, Berlin, 2006. Based on the original Russian edition, translated from the original Russian by M. Goncharenko and D. Shepelsky.
- [90] Meshkova, Y. M., and Suslina, T. A. Homogenization of initial boundary value problems for parabolic systems with periodic coefficients. *Applicable Analysis* 95, 8 (2016), 1736–1775.
- [91] Meyers, M. A., and Chawla, K. *Mechanical Behavior of Materials*, 2nd ed. Cambridge University Press, Cambridge, UK, 1999.
- [92] Mikelić, A. A global existence result for the equations describing unsaturated flow in porous media with dynamic capillary pressure. *J. Differential Equations* 248 (2010), 1561–1577.
- [93] Milisic, J. The unsaturated flow in porous media with dynamic capillary pressure. *J. Differential Equations* 264 (2018), 5629–5658.
- [94] Monteiro, P. J. M. *Interfacial Transition Zone in Concrete*, 1st ed. No. 11 in RILEM Report. E & FN SPON, London, UK, 1996, ch. 4. Mechanical modelling of the transition zone. State-of-the-Art Report prepared by RILEM Technical Committee 108-1CC, Interfaces in Cementitious Composites.
- [95] Morro, A. Diffusion in mixtures of reacting thermoelastic solids. *J. Elast.* 123 (2015), 59–84.
- [96] Muntean, A. *Continuum Modeling. An Approach Through Practical Examples*. Springer, Heidelberg New York Dordrecht London, 2015.
- [97] Muntean, A., and Chalupecký, V. *Homogenization Method and Multiscale Modeling*. No. 34 in COE Lecture Note. Institute of Mathematics for Industry, Kyushu University, Japan, 2011.

- [98] Muntean, A., and Reichelt, S. Corrector estimates for a thermodiffusion model with weak thermal coupling. *SIAM Journal on Multiscale Modeling and Simulation* 16, 2 (2018), 807–832.
- [99] Nguetseng, G. A general convergence result for a functional related to the theory of homogenization. *SIAM J. Math. Anal.* 20, 3 (1989), 608–623.
- [100] Nguetseng, G. Homogenization structures and applications I. *Z. Anal. Anwend.* 22, 1 (2003), 73–107.
- [101] Nikolopoulos, C. V. A mushy region in concrete corrosion. *Appl. Math. Model.* 34 (2010), 4012–4030.
- [102] Nikolopoulos, C. V. Macroscopic models for a mushy region in concrete corrosion. *J. Engrg. Math.* 91, 1 (2014), 143–163.
- [103] Nikolopoulos, C. V. Mathematical modelling of a mushy region formation during sulphation of calcium carbonate. *Netw. Heterog. Media* 9, 4 (2014), 635–654.
- [104] Ortiz, M., and Popov, E. P. Plain concrete as a composite material. *Mechanics of Materials* 1 (1982), 139–150.
- [105] Papanastasiou, T. C., Georgiou, G. C., and Alexandrou, A. N. *Viscous Fluid Flow*. CRC Press LLC, Boca Raton, FL, 2000.
- [106] Pavliotis, G. A., and Stuart, A. M. *Multiscale Methods - Averaging and Homogenization*. No. 53 in Texts in Applied Mathematics. Springer, Berlin, 2008.
- [107] Peszyńska, M., Showalter, R., and S.-Y. Yi. Homogenization of a pseudoparabolic system. *Applicable Analysis* 88, 9 (2009), 1265–1282.
- [108] Piatnitski, A., and Ptashnyk, M. Homogenization of biomechanical models for plant tissues. *Multiscale Model. Simul.* 15, 1 (2015), 339–387.
- [109] Plachy, T., Tesarek, P., Padevet, P., and Polak, M. Determination of Young’s modulus of gypsum blocks using two different experimental methods. In *Recent Advances in Applied and Theoretical Mechanics* (www.wseas.org, 2009), C. A. Bulucea, Ed., 5th WSEAS Int. Conf. Appl. Theor. Mech., WSEAS Press.

- [110] Polyanin, A. D., and Zaitsev, V. F. *Handbook of Exact Solutions for ODEs*, 1st ed. CRC Press Inc, 1995.
- [111] Pop, I. S., Bogers, J., and Kumar, K. Analysis and upscaling of a reactive transport model in fractured porous media with nonlinear transmission condition. *Vietnam J. Math.* 45 (2017), 77–102.
- [112] Ptashnyk, M. *Nonlinear Pseudoparabolic Equations and Variational Inequalities*. PhD thesis, University of Heidelberg, 2004.
- [113] Ptashnyk, M. Nonlinear pseudoparabolic equations as singular limit of reaction-diffusion equations. *Applicable Analysis* 85, 10 (2006), 1285–1299.
- [114] Ptashnyk, M. Degenerate quasilinear pseudoparabolic equations with memory terms and variational inequalities. *Nonlinear Anal.* 66 (2007), 2653–2675.
- [115] Ptashnyk, M. Pseudoparabolic equations with convection. *IMA J. Appl. Math.* 72 (2007), 912–922.
- [116] Radu, M. *Homogenization Techniques*. Diplomarbeit, University of Heidelberg, 1992.
- [117] Reichelt, S. Error estimates for elliptic equations with not-exactly periodic coefficients. *Advances in Mathematical Sciences and Applications* 25 (2016), 117–131.
- [118] Rendell, F., Jauberthie, R., and Grantham, M. *Deteriorated Concrete*. Thomas Telford Publishing, London, UK, 2002.
- [119] Rice, J. A. *Mathematical Statistics and Data Analysis*, 3rd edition ed. Duxbury Advanced Series. Thomson Brooks/Cole, Pacific Grove, California, 2007. International Student Edition.
- [120] Rothe, F. *Global Solutions of Reaction-Diffusion Systems*. Springer-Verlag, Berlin Heidelberg New York Tokyo, 1984.
- [121] Roubíček, T. *Nonlinear Partial Differential Equations with Applications*. No. 153 in International Series of Numerical Mathematics. Birkhäuser Verlag, Berlin, 2005.
- [122] Sanchez-Palencia, E. *Non-Homogeneous Media and Vibration Theory*. No. 127 in Lecture Notes in Physics. Springer, Berlin, 1980.

- [123] Sand, W. *Materials Science and Technology - A Comprehensive Treatment*, vol. 1 of *Corrosion and Environmental Degradation*. WILEY-VCH, Chichester, 2000, ch. 4. Microbial Corrosion. Volume Editor: Michael Schütze.
- [124] Schweizer, B. The Richards equation with hysteresis and degenerate capillary pressure. *J. Differential Equations* 252 (2012), 5594–5612.
- [125] Seam, N., and Vallet, G. Existence results for nonlinear pseudoparabolic problems. *Nonlinear Anal. Real World Appl.* 12 (2011), 2625–2639.
- [126] Shampine, L. F., Reichelt, M. W., and Kierzenka, J. Solving boundary value problems for ordinary differential equations in matlab with `bvp4c`. Tech. rep., Math. Dept., SMU, Dallas, 2000. The tutorial and programs are available at http://www.mathworks.com/bvp_tutorial.
- [127] Showalter, R. E. *Monotone Operators in Banach Space and Nonlinear Partial Differential Equations*. No. 49 in *Mathematical Surveys and Monographs*. American Mathematical Society, 1996.
- [128] Showalter, R. E., and Ting, T. W. Pseudoparabolic partial differential equations. *SIAM J. Math. Anal.* 1, 1 (1970), 1–26.
- [129] Simon, J. Compact sets in the space $L^p(0, T; B)$. *Ann. Mat. Pura Appl.* (4) 146 (1987), 65–96.
- [130] Simon, L. *Application of monotone type operators to nonlinear PDE's*. 2011. http://eta.bibl.u-szeged.hu/1293/1/application_of_monotone_type_operators.pdf.
- [131] Taylor, H. F. W. *Cement Chemistry*, 2nd ed. Thomas Telford Publishing, London, UK, 1997.
- [132] Trethewey, K. R., and Chamberlain, J. *Corrosion for Science & Engineering*, 2nd ed. Longman Group, Harlow, UK, 1995.
- [133] van Duijn, C. J., and Pop, I. S. Crystal dissolution and precipitation in porous media: pore scale analysis. *J. Reine Angew. Math.* 577 (2004), 171–211.
- [134] Verdink Jr., E. D. *Uhlig's Corrosion Handbook*, 3rd ed. John Wiley & Sons, Hoboken, New Jersey, 2011, ch. Economics of Corrosion.
- [135] Visintin, A. Homogenization of a doubly nonlinear Stefan-type problem. *SIAM J. Math. Anal.* 39, 3 (2007), 987–1017.

- [136] Vromans, A. J. *A Pseudoparabolic Reaction-Diffusion-Mechanics System: Modeling, Analysis and Simulation*. Licentiate thesis, Karlstad University, 2018.
- [137] Vromans, A. J., Muntean, A., and van de Ven, A. A. F. A mixture theory-based concrete corrosion model coupling chemical reactions, diffusion and mechanics. *Pacific Journal of Mathematics for Industry* 10, 5 (2018), Online Press.
- [138] Vromans, A. J., van de Ven, A. A. F., and Muntean, A. Existence of weak solutions for a pseudo-parabolic system coupling chemical reactions, diffusion and momentum equations. Tech. Rep. 17-03, CASA (Centre for Analysis, Scientific computation and Analysis), Eindhoven University of Technology, 2017.
- [139] Vromans, A. J., van de Ven, A. A. F., and Muntean, A. Periodic homogenization of a pseudo-parabolic equation via a spatial-temporal decomposition. Tech. Rep. 18-06, CASA (Centre for Analysis, Scientific computation and Analysis), Eindhoven University of Technology, 2018.
- [140] Vromans, A. J., van de Ven, A. A. F., and Muntean, A. Homogenization of a pseudo-parabolic system via a spatial-temporal decoupling: upscaling and corrector estimates for perforated domains. *Mathematics in Engineering* 1, 3 (2019), 548–582.
- [141] Vromans, A. J., van de Ven, A. A. F., and Muntean, A. Homogenization of a pseudo-parabolic system via a spatial-temporal decoupling: upscaling and corrector estimates for perforated domains. Tech. Rep. 19-01, CASA (Centre for Analysis, Scientific computation and Analysis), Eindhoven University of Technology, 2019.
- [142] Vromans, A. J., van de Ven, A. A. F., and Muntean, A. Parameter delimitation of the weak solvability for a pseudo-parabolic system coupling chemical reactions, diffusion and momentum equations. *Advances in Mathematical Sciences and Applications* 28, 1 (2019), 273–311.
- [143] Vromans, A. J., van de Ven, A. A. F., and Muntean, A. Periodic homogenization of a pseudo-parabolic equation via a spatial-temporal decomposition. In *Progress in Industrial Mathematics at ECMI 2018* (Berlin, 2019), I. Faragó, F. Izsák, and P. Simon, Eds., vol. 20 of *The European Consortium for Mathematics in Industry Series in Mathematics in Industry*, Scientific Committee of The 20th European Conference on Mathematics for Industry, Springer, p. to be communicated.

- [144] Watanabe, K., Kametaka, Y., Nagai, A., Takemura, K., and Yamagishi, H. The best constant of Sobolev inequality on a bounded interval. *J. Math. Anal. Appl.*, 340 (2008), 699–706.
- [145] Wittmann, H. F. Estimation of the modulus of elasticity of calcium hydroxide. *Cement and Concrete Research* 16 (1986), 971–972.
- [146] Zeidler, E. *Nonlinear Functional Analysis and its Applications II/A - Linear Monotone Operators*, vol. 2 part a. Springer-Verlag, 1990.

About the author

Arthur Vromans was born on February 16, 1989 in Vlaardingen, The Netherlands. There he attended primary school *Katholieke Basisschool De Hoeksteen*. In 2001 he was admitted to the pre-university level (VWO) secondary school *Stedelijk Gymnasium Schiedam*. In 2007 he was admitted to the bachelor programs of physics, mathematics and astronomy at *Leiden University*. In January 2011 he received his bachelor degrees in mathematics, physics, and astronomy. Arthur continued by enrolling in the Leiden University master programs of Applied Mathematics, Theoretical Physics, and Research in Astronomy. In August 2013 he received the master degree in Applied Mathematics and in August 2015 he received the master degrees in Theoretical Physics and Research in Astronomy.

Already in July 2015 Arthur started his PhD-research in applied mathematics at the Centre for Analysis, Scientific computing and Applications (CASA) at the *Eindhoven University of Technology* under supervision of dr. Adrian Muntean. In March 2017 Arthur was enrolled in the Swedish PhD-program of *Karlstad University* as well under supervision of prof.dr. Adrian Muntean via a dual degree agreement between Eindhoven and Karlstad. In September 2018 he obtained his Swedish Licentiate degree after a successful defense of his Licentiate thesis.

Summary

Homogenization of pseudoparabolic reaction-diffusion-mechanics systems: multiscale modeling, well-posedness and convergence rates

In this dissertation, we study a coupled system of partial differential equations describing a possible coupling between mechanics, flow, reaction-diffusion, chemistry and heterogeneous media. As indicated in chapter 2, we are interested in topics related to handling heterogeneities, model validation, parameter delimitation, vanishing multi-domains, convergence rates and other subjects beyond the standard research questions like model derivations, well-posedness, and formulation of limit systems and effective coefficients.

Specifically, in chapter 3, we derive a model based on physical laws and empirical relationships, for describing the effect of a chemical reaction in a mixture on its constitutional fractions, the domain thickness, and the velocities of its constituents. A specific application of this model is a theoretical formulation able to capture the onset of concrete corrosion of sewer pipes, where the mixture describes the penetration of acid into the concrete, where it reacts to form gypsum.

The physical validation of the model asks whether or not the model behaviour adheres to physical laws and assumptions if these laws and assumptions were not explicitly incorporated in the model. Positivity of the concentrations and boundedness of the velocities were obtained for several parameter regions. Similarly, the mathematical validation of the model from chapter 3 is invest-

igated in chapter 4. The mathematical validation focuses on the existence of a weak solutions to the model equations, and on the existence of a parameter region for which the physical validation is proven to hold. Moreover, in chapter 4, we tested numerically these parameter regions in order to determine their sharpness. It turns out that the obtained parameter regions are not sharp and that physical model behaviour exists even outside the obtained parameter regions.

The equations derived in chapter 3 describe a microscopic model for concrete corrosion. This material is heterogeneous, consisting of grains in a matrix. We assume that either grain or matrix is susceptible to corrosion. We take into account this small microscopic structure of grains in order to obtain correct corrosion speeds. In chapter 5, we employ the method of periodic homogenization to average out in some sense this microscopic structure and obtain effective behaviour at a large, macroscopic scale. Our main technique for periodic homogenization is the two-scale convergence, which copes with fast oscillating behaviour such as microscopically sized changes due to the grain-matrix differences, and gives an effective average behaviour in the limit these oscillations have positive amplitudes but infinitesimal wavelengths. Moreover, a convergence speed is obtained. This states that the deviation from the limit value becomes smaller as ϵ^p , when the microscopic scale ϵ tends to 0. For finite times we have $p = \frac{1}{2}$, while for infinite times we have $p < \frac{1}{2}$.

In chapter 5 we study the effect of perforated domains. On the contrary, the domain used in chapter 6 can be identified with only the grains and not the matrix. The exact geometric shape of the domain can be seen as a “forest” of tubes on a thin layer called the substrate. This geometry is reminiscent of the famous bed of nails and it is a geometry found on a microscopical level also in the context of solar cells design. In chapter 6, for this bed of nails geometry, the effective macroscopic behaviour and the convergence speed to it in the limit where both the nails and the substrate become infinitesimally thin, are obtained for a nonlinear version of the system looked at in chapter 5.

List of publications

Published or accepted papers

1. A.J. Vromans, A.A.F. van de Ven, and A. Muntean, “Homogenization of a pseudo-parabolic system via a spatial-temporal decoupling: upscaling and corrector estimates for perforated domains”, *Mathematics in Engineering*, vol. 1, no. 3, 2019, pp. 548-582.
2. A.J. Vromans, A.A.F. van de Ven, and A. Muntean, “Periodic homogenization of a pseudo-parabolic equation via a spatial-temporal decomposition”, in *Progress in Industrial Mathematics at ECMI 2018*, (I. Faragó, F. Izsák, and P. Simon, eds.), vol. 20 of *The European Consortium for Mathematics in Industry Series in Mathematics in Industry*, Scientific Committee of The 20th European Conference on Mathematics for Industry, Springer, Berlin, 2019, pp. *to be communicated*
3. A.J. Vromans, A.A.F. van de Ven, and A. Muntean, “Parameter delimitation of the weak solvability for a pseudo-parabolic system coupling chemical reactions, diffusion and momentum equations”, *Advances in Mathematic Sciences and Applications*, vol. 28, no. 1, 2019, pp. 273-311
4. G.E. Comi, R.J. Fitzner, S. Kolumbán, F.P. Pijpers, R.M. Pires da Silva Castro, R.A.J. Post, A.J. Vromans, “Causal effects of government decisions on earthquakes in Groningen” in *Proceedings of the Studygroup Mathematics with Industry. SWI 2018. Eindhoven, January 29 - February 2, 2018* (A. Di Bucchianico, S. Kapodistria, C. Hurkens, P. Koorn, O. Tse, S. Kolumbán, eds.), pp 1-25, 2019.

5. A.J. Vromans, A. Muntean, and A.A.F. van de Ven, “A mixture theory-based concrete corrosion model coupling chemical reactions, diffusion and mechanics”, *Pacific Journal of Mathematics for Industry*, vol. 10, no. 5, on-line press, 2018.
6. A.J. Vromans, *A Pseudoparabolic Reaction-Diffusion-Mechanics System: Modeling, Analysis and Simulation*. Licentiate thesis, Karlstad University, 2018.
7. R. Castelli, P. Frolkovic, C. Reinhardt, C.C. Stolk, J. Tomczyk, A. Vromans, “Fog detection from camera images”, in *Proceedings of the 114th European Study Group Mathematics with Industry. SWI 2016. Nijmegen, January 25 29, 2016* (E. Cator, R.J. Kang, eds.), pp 25-43, 2016.
8. A.J. Vromans and L. Giomi, “Oriental properties of nematic disclinations”, *Soft Matter*, vol. 12, pp. 6490-6495, 2016.
9. M. Bosmans, S. Gaaf, C. Groothede, R. Gupta, M. Regis, M. Tsardakas, A. Vromans and K. Vuik, “Nonlinear Cochlear Dynamics”, in *Proceedings of the Study Group Mathematics With Industry held at the TU Delft on January 27th - January 31st, 2014* (J. Dubbeldam, W. Groenevelt, A. Heemink, D. Lahaye, C. Meerman, F. van der Meulen, eds.), pp 94-110, 2014.

Submitted or to be submitted papers

10. A.J. Vromans, A.A.F. van de Ven, and A. Muntean, “Upscaling nonlinear pseudoparabolic-like systems on vanishing thin multidomains”, 2019. **To be submitted.**

Acknowledgments

Four years of being a PhD-student in CASA have passed in a blink of an eye. This is probably due to relativity: the more you enjoy something, the faster time seems to pass. And indeed the past four years I have had a lot of fun. So much so that I wish I could have made this experience last longer. Therefore, I would like to thank everyone who has helped me reach this point in my life.

Adrian, you managed to learn me valuable lessons: always ask questions; go to every social event for networking; advertise your work wherever you can. You showed me the joy of homogenization and the beautiful results that connect different descriptions of physical phenomena. Your energy and drive always amazes me and I tried to keep up with you, but it is like you contain a never depleting battery. You just keep going on.

Mark, you have helped me become a better presenter. Your quality of always being able to find the problem at the root of a question has influenced me greatly. Furthermore, the task of being a paper reviewer, which you asked me to do, opened my eyes and helped me with submitting my work. I am also very grateful for your support in my first year by funding my trips to Karlstad, AIMS2016 in Orlando, and Loka Brunn.

Fons, of all the people who have helped me during my PhD, I am indebted the most to you. With Adrian leaving for Sweden, you stood up and naturally rose to the positions of daily supervisor, confidant, proof checker, and collaborator. At moments, when I believed I was right and you believed I was wrong, you always pushed me to checking that part again, which often led to me agreeing with you that I was wrong. You have prevented me from making mathematical, grammatical, and most importantly social errors or even blunders when writing/submitting a paper or replying to a referee report.

Martin, it was always nice talking to you about science. Your advice helped me to grasp the cultural differences between Sweden and The Netherlands.

I thank the doctorate committee and the licentiate committee and opponent for their time and effort and especially their comments, which allowed me to improve this dissertation and its foundation, my Licentiate thesis. Next to them, I also thank the anonymous referee of AMSA, whose comments in all the reports have been vital in shaping Chapter 4 and paper [142]. Furthermore, I thank the Netherlands Organisation for Scientific Research (NWO) for the MPE-grant 657.000.004, and their cluster Nonlinear Dynamics in Natural Systems (NDNS+) for funding a research stay at Karlstad. Moreover, I thank the Kungliga Vetenskapsakademien (KVA) in Sweden for granting me grant MG2018-0020 for attending AIMS 2018 in Taipei.

I wouldn't have ended up at CASA if it weren't for Arjen Doelman, Sarah Gaaf and Barry Koren as Arjen advised me to go to CASA, and I knew it wouldn't be a place with only strangers as Barry had taught me in Leiden and I had met Sarah in SWI Delft. My time at both CASA and Karlstad would have been so much more difficult without the indispensable help and advice from the secretaries: Marèse, Enna, Jolijn, Diane, Stina and Birgitta. Every day was a nice day at the office with Joep, Patrick, Alessandro, Erik and Wim present. At lunch time and at Fika time I enjoyed all the conversations with Bart, Rien, René, Nikhil, Pranav, Koondi, Yuriy, Professor, Jens, Onur, Gianluca, Behnaz, Melania, Lotte, Ian, Nhung, Anuj, Nitin, Harshit, Xingang, Xiulei, Saeed (we still need to go to TEFAF), Jasper, Mikola (Zigge-zagge), Anastasiia, Anne, Jan-Cees, Georg, Jim, Jorg, Giovanni, Bjoern, Omar, Niklas, Mirela, Sorina, Jorryt, Anders, and everybody else.

My free time was quickly filled with many social groups: math and party in a *dude like* way with the Mathia group, parties and sports with PhD-council under leaderships of the Godfather, the Supreme Leader, and Sarah, sports with Above Average, roleplaying in Dungeons and Dragons, dining with Pranav, Niels, Quirijn, and Yuriy, so many board games with Dion, Jan-Willem, Niels, Rob, Patrick, Aleks, Max, and many others, poker with the unofficially official CASA poker group of Niels, Dion, Jaba, Rob, Craig, Straightchaser, Akshay, Lekhaj, Oleg, Lena, Mr. X., and Hossein, playing squash with Valliappan, Upanshu, Frank, Mr. Boogers, Auke, Pranav, Anweesha, Nikhil, Rien, Tarun, and Koondi, and playing field hockey at Oranje-Rood with Youri, Ditmar, Casper, Bas, Dennis, Sander, Marc, Olof, Stijn, Jillis, Edwin, Freek, Sander, Jelle, Jeroen, Hauke, Leon, Bas, Koen, Marijn, Cees, Paul, Bart, Chris, Roza, Siebe, Ivo, Patrick, Willem, Timo, and Jolanda.

Thank you all for all adventures, laughter and parties we had together.

Rico, Kasper, en Rick. De afgelopen vier jaar zag de grootste verandering in onze vriendschap. In plaats van elke vrijdag en zaterdag te snookeren of vele pubs en barren af te gaan, kon ik alleen deze oude tijden laten herleven als ik een heel weekend bleef. Een positieve verandering was de toon van onze gesprekken. We verdiepten onze band door meer over onze karakters, verlangens, dromen en nachtmerries te praten of elkaar advies te geven. Bedankt voor alle leuke tijden, advies, slechte grappen, discussies en steun.

Gerard, Marian, Eveline, Brian, opa Jan, oma Nel, opa Gerard, en oma Toos. Al die jaren dat ik aan de universiteit heb gestudeerd en nu promoveer, hebben jullie mij gesteund in al mijn beslissingen. Jullie hebben me laten zien waarom voor Eindhoven kiezen goed voor mijn toekomst en ontwikkeling zou zijn. Jullie hebben me van advies voorzien, zelfs wanneer ik er niet om vroeg, juist om te zorgen dat ik niet in een negatieve spiraal zou belanden en gewoon zou doorzetten om mijn doel te bereiken, hoe onmogelijk dat doel soms ook leek te zijn. Jullie hebben telkens laten weten hoe trots jullie waren bij het bereiken van elke mijlpaal. Dank jullie voor alle steun en advies die mij hebben gebracht op dit punt en die mij zullen helpen toekomstige keuzes te maken.

Statements

accompanying the dissertation

“Homogenization of Pseudoparabolic Reaction-Diffusion-Mechanics Systems:
Multiscale Modeling, Well-Posedness and Convergence Rates”

by

Arthur Johannes Vromans

1. Validation of a model for a physical problem described by partial differential equations cannot simply follow from well-posedness alone, but needs a-priori tests for adhering to reasonable physical properties and for accuracy determination based on real world data; see Chapters 3 and 4.
2. It is possible to describe smooth non-oscillating macroscopic behaviour of a pseudoparabolic system with fast oscillating periodic microscopic behaviour with a wavelength of size ϵ ; see Section 5.4.
3. The convergence error between the actual behaviour of the microscopic pseudoparabolic system with oscillations of wavelength ϵ and the $\epsilon = 0$ limit macroscopic behaviour is of size ϵ^p with $p = \frac{1}{2}$ for finite sized time intervals and with $p < \frac{1}{2}$ for infinite sized time intervals; see Chapter 5.
4. Solutions of pseudoparabolic systems lose dependence on and have a decrease in regularity in the directions with vanishing thickness of a multidomain; see Chapter 6.
5. Students need interdisciplinary projects in their curriculum to spark in them an appreciation of handling a problem using different viewpoints and to improve their communication with people of different knowledge backgrounds.
6. Communication in science is as important as research and learning. However, scientific education focuses predominantly on the latter two.
7. Poincaré said “*The wise must declare; science is built up with facts like a house is with bricks; but a collection of facts is no more a science than a heap of bricks is a house.*” (Ch. IX: Hypotheses in Physics, Translated by George Bruce Halsted 1913) However, some students perceive their collection of facts to be a theory.
8. Universities should embrace scientific channels on YouTube such as Numberphile, PBS Infinite Series and 3Blue1Brown as valuable tools in undergraduate education.
9. Playing board games with mathematicians will ultimately result in a long awkward silence followed by agitation due to one of the players using his/her turn to try to calculate the optimal strategy beyond the decimal point.
10. In the Dutch euthanasia protocol, discrepancies between the subjective definition of *unbearable and hopeless suffering* stated by a patient in a written declaration containing reasons for euthanasia, and the interpretation of this definition by a doctor when checking the criteria for legal performance of euthanasia, leads to unbearable and hopeless suffering by the patient.



Homogenization of pseudoparabolic reaction-diffusion-mechanics systems

In this dissertation, parabolic-pseudoparabolic equations are proposed to couple chemical reactions, diffusion, flow and mechanics in heterogeneous materials using the framework of mixture theory. The weak solvability is obtained in a one dimensional setting for the full system posed in a homogeneous domain - a formulation which we have obtained using the classical mixture theory. To give a glimpse of what each component of the system does, we illustrate numerically that approximate solutions according to the Rothe method exhibit realistic behaviour in suitable parameter regimes. The periodic homogenization in higher space dimensions is performed for a particular case of the initial system of partial differential equations posed in perforated domains. Besides obtaining upscaled model equations and formulas for computing effective transport coefficients, we also derive corrector/convergence estimates which delimitate the precision of the upscaling procedure. Finally, the periodic homogenization is performed for a thin vanishing multidomain. Corrector estimates are obtained for a comb-like domain placed on a thin plate in a monotone operator setting for pseudoparabolic equations.

ISBN 978-91-7867-033-8 (print)

ISBN 978-91-7867-038-3 (pdf)

ISSN 1403-8099

DOCTORAL THESIS | Karlstad University Studies | 2019:19
